

- I. Development of an isoxylitone analog as an anti-epileptic drug candidate
- II. Synthesis of SOX9 inhibitors as promoters of recovery from spinal cord injury

Julien Haeck

Thesis submitted in partial fulfillment of the requirements for the Master of  
Science degree in Chemistry

Department of Chemistry and Biomolecular Sciences

Faculty of Science

University of Ottawa

Candidate

Supervisor

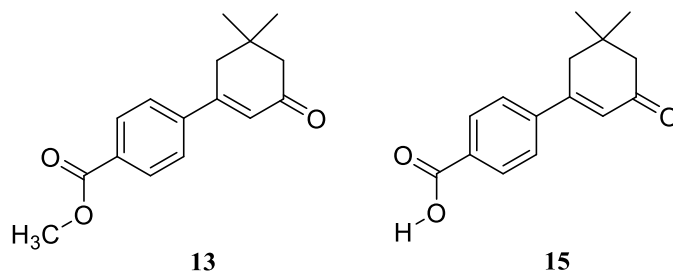
-----  
Julien Haeck

-----  
Dr. Tony Durst

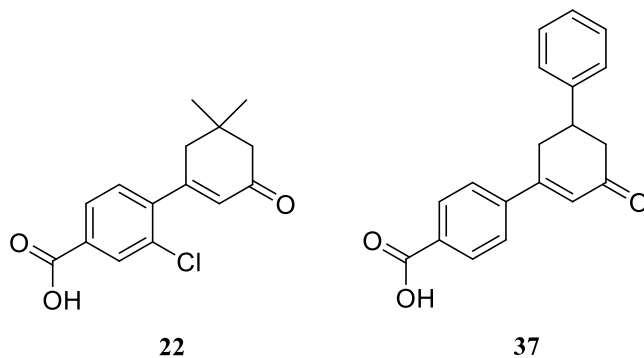
## Abstract

### Part I. Development of an isoxylitone analog as an antiepileptic drug candidate

*Delphinium denudatum* is a medicinal plant traditionally used to treat a variety of conditions in Central Asia. Its interesting anticonvulsant effects were determined to be a property of the compound isoxylitone. Prior work from our group in collaboration with the Poulter group from Western University investigated this compound and generated a large number of isoxylitone analogs in order to optimize its antiepileptic activity. This led to the discovery of the prodrug **13** and the active form **15** shown below, which emerged as the most potent.



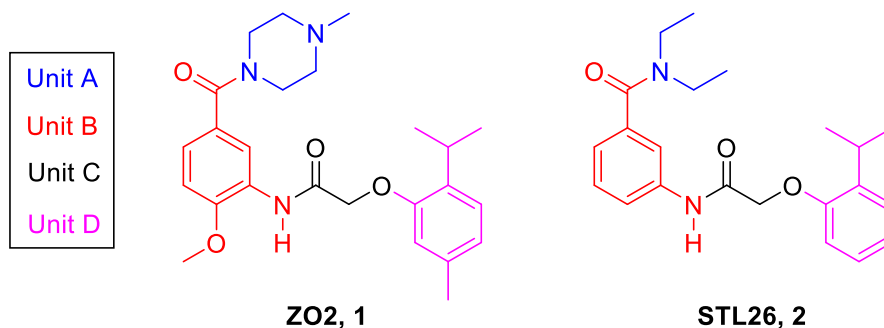
In this work, the library of analogs was further expanded with 22 new compounds with several which matched the activity of **13** and **15**, such as compounds **22** and **37**, which led to valuable new insights on the activity of these analogs, and suggested other possible future improvements.



In addition, efforts were continued regarding developing compound **15** as a clinical trial candidate. Optimization of the synthesis was performed to drastically reduce costs and waste of chemicals, as well as accelerating the duration of the synthesis. The purification of the final product was also greatly facilitated by the direct synthesis of **15**, compared to the prior process of first preparing **13** and hydrolyzing the ester. Efforts were exerted to gather additional knowledge on the characteristics of the compound, with structural and conformational analysis via X-ray crystallography and NOE NMR as well as accelerated stability studies to test the viability of **15** in long-term storage under various conditions. All the information gathered throughout this work supported **15** and its sodium salt as excellent clinical trial candidates as treatments for epilepsy.

## **Part II. Synthesis of SOX9 inhibitors as promoters of recovery from spinal cord injury**

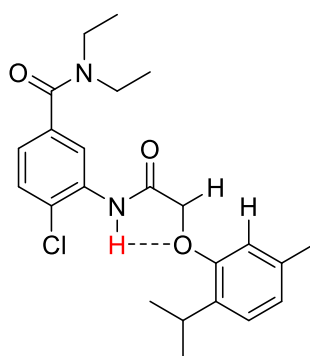
According to the World Health Organization, 250 to 500 thousand people develop a spinal cord injury each year with a large portion resulting in tetraplegia. A common misconception is that this is permanent because the damaged nerves cannot be repaired. In fact, nerves can and do regrow after being damaged, but cannot do so after spinal cord injuries due to formation of scar tissues which physically and chemically prevents the healing. The Brown group at Western University identified the SOX9 transcription factor as an important promoter of the formation of this scar and showed that SOX9 inhibitors could improve recovery and mobility in mice affected by spinal cord injuries. In collaboration with their group, previous work in our lab performed and SAR study on the lead compounds ZO2(**1**) and STL26 (**2**), shown below. The different sections of the molecule have been designated units A to D, to simplify discussion.



Initial work by our group established an efficient method to prepare a library of analogs of the lead compounds. A number of compounds were prepared, which primarily investigated small amines as unit A and phenols with small aliphatic substituents as unit D. The initial SAR data confirmed the validity of STL26 as lead compound, as most alterations to the structure were detrimental to the SOX9 inhibitory activity.

The objective of this work was to build on these preliminary SAR results, and expand the library of analogs. Larger substituents were introduced in unit A and D and showed that any group larger or smaller than diethylamide in unit A was detrimental to the activity, but that there seemed to be ample space to increase the size of the unit D isopropyl group. Analogs investigating unit B showed that adding substituents at most of the positions was detrimental, as well as changing the relative positions of unit A and B to be ortho or para to each other. However, the C4 on ring B seemed to be very tolerant to various electron donating or withdrawing functional groups. During this SAR study, a recurring theme was the awful solubility of the compounds in water, which heavily complicated their administration to mice during the bioassays. While none of the analogs tested proved superior to **2**, the knowledge accrued during this work painted a clear path forward on which areas of the structure could be safely altered to improve solubility without negative impacts on SOX9 inhibition.

Some additional efforts were put into obtaining an accurate three-dimensional structure of an active STL26 (**2**) analog, and information on the primary conformation in solution. Achieving these goals required the use of NOE NMR experiments and X-ray crystallography. One conformation was discovered to be strongly favoured as a result of an intramolecular hydrogen bond even in protic solvents. Subsequently, a small number of additional analogs were prepared containing modifications that would strongly favor or hinder the preferred conformation, in order to better understand its role in the inhibitory activity. The presence of this hydrogen bond appeared to be key to the activity of the compounds.



## Acknowledgements

Firstly, I want to express my appreciation for my supervisor Dr. Tony Durst for taking me in despite my lack of any prior research experience, and the mentorship and guidance throughout my degree. I am blessed to have had the opportunity to work on a number of interesting and unique projects. The experience has shaped me as a chemist, and helped clear up my path for the future.

I would further like to thank both Dr. Tony Durst and Dr. André Beauchemin for their unwavering patience despite the particularly long process. This thesis would have never come to be complete without their support and encouragements during the difficult times and I will be forever grateful.

I am grateful for my seniors Adrien, Vik and Amanda for showing me the ropes and helping me acclimatize to my first research lab, as well as paving the way for the projects I worked on. I would also like to recognize the assistance of all the amazing undergraduates and visiting student researchers I have had the pleasure to work with. Special thanks to David, Ashleigh and Lotty for the great memories.

Thank you to my friends and family for always being there for me. To my biggest supporter Sabrina, thank you for believing in me and always pushing me forward. I couldn't ask for a better partner.

## Table of Contents

Abstract	ii
Acknowledgements	vi
List of Figures	xi
List of Tables	xv
List of abbreviations	xvi
Part I. Development of an isoxylitone analog as an anti-epileptic drug candidate.	1
1.1 Introduction	2
1.1.1 Epilepsy and its symptoms	2
1.1.2 Effects of epilepsy on health and quality of life	4
1.1.3 Anti-epileptic drugs (AED)	5
1.1.3.1 History of treatments for epilepsy and seizures	5
1.1.3.2 Recent and future AEDs	8
1.1.4 <i>Delphinium denudatum</i> , traditional uses and antiepileptic activity	10
1.1.5 The Poulter group & OB Pharma	12
1.1.5.1 Voltage-sensitive dye imaging (VSDI)	13
1.1.5.2 The kindling model	14
1.1.6 Previous works	16
1.1.6.1 Amanda Saikaley M.Sc. Thesis	16
1.1.6.2 Adrien Fluet-Chouinard M.Sc. Thesis	18
1.2 Discussion	23
1.2.1 Introduction	23
1.2.2 Synthesis of amide analogs of 13	23

1.2.2.1	Objective	23
1.2.2.2	Synthesis	25
1.2.3	Optimization of the synthesis of 3-(4-carboxyphenyl)-5,5-dimethylcyclohex-2-enone	28
1.2.3.1	Justification of the acid 15 and the salt 18 as the lead clinical trial candidates	28
1.2.3.2	Optimization of the synthesis	35
1.2.3.3	Conclusion	46
1.2.4	Stability studies of TD562 and TD567	49
1.2.5	Structure-activity relationship studies	53
1.2.5.1	Objective	53
1.2.5.2	Preparation of halogenated aryl ring analogs	53
1.2.5.3	Modifications to the aryl-carboxylic acid substituent	55
1.2.5.4	Preparation of analogs with variations to C5 substituents	57
1.2.5.5	Changes in activity resulting from the various structural modifications	60
1.2.6	Conclusion and future work	73
1.3	Experimental Data	77
1.3.1	General information	77
1.3.2	General procedures	79
1.3.2.1	Preparation of enol tosylates in acetone and water	79
1.3.2.2	Palladium-catalyzed Suzuki cross-coupling	80
1.3.2.3	Conversion of carboxylic acids into sodium salts	81
1.3.3	Experimental procedures and product characterization	82
1.4	References	168
Part II.	Synthesis of SOX9 inhibitors as promoters of recovery from spinal cord injury.	173

2.1	Introduction	174
2.1.1	Overview on spinal cord injuries	174
2.1.2	Symptoms and effects of SCI on quality of life	175
2.1.3	Current treatments for SCI	176
2.1.4	Natural inhibition of neuronal regeneration by CSPGs	176
2.1.5	Finding a lead structure	178
2.1.5.1	The SOX9 gene plays a key role in the inhibition of recovery from SCI	178
2.1.5.2	ZO2 as SOX9 inhibitor	178
2.1.6	Previous work by the Durst group	180
2.1.6.1	Modifications of Unit A	182
2.1.6.2	Modifications of Unit B	183
2.1.6.3	Modifications of unit C	184
2.1.6.4	Modifications of unit D	185
2.2	Discussion and results	186
2.2.1	Introduction	186
2.2.2	Synthesis of the ZO2 analogs	186
2.2.2.1	General synthetic process	186
2.2.2.2	Using EDCI as coupling reagent for a cleaner amide bond formation	189
2.2.2.3	Using EDCI to circumvent the nitro reduction step	191
2.2.3	Analogs containing unit A modifications	192
2.2.4	Analogs containing unit B modifications	195
2.2.4.1	Structural and conformational analysis	198
2.2.4.2	Additional unit B analogs	202
2.2.5	Analogs containing unit D modifications	206

2.2.6	Conclusion and future work	209
2.3	Experimental Data	212
2.3.1	General information	212
2.3.2	General procedures	214
2.3.2.1	Amide coupling via acyl chloride intermediate	214
2.3.2.2	EDCI & DMAP amide coupling	215
2.3.2.3	Reduction of nitro groups to amines using Iron	216
2.3.2.4	Nucleophilic substitution of chloroacetic chloride by phenols	217
2.3.2.5	Palladium-catalyzed substitution of aromatic bromine by amines	217
2.3.3	Experimental procedures and product characterization	218
2.4	References	280

## List of Figures

<b>Figure 1.1.3.1.1.</b> Chemical structures of first generation antiepileptic drugs.	6
<b>Figure 1.1.3.2.1.</b> Chemical structures of third generation AEDs.	9
<b>Figure 1.1.3.2.2.</b> Chemical structures of novel potential AEDs that were ultimately unsuccessful.	10
<b>Figure 1.1.4.1.</b> Structures of isoxylitone E ( <b>1a</b> ) and Z ( <b>1b</b> ).	11
<b>Figure 1.1.4.2.</b> ISOX analogs described in the second Rahman group patent.	12
<b>Figure 1.1.6.1.1.</b> Reaction scheme for the synthesis of isoxylitone and the first set of analogs.	16
<b>Figure 1.1.6.1.2.</b> Main series of analogs in the A. Saikaley Thesis.	16
<b>Figure 1.1.6.1.3.</b> Structures of isophorone <b>6</b> , TD532 ( <b>7</b> ) and a proposed pharmacophore.	18
<b>Figure 1.1.6.2.1.</b> Chemical structure of dimedone ( <b>8</b> ).	18
<b>Figure 1.1.6.2.2.</b> Synthesis and chemical structures of analogs <b>10</b> and <b>11</b> .	19
<b>Figure 1.1.6.2.3.</b> General method for preparing 3-aryl substituted-5,5-dimethylcyclohex-2-enones.	19
<b>Figure 1.1.6.2.4.</b> Chemical structures of analogs <b>13</b> , <b>14</b> and <b>15</b> .	20
<b>Figure 1.1.6.2.5.</b> Synthesis of 3-(4-methoxycarbonylphenyl)-5,5-dimethylcyclohex-2-enone, <b>13</b> .	21
<b>Figure 1.2.2.1.1.</b> Chemical structure of the amide <b>14</b> (TD569).	24
<b>Figure 1.2.2.1.2.</b> Chemical structures of Lipitor, Crestor and Celebrex: examples of halogen-protected aromatic metabolic soft spots on currently marketed drugs.	24
<b>Figure 1.2.2.2.1.</b> Synthesis of the amide analogs <b>17a-g</b> .	25
<b>Figure 1.2.2.2.2.</b> General mechanism for the EDCI amide coupling.	26
<b>Figure 1.2.2.2.3.</b> Chemical structure of the amide analogs <b>17a-g</b> .	27
<b>Figure 1.2.3.1.1.</b> Seizure stage in kindled rats after administration of antiepileptic treatment.	29
<b>Figure 1.2.3.1.2.</b> Daily treatment with TD567 <b>18</b> prevents establishment of chronic epilepsy in rats following kindling model epileptogenesis.	30
<b>Figure 1.2.3.1.3.</b> TD 567 <b>18</b> can prevent stage 1 seizures in drug-resistant in kindled TBI rats.	31
<b>Figure 1.2.3.1.4.</b> TD567 <b>18</b> reduced neuron activation in brain slices from human brain slices obtained from patients with refractory epilepsy.	32

<b>Figure 1.2.3.1.5.</b> Concentrations of <b>15</b> in the plasma and the brain over 24h hours after administration of an oral dose.	<b>33</b>
<b>Figure 1.2.3.1.6.</b> Survival rates of mice treated with various concentrations of TD561 <b>13</b> .	<b>34</b>
<b>Figure 1.2.3.2.1.</b> Visualization of the inverse proportional correlation between catalyst loading and reaction time based on table 1.2.3.2.6.	<b>43</b>
<b>Figure 1.2.3.3.1.</b> <sup>1</sup> H NMR of the acid <b>15</b> .	<b>47</b>
<b>Figure 1.2.4.1.</b> Comparison of the <sup>1</sup> H NMR spectrum of compound <b>18</b> before and after the stability study.	<b>52</b>
<b>Figure 1.2.5.2.1.</b> Structures and chemical properties of halogenated analogs <b>20-21</b> , compared to <b>15</b> .	<b>54</b>
<b>Figure 1.2.5.2.2.</b> Overview of the preparation of analogs <b>20-22</b> .	<b>55</b>
<b>Figure 1.2.5.3.1.</b> Structures of analogs <b>26</b> and <b>27</b> .	<b>55</b>
<b>Figure 1.2.5.3.2.</b> Overview of the preparation of analogs <b>28-30</b> and their chemical structures.	<b>57</b>
<b>Figure 1.2.5.4.1.</b> Overview of the preparation of analog <b>34</b> .	<b>58</b>
<b>Figure 1.2.5.4.2.</b> Overview of the preparation of analog <b>37</b> .	<b>58</b>
<b>Figure 1.2.5.4.3.</b> Aliphatic region (2.0 to 4.0 ppm) of the <sup>1</sup> H NMR of compound <b>37</b> .	<b>59</b>
<b>Figure 1.2.5.4.3.</b> Overview of the preparation of analogs <b>42</b> and <b>43</b> .	<b>60</b>
<b>Figure 1.2.5.5.1.</b> pKa values for the benzoic acids corresponding to the acid <b>15</b> and its analogs <b>20</b> to <b>22</b> .	<b>62</b>
<b>Figure 1.2.5.5.2.</b> Tridimensional structure of the acid <b>15</b> obtained via X-ray crystallography viewed from various angles.	<b>63</b>
<b>Figure 1.2.5.5.3.</b> UV-vis Absorption spectra of <b>15</b> (left) and <b>22</b> (right).	<b>64</b>
<b>Figure 1.2.5.5.4.</b> 1D NOESY experiments of compounds <b>15</b> and <b>22</b> irradiating the sp <sup>2</sup> protons of the cyclohexenone rings at 6.44 ppm and 6.02 ppm.	<b>66</b>
<b>Figure 1.2.5.5.5.</b> <sup>1</sup> H NMR comparison between the initial quinine salt mixture of compound <b>37</b> and the recrystallised product.	<b>71</b>
<b>Figure 1.2.5.5.6.</b> Structures and LogP of the various analogs with C5 modifications.	<b>72</b>
<b>Figure 1.2.5.5.7.</b> Structures and LogP of potential analogs <b>44-46</b> . <i>The LogP values are calculated by ChemDraw.</i>	<b>73</b>
<b>Figure 1.2.5.5.8.</b> Reaction scheme for the preparation of the various cyclohexane-1,3-dione starting materials.	<b>73</b>

<b>Figure 1.2.6.1.</b> Revised proposed pharmacophore of the ISOX analogs family of antiepileptic compounds.	<b>74</b>
<b>Figure. 1.2.6.1.</b> Structures of analogs to be completed.	<b>75</b>
<b>Figure. 1.2.6.2.</b> Examples of analogs containing aryl electron donating groups.	<b>75</b>
<b>Figure. 1.2.6.2.</b> Examples of analogs containing polar C5 substituents.	<b>76</b>
<b>Figure 1.3.2.1.1.</b> Two methods of preparation of dimedone enol tosylates.	<b>80</b>
<b>Figure 1.3.2.2.1.</b> Preparation of 3-aryl cyclohexenones.	<b>81</b>
<b>Figure 1.3.2.3.1.</b> Preparation of the sodium salts.	<b>82</b>
<b>Figure 2.1.4.1.</b> The CSPG-heavy perineuronal nets block axonal sprouting.	<b>178</b>
<b>Figure 2.1.5.2.1.</b> Chemical structure of the lead compound ZO2 (1).	<b>180</b>
<b>Figure 2.1.6.1.</b> The four main units in the ZO2 (1) structure.	<b>181</b>
<b>Figure 2.1.6.2.</b> Chemical structure of the compound STL26 (2).	<b>182</b>
<b>Figure 2.1.6.1.1.</b> Structures of the various A units tested by Raina and Swan, sorted by decreasing potency.	<b>183</b>
<b>Figure 2.1.6.2.1.</b> Structures of the B ring C4 analogs.	<b>184</b>
<b>Figure 2.1.6.2.2.</b> Structure of the ortho-CD analogs.	<b>185</b>
<b>Figure 2.1.6.3.1.</b> Structures of the unit C analogs.	<b>185</b>
<b>Figure 2.1.6.4.1.</b> Structures of the unit D analogs, ordered by decreasing potency.	<b>186</b>
<b>Figure 2.2.2.1.1.</b> Formation of the AB amide bond via acyl chloride intermediate.	<b>189</b>
<b>Figure 2.2.2.1.2.</b> Reduction of the 3-nitro protecting group.	<b>189</b>
<b>Figure 2.2.2.1.3.</b> Preparation of the CD unit, thymol acetic acid (3), and its conversion to the acyl chloride.	<b>190</b>
<b>Figure 2.2.2.1.4.</b> Amide bond formation between the AB and CD units.	<b>190</b>
<b>Figure 2.2.2.2.1.</b> Formation and reaction of an active ester intermediate.	<b>191</b>
<b>Figure 2.2.2.2.1.</b> Amide bond formation using EDCI.	<b>192</b>
<b>Figure 2.2.2.3.1.</b> <sup>1</sup> H NMR spectrum of the EDCI/DMAP coupling on 3-aminobenzoic acid.	<b>193</b>
<b>Figure 2.2.2.2.2.</b> Attempted one pot formation of an ABCD analog.	<b>194</b>
<b>Figure 2.2.3.1.</b> Chemical structure of compounds 4 to 9.	<b>195</b>
<b>Figure 2.2.3.2.</b> Luciferase expression assay results of compounds 4 to 9. Compound 6 was prepared and sent, but not tested.	<b>197</b>
<b>Figure 2.2.4.1.</b> Chemical structure of the unit B para (11) and ortho (12) conformations.	<b>197</b>

<b>Figure 2.2.4.2.</b> Chemical structure of the analogs containing various C4 substituents on unit B.	<b>198</b>
<b>Figure 2.2.4.3.</b> Luciferase expression assay results of ring B C4-modified analogs. Compounds <b>12</b> and <b>13</b> were prepared and sent, but results were not received.	<b>199</b>
<b>Figure 2.2.4.4.</b> Preparation of C4 thioether analogs.	<b>200</b>
<b>Figure 2.2.4.3.1.</b> Tridimensional structure of compound <b>4</b> in a crystal lattice, obtained by single crystal X-ray diffraction.	<b>201</b>
<b>Figure 2.2.4.3.2.</b> Relevant protons in the NOE experiment on compound <b>4</b> in both possible major conformations.	<b>202</b>
<b>Figure 2.2.4.3.3.</b> 1D <sup>1</sup> H NOE spectrum of compound <b>4</b> , with irradiation of the 4.71ppm CH <sub>2</sub> peak.	<b>203</b>
<b>Figure 2.2.4.2.1.</b> Chemical structure of the conformation-altering analogs <b>14-17</b> .	<b>204</b>
<b>Figure 2.2.4.2.2.</b> Preparation of analogs <b>14-17</b> .	<b>205</b>
<b>Figure 2.2.4.2.3.</b> Luciferase expression assay results of analogs <b>14-17</b> .	<b>206</b>
<b>Figure 2.2.4.3.</b> Chemical structure of compounds <b>18</b> and <b>19</b> as well as their respective final coupled products.	<b>208</b>
<b>Figure 2.2.5.1.</b> Chemical structure of analogs <b>20-25</b> , containing unit D modifications.	<b>209</b>
<b>Figure 2.2.5.2.</b> Luciferase expression assay results of analogs <b>20-25</b> .	<b>210</b>
<b>Figure 2.2.6.1.</b> Structure of the three analogs prepared by the Organ group ( <b>26-29</b> ).	<b>211</b>
<b>Figure 2.2.6.2.</b> Structure of potential water-soluble analogs.	<b>212</b>
<b>Figure 2.2.6.3.</b> Structure of potential analogs containing a cyclic unit C.	<b>213</b>
<b>Figure 2.3.2.1.1.</b> Preparation of amides from an acyl chloride intermediate.	<b>216</b>
<b>Figure 2.3.2.2.1.</b> Amide bond formation using EDCI as coupling reagent.	<b>217</b>
<b>Figure 2.3.2.3.1.</b> Fe reduction of nitro groups.	<b>218</b>
<b>Figure 2.3.2.4.1.</b> Formation of 2-phenoxyacetic acid derivatives.	<b>219</b>
<b>Figure 2.3.2.5.1.</b> Substitution of aromatic bromines by amines.	<b>219</b>

## List of Tables

<b>Table 1.1.1.1.</b> Categories of seizures.	2
<b>Table 1.1.6.2.1.</b> Summary of the neuron firing reduction at 20Hz and 60Hz from VSDI <i>in vitro</i> bioassays on kindled rat brain slices.	20
<b>Table 1.2.3.2.1.</b> Cost per mole for the various reagents used in the synthesis of <b>15</b> .	37
<b>Table 1.2.3.2.2.</b> Initial reaction conditions for the Suzuki coupling at the start of the optimization process.	38
<b>Table 1.2.3.2.3.</b> Reaction conditions for the first 6 sets of Suzuki couplings with diminishing catalyst loading percentages.	39
<b>Table 1.2.3.2.4.</b> Reaction conditions for the sets 7 to 9 of Suzuki couplings with diminishing catalyst loading percentages and modified workup procedure, compared to a previous result.	41
<b>Table 1.2.3.2.5.</b> Summary of the sets of Suzuki reaction conditions with varying reaction time. <i>Equivalents for the reagents are based on 1.00 equivalents of boronic acid 19.</i>	42
<b>Table 1.2.3.2.6.</b> Overview of the effect of reaction time and catalyst loading on yield.	43
<b>Table 1.2.3.2.7.</b> Results from the reaction conditions investigating the importance of the base in the Suzuki cross-coupling.	44
<b>Table 1.2.3.2.8.</b> Comparison of the results from reactions under inert atmosphere or in air.	45
<b>Table 1.2.3.3.1.</b> Sample table of reagents for a large scale synthesis of compound <b>15</b> .	49
<b>Table 1.2.4.1.</b> Calculations for the estimated acceleration factor of the stability study.	51
<b>Table 1.2.5.5.1.</b> After-discharge duration (ADD) after electrical stimulus in amygdala of kindled rats treated with analogs <b>20-22</b> and compared to <b>18</b> .	61
<b>Table 1.2.5.5.2.</b> After-discharge duration (ADD) after electrical stimulus in amygdala of kindled rats treated with analogs <b>28-30</b> and compared to <b>18</b> .	67
<b>Table 1.2.5.5.3.</b> After-discharge duration (ADD) after electrical stimulus in amygdala of kindled rats treated with analogs <b>34, 37, 42</b> and <b>43</b> , and compared to <b>18</b> .	69

## List of abbreviations

°C	Degrees Celcius
<sup>1</sup> H NMR	Proton NMR
<sup>13</sup> C NMR	Carbon 13 NMR
ACSF	Artificial Cerebral Spinal Fluid
ADD	After-Discharge Duration
AED	Anti-Epileptic Drug
CBD	Cannabidiol
CCI	Controlled Cortical Impact
CDCl <sub>3</sub>	Chloroform-D <sub>3</sub>
CDRD	Center for Drug Research and Development
CNS	Central Nervous System
CSPG	Chondroitin sulfate proteoglycan
DCM	Dichloromethane
DMAP	N,N-Dimethylaminopyridine
DMF	N,N-Dimethylformamide
EDCI	1-Ethyl-3-(3-dimethylaminopropyl)carbodiimide
EDG	Electron Donating Group
eq.	Equivalents
EtOH	Ethanol
EWG	Electron Withdrawing Group
FDA	US Food and Drug Administration
g	Grams
GABA	γ-Aminobutyric acid
H <sub>2</sub> O	Water
HCl	Hydrochloric Acid
HPLC	High Performance Liquid Chromatography
HRMS	High-Resolution Mass Spectrometry
Hz	Hertz

ISOX	Isoxylitone
kg	Kilograms
L	Liters
MeOD	Methanol-D4
mg	Milligrams
MgSO <sub>4</sub>	Magnesium Sulfate
min	Minutes
mL	Milliliters
MM	Molar Mass
mmol	Millimoles
mp	Melting Point
NaCl	Sodium Chloride
NaOH	Sodium Hydroxide
n-BuLi	n-Butyllithium
nM	nanomoles per Liter
NMR	Nuclear Magnetic Resonance
NOE	Nuclear Overhauser Effect
Pd(PPh <sub>3</sub> ) <sub>4</sub>	Tetrakis(triphenylphosphine)palladium(0)
PhMgBr	Phenyl Magnesium Bromide
PNN	Perineuronal nets
ppm	Parts per million
SAR	Structure-Activity relationship
sbPTZ	Subcutaneous Pentylenetetrazole
SCI	Spinal Cord Injury
TBI	Traumatic Brain Injury
TLC	Thin Layer Chromatography
TMS	Tetramethylsilane
UV-Vis	Ultraviolet – Visible light
VSDI	voltage-sensitive dye imaging

Part I. Development of an isoxylitone analog as an anti-epileptic drug candidate.

## 1.1 Introduction

### 1.1.1 Epilepsy and its symptoms

Epilepsy is a chronic neurological disorder that is affecting, according to the US NIH, more than 700 000 children below eighteen and 3 000 000 adults in the United States. Almost 65 million people are affected worldwide making epilepsy and seizures among the most common neurological diseases.<sup>1</sup> People of all ages, genders and ethnicities are affected, but there is a significantly higher prevalence of epilepsy in lower income countries.<sup>2</sup> Epilepsy can be symptomatic (caused by various diseases or brain injuries) or idiopathic (genetic factors). Due to this, the term Epilepsy describes the spectrum of symptoms exhibited by those affected by the disorder, rather than the cause. For all patients, epilepsy manifests as recurring seizures of various intensities. Seizures are typically a fit of uncontrolled muscle contractions and jerking movements affecting local areas or the entire body, depending on the affected parts of the brain, caused by abnormal rapid neuron firing.<sup>3</sup> There are however several variants of seizures, which do not always involve the full-body convulsions commonly associated with epilepsy.

**Table 1.1.1.1.** Categories of seizures.

Type of seizure		Symptoms
Generalized Onset Seizures	Motor	Jerking movements (clonic), loss of muscle tone (atonic) or tension of the muscles (tonic), throughout the entire body.
	Non-motor	Short absence of movement and blank staring (Typical) or small unusual movements such as blinking repeatedly or hand movements (Atypical). Both involve loss of consciousness.
Focal Onset Seizures (Retained or Impaired Awareness)	Motor	Jerking movements (clonic), loss of muscle tone (atonic) or tension of the muscles (tonic), in specific parts of the body.
	Non-motor	Cognitive symptoms, absence of movement, emotional changes, hallucinations or other abnormal sensory experiences.

In 2017, the classification of seizures was revised by the International League Against Epilepsy to include some types of seizures that weren't included in previous classifications, and to make the terminology more practical and descriptive.<sup>4</sup> In this new classification seizures are first differentiated by onset type, or the origin of the seizure in the brain. The new unknown onset category was added, allowing the classification of seizures that were not observed by another party or where the onset type could not be determined.

A seizure will additionally be classified according to whether the patient is aware or has impaired awareness. As generalized onset seizures always impair awareness in some way, only focal onset seizures are separated between the two, previously known as simple partial seizures or complex partial seizures. Impaired awareness seizures do not necessarily involve loss of consciousness, as a confused or disoriented state is sufficient to fall under this category.

The last main classification is done based on the symptoms, separating them as motor or non-motor symptoms. Motor symptoms cover the common muscle tensing (tonic) and jerking (clonic), as well as loss of muscle tone (atonic). Motor symptoms can also include tics, such as twitching or small spasms. Motor symptoms are similar between both generalized and focal onset seizures. The parts of the body affected and the intensity of the effect are dependent on the onset type.

On the other hand, non-motor symptoms consist of various cognitive symptoms such as hallucinations and emotional changes, or blank staring/loss of consciousness with no motor symptoms (absence seizures).<sup>5</sup>

### **1.1.2 Effects of epilepsy on health and quality of life**

Epilepsy is a condition that has significant effect on the quality of life of those affected. In addition to the direct symptoms of the seizures, patients also have to contend with many comorbidities<sup>6,7</sup> and decreased life expectancy.<sup>8</sup> The prevalence of several conditions, such as cardiovascular disease and respiratory disorders, has been found to be higher in epileptic patients than in the general population.<sup>7</sup>

A significant challenge for people afflicted by epilepsy is the strong social stigma that has left many patients isolated from the rest of society. Though the general population's perception and understanding of the disease has come a long way, epileptic patients are still subject to increased challenges, especially regarding driving and employment.<sup>3,9</sup> It was found that over a third of people suffering from epilepsy kept the condition a secret for fear of being treated differently.<sup>10</sup>

Patients suffering from epilepsy are much more likely than the average person to also be affected by anxiety disorders, suicidal thoughts, depression or other mental health disorders, although it can be unclear whether that is due to the social and psychological aspect, or a direct effect of seizures on the brain.<sup>11</sup> Due to the major, long-lasting effects of epilepsy on quality of life and the fact that for some patients the condition never goes away, availability of accessible and safe medication is crucial.

### 1.1.3 Anti-epileptic drugs (AED)

#### 1.1.3.1 History of treatments for epilepsy and seizures

Epilepsy is one of the oldest known conditions with records going back as far as 2000 B.C., and descriptions of the various known seizure types being found as early as around 1000 B.C.<sup>12</sup> Some, such as Hippocrates, correctly attributed epilepsy to brain dysfunctions and tried to treat what he called the great disease (tonic-clonic generalized onset seizures are still commonly referred to as Grand mal). For the longest time however, most people attributed the symptoms to spirits, curses, punishments from the gods and other superstitions.<sup>12</sup>

Although many aspects of epilepsy, such as the various types and onsets or it being a disease of the brain, were discovered or guessed correctly thousands of years ago, little was understood about how seizures occurred and how to prevent them. Ancient treatments were thus at best ineffective and at worst harmful to the patient. These mainly consisted in specific diet recommendations or avoiding seizure triggers.<sup>12</sup> The first legitimate treatment of seizures was potassium bromide<sup>13</sup> that started seeing use in 1857. While useful in dampening epilepsy symptoms, the use of bromides was accompanied by severe dermatological and psychological side effects. This collection of adverse effects is referred to as bromism. The dermatological symptoms can include rashes, pustules and angiomas, while the psychological symptoms consist of irritability, confusion and psychosis. Ironically, severe case of bromism can induce seizures.<sup>14,15</sup>

Bromide remained the major method of treatment for epilepsy until 1912, when phenobarbital was discovered to be an effective anticonvulsant.<sup>13</sup> Phenobarbital and other barbiturates were well-known drugs for use as sedatives, but were found to be more effective than bromide at preventing seizures.<sup>13</sup> Benzodiazepines, the successors of barbiturates, also show anticonvulsant properties, but superior antiepileptic alternatives were found before benzodiazepines were discovered. As expected considering their

primary use, barbiturates and benzodiazepines are depressants and display strong sedative side effects. Both drug classes are highly addictive and can cause painful withdrawal symptoms.

The study of epilepsy on animal models led to the discovery of phenytoin in 1937.<sup>16</sup> Phenytoin is structurally very similar to phenobarbital, but was effective on some patients that did not respond to previous existing treatments. In addition, it did not display the sedative effects of the barbiturates although many other severe adverse effects were observed instead. The use of animal models allowed researchers to develop many effective analogs of phenobarbital and phenytoin, such as primidone which is used to this day.

In 1953, one of the most important AEDs was discovered. Carbamazepine was the most prescribed medication to treat epilepsy for many years, and remains the standard against which new AEDs in development are compared.<sup>13</sup> As with every successful drug, analogs of carbamazepine have been developed, but potency or reduction of adverse effect have not been improved significantly enough for carbamazepine to be replaced.

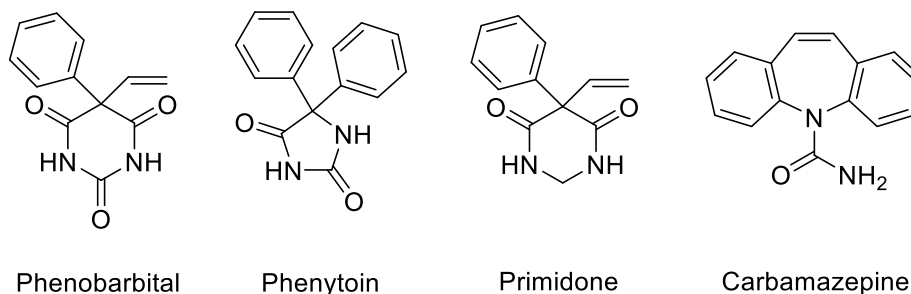


**Figure 1.1.3.1.1.** Chemical structures of first generation antiepileptic drugs.

The numerous available AEDs do not all share the same mode of action. The mechanisms of antiseizure activity can be separated into two main classes: drugs affecting GABA neurotransmitter activity, and drugs affecting neuron ion channels.

The antiepileptic effect on drugs affecting ion channels is a result of inhibition of the sodium or calcium channels on neuron membranes. The role of these channels is to initiate an action potential upon their opening, by depolarization of the membrane caused from releasing sodium ions back into the cell.<sup>17,18</sup> Inhibition of these channels can increase the threshold needed to initiate an action potential, and reduce neuron firing rate. Sodium channel blockers are more common and comprises all the carbamazepine and phenytoin analogs, although some AEDs such as Lamotrigine can block both types of channels.<sup>19-21</sup>

GABA is a major inhibitory neurotransmitter, that modifies the resting potential of neuron membranes to increase the threshold required to initiate an action potential. AEDs can promote the natural activity of GABA by binding to allosteric sites of the GABA<sub>A</sub> receptor to increase the response when a binding event occurs.<sup>21,22</sup> All barbiturates and benzodiazepines follow this mode of action.<sup>23</sup> A second pathway to increase the natural activity of GABA is to increase the concentration of the neurotransmitter in the brain. This is achieved by slowing the degradation of GABA by inhibition of the GABA-T enzyme which metabolizes it.

While the extent to which AEDs display their adverse effects varies from one to another, many of these effects are common to most AEDs. One of the most widespread side effects is an increased risk of suicidal behaviours, displayed by almost all major AEDs. While not every patient is affected in this way, they are significantly more likely to report having suicidal thoughts than people who are not under epilepsy treatment. Many AEDs are depressants and cause drowsiness, difficulty of breathing or slowing down heart rate. AEDs also tend to interact with cytochrome metabolic enzymes, either as activators or inhibitors, and often interfere with the metabolism of other medication. Ensuring effective treatment or preventing overdoses therefore requires careful dosage of every drug involved, for patients that require concomitant treatment. Many of these drugs,

such as but not limited to barbiturates and benzodiazepines, can be addictive and lead to withdrawal symptoms or substance abuse.<sup>24,25</sup>

Medication remains the primary treatment of epilepsy and seizures despite the adverse effects involved, however alternatives do exist. For patients suffering from focal onset seizures that always originate in the same lobe of the brain, the condition can be cured via cerebral lobectomy, the surgical removal of the entire lobe. The surgery is highly effective and can completely prevent seizures or greatly reduce the dosage of medication required to keep seizures under control.<sup>26</sup> While there are initial side effects, they are temporary and rarely persist. Despite being an effective treatment for specific types of epilepsy, the specificity of the surgery doesn't change the fact that most patients cannot have their condition cured and need to rely on AEDs.

### **1.1.3.2 Recent and future AEDs**

As development of AEDs has accelerated, new drugs have become available at an increasing pace and a large library of AEDs is now available to patients. Unfortunately, the increase in options available has not significantly lowered the rates of non-responding patients or reduced the severity of the adverse effects.<sup>13</sup> In fact, drugs such as carbamazepine, phenytoin and primidone are still commonly used despite the development of dozens of alternatives since. There have been around 20 AEDs developed after 2000, which have been termed third generation antiepileptic drugs. Most of these new AEDs have been unremarkable compared to their predecessors, however a few novel families of AEDs have emerged with structures or characteristics that make them stand out from the rest.

Despite ancient texts describing the anticonvulsant properties of the plant, the medicinal component of cannabis, cannabidiol (CBD), has only recently undergone clinical trials in the United States and has been approved by the FDA. Branded as Epidiolex, it is

used to treat the Lennox-Gastaut syndrome and Dravet syndrome seizure disorders.<sup>27,28</sup> CBD can be used to reduce seizure frequency for patients suffering from refractory epilepsy of the two mentioned syndromes. An advantage of CBD treatment is that the drug is unusually low in side effects for an anticonvulsant, with most patients only showing decreased appetite, fatigue or poor quality of sleep.<sup>27</sup>

Ganaxolone is an interesting AED currently in development. It has been found to prevent seizures via allosteric activation of the GABA<sub>A</sub> receptor, but stands out from the other drugs in the category due to its unique structure, being the only steroid AED. Initial clinical trials for the drug have been promising and show no drug interactions and mild side effects.<sup>29-31</sup>

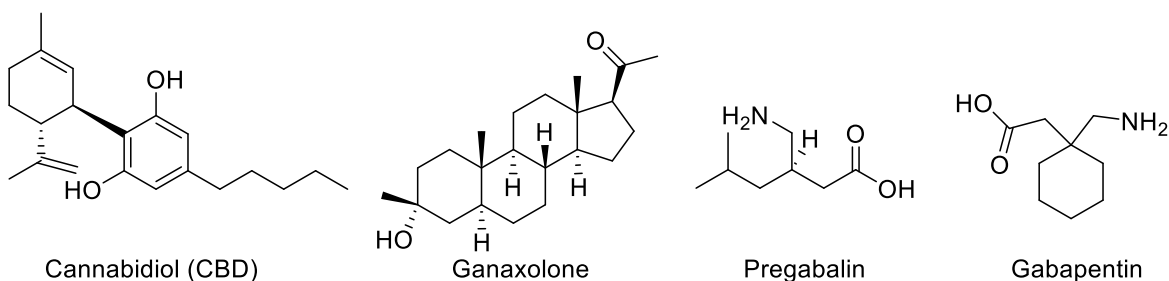


**Figure 1.1.3.2.1.** Chemical structures of third generation AEDs.

Pregabalin and gabapentin stand out by the fact they are some of the few current AEDs that do not contain a heterocycle. However, gabapentin is plagued by a similar side effect profile as first generation AEDs and pregabalin is not effective enough to be used on its own, always being prescribed in addition to another AED.<sup>24,31</sup> Many other potential candidates with novel structures were investigated, such as Carabersat and Carisbamate, but ultimately failed to prove effective.<sup>31</sup> Until ganaxolone is approved and available to patients outside of clinical studies, this makes cannabidiol the only currently marketed nitrogen-free AED.

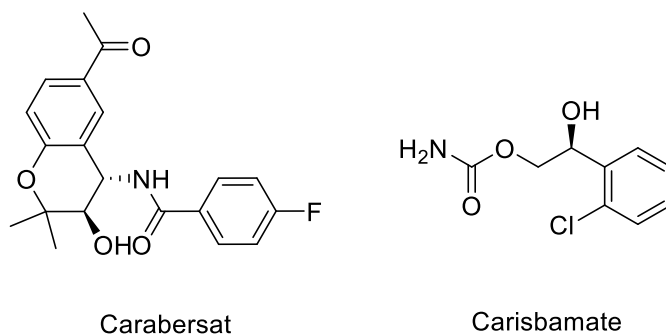


**Figure 1.1.3.2.2.** Chemical structures of novel potential AEDs that were ultimately unsuccessful.

In conclusion, the key modern issue with AEDs is the side effects of the drugs. Severe adverse effects can often force early termination of treatment, in addition to preventing the use of a sufficient dosage to properly treat the condition.<sup>24,25</sup> Despite the current selection of treatments, up to a third of patients receiving proper treatment and appropriate medication will be non-responders, and can suffer seizures throughout their lifetime.<sup>3,32</sup> Drug-resistant or refractory epilepsy is defined as cases where the seizures fail to be prevented by the proper usage of at least two separate AEDs. Very few patients with refractory epilepsy ever get better, despite the variety of drug and non-drug treatments.<sup>33</sup> There is therefore still a strong need for novel antiepileptic compounds that can deal with these issues.

#### 1.1.4 *Delphinium denudatum*, traditional uses and antiepileptic activity

*Delphinium denudatum* is an endangered plant native to the Western Himalayas, locally known as Jadwar. The roots have seen wide use in local traditional medicine to treat various conditions, and have a well researched use in the treatment of opioid addiction as a means of reducing withdrawal symptoms.<sup>34</sup> Investigation of its traditional use for epilepsy treatment through various anticonvulsant screenings confirmed the antiepileptic activity of the plant when administered as an aqueous extract.<sup>35–38</sup>

Researchers of the Rahman group from the University of Karachi determined the active compounds of the extract by assay-guided isolation. Most organic fractions were found to be highly toxic to mice, but anticonvulsant activity was only found in the non-alkaloidal aqueous extract which was also the least toxic. This extract was further separated via liquid chromatography, affording an oily fraction from which an isomeric mixture of the active compounds was isolated. These compounds were dubbed isoxylitone (ISOX) E and Z. The two isomers were found to be easily interconvertible between each other, and to both be active.<sup>39</sup> The activity of both compounds was confirmed *In vivo* in kindled mice.<sup>40</sup>

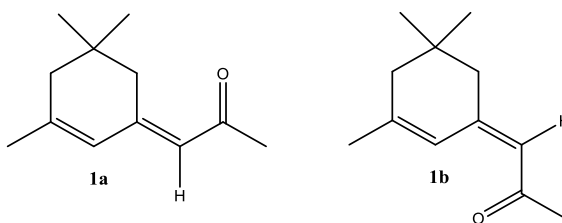


**Figure 1.1.4.1.** Structures of isoxylitone (ISOX) E (**1a**) and Z (**1b**).

In a second patent<sup>41</sup>, the same group described the synthesis of the isoxylitone isomeric mixture and made a few analogs (**2** to **5**), comparing them to the natural product which proved to be much more potent than any of the synthetic compounds. As the acid (**3**) was the only analog with some activity, these bioassay results demonstrated a clear loss of potency when increasing the size of the alkyl group adjacent to the ketone. The Maximal Electroshock Test (MEST) and the subcutaneous pentylenetetrazol test (sbPTZ) were the *In vitro* assays used to determine anticonvulsant activity, and are described in detail in the patent.<sup>41</sup>

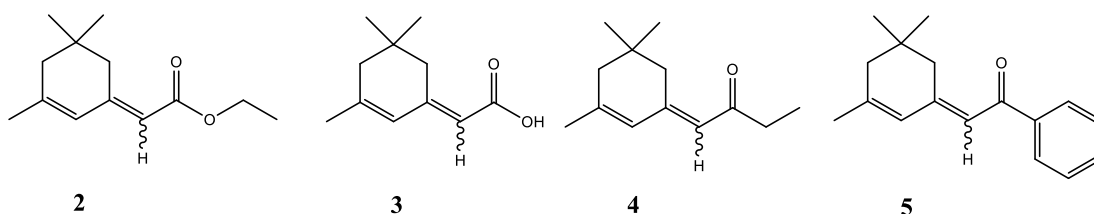


**Figure 1.1.4.2.** ISOX analogs described in the second Rahman group patent.

### 1.1.5 The Poulter group & OB Pharma

A sample of ISOX was brought to the Poulter group in 2011 by Muhammad N. Ashraf from the Rahman group. They worked together to confirm the antiepileptic activity of isoxylitone *In vivo* on kindled rats. They were entirely unable to kindle rats that were being treated with ISOX at 30 mg/kg doses.<sup>42,43</sup> Dr. Michael Poulter, a late member of the Ontario Brain Institute, who had been researching epilepsy for over 20 years, was impressed by the results and saw huge potential in the novel compound. Isoxylitone is the first antiepileptic compound that is completely nitrogen free, and lacks the heterocycles of the previous AEDs. Its structure is much simpler than most of the existing drugs, and would be relatively easy to synthesize on a large scale. The novelty of the structure indicates potential for ISOX to be effective in situations where the other AEDs are not, and be useful in treating refractory epilepsy. Poulter recognized the possibility that ISOX, because of its novel structure, might have a mode of action different from the various currently used heterocyclic AEDs and might thus be effective in treating the more recalcitrant cases.

In addition, the initial tests on mice and rats showed none of the usual side effects that plague modern antiepileptic drugs. The novelty of ISOX means it could possibly free patients from those usual side effects, although there could be different side effects associated with it.

Seeing this potential, ISOX became the lead compound on the project to develop new AEDs. Dr. Poulter founded Owen-Barry Pharmaceuticals (OB Pharma) to fund and work on this project. He tasked the Durst lab with synthesizing a library of isoxylitane analogs, in the hope of discovering analogs with greater antiepileptic activity than ISOX. Meanwhile, the Poulter group was responsible for the initial *in vitro* bioassays of the synthesized analogs via VSDI. The most potent analogs would then be advanced, further testing their ability to prevent epilepsy in kindled rats.

#### **1.1.5.1 Voltage-sensitive dye imaging (VSDI)**

Voltage-sensitive dye imaging is a technique used to visualize and quantify neuron electrical activity. Special dyes are used that react to changes in surrounding electrical potential during neuron firing.<sup>44</sup> The fluorescence profile of the dyes changes proportionally to the voltage applied, which allows the measurement of membrane excitation potential.

The dyes are introduced to neurons in rat brain slices in artificial cerebrospinal fluid (ACSF) and incubated to allow the dye to permeate in the cell membranes. The brain slices are then washed with clean ACSF to remove excess dye in the medium, followed by the addition of the analogs being assayed. The treated brain slices are electrically stimulated at 20Hz and 60Hz via implanted electrodes to induce neuronal firing. A strong reduction of neuronal firing at 60Hz is a good indicator of antiepileptic activity, while a reduction below 20Hz is undesirable as it could interfere with the electrical signals of the heart muscles.<sup>45,46</sup>

The results are expressed as a percentage reduction compared to base activity of control brain slices in absence of inhibitor. VSDI is a well-known method, and a good test to easily measure antiepileptic activity.

### 1.1.5.2 The kindling model

The kindling model is a model explaining epileptogenesis, the development of epilepsy, by the fact that seizures increase the sensitivity of the individual to further seizures.<sup>47</sup> The application of the kindling model to humans has been controversial as some patients with long lasting seizure disorders can sometimes have the condition go away on its own, but there is also solid evidence of artificially induced epilepsy according to this model.<sup>48</sup> The kindling model is based on the same phenomenon that explains the recurring seizure clusters that some patients experience, where months or years can pass without a seizure, followed by several seizures in a short span of time due to increased sensitivity after the first seizure of the cluster.<sup>49</sup>

The kindling model is a well documented method of preparing animal test subjects for *In vivo* bioassays of antiepileptic activity. Sub-epileptic electrical stimuli are administered regularly over an extended period of time directly to the animal's hippocampus. This slowly increases the sensitivity and ramps up the response to the stimuli, eventually leading to full-strength seizures in the animal.<sup>50</sup> Seizures are classified based on the intensity of the symptoms, according to the Racine scale. Severity of seizures is classed from 1 to 5, with class 1 seizures only exhibit facial movements & tics and class 5 seizures being a "Grand Mal" generalized onset tonic-clonic seizure. Once the rats exhibit class 5 seizure symptoms when receiving the same initial stimulus, they are considered fully kindled, ready for bioassays.

Furthermore, electrical stimulation is not the only kindling method and other epileptogenic stimuli have also been successful. The sbPTZ test described by the Rahman group in their second patent is referred to as chemical kindling, as the kindling process was carried out by regular doses of pentylenetetrazol (PTZ), a compound with strong convulsant activity.<sup>41</sup> A recent publication showed that light is also a functional kindling stimulus. The Sjöström group used lasers to excite light-sensitive brain cells and obtained results consistent with the traditional kindling model.<sup>51</sup> This new method has the

advantages of causing less physical damage to the brain cells, allows the researchers to target specific regions of the brain to simulate focal seizures and diminishes the ethical concerns of regularly shocking the animals.

As the kindling model cannot represent all types of seizures, some of the more important isoxylitane analogs described in this work required additional *In vivo* assays on rats kindled via a different method. This second method of epileptogenesis induced traumatic brain injury via controlled cortical impacts (CCI TBI). Although this is different to the kindling model as the epilepsy is induced immediately rather than over time, obtaining the data from both types of epileptic rats was important in evaluating the scope of activity of the analogs on the epilepsy spectrum.

## 1.1.6 Previous works

### 1.1.6.1 Amanda Saikaley M.Sc. Thesis

The first contribution to this project in the Durst lab was reported by Amanda Saikaley. Her M. Sc. thesis describes her synthesis of isoxylitone as an *E/Z* mixture from isophorone (**6**), a readily available and inexpensive starting material.<sup>52</sup> More than forty analogs were prepared via this method, most of which can be classified as either ketones, sulfones or nitriles. When tested by VSDI assays or on kindled rats, the anticonvulsant activity of these compounds decreased progressively as the alkyl chains on the EWG became larger, confirming the findings of the Rahman group.<sup>41</sup>

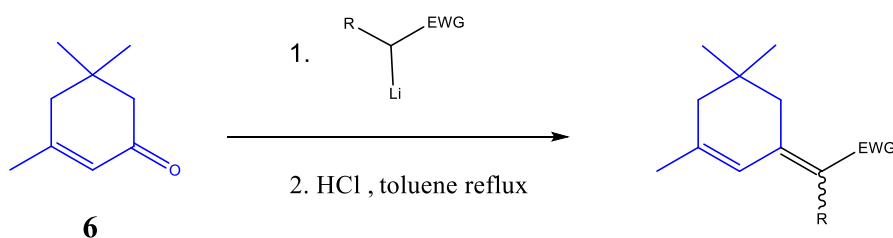
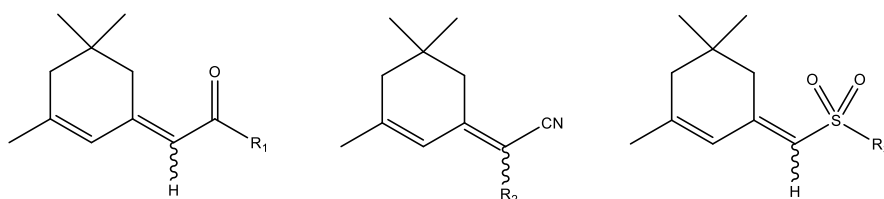


**Figure 1.1.6.1.1.** Reaction scheme for the synthesis of isoxylitone and the first set of analogs.



R<sub>1</sub> = OH, OMe, OEt, NHPH, ...

R<sub>2</sub> = H, Me, iPr, ...

R<sub>3</sub> = Me, Ph

**Figure 1.1.6.1.2.** Main series of analogs in the A. Saikaley Thesis.

The most potent compound of the analogs reported in the thesis was the nitrile **7**, internally named TD532, which was noticeably more active than isoxylitone and reduced neuron firing in VSDI assays by 50% at a 200nM. A number of additional nitrile analogs were made based on **7** but none matched the activity, once again showing that increasing

the size of the alkyl chain on the EWG is detrimental. Despite having the best activity so far, **7** had a few major downsides. Importantly the synthesis yielded **7**, initially as a mixture of all four dehydration products. These were converted to a mixture of mainly **E-7** and **Z-7** by heating the dehydration mixture with tosic acid in refluxing toluene. The <sup>1</sup>H NMR should clearly show the presence of the two isomers however when the amplitude of the spectrum was increased evidence of the presence of the other dehydration isomers could be seen. The two isomers were shown to be rapidly interconvertible under acidic conditions, as they would be in the stomach. The interconversion of the isomers also meant that separation of the isomers or modifications to the synthetic pathway to obtain a pure isomer would be pointless. Health Canada and the FDA are reluctant to accept drugs that are mixtures of isomers or enantiomers, and additional efforts would have needed to be made to ensure both structures were safe for use. A second major problem of **7** was its relatively low thermal stability, showing significant degradation after a few months at room temperature. Such a short expiration date would be a significant hurdle to the availability of any drug, regardless of its safety or activity. While the activity of the analogs was highly encouraging, these two issues needed to be addressed before the compounds had a chance to go to clinical trials.

Due to the success with small EWGs, the group decided to test the activity of the isophorone **6**. A moderate 22% reduction of neuron firing was observed for a 200nM concentration. While weaker than **7**, this activity was similar to some of the other analogs described in the thesis. This led to the proposed pharmacophore shown below.<sup>52</sup> The presence of an electron withdrawing group was shown to be important, but size and complexity negatively affected activity. As such, further analogs would aim to explore modifications to the C3 position of the cyclohexanone ring while retaining a ketone as EWG for simplicity of synthesis and to resolve the issue of isoxylitone analogs being obtained as E/Z isomeric mixtures.

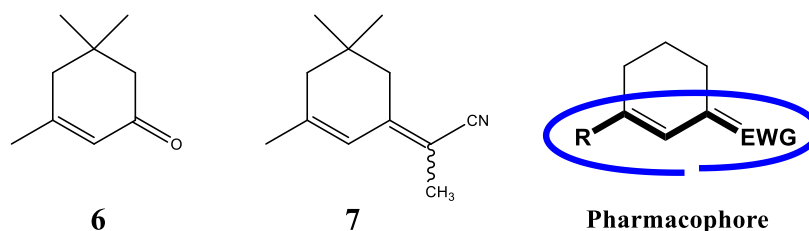


**Figure 1.1.6.1.3.** Structures of isophorone **6**, TD532 (**7**) and a proposed pharmacophore.

### 1.1.6.2 Adrien Fluet-Chouinard M.Sc. Thesis

The project was continued by Adrien Fluet-Chouinard, who investigated the proposed pharmacophore from the Saikaley thesis focusing mainly on 3-substituted cyclohexenones and added more than fifty new analogs to the library.<sup>53</sup>

In order to introduce modifications to the C3 position of isophorone, dimedone (5,5-dimethylcyclohexane-1,3-dione) **8** was used as starting material. Dimedone is easily available and almost as inexpensive as isophorone.

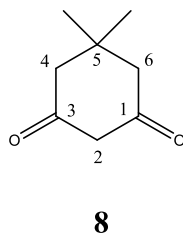


**Figure 1.1.6.2.1.** Chemical structure of dimedone (**8**).

Fluet-Chouinard expanded the library of analogs via two simple two-step processes. In the first, dimedone was converted to the enol ether **9** under acidic conditions in ethanol. The ether was then replaced by various alkyl groups via nucleophilic substitution with Grignard or organolithium reagents. The first two analogs produced by this method, **10** and **11** shown below, were synthesized using respectively *n*-BuLi and PhMgBr as nucleophiles. Both of these analogs exhibited a significantly improved activity

when compared to isophorone, boasting neuron firing reductions at 200nM of -36% (**10**) and -40% (**11**).<sup>53</sup> These impressive results confirmed the potential of investigating a diversity of substituents at C3. Analogs containing both the C3 butyl or phenyl groups and the C1 nitrile, as in compound **7**, were synthesized and assayed. This showed once and for all that the difference in activity between the ketone and other EWGs was not significant enough to warrant the additional synthetic steps or make up for the other downsides mentioned previously.

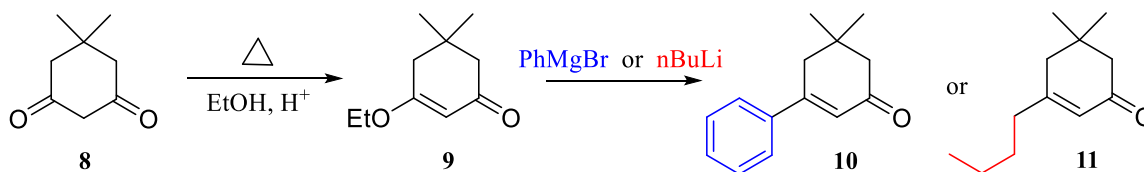


**Figure 1.1.6.2.2.** Synthesis and chemical structures of analogs **10** and **11**.

Many 3-arylcyclohexenone analogs were prepared to build on the bioassay results obtained with **10**. Virtually all of these analogs were prepared via a Suzuki coupling involving the enol tosylate **12** and a commercially available boronic acid.

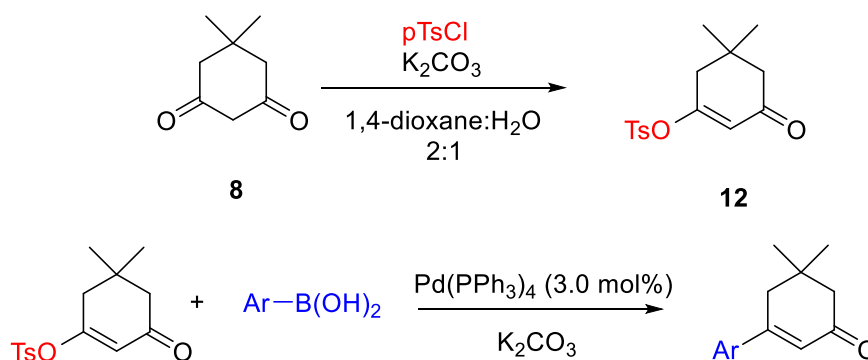


**Figure 1.1.6.2.3.** General method for preparing 3-aryl substituted-5,5-dimethylcyclohex-2-enones.

Most of the newly prepared compounds had somewhat similar activity in the VSDI assay as the simple 3-phenyl compound **10**, which was expected considering the similarities between the structures. Two standouts were the 4-(carboxymethyl)phenyl

(**13**) and 4-*N*-phenyl benzamide (**14**) analogs. Both had excellent activity in VSDI assays, causing reduction of neuronal firing of 48% (**13**) and 42% (**14**) at 200 nM concentration when excited at 60 Hz. Importantly, these compounds had very little activity when the excitation was carried out at 20 Hz.<sup>53</sup>

**Table 1.1.6.2.1.** Summary of the neuron firing reduction at 20Hz and 60Hz from VSDI *in vitro* bioassays on kindled rat brain slices.

Compound	Average reduction (%) at 200	Average reduction (%) at 200
	nM - 60Hz	nM - 20Hz
4-(carboxymethyl)phenyl <b>13</b>	-48 +/- 5	-13 +/- 13
4- <i>N</i> -phenyl benzamide <b>14</b>	-42 +/- 7	47 +/- 33

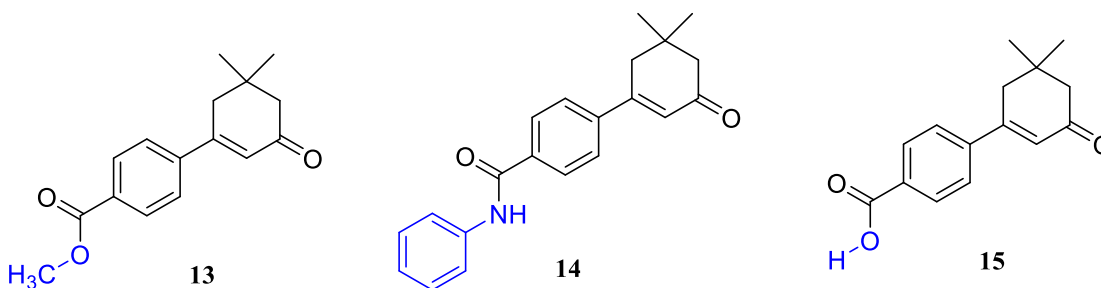


**Figure 1.1.6.2.4.** Chemical structures of analogs **13**, **14** and **15**.

The methyl ester **13**, internally referred to as TD561, became the new lead compound of the project. Several other esters including ethyl, isopropyl and butyl were prepared, but none of them had a statistically significant increase in activity over the methyl ester **13**. It was eventually discovered as part of a metabolism study that **13** administered orally was rapidly converted, presumably by esterases, to the corresponding acid **15**. Indeed, the acid **15** is the only metabolite observable by HPLC. As the half-life of the acid was of the order of 6 hours, the antiepileptic activity observed when administering compound **13** is therefore due to the activity of acid **15** itself. The

absence of additional metabolites makes either **13** or **15** attractive potential clinical trial candidates, especially if the safety of these compounds can be established.

As shown in **Figure 1.1.6.2.5**, the ester **13** was synthesized in two steps from dimedone and 4-(carboxymethyl)phenylboronic acid **16** as starting substrates. Dimedone was first converted to the enol tosylate **12** by reaction with p-toluenesulfonyl chloride in the presence of potassium carbonate as base. The dimedone tosylate was then coupled to the boronic acid **16** via a palladium-catalyzed Suzuki cross coupling to yield the desired product **13**.

Based on literature precedent this sequence was initially carried out in one pot without isolating the tosylate intermediate. The yield for the one pot synthesis was typically 55% based on the boronic acid as limiting reagent. These reaction conditions led quickly to the desired product however significant downsides are associated with isolation of **13** which required a difficult and lengthy column chromatography and at times even a second chromatography. The synthesis of **13** was improved considerably by first isolating and purifying by recrystallization the enol tosylate before carrying out the coupling reaction in a separate pot. As a result, the yield of **13** based on 4-(methoxycarbonyl)phenylboronic acid **16** as limiting reagent was improved to 85%. In this case too, a combination of crystallization and chromatography was necessary to produce a pure product. These reactions were typically carried out to yield 5 to 8 g of ester. This amount was sufficient to fulfill the need of material for the more extensive additional *in vitro* and *in-vivo* testing.

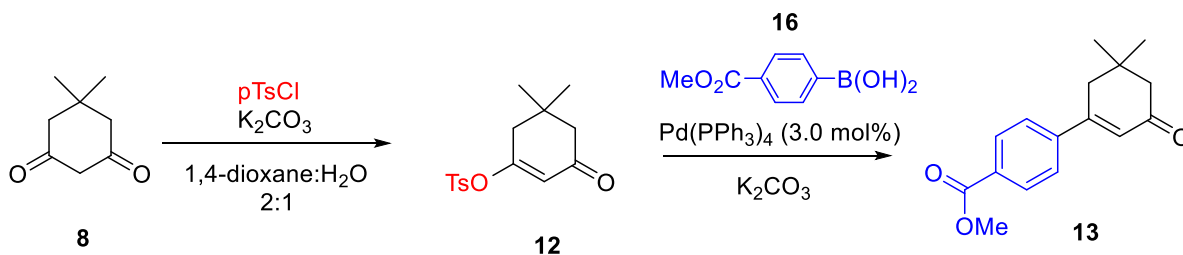


**Figure 1.1.6.2.5.** Synthesis of 3-(4-methoxycarbonylphenyl)-5,5-dimethylcyclohex-2-enone, **13**.

By the end of Fluet-Chouinard's work on the project, 3-(4-methoxycarbonylphenyl)-5,5-dimethylcyclohex-2-enone **13** had been established as a convincing clinical trial candidate. A number of the biological and physical properties of this analog, gathered by OB Pharma, support its development as a viable and potentially superior alternative to current epilepsy drug treatments.<sup>53,54</sup>

Compound **13** is effective at substantially smaller doses than its competitors. In comparison to Phenytoin, Lamotrigine and Carbamazepine that exhibit *in vitro* IC50 values between 50  $\mu$ M and 150  $\mu$ M<sup>19</sup>, **13** only requires a concentration of 25 pM to deliver the same activity.<sup>55</sup> When administered to rats during the kindling process, **13** showed antiepileptogenic properties, preventing the rats from becoming fully kindled.<sup>42,43</sup>

Despite being significantly more potent, no side effects were detected at up to 25 times the effective dose of the compound. Autopsies on treated kindled rats revealed no evidence of tissue damage or toxicity. Due to having a high selectivity for reducing neuron firing at high excitation frequencies only and no effect on hERG Potassium ion channels, **13** does not affect natural cardiomyocyte activity in a meaningful way. Compound **13** also passes the Ames test for mutagenicity and carcinogenicity.

As mentioned previously, the heterocycle and nitrogen-free novel structure of **13** sets it apart from any previous AED with the potential to treat refractory epilepsy. However, the compound still follows the Lipinski rules. Due to a calculated logP of 2.7, **13** has good bioavailability and distribution in the body. The compound is simple to prepare, and preliminary accelerated stability studies demonstrated a good thermal stability, showing no deterioration at room conditions for long term storage.

## 1.2 Discussion

### 1.2.1 Introduction

The initial goal of this work was to expand the library of isoxylitane analogs by exploring additional potential structural changes both in positions C3 and C5 of the cyclohexenone ring. It should be kept in mind that this project was funded by OB Pharma and thus it was often necessary to react to their priorities and put on hold the library expansion. Not unexpectedly, the company goals changed from time to time as new results were generated. In the end we were able to make considerable progress both in the initial goal and begin to establish structure activity relationships and satisfy to a considerable extent the company requests. The company goals and the expansion of the library intersected from time to time. The sub sections in this chapter of this thesis represent the chronological order in which the OB Pharma priorities were addressed.

### 1.2.2 Synthesis of amide analogs of **13**

#### 1.2.2.1 Objective

At the outset of this work there was considerable interest in the amide **14** since it gave not only very promising VSDI results but also prevented seizures in kindled rats when given at 20 mg per kg; the latter results were comparable to those for the methyl ester **13**. Part of the impetus for the interest in the amide stemmed from patent concerns. The ester **13** had been reported in the literature as part of a synthetic methods study describing the generation of a 300 compound library based on a Suzuki coupling of enol tosylates derived from 1,3-diketones with different boronic acids.<sup>56,57</sup> As the ester **13** was in this library, OB Pharma could patent the use of **13** but not the composition of matter. In contrast, the amide **14** had not been reported and thus could be patented for both the use and composition of matter thereby leading to a much stronger intellectual property position, the type highly preferred in the pharmaceutical industry.



### 1.2.2.2 Synthesis

The synthesis of these compounds was straightforward. The acid **15** was obtained from saponification of the methyl ester **13** and was then coupled to the appropriate anilines in presence of *N*-(3-dimethylaminopropyl)-*N'*-ethylcarbodiimide hydrochloride (EDCI) and 4-(dimethylamino)pyridine (DMAP) in dichloromethane (DCM) to yield the amides **17a-g**. The desired product was formed quickly at room temperature, but was typically left to react overnight. The product was isolated via acid and base washes and purified via recrystallization in a mixture of DCM and hexanes. Eight analogs were prepared in yields ranging from 15% to 81% and characterized by <sup>1</sup>H NMR and <sup>13</sup>C NMR which supported the assigned structures.

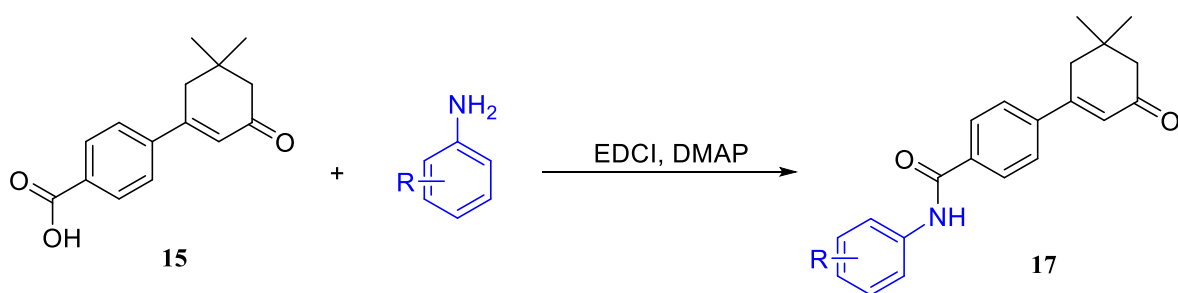


**Figure 1.2.2.2.1.** Synthesis of the amide analogs **17a-g**.

The EDCI amide coupling was chosen over other amide coupling reactions due to its reliability and ease of purification. EDCI reagent is significantly more expensive than oxalyl chloride or thionyl chloride, two common reagents used to convert carboxylic acids to acyl chlorides for amide coupling. However, the acyl chloride synthetic pathway makes use of harsher reagents and reaction conditions, as well as requiring an additional step. EDCI readily forms hydrochloride salts, and is trivial to remove via simple acid washes once the reaction is done. Due to this, multiple analogs could be made in parallel each day. All the analogs mentioned above were prepared within two weeks including the preparation of the starting acid **15**, the time saved due to the choice of reaction thus outweighed the increased cost of reagents. EDCI activates the carboxylic acids by forming an isourea-type leaving group facilitating the nucleophilic substitution by amines.

In addition to providing the required basic conditions for the reaction, the role of DMAP is to act as a transition amine and prevent the activated o-acylisourea ester from being hydrolyzed back into the carboxylic acid.<sup>59</sup>

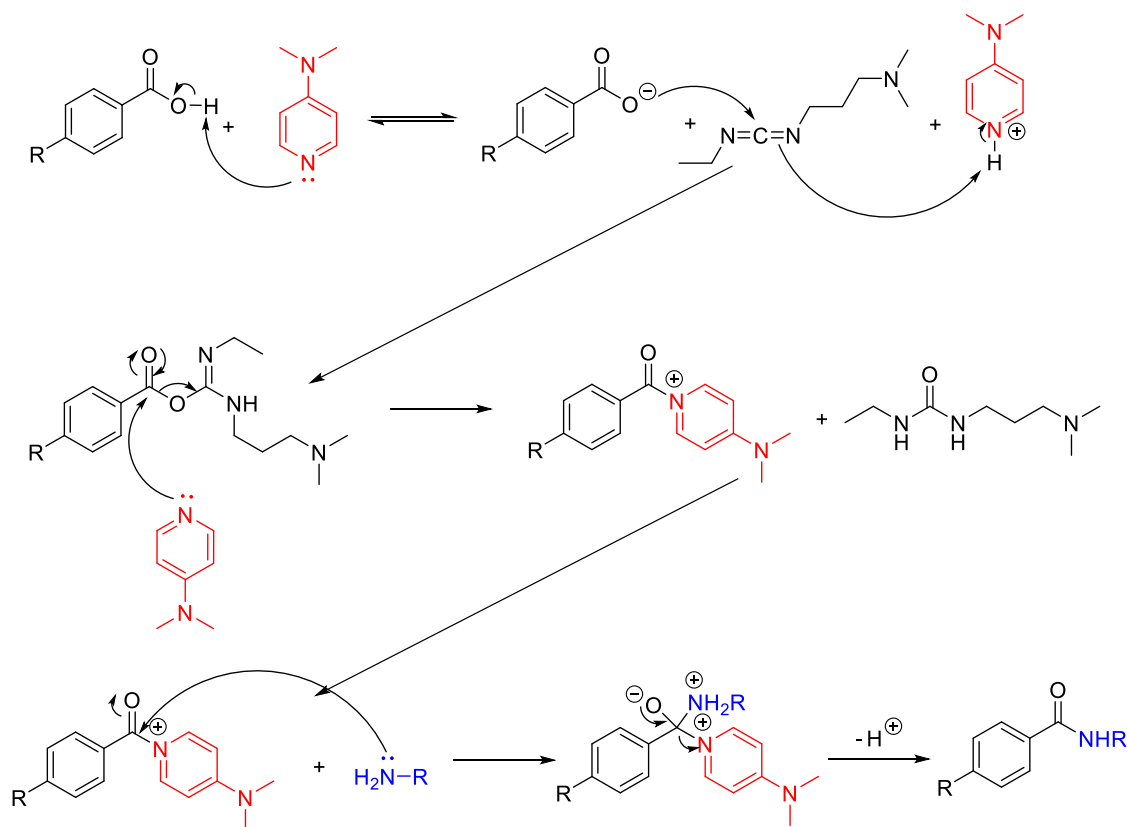


**Figure 1.2.2.2.** General mechanism for the EDCI amide coupling.

The amide compounds, **17a-g** prepared were submitted to OB Pharma for evaluation. Unfortunately, from this thesis point of view, the interest in these amides had waned considerably mainly because studies carried out at the Center for Drug Research and Development (CDRD) at the University of British Columbia indicated that the pharmacodynamics of the parent amide **14** were much more complicated than expected. Surprisingly, it was reported that some of this compound was metabolized back to the parent acid and none of the amide could be detected in the blood. Also, and very importantly, it was discovered that the US patent examiner had accepted the sodium salt as a new chemical entity and thus suddenly the company focus shifted to **15** and its

sodium salt **18**. None of the amides have been evaluated to date in the *in vitro* or *in vivo* bioassays, thus no comment can be made on the potency of these analogs.

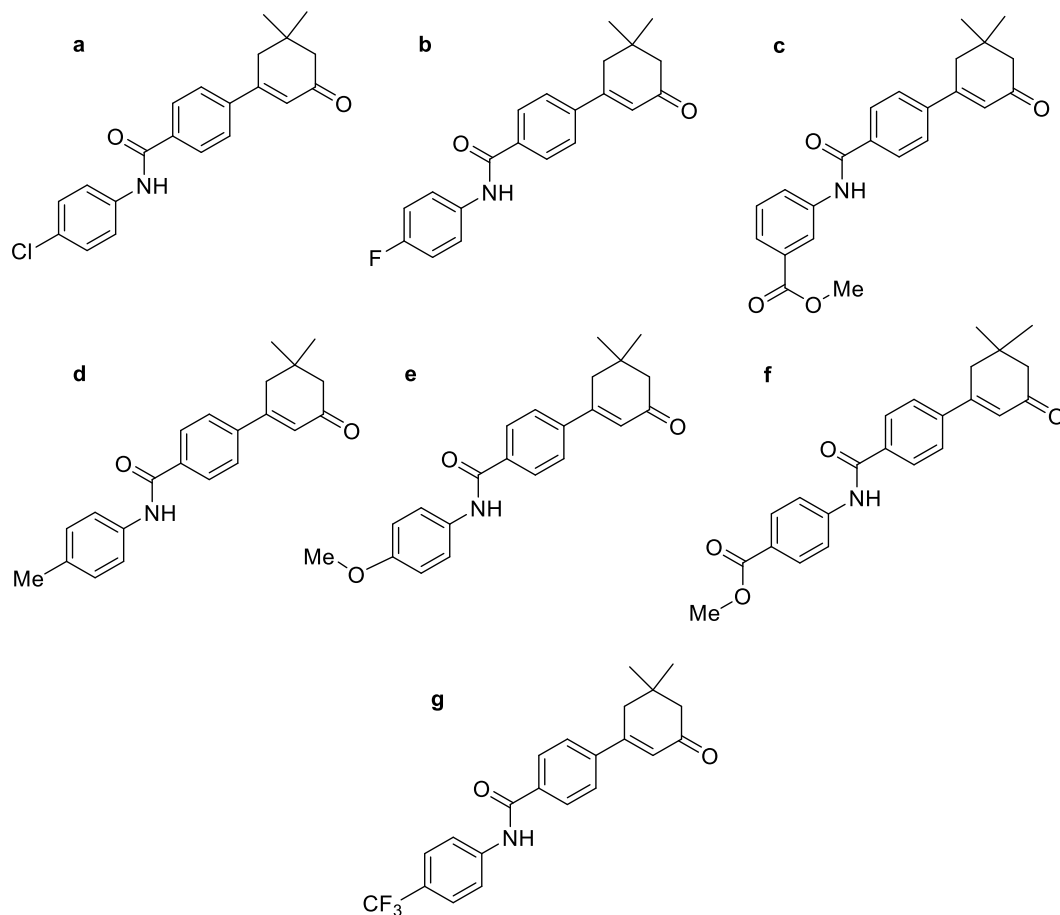


**Figure 1.2.2.2.3.** Chemical structure of the amide analogs **17a-g**.

### 1.2.3 Optimization of the synthesis of 3-(4-carboxyphenyl)-5,5-dimethylcyclohex-2-enone

#### 1.2.3.1 Justification of the acid **15** and the salt **18** as the lead clinical trial candidates

At this point in time, the scientists and management of OB Pharma decided that the acid **15** and the related sodium salt **18** were the best candidates for clinical trials. Since the ester **13** had been identified as the pro-drug of the acid **15**, much of the in vivo data available for the ester **13** was applicable to **15** and its sodium salt **18**. OB Pharma in cooperation with the Center for Drug Research and Development (CDRD) had gathered much additional data to support the decision to advance the acid **15** or its sodium salt **18** to clinical trials. Since this data was not generated by us, only a few critical results are described below in order to illustrate that this decision was based on solid scientific evidence.

##### a) Comparison of **18** activity to Carbamazepine and Levetiracetam.

A head-to-head comparison with levetiracetam and carbamazepine showed that **18** almost completely attenuated behavioral seizures to below Stage 1 when administered at 20 mg/kg intraperitoneally. On the other hand, the other two currently used AEDs at their maximally effective doses reduced the severity of seizures only to the still rather severe Stage 3-4.<sup>54</sup>

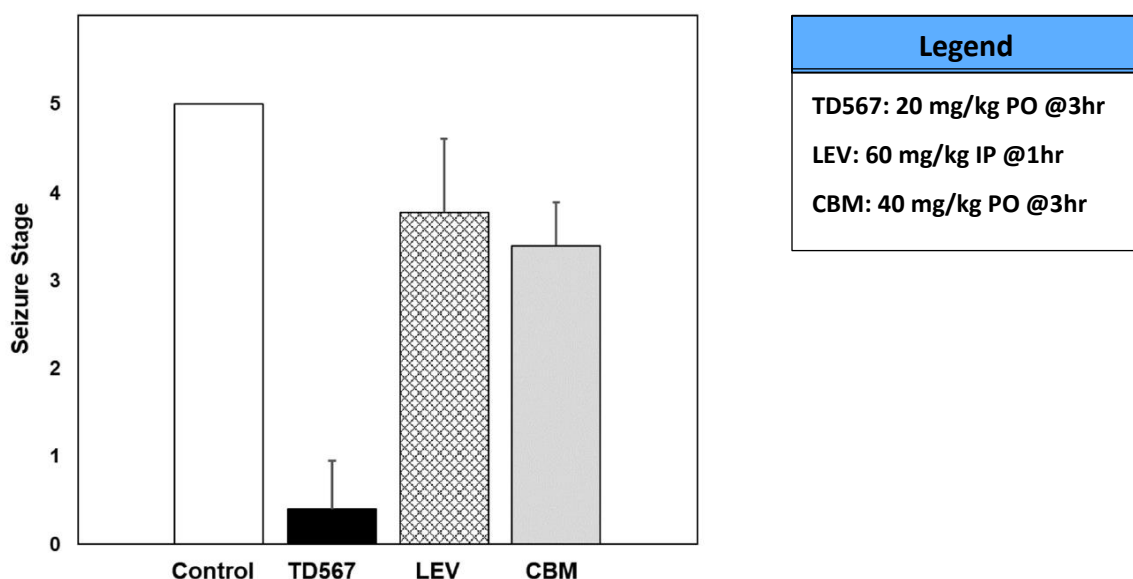


**Figure 1.2.3.1.1.** Seizure stage in kindled rats after administration of antiepileptic treatment. TD567 **18** and Carbamazepine (CBM) were administered orally and tested 3 hours after administration. Levetiracetam (LEV) was administered by intraperitoneal injection and tested 1 hour afterwards. CBM and LEV were administered at maximal effective non-toxic dosage based on previously published results.

b) **18** prevents rats from becoming fully kindled

Rats undergoing the regular kindling process while treated with **18** would not exhibit severe seizures up to two weeks after the control rats were fully kindled. Full kindling was prevented in the treated animals despite doubling the usual treatment duration, thus demonstrating **18** possesses antiepileptogenic properties in addition to its antiepileptic activity. Similar results were observed for tests on TD561 **13** and TD562 **15**.<sup>54</sup>

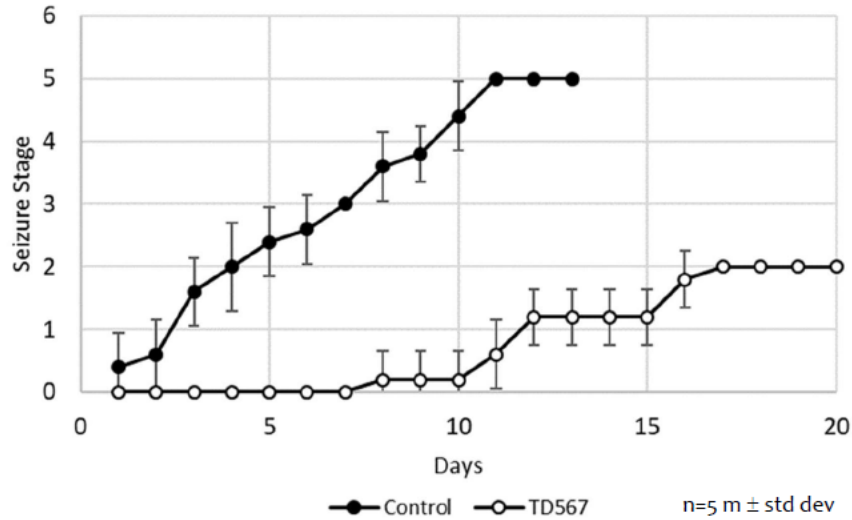


**Figure 1.2.3.1.2.** Daily treatment with TD567 **18** prevents establishment of chronic epilepsy in rats following kindling model epileptogenesis. Rats were administered 20 mg/kg orally each day, and electrically stimulated with 2s 70Hz currents once daily for three weeks. Treated rats subsequently stopped being administered with TD567 and were fully kindled within the following two weeks of daily stimulations.

c) Seizures in subjects exhibiting refractory epilepsy can be prevented by treatment with **18**.

Traumatic brain injury (TBI) can be administered in a reproducible manner by a pneumatic or electromagnetically controlled piston to deliver controlled impacts (CCI) to the head.<sup>60</sup> Following a CCI TBI, and for several weeks after the injury, the animals can be kindled extremely easily. Compared to regular control rats, CCI TBI rats would become fully kindled more than twice as fast, in as little as four days after the injury.<sup>54</sup>

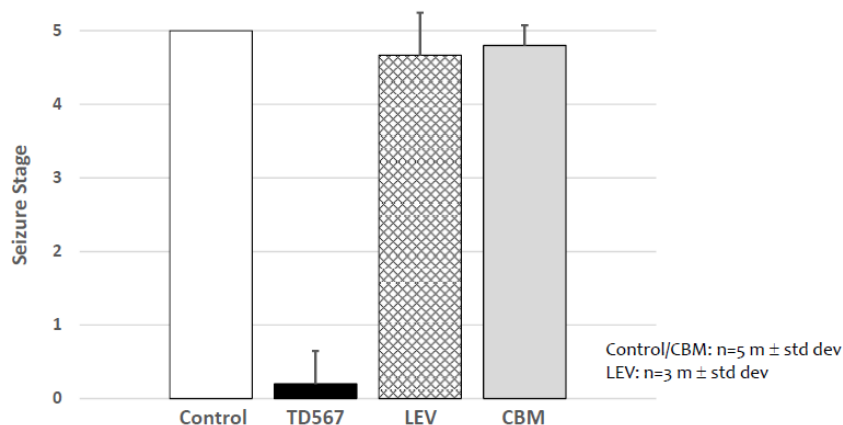


**Figure 1.2.3.1.3.** TD 567 **18** can prevent stage 1 seizures in drug-resistant in kindled TBI rats. *The subject rats were administered CCI TBI then allowed to recover for a week, after which electrical kindling was performed. When the animals were treated with Carbamazepine (CBM) or Levetiracetam (LEV) and subjected to electrically-induced seizures, they exhibited drug-drug resistant epilepsy. Meanwhile, TD567 **18** was effective at completely preventing seizure symptoms. Maximal effective non-toxic oral dose for each drug was administered. The animals received 20 mg/kg of TD567, 60 mg/kg of LEV or 50 mg/kg CBM.*

OB pharma additionally obtained drug-resistant human brain tissue from seven different patients, for use in *ex vivo* VSDI bioassays. Compounds **15** and **18** both showed major reductions in neuron firing on tissues where Levetiracetam and Carbamazepine had little effect.<sup>54</sup>

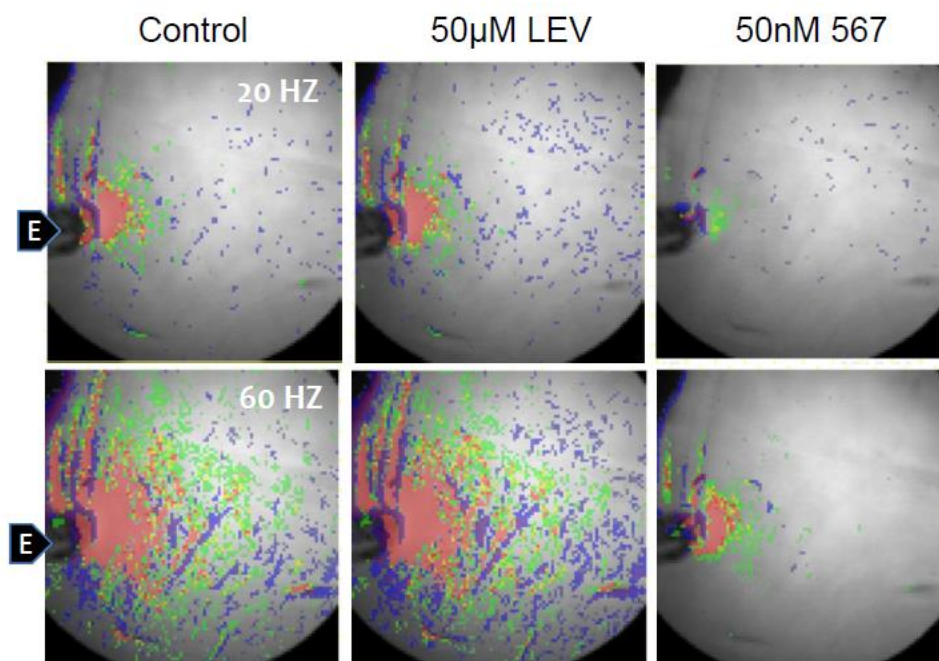


**Figure 1.2.3.1.4.** TD567 **18** reduced neuron activation in brain slices from human brain slices obtained from patients with refractory epilepsy. *Ex vivo* VSDI bioassays were performed on brain slices from a 21-year-old female patient suffering from drug resistant epilepsy. Treatment with Levetiracetam shows very little effect, despite a thousand-fold higher concentration than TD567.

#### d) Pharmacokinetics and metabolism

Compounds **15** and **18** have desirable pharmacokinetic and metabolic profiles. Ester prodrugs are readily hydrolyzed into the active compound. The ester **13** has a half-life of 27.4 min in human plasma, going down to 2.4 min in the liver. Compound **15** and **18** were detected in the brain at concentrations 400 +/- 63 ng/mL from a 10 mg/kg oral dose. With the above dosage, the half life of the compounds in the brain was calculated to be 7.57 hours. Compounds **15** and **18** therefore have no issue crossing the blood brain barrier to reach the origin of the seizures and provide their antiepileptic activity where needed for an acceptable duration. The half-life of the compounds is at a good level to be effective with only one dose per day, without causing accumulation issues from being too difficult for the body to evacuate. As mentioned previously, it is important to note that no metabolite of **15** was detected in the samples taken.<sup>54</sup>

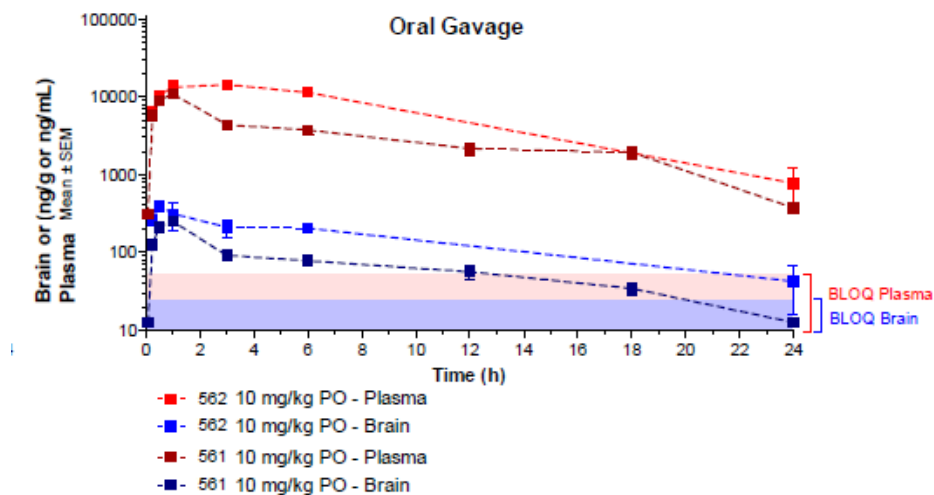


**Figure 1.2.3.1.5.** Concentrations of **15** in the plasma and the brain over 24h hours after administration of an oral dose. Concentrations of *TD562 15* rather than *TD561 13* are displayed when *TD561* was administered, due to the fast hydrolysis of the latter.

e) Off-target safety and potential adverse effects

Compounds **13** and **15** were tested by the Center for Drug Research and Discovery (CDRD) via the SafetyScreen 44 panel.<sup>61</sup> The screen tests off-target binding to 44 important targets, that are essential to pass a safety evaluation. Compound **15** showed no significant inhibition to any of the 44 targets. There was no inhibition of the hERG potassium channels responsible membrane polarization in the heart muscle, at up to  $10^5$  times the concentration that is effective for seizure prevention<sup>62</sup>. Compound **13** demonstrated slight inhibitory binding to a few transporters at high concentrations. However, this would not be an issue as long as the compound is administered at its normal effective concentration, especially considering the rapid metabolism into **15**.<sup>54</sup>

Preliminary toxicity testing was carried out by InterVivo Solutions. To investigate a maximum tolerated dose, mice were administered doses of 300 mg/kg to 1 g/kg, fifty times the effective dose, by intraperitoneal injections and monitored over three days. No deaths or behavioural differences were observed between any of

the treated mice and the controls, and the administration of the drug caused no lasting change to the body temperature of the animals.

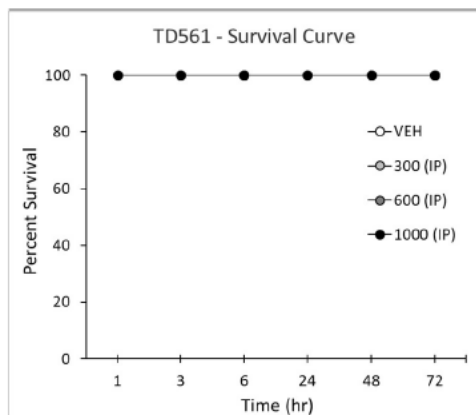


**Figure 1.2.3.1.6.** Survival rates of mice treated with various concentrations of TD561 **13**.

The acceptance by the US patent examiner that the sodium salt **18** represented a novel patentable structure resulting in a strong intellectual property position for the company was also important in identifying **18** as the prime clinical trial candidate. It should be appreciated that the sodium salt **18** and the free acid **15** are identical when taken orally since both exist in the acid form in the stomach.

Health Canada as well as the US FDA enforce strict limits on elemental impurities in drug regulations. The daily intake of heavy metals has to be limited as they are known to be health hazards at high levels. Both regulatory agencies follow the ICH elemental impurities guidelines, which states a maximum permitted daily exposure for palladium via oral administration of 100 ug.<sup>63</sup> Since the synthesis of **15** includes a palladium-catalyzed coupling reaction, it was necessary to show that our process and finished product follow these regulations and ensure that administration of **15** would not pose a health risk to patients.

A sample of **15** was sent to Huffman Hazen Laboratories in Golden, Colorado for analysis. They reported an average of 1.23 ug of palladium per gram of

sample. Extrapolating a high dose of double the 20 mg/kg concentration from the bioassays to a 80 kg patient would result in a large 3.2 g dose. Even at this quantity, the resulting daily palladium exposure would be less than 4 ug. Administration of **15** should therefore be perfectly safe even at much higher levels than what would be prescribed, in regards to palladium toxicity.

### 1.2.3.2 Optimization of the synthesis

The goal that OB Pharma now presented to us was to develop a synthesis of **15** that could be used to prepare the tens of grams and eventually hundreds of grams of **15**, or **18** that would be required for preclinical toxicity studies. If a sufficiently efficient process could be developed, it might also serve as the basis for the preparation of the multi-kilogram quantities that would be needed for clinical trials and, assuming successful clinical trials, for the preparation of commercial quantities.

The acid **15** and its sodium salt **18** had been prepared by Fluet-Chouinard by hydrolysis of the ester **13** and then salt formation from **15** using sodium hexamethyldisilazide (NaHMDS). As explained in the introduction, the synthesis of **13** even via the two-step process required a combination of recrystallization and multiple chromatographies in order to obtain a good quality product. It would be expensive and time consuming to prepare hundred gram quantities via this sequence.

During an effort to look for less expensive commercial sources of 4-carboxymethylphenyl-boronic acid, the reagent used to prepare the ester **13**, we became aware the 4-caboxyphenylboronic acid, **19**, was not only available from many sources but that it also was considerably less expensive than its methyl ester. Additionally, it was clear from the literature that 4-caboxyphenylboronic acid could be used in Suzuki coupling reactions.<sup>64,65</sup>

In an initial attempt following literature precedent 10 mmol of boronic acid **19**, 11 mmol of enol tosylate **12**, 3 mol% of tetrakis(triphenylphosphine)palladium(0) and 3 equivalents of potassium carbonate dissolved/suspended in 15 mL of water and 30 mL of ethanol were refluxed for 5 h. The reaction mixture was cooled and much of the ethanol was evaporated via a rotary evaporator. The remaining material was diluted with 30 mL of water and extracted 2 times with 15 mL of dichloromethane. The dark organic extracts were discarded. The aqueous layer was carefully acidified with concentrated HCl until red to litmus paper. The white precipitate which formed when the solution became acidic was filtered off and allowed to dry. The  $^1\text{H}$  NMR of this product, obtained in 92 % yield, was identical to that reported in the Fluet-Chouinard thesis. This reaction was subsequently repeated on five times the above scale with similar results.

This was a much superior route to **15** than that described by Fluet-Chouinard. Particularly noteworthy was the ease of isolation which required only precipitation from the aqueous extraction fraction. All organic byproducts, including any remaining starting material or decomposition products as well as any remaining or partly decomposed catalyst, were found in the organic extract. The replacement of 1,4-dioxane by ethanol in the solvent system of the reaction proved to have no negative effect on the yield of the reaction. This change was done as ethanol is safer for longer term storage, significantly less expensive and easier to obtain in bulk, and has a smaller impact on the environment as it is mostly produced via fermentation of grains.

The price of each of the components required for the synthesis of **15** is given below. Aside from the catalyst, the reagents are available from many suppliers in essentially bulk quantities. Considering the most expensive component in the synthesis is the palladium catalyst, one obvious way to reduce cost would be to reduce the amount of catalyst necessary to obtain at least an 85 % yield of crude **18** after filtration of the acidified aqueous phase. While the boronic acid is also relatively costly compared to the rest of the reagents used, it is the limiting reagent for the synthesis against which the yield

was optimized, therefore amounts used could not be reduced without a proportional reduction of the product obtained. Optimization thus focused primarily on lowering catalyst loading and investigating the relationship between reaction time, catalyst loading and yield.

**Table 1.2.3.2.1.** Cost per mole for the various reagents used in the synthesis of **15**. *Prices assume purchases of 1kg of material at once, except in the case of the palladium catalyst, where price is given for a 25 g purchase. Prices are given for highest available reagent purity and rounded up. The prices were taken from AK Scientific<sup>66</sup>, where the materials were purchased.*

Reagent	Price per weight <sup>66</sup>	Price per mole (\$)
Dimedone <b>8</b>	250 \$/kg	35
p-Toluenesulfonyl chloride	66 \$/kg	13
4-carboxyphenyl boronic acid <b>19</b>	962 \$/kg	160
Pd[PPh <sub>3</sub> ] <sub>4</sub>	427 \$/25 g	19 737 \$

Reaction conditions were investigated by performing the Suzuki coupling on 9.3 mmol of starting boronic acid **19**. The synthesis of **15** was performed in duplicates for sixteen different reaction conditions, only changing one variable from one set of duplicates to the next. The variables changed included catalyst loading, equivalents of dimedone tosylate and base as well as the base used, reaction time and workup procedure.

**Table 1.2.3.2.2.** Initial reaction conditions for the Suzuki coupling at the start of the optimization process. The reaction was carried out with 1.53 grams of boronic acid **19**. The workup was done as described above. 1.98 grams of crude product (88%) were obtained, which lowered to 1.78 grams (79%) after drying at 40°C overnight.

Reagent	Equivalents	Time	Yield (%)
Boronic acid <b>19</b>	1.00		
Dimedone Tosylate <b>12</b>	1.08	3 hours	79
Sodium Carbonate	3.22		
Pd(PPh <sub>3</sub> ) <sub>4</sub>	2.8 mol%		

The approach for the first sets of reactions was to simply lower the catalyst loading with no other changes to the reagents or procedure, to find out the minimum amount that would produce satisfactory yields. The goal was to lower catalyst loading until reaction yields reached roughly 50%, at which point reaction time would be increased to increase the yield back towards starting values. The amount of palladium was lowered by half for each successful set of duplicate reactions.

**Table 1.2.3.2.3.** Reaction conditions for the first 6 sets of Suzuki couplings with diminishing catalyst loading percentages. *Equivalents for the reagents are based on 1.00 equivalents of boronic acid 19. All reactions used 3.10 to 3.20 equivalents of sodium carbonate as base, and a 3 hours reflux duration. The melting point for the first reaction of a set of duplicates is shown in the table.*

Reaction #	Dimedone Tosylate (eq)	Palladium Catalyst (% mol)	Melting Point (°C)	Average Yield (%)
OP-01*	1.08	2.80	181.7 - 182.9	79
OP-02*	1.07	1.96	183.1 - 183.4	80
OP-03*	1.08	1.00	182.9 - 184.7*	89*
OP-04*	1.08	0.46	182.0 - 183.2	81
OP-05	1.07	0.21	184.3 - 184.9	76
OP-06	1.08	0.11	not melting	84

\*reactions 01, 02 and 04 were not performed as duplicates. Results from the first reaction of OP-03 are shown only as some product was spilled for the second reaction. Estimated yield of OP-03D was around 80%.

The results from the last three sets offered unintended interesting insights on the workup procedure used to obtain the product. As the catalyst loading was being lowered from one set of experiments to the next, the yield did not seem to follow the trend, and stayed relatively consistent. However, it was noticed that for reactions using less than 0.5% catalyst, a high melting point impurity started appearing that was not previously observed. The impurity was undetectable in both <sup>1</sup>H- and <sup>13</sup>C NMR indicating it was likely a salt. Some amount of time was spent investigating this unknown component of the product, as it was thought to be unlikely to be leftover starting materials. While the vacuum filtration was effective at isolating the product **15**, this acid was retaining a lot of water, trapped within the solid. This was not an issue as the product was always dried overnight at 40°C, however it was eventually determined that the evaporation of the small amount of excess water would leave behind NaCl formed during the precipitation of **15** with HCl. This was more significant at lower yields and, ironically, when the filtration was performed more skillfully and needing less rinses to transfer all the solid to the filter. Two different workup procedures were developed to solve this issue. The first method

was to simply wash the solid on the filter with a large amount of distilled water, while mixing the solid into suspension after each addition of water. However, it was uncertain how much water would be needed to ensure no salt remained as low amounts of salt would be difficult to detect with the methods used, as seen in the set **OP-05** in the table above. The second method was to dissolve the acid **15** obtained from the filtration in an organic solvent and wash once with water. This ensured no salt would be left in the product, using a minimal amount of water. Unfortunately the solubility of the acid **15** in organic solvents was quite poor, requiring around 50 mL of ethyl acetate to fully dissolve 2 grams of product. In the end, the first method was selected going forward as it was more economical and less wasteful despite the higher total volume of liquids used. The reaction conditions for 1.0%, 0.5% and 0.25% catalyst loading were repeated with the addition of the ethyl acetate wash after the filtration to confirm the previously obtained results. The melting points from the products obtained from then on were generally lower by 1-2°C than those previously obtained, indicating the melting point of pure acid **15** should be closer to 182°C. The repeats of these three sets of reaction conditions confirmed that the yields obtained with the previous methods were inflated due to the presence of salt. The actual yields were quite similar at higher catalyst loadings, but significantly lower at low catalyst percentages. The largest difference in yield from washing out the salt was observed for reactions at 0.22 mol% of palladium catalyst, dropping from averages of 77% to 57%.

**Table 1.2.3.2.4.** Reaction conditions for the sets 7 to 9 of Suzuki couplings with diminishing catalyst loading percentages and modified workup procedure, compared to a previous result. *Equivalents for the reagents are based on 1.00 equivalents of boronic acid 19. All reactions used 3.00 to 3.20 equivalents of sodium carbonate as base, and a 3 hours reflux duration. The melting point for the first reaction of a set of duplicates is shown in the table.*

Reaction #	Palladium Catalyst (% mol)	Post-filtration wash performed	Melting Point (°C)	Average Yield (%)
OP-03	1.00	No	182.9 - 184.7	89
OP-07	0.98	Yes	181.3 – 183.4	78
OP-08	0.51	Yes	180.1 – 183.0	62
OP-09	0.22	Yes	175.9 – 179.1	57

The results from the progressively diminishing catalyst loading of reaction conditions 7 to 9 were much closer to what was originally expected. A catalyst loading of 0.5 mol% was decided as the new value to work from while modifying other condition variables. From this point, the low hanging fruit to easily improve yield was to increase the reflux duration of the reaction mixture. Reactions with 0.5 mol% of the palladium catalyst were performed with 5, 6 and 8 hour durations. Based on the results, an 8 hour reaction time was unnecessary as the yield obtained was within regular variance of results when compared to 6. Additionally, the reaction was mostly complete by 5 hours.

**Table 1.2.3.2.5.** Summary of the sets of Suzuki reaction conditions with varying reaction time. *Equivalents for the reagents are based on 1.00 equivalents of boronic acid 19. All reactions used 3.00 to 3.20 equivalents of sodium carbonate as base, and a 3 hours reflux duration. The melting point for the first reaction of a set of duplicates is shown in the table.*

Reaction #	Palladium Catalyst (% mol)	Reaction Time (h)	Melting Point (°C)	Average Yield (%)
OP-10*	0.55	6	179.6 – 181.1	78
OP-12	0.54	5	181.3	69
OP-13*	0.55	8	180.1 – 183.0	74

\*4 reactions were performed for OP-10. Two outlier data sets were excluded. One had an unusually low melting point and was obtained with a 67% yield. The second excluded reaction was not washed properly and resulted in a 103% yield. Only one reaction was performed for OP-013.

As the additional two hours of an eight hour reaction did not improve the yield, 6 hours was chosen as ideal reaction time. This duration allowed maximization of the yield at 0.5 mol% of catalyst, while being short enough to complete the set up, reaction time, workup and analysis within a regular work day. This duration was also long enough to prepare dimedone enol tosylate **12** starting material or convert previous obtained product **15** to the salt **19** in the meantime. However, what constitutes a desirable reaction time can vary on the needs and deadlines of those carrying out the reaction. It was deemed valuable to perform additional reactions at different catalyst loadings while aiming for consistent yields, to verify the relationship between the two variables.

**Table 1.2.3.2.6.** Overview of the effect of reaction time and catalyst loading on yield. *Values entered are a rough average of the results from all applicable reactions to indicate a general trend only.*

Catalyst loading (%)	Reaction Time (h)	Average Yield (%)	Turnover Number
1.00	3	78	78
0.75	6	76	101
0.50	6	80	160

As expected, the amount of catalyst required is inversely proportional to the reaction time. At the concentrations tested, a twofold increase in catalyst loading resulted in a roughly twofold increase in reaction rate, cutting time by half. Further testing would be required at different concentrations to get a more accurate representation on how this relationship translates to other reaction conditions and whether it would be applicable to long duration reactions with extremely low catalyst use. This would be interesting information as the product yield per amount of palladium catalyst used drastically increases as this amount lowers. Regardless, the values above represent the best compromise between catalyst efficiency and time efficiency.

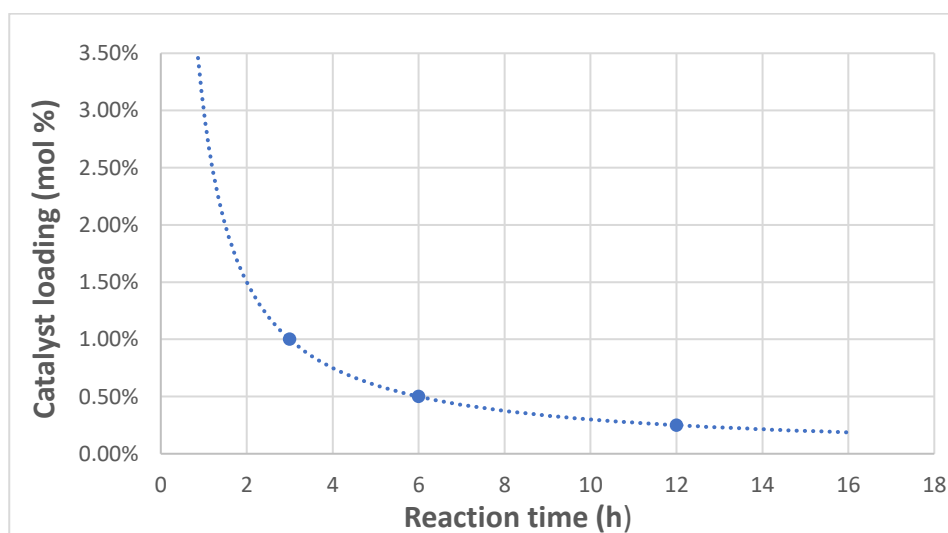


**Figure 1.2.3.2.1.** Visualization of the inverse proportional correlation between catalyst loading and reaction time based on table 1.2.3.2.6.

Some additional testing was done to investigate variations on the base used and the amounts. During all of the previous experiments mentioned, the 3 equivalents of sodium carbonate were saturating the solution and not fully dissolving even at high temperatures. Suzuki cross-couplings typically require at least two equivalents of base, but 3 equivalents were used due to the presence of the boronic acid **19**'s carboxylic acid functional group which would be deprotonated first and use up one equivalent of base. However since there was always noticeable amounts of undissolved sodium carbonate, several reactions were performed with reduced equivalents of base.

**Table 1.2.3.2.7.** Results from the reaction conditions investigating the importance of the base in the Suzuki cross-coupling. *Equivalents for the reagents are based on 1.00 equivalents of boronic acid 19. All reactions used 0.5 mol% of tetrakis(triphenylphosphine)palladium, and a 6 hours reflux duration. The melting point for the first reaction of a set of duplicates is shown in the table.*

Reaction #	Base used	Amount of base (eq)	Melting Point (°C)	Average Yield (%)
OP-10*	Na <sub>2</sub> CO <sub>3</sub>	3.20	179.6 – 181.1	78
OP-11	NaOH	3.55	178.9 – 182.4	36
OP-16	Na <sub>2</sub> CO <sub>3</sub>	2.10	180.1 – 183.0	80

\*4 reactions were performed for OP-10. Two outlier data sets were excluded. One had an unusually low melting point was obtained with a 67% yield. The second excluded reaction was not washed properly and resulted in a 103% yield.

The result showed clearly that any sodium carbonate above 2 eq. is wasted, and that NaOH led to a dramatically worse performance even when using almost twice as much. It is possible this is due to sodium carbonate being a diprotic base, even if it is weaker. While the pKa of bicarbonate is too high for there to be much carbonic acid formed, the temperatures used for the reaction would force the carbonic acid to dissociate into water and carbon dioxide which would then evaporate. This could allow bicarbonate to deprotonate more molecules than it would otherwise be able to.

While no issues were observed with the conditions described above, Suzuki cross-coupling reactions are often performed under inert atmosphere. A single reaction was therefore performed under Argon to explore a potential increase in yield. In this test reaction, the palladium was added last, after the reaction mixture had been purged with argon and after the solution was brought to a boil. The reaction was only performed once resulting in a 91% yield, which is on par with the top end of the results from the OP-16 conditions. While this is a good result, the yield is not high enough to determine that the controlled atmosphere had a beneficial effect. A higher number of repeats would be necessary to determine whether or not performing the reaction under Argon or Nitrogen would be worth the additional effort.

**Table 1.2.3.2.8.** Comparison of the results from reactions under inert atmosphere or in air. *Only one reaction was performed under argon, however the scale was double that of the OP-16 reaction.*

Reaction #	Catalyst loading (%)	Reaction Time (h)	Atmosphere	Yield (%)
OP-16	0.55	6	Air	80
OP-18	0.55	6	Argon	91

Finally, the one-pot reaction was attempted again, under the new conditions. A clean product was obtained, but the yield was poor compared to the 2-step synthesis. Tracking by TLC showed significant presence of dimedone after 2h of reflux, indicating the poor overall yield is likely due to low conversion of dimedone into the enol tosylate form. This is likely due to the fact that running a one-pot reaction requires the same solvents for both steps, and that the ethanol:water mixture that was effective for the Suzuki coupling was not appropriate for the first step.

### 1.2.3.3 Conclusion

In conclusion, several key conditions for the synthesis were determined thanks to the efforts mentioned in the previous section. The 1,4-dioxane cosolvent was replaced by the more environmentally friendly ethanol, and the synthesis moved away from a one-pot reaction to reduce possibility of byproduct formation. It was also shown that sodium carbonate is an effective base at 2.0 equivalents, but that any excess is unnecessary and wasted. The necessity of an inert atmosphere was tested, with inconclusive data, showing no significant differences between a reaction performed under argon and a control experiment. The catalyst loading was decreased six-fold compared to the original literature value, while retaining similar yields as long as reaction duration was increased to 6 hours, leading to significant cost savings. The catalyst efficiency drastically increased at low percentages used, however the most optimal overall conditions would be in the ranges mentioned above. There are examples in the literature of industrial-scale reactions on very similar conditions as the ones described above, proving that this process would be viable and successful when scaled up, without any further necessary modifications.<sup>67</sup>

As mentioned, isolation of the acid **15** is extremely easy when compared to the methyl ester. Below is a <sup>1</sup>H NMR from the product directly after the filtration under vacuum, without any additional purification steps.

**<sup>1</sup>H NMR (400 MHz, CDCl<sub>3</sub>) δ, ppm:** 8.13 (d, J = 7.6 Hz, 2H), 7.60 (d, J = 8.3 Hz, 2H), 6.46 (s, 1H), 2.65 (s, 2H), 2.36 (s, 2H), 1.13 (s, 6H)

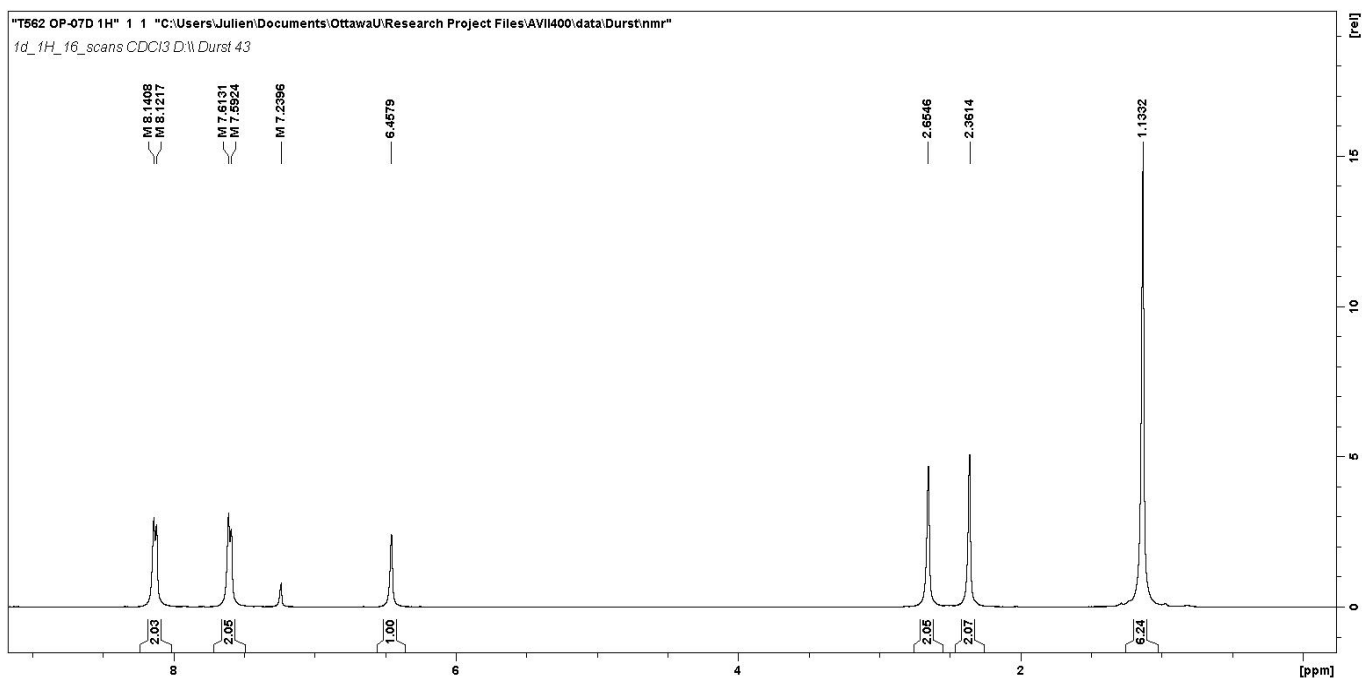


**Figure 1.2.3.3.1.** <sup>1</sup>H NMR of the acid **15**. The spectrum was obtained from a roughly 10 mg sample dissolved in CDCl<sub>3</sub>, with a Bruker Avance 400Hz spectrometer.

The synthesis of **15** described is extremely easy to carry out, and would allow for easy and inexpensive bulk synthesis of the compound. There are a few potential other areas of improvement that could improve the synthesis further given the time to investigate them. First would be the use of more specialized catalysts. A plethora of palladium ligands have been developed for specific uses and substrates, and modifications to the phosphine ligands could improve the catalytic activity. Second would be further testing of stronger bases. While NaOH was used unsuccessfully, a variety of other bases could also be used that might improve reaction rate. In an industrial setting, the workup procedure could also be improved to minimize losses of product during purification and lower the quantities of solvents used. Finally, At the end of the reaction, a yellow shiny solid could be filtered out of the solution after evaporation of the ethanol. Although the solid was not characterized, the behaviour and appearance are consistent with that of the tetrakis(triphenylphosphine)palladium(0) used. This suggests the possibility of a very simple method for recovering the catalyst to recycle it for subsequent

reactions. A confirmation of the identity and quality of this potential recovered catalyst by  $^{31}\text{P}$  NMR or X-ray crystallography would be important to obtain.

The final yields from the optimized reaction conditions were ranging between 80% and 90%, and were highest on larger reaction scales. A larger scale test was performed on 21 grams of dimedone tosylate **12** by undergraduate student Hannah Mayer, yielding 97% of crude product and 90% after purification, on her first attempt. When performed at industrial scales with specialized equipment, yields of 90% should be obtained reliably. A sample protocol for the synthesis of 100 grams of product is described below.

### **Large Scale TD 562 (15) Suzuki Coupling Procedure**

p-Carboxyphenylboronic acid (80 g, 480 mmol, 1.0 eq.), dimedone tosylate (160 g, 540 mmol, 1.1 eq.), sodium carbonate (105 g, 990 mmol, 2.1 eq) and tetrakis(triphenylphosphine)palladium(0) (4 g, 3 mmol, 0.7 mol%) were weighed and placed in a 3 L round bottom flask. A mixture of 1.3 L of ethanol 95% and 0.7 L H<sub>2</sub>O was prepared, and poured in the flask on top of the solids. The solids were mostly dissolved within a few minutes, except for some sodium carbonate deposits at the bottom.

The solution was heated to reflux in a ~100°C oil bath while mixing with a magnetic stirrer, and left to react for 6 hours. After the time has elapsed, the magnetic stirrer was removed and the solution was filtered out into a different flask to remove leftover solids. The flask was then placed on the rotary evaporator to remove a majority of the ethanol. An additional 1 L of water was added to the flask, and the solution was subsequently washed 3x with 500 mL of dichloromethane.

The resulting aqueous phase was transferred into an Erlenmeyer flask and acidified by adding concentrated HCl (12 M) until the desired product precipitated out as a white solid. The flask was placed in a -20°C freezer to allow further precipitation.

The solid was filtered by suction and washed by passing 3x 500 mL of distilled water through the funnel. The solid obtained was placed in a wide container at 40°C for a few hours, until the melting point of the solid is within the 181-183°C range, to evaporate residual water trapped in the solid.

**Table 1.2.3.3.1.** Sample table of reagents for a large scale synthesis of compound **15**.

Reagents	MW (g/mol)	Quantity	mmol	Equivalents
p-Carboxyphenylboronic acid	165.94	80 g	480	1.0
Dimedone enol tosylate	294.37	160 g	540	1.1
Sodium Carbonate	105.99	105 g	990	2.1
Pd(PPh <sub>3</sub> ) <sub>4</sub>	1155.56	3 g	2.6	0.5 mol%
Ethanol 95%	46.07	1.3 L	-	Solvent
Distilled water	18.01	0.7 L	-	Solvent

#### 1.2.4 Stability studies of TD562 and TD567

As part of the Fluet-Chouinard thesis, stability studies were performed on the methyl ester **13**. As the focus of the project shifted to the acid **15** and salt **18**, stability testing experiments had to be performed on both forms of the compound. The data on degradation of the chemicals over time at ambient conditions is an important factor in the marketability and availability of a drug product, as this ties directly to the shelf life and expiry date. In a perfect scenario, drug compounds should have the capability of being stored at room conditions without degradation for at least five years, although many products expire after a year or two which is still perfectly acceptable.

To obtain this information in a timely manner in a laboratory setting, simply storing the samples at room conditions for the desired time period is not a viable option. Fortunately, as with the stability testing procedures for pharmaceutical products, accelerated studies can be performed by increasing the storage temperature and room humidity, as per the protocols from the World Health Organization.<sup>68</sup> Five separate studies were performed as part of this project, and are described below. The testing time points were selected based on the estimate that an increase of 10°C would double the rate of decomposition. With the stability studies being performed at 70°C, the decomposition rate would increase by a factor of 22.6x. It was decided that the samples would be tested every 7 days, which would roughly correspond to 6 months at room temperature. Some of the samples were dissolved and stored in water, to simulate a worst-case scenario of long-term storage in high humidity conditions.

In the first two studies, a sample of the acid **15** was stored at 70°C under room humidity conditions and controlled light exposure. The first sample was placed in a round bottom flask which was capped with cotton, covered in aluminum foil and stored in an oil bath. The second sample was simply placed in a small beaker, stored in an oven.

The third study observed the salt **18**, stored in D<sub>2</sub>O for ease of monitoring by <sup>1</sup>H NMR. Unfortunately, a significant amount of proton exchange with the solvent was observed, making most proton peaks disappear. The fourth and fifth stability studies were therefore performed with **18** dissolved in water and heated in an oil bath, and dry **18** placed in a beaker in the oven.

Aside from the third study which was cancelled due to the NMR spectrum in D<sub>2</sub>O being unreadable, none of the samples showed any sign of degradation under any conditions at all time points tested. For up to a calculated two years, or one month under accelerated conditions, no new visible peaks or changes to the existing peaks of the compounds were observed by NMR. Compounds **15** and **18** demonstrated excellent

thermal stability under normal and high humidity conditions, which should translate directly to a long shelf-life of the potential finished drug product. Of course, as per regulations requirements, stability studies for marketed drug products have to be performed in the final packaging for accuracy of results. While this means more studies will need to be performed in the future, obtaining this data in early on provides reassurance against the possibility of it becoming a problem later in the development of the compound. The results of the fifth study with compound **18** in water are shown below.

**Table 1.2.4.1.** Calculations for the estimated acceleration factor of the stability study. *The temperature was measured 4 times over the duration of the study at 0, 7, 14 and 28 days. The temperatures measured varied between 73.5°C and 77.0°C. Acceleration factor is calculated between the calculated 75.4°C average temperature and room conditions of 25°C, and assumes a doubling of reaction rates for each 10°C increments*

<b>Average temperature</b>	75.4°C
<b>ΔT</b>	50.4
<b>Acceleration factor</b>	2 <sup>5.04</sup> or 32.9
<b>Equivalent room conditions duration after 28 days</b>	921 days or 2.5 years

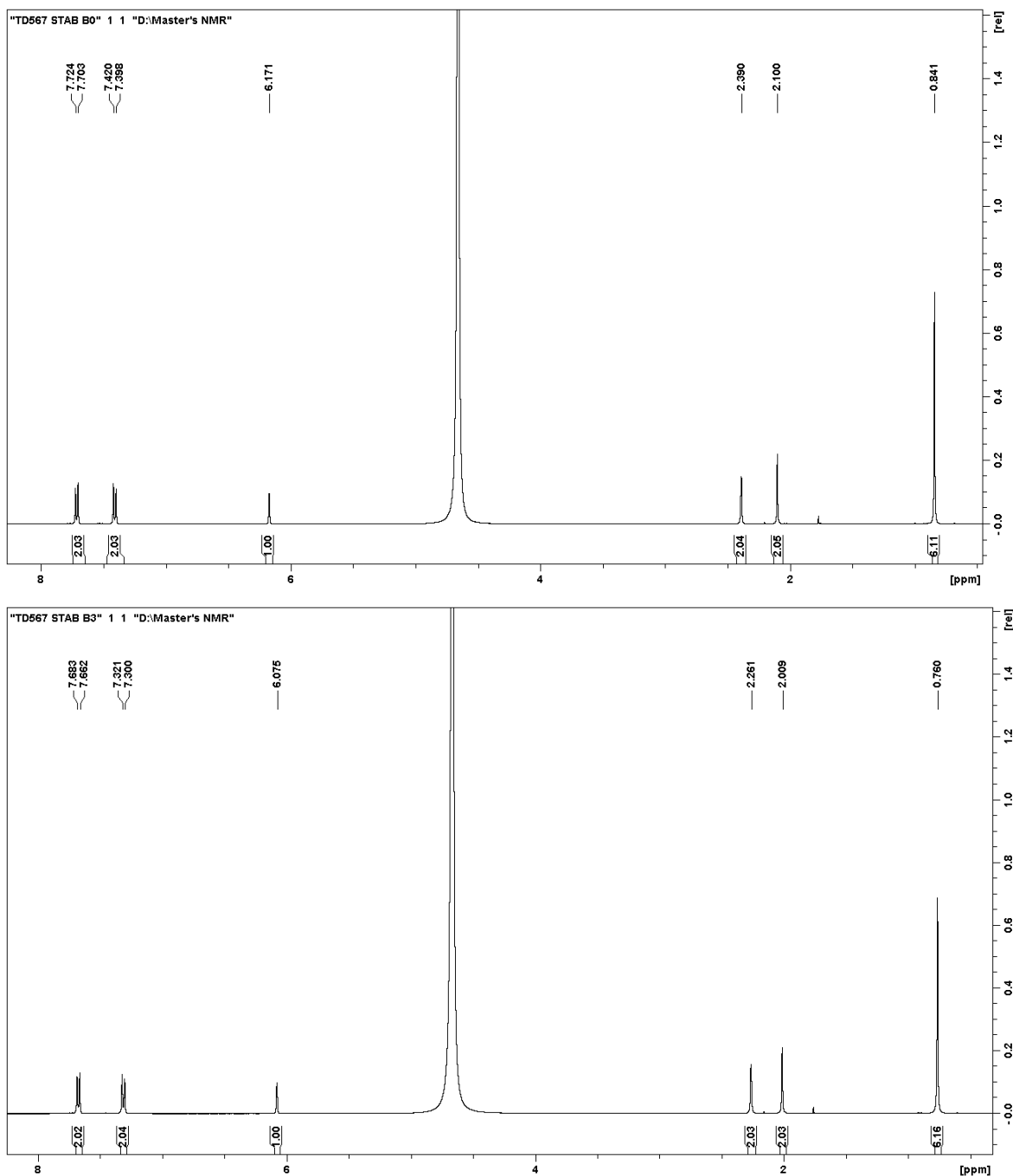


**Figure 1.2.4.1.** Comparison of the <sup>1</sup>H NMR spectrum of compound **18** before and after the stability study. Both samples were prepared by evaporating a 1.0 mL aliquot of the stability sample, then re-dissolving the solid obtained in D<sub>2</sub>O with a few small grains of sodium carbonate. The first spectrum (B0) represents the initial sample. The second spectrum (B3) was taken 28 days later and corresponds to a room-conditions storage time of more than two years. The sample was stored dissolved in water in an uncovered round bottom flask closed with a glass stopper. The temperature was measured before each aliquot was taken for NMR analysis at 0, 7, 14 and 28 days, and stayed between 73.5°C and 77.0°C.

## 1.2.5 Structure-activity relationship studies

### 1.2.5.1 Objective

Once the decision to move forward with the acid **15** and its sodium salt **18** as clinical trial candidates had been made and the synthesis of **15** had been optimized, we had an opportunity to generate new analogs of **15**. Of course, it would be easy to convert any new acid into its corresponding sodium salt.

### 1.2.5.2 Preparation of halogenated aryl ring analogs

The initial focus was on introducing substituents into the meta (C3) position of the aromatic ring. The first targets were the halogenated analogs **20-22**. The introduction of either a Chlorine or Fluorine substituent into the aromatic ring was anticipated to have two positive effects, the most important being that these compounds would be significantly less polar than **15** and thus potentially facilitate their uptake into the brain. While the acid **15** is able to penetrate the blood-brain barrier as is, its partition coefficient between the brain and plasma is only  $K_p = 0.022$ . There is therefore much room to improve its membrane permeability and bioavailability. The increase in lipophilicity is indicated by the estimated logP values which are given below alongside the structures and compared to **15** itself. The estimated logP values are calculated by ChemDraw. The other anticipated effect of these halogen substituents is a diminution of the compound's susceptibility to aromatic hydroxylation catalyzed by liver CYP450 enzymes. However, since **15** itself had been shown to be essentially inert to aromatic hydroxylation, this was not a significant consideration.

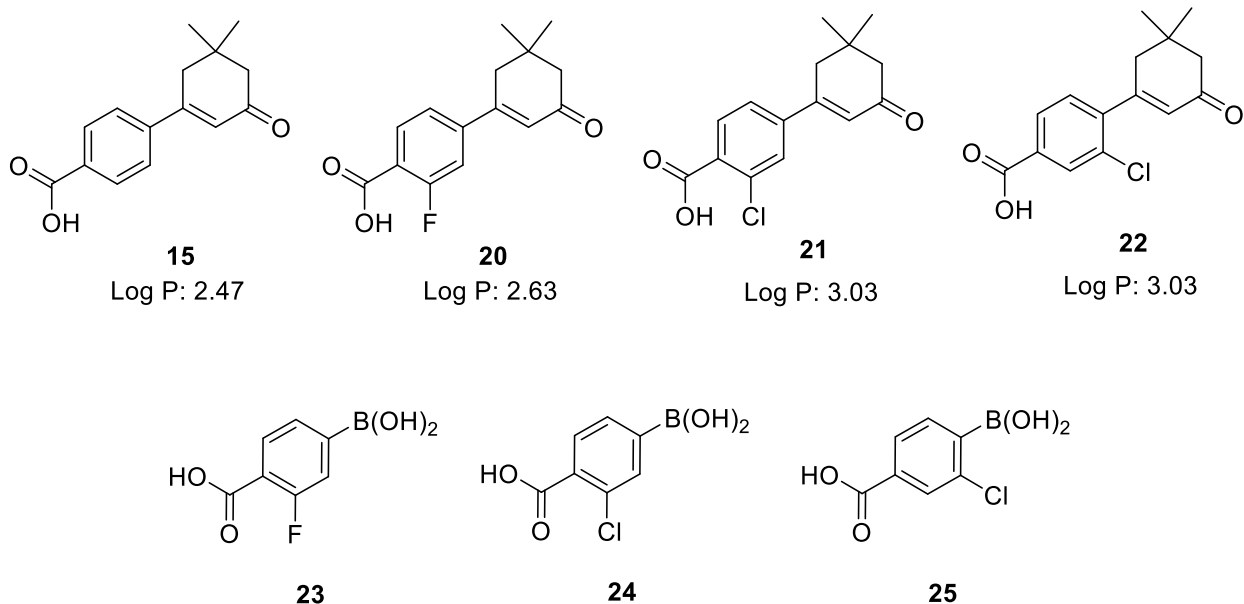


**Figure 1.2.5.2.1.** Structures and chemical properties of halogenated analogs **20-21**, compared to **15**. LogP values are calculated by ChemDraw.

The synthesis of these three derivatives was performed following the optimized procedure for **15** utilizing the commercially available boronic acids **23-25**, respectively. The structures of the new compounds were readily confirmed by their  $^1\text{H}$  and  $^{13}\text{C}$  NMR data. For example, the doublets ( $\delta$  8.13, 7.60) seen in aromatic region of the spectrum of **15** were replaced by the expected three multiplets for **21** and **22** (NMR peaks in the aromatic region only are shown below). For **20**, the additional coupling of all three aromatic hydrogens to the fluorine was also observed.

**20**  $^1\text{H}$  NMR (400 MHz,  $\text{CDCl}_3$ )  $\delta$ , ppm: 8.05 (t,  $J = 8.0$  Hz, 1H), 7.380 (dd,  $J = 8.4$  Hz,  $J_2 = 1.6$  Hz, 1H), 7.29 (dd,  $J_1 = 11.6$  Hz,  $J_2 = 1.6$  Hz, 1H), 6.45 (s, 1H),

**21**  $^1\text{H}$  NMR (400 MHz,  $\text{CDCl}_3$ )  $\delta$ , ppm: 8.02 (d,  $J = 8.0$  Hz, 1H), 7.59 (d,  $J = 1.6$  Hz, 1H), 7.46 (dd,  $J_1 = 8.0$  Hz,  $J_2 = 1.6$  Hz, 1H), 6.44 (s, 1H),

**22**  $^1\text{H}$  NMR (400 MHz,  $\text{CDCl}_3$ )  $\delta$ , ppm: 8.14 (s, 1H), 8.00 (d,  $J = 7.6$  Hz, 1H), 7.27 (d,  $J = 8.0$  Hz, 1H), 6.07 (s, 1H).

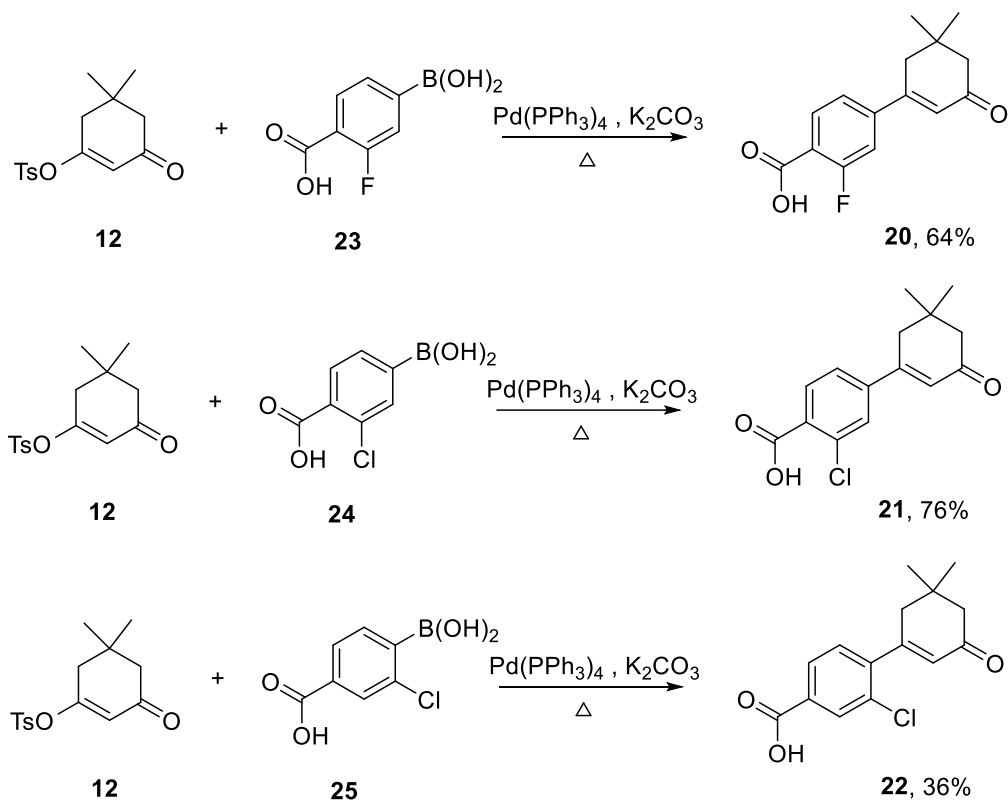


Figure 1.2.5.2.2. Overview of the preparation of analogs **20-22**.

### 1.2.5.3 Modifications to the aryl-carboxylic acid substituent

Following analogs **20-22**, the importance of the position of the carbonyl on the aromatic ring was investigated. In the Fluet-Chouinard thesis, it was determined that the presence of an oxygen substituent was important to the activity, as compound **26** had much lower activity than the acid **15** and most other analogs made. However, ether analogs such as **27** had good activity despite lacking a double-bonded oxygen.<sup>53</sup>

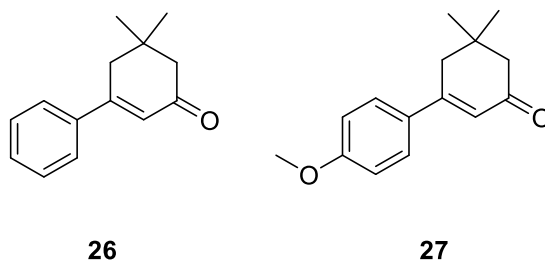


Figure 1.2.5.3.1. Structures of analogs **26** and **27**.

Three analogs were prepared to probe the importance of the position of the carboxylic acid function. The first compound, **28**, tested the effect of moving the carboxylic acid meta to the connection at C3 in the cyclohexenone compared to para in **15**. In the second, compound **29**, a CH<sub>2</sub> group is inserted between the benzene ring and the carboxylic acid. In the third, compound **30**, a vinyl spacer is inserted instead. Bioassay results for these three compounds would be compared to **15** thereby indicating whether the distance between the oxygen of the cyclohexenone and the carboxylic acid was an important structural parameter.

The synthesis of compounds **28-30** again utilized a Suzuki coupling reaction between enol tosylate of dimedone, **8**, and commercially available boronic acids **31-33** respectively. As usual the structures were confirmed by NMR spectroscopy.

**28** <sup>1</sup>H NMR (400 MHz, CDCl<sub>3</sub>) δ, ppm: 8.25 (s, 1H), 8.14 (d, J = 7.6 Hz, 1H), 7.56 (d, J = 8.0 Hz, 1H), 7.52 (t, J = 8.0 Hz, 1H), 6.47 (s, 1H), 2.68 (s, 2H), 2.36 (s, 2H), 1.14 (s, 6H).

**29** <sup>1</sup>H NMR (400 MHz, CDCl<sub>3</sub>) δ, ppm: 7.49 (d, J = 8.4 Hz, 2H), 7.32 (d, J = 8.0 Hz, 2H), 6.40 (t, J = 1.2 Hz, 1H), 3.67 (s, 2H), 2.61 (d, J = 1.2 Hz, 2H), 2.33 (s, 2H), 1.10 (s, 6H).

**30** <sup>1</sup>H NMR (400 MHz, CDCl<sub>3</sub>) δ, ppm: 7.67 (d, J = 16.0 Hz, 1H), 7.54 (s, 4H), 6.47 (d, J = 16.0 Hz, 1H), 6.42 (s, 1H), 3.80 (s, 3H), 2.62 (s, 2H), 2.33 (s, 2H), 1.12 (s, 6H).

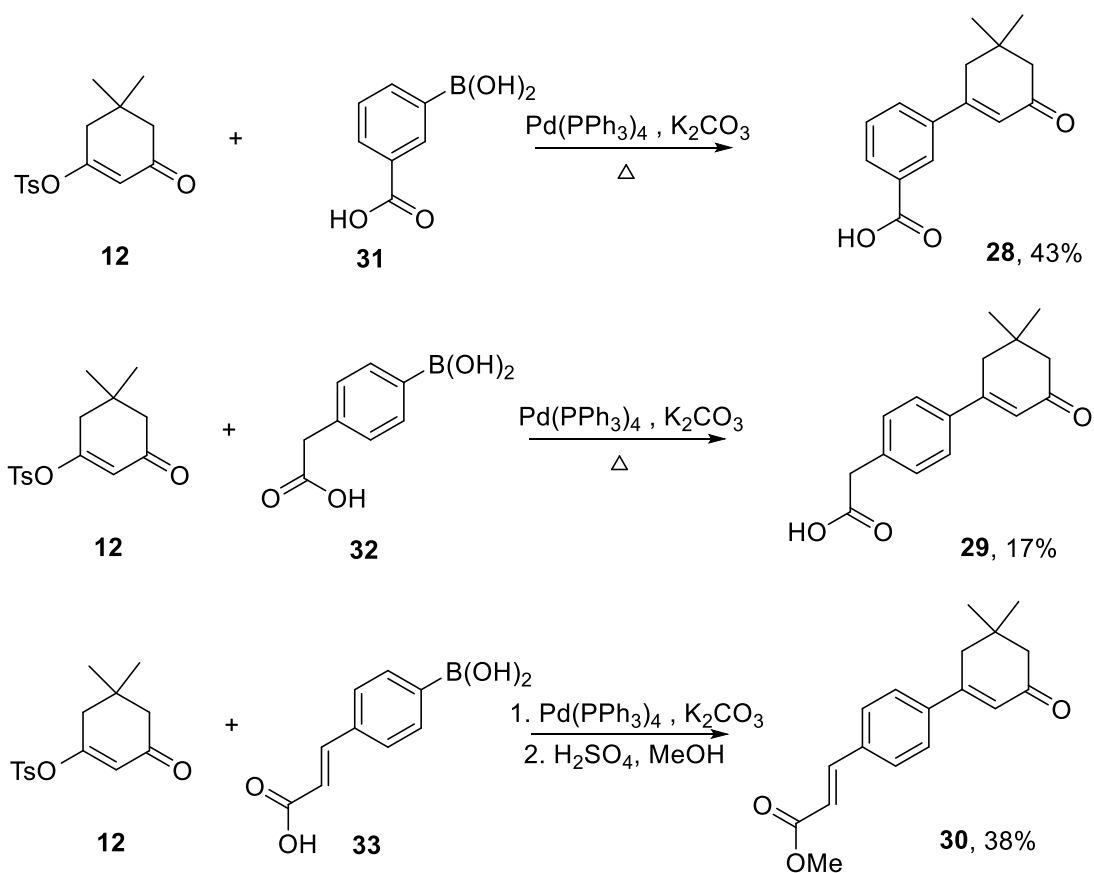


**Figure 1.2.5.3.2.** Overview of the preparation of analogs **28-30** and their chemical structures. *The methyl ester **30** was prepared from the corresponding acid for ease of purification, as a significant amount of **12** remained with the initial product. The compound was then sent to be analyzed as an ester.*

#### 1.2.5.4 Preparation of analogs with variations to C5 substituents

Based on the observation that compound **34** which lacked the 5,5-dimethyl groups was considerably less potent than **15** in the kindled rat bioassays, the hypothesis was made that larger hydrophobic substituents at the C5 position would demonstrate potent antiepileptic activity. The preparation of a representative set of compounds which would test this hypothesis became the final goal in this project.

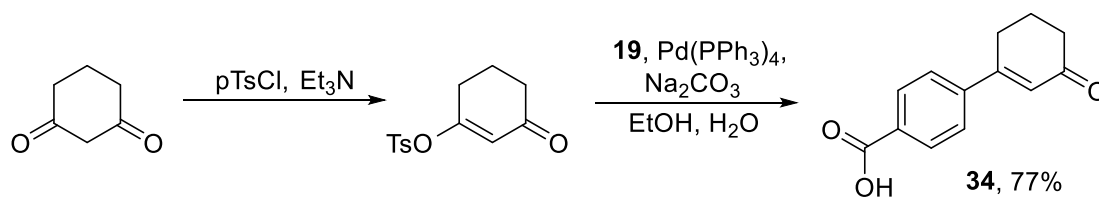


**Figure 1.2.5.4.1.** Overview of the preparation of analog **34**.

As per the synthesis of **15** and the other analogs made, the appropriate starting materials would be 5-substituted 1,3-cyclohexanediones. A few of these were commercially available at a reasonable price, but the selection was limited and some of the diketones would need to be prepared from scratch. 5-phenylcyclohexane-1,3-dione **35** was purchased from Alfa Aesar and converted to the corresponding enol tosylate **36** in a 62% yield. The palladium-catalyzed Suzuki coupling with the boronic acid **19** following the established procedure for **15** afforded the desired 3-(4-carboxyphenyl)-5-phenylcyclohex-2-en-1-one **37** as a white solid in 71% yield. The aliphatic hydrogen portion of the  $^1\text{H}$  NMR spectrum of **37** was much more interesting than that of **15**, due to the presence of the chiral center at C5. Two ABX patterns were visible due to the coupling between the C4 and C6 hydrogens and the chiral C5 hydrogen.

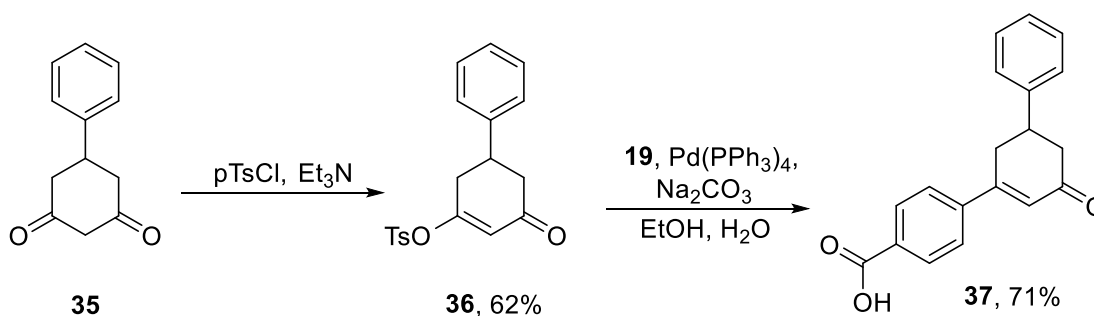


**Figure 1.2.5.4.2.** Overview of the preparation of analog **37**.

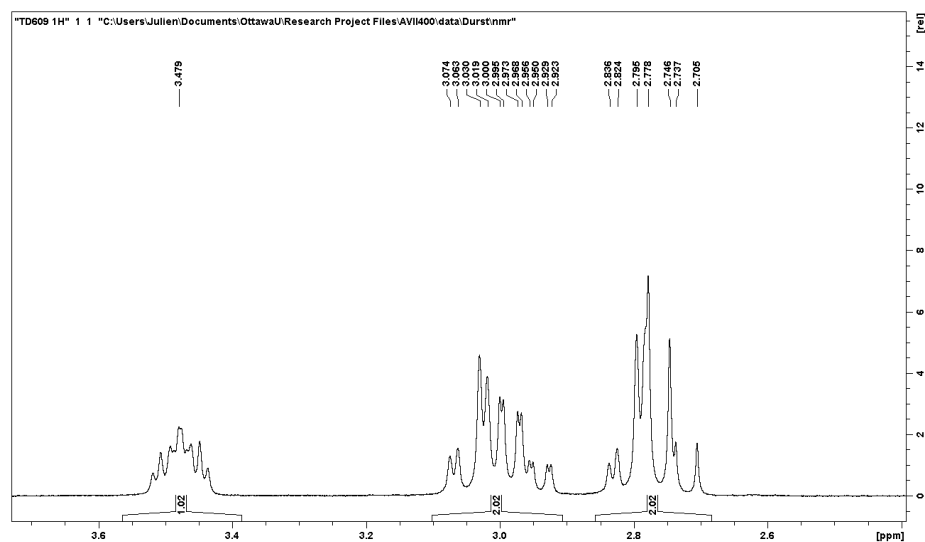


**Figure 1.2.5.4.3.** Aliphatic region (2.0 to 4.0 ppm) of the  $^1\text{H}$  NMR of compound **37**.

Satisfyingly, this compound prevented epilepsy to almost the same extent as **15** or the salt **18**. None of the rats treated with **37** at 20 mg/ kg reached stage 1 seizures, confirming our hypothesis that hydrophobic groups at C5 are necessary for good potency in the fast kindling rat model. Two additional compounds, **42** and **43** were prepared from the corresponding commercially available diketones **38** and **39**. These compounds were prepared jointly with undergraduates Sofi Liu, Yasmin Elsaddik and Catalina Fernandez. Their structures were verified by NMR and HRMS.

**37**  $^1\text{H}$  NMR (400 MHz,  $\text{CDCl}_3$ )  $\delta$ , ppm: 8.13 (d,  $J = 8.8$  Hz, 2H), 7.63 (d,  $J = 8.4$  Hz, 2H), 7.39-7.27 (m, 5H), 6.56 (d,  $J = 2.0$  Hz, 1H), 3.48 (m, 1H), 3.07-2.92 (m,  $J_1 = 17.6$  Hz,  $J_2 = 10.8$  Hz,  $J_3 = 4.4$  Hz,  $J_4 = 2.0$  Hz, 2H), 2.84-2.71 (ddd,  $J_1 = 16.4$  Hz,  $J_2 = 12.8$  Hz,  $J_3 = 4.8$  Hz, 2H).

**42**  $^1\text{H}$  NMR (400 MHz,  $\text{CDCl}_3$ )  $\delta$ , ppm: 8.05 (d,  $J = 8.4$  Hz, 2H), 7.73 (d,  $J = 8.8$  Hz, 2H), 7.39 – 7.33 (m,  $J = 8.4$  Hz, 4H), 6.51 (s, 1H), 3.53-3.45 (m,  $J = 4.4$  Hz, 1H), 3.06 (d,  $J = 6.8$  Hz, 2H), 2.80 (dd,  $J_1 = 16.4$  Hz,  $J_2 = 13.2$  Hz, 1H), 2.65 (dd,  $J_1 = 16.4$  Hz,  $J_2 = 4.4$  Hz, 1H).

**43**  $^1\text{H NMR}$  (400 MHz,  $\text{CDCl}_3$ )  $\delta$ , ppm: 8.12 (d,  $J = 8.8$  Hz, 2H), 7.61 (d,  $J = 8.4$  Hz, 2H), 6.44 (d,  $J = 2.4$  Hz, 1H), 2.78 (dd,  $J_1 = 17.6$  Hz,  $J_2 = 3.2$  Hz, 1H), 2.62-2.52 (m, 2H), 2.21 (dd,  $J_1 = 16.0$  Hz,  $J_2 = 13.6$  Hz, 1H), 2.03 (m, 1H), 1.72 (m,  $J = 6.8$  Hz, 1H), 0.99 (dd,  $J_1 = 6.8$  Hz,  $J_2 = 4.8$  Hz, 6H).

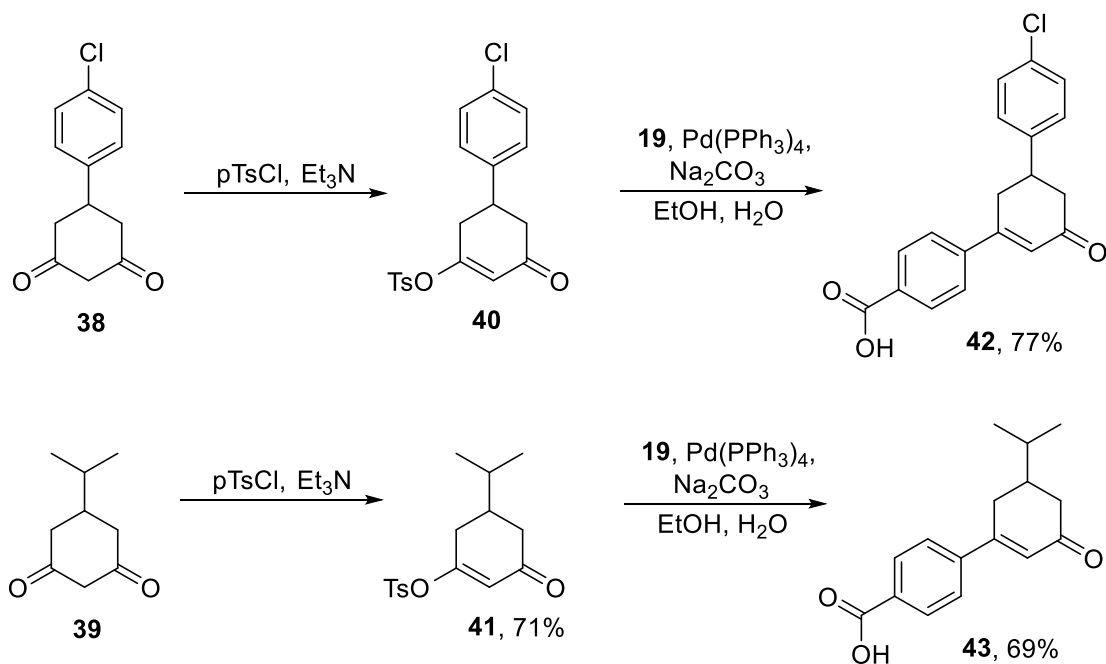


**Figure 1.2.5.4.3.** Overview of the preparation of analogs **42** and **43**.

### 1.2.5.5 Changes in activity resulting from the various structural modifications

At this stage in the project, all of the compounds tested were expected to have good antiepileptic activity. As such, each of the analogs prepared as part of this SAR study was directly assayed *in vivo* without being first tested by VSDI. Their activity was compared to **15** to determine the effect of the various changes to the structure. The effect of the compound on the kindled rats was measured in two ways, a qualitative assessment of the seizure stage exhibited by the rats based on their symptoms, and a quantitative measure of the after-discharge duration (ADD). The after-discharge duration represents the length of time of neuron firing after the stimulus was administered. Longer durations

are correlated with increased neuron firing and sensitivity to seizures, while a reduction in ADD is a good indicator of antiepileptic activity.

The result from the first set of analogs, **20-22**, probing the effect of halogenated substituents is shown below. To reiterate, the goal with this set of analogs was to improve bioavailability of the compounds by increasing their lipophilicity due to the addition of halogen groups.

**Table 1.2.5.5.1.** After-discharge duration (ADD) after electrical stimulus in amygdala of kindled rats treated with analogs **20-22** and compared to **18**. A lower after-discharge duration is correlated to a stronger reduction in neuron firing from the administered compound. Results were obtained from OB Pharma; sample size information of the tests was not provided.

Compound	ADD at 5 mg/kg (s)	ADD at 20 mg/kg (s)
<b>18</b>	37.2 +/- 7.0	3.2 +/- 4.4
<b>20</b>	66.2 +/- 7.3	54.8 +/- 5.1
<b>21</b>	67.2 +/- 8.1	56.8 +/- 7.3
<b>22</b>	52.6 +/- 8.4	7.6 +/- 10.4

Contrary to the expectations, compounds **20** and **21** demonstrated nearly nonexistent activity, despite the modifications to the structure being minor. These results were unexpected, but made sense after reflection. The addition of halogens ortho to the carboxylic acid of the analogs would have a strong increase in the acidity of the compound, which would in turn diminish the portion of protonated acid in the blood that would be available to cross the blood-brain barrier. This change would significantly lower the bioavailability instead of increasing it as desired. While the pKas of the analogs were not measured, their relative values can be estimated based on the corresponding benzoic acids. The acid **15** is expected to have a pKa very similar to that of 4-acetylbenzoic acid **40**. It is reasonable to assume that analogs **20-21** and **22** would have pKas lower than that of 2-chlorobenzoic acid **42** and 3-chlorobenzoic acid **43**, in a similar fashion as observed between **40** and **41**. As the portion of protonated 2-Chlorobenzoic acid **42** is almost

exactly 20 times smaller than that of benzoic acid, one could expect a similar ratio between **15** and **21**. This should roughly correlate to a 20-fold decrease in bioavailability and resulting activity at a given dose. On the other hand, while **43** is still more acidic than **41**, this effect is much less pronounced as the concentration of protonated species in **43** would only diminish by half. The pKa of the various benzoic acids corresponding to the analogs prepared are shown below.

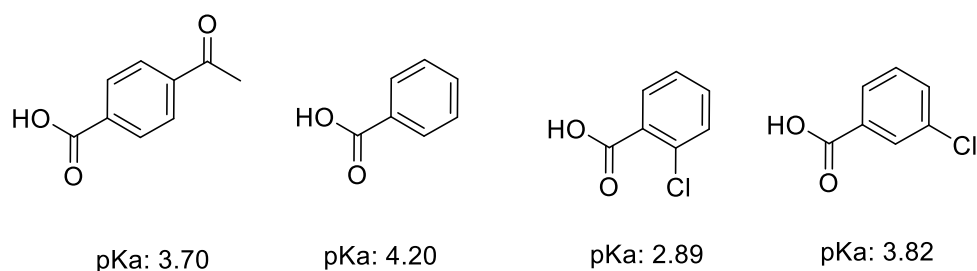


**Figure 1.2.5.5.1.** pKa values for the benzoic acids corresponding to the acid **15** and its analogs **20** to **22**.

However, the minor increase in acidity from the 3-chloro substituent of compound **22** would be expected to cause a more significant decrease in activity than what was observed in the bioassays performed. This could partially be explained by the presence of the chlorine substituent as a larger group improving the membrane permeability of this analog. Another explanation is that the presence of this bulkier atom close to the cyclohexyl ring can force the two rings to rotate away from each other, increasing the angle between both. By looking at the chemical structure, it would be expected that both rings be on the same plane, due to the conjugated  $\pi$  system. In practice, a small angle is present even with the absence of any additional substituents, which then increases as the hydrogens are replaced by larger substituents. This effect was observed by various analytical methods.

The initial value of this angle was determined via X-ray crystallography. High energy X-ray radiation is used to get an accurate tridimensional structure of molecules in

a crystal lattice. The sample was prepared by dissolving **15** in methanol in a small Erlenmeyer flask, and sealing the opening with parafilm. Small holes were poked through the seal to let the solvent slowly evaporate over two weeks. The large crystals formed were filtered out of the leftover solvent, and analyzed via single crystal X-ray diffraction.

The structure was viewed with the CCDC's Mercury crystal structure visualisation tool, which was also used to calculate the angle between the two planes. In the acid **15**, this angle was found to be  $37.2^\circ$ , which was already significantly larger than expected. X-ray crystallography analysis was not performed on **22** to obtain the exact angle.

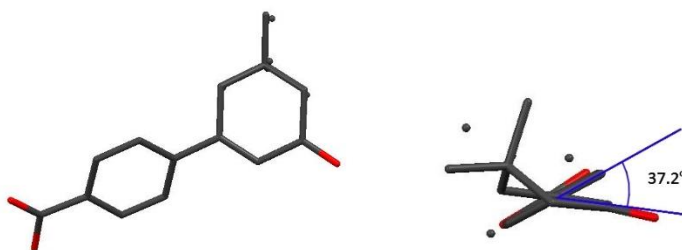


**Figure 1.2.5.5.2.** Tridimensional structure of the acid **15** obtained via X-ray crystallography viewed from various angles.

This effect was also confirmed via UV-vis spectrometry. The spectrometers measure the capacity of the samples to absorb light over a spectrum of wavelengths. There is a known correlation between the number of bonds in a conjugated  $\pi$  systems and the resulting absorbance profile of the molecule. Generally, longer chains of conjugated bonds lead to absorption at longer wavelengths and vice-versa with shorter  $\pi$  systems. This was used to qualitatively determine whether or not the addition of the chlorine substituent in compound **22** was inhibiting conjugation between the benzoic acid and vinyl ketone portions of the molecule. The absorption spectrum of the acid **15** was collected and used as a point of comparison. The UV-vis absorption spectra of compounds **15** and **22** are displayed below. From the data gathered, it was indisputable that presence of the chlorine inhibited conjugation in the  $\pi$  system of **22**. The intensity of the major

absorption peak around 300 nm of compound **15** was reduced by more than half in the spectrum of **22**, and the edge of a new peak could be observed at the 200 nm detection limit. The fact that the 300 nm peak did not completely disappear means that conjugation between the two regions of the molecule is still possible and present, but much less pronounced than in **15**.

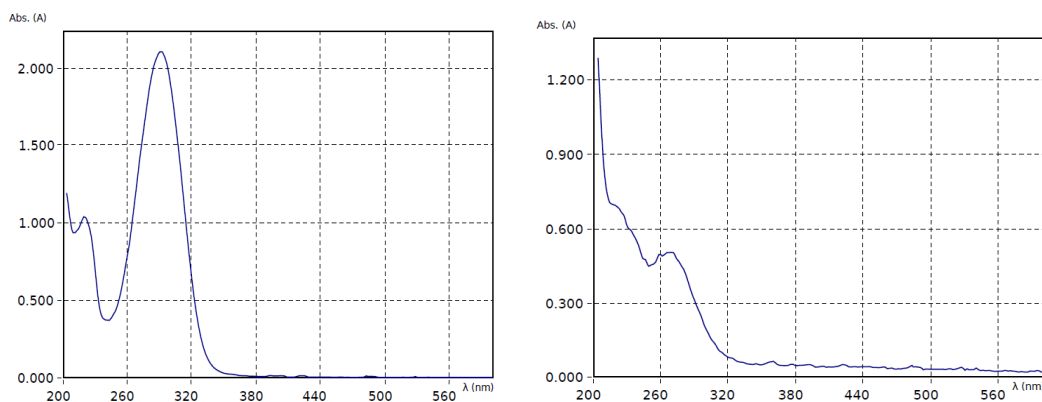


**Figure 1.2.5.5.3.** UV-vis Absorption spectra of **15** (left) and **22** (right). *The samples of the two compounds were dissolved in 99% methanol in concentrations of 0.078 and 0.075 mmol/L respectively. Analysis was performed on an Eppendorf Biospectrometer Basic.*

Finally, NOE NMR experiments were performed to confirm the data obtained via X-ray crystallography and UV-vis spectrometry. While not as precise as the previous methods mentioned, the NOE spectra of **15** and **22** clearly show the disappearance of the small peak ( $\delta$  7.71 ppm) representing the interaction between the adjacent protons on the two cycles, which indicates a larger gap between the two protons in analog **22**. The spectra below were obtained on a Bruker Avance II 300 MHz spectrometer, by irradiating the  $sp^2$  singlet via a selective  $180^\circ$  pulse in a 1D NOESY experiment. The irradiated peak appears normally, while the other protons in the molecule only show on the spectrum according to their spatial proximity to the targeted proton. The relative distance between different protons can be qualitatively assessed from the integration of the peaks. The NOE spectrum of **15** shows a spatial interaction between the irradiated proton (6.44 ppm) and the doublet of the closest pair of protons (7.71 ppm) on the neighbouring aromatic ring.

On the other hand, no interactions are visible when the equivalent proton in **22** is irradiated.

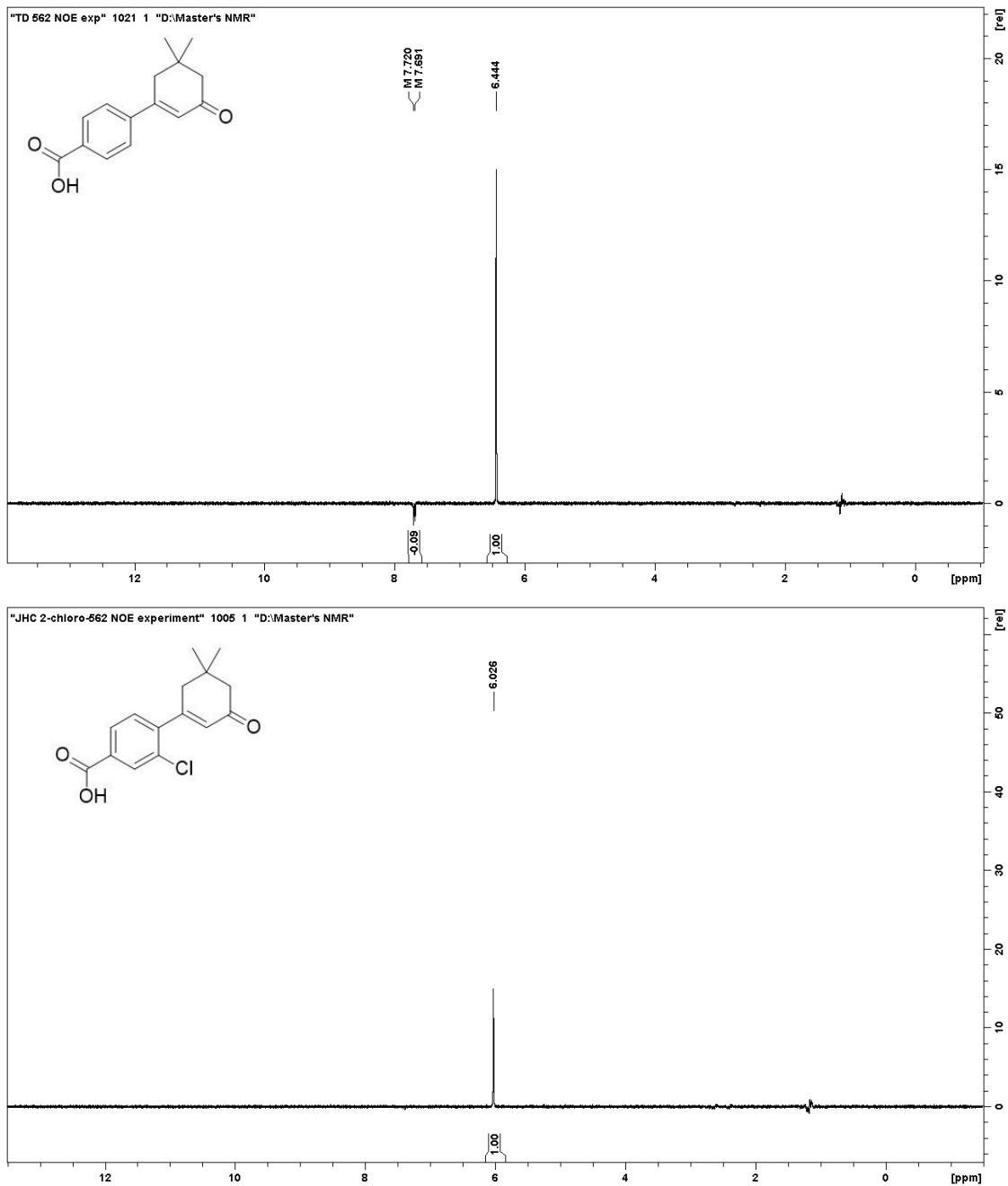


**Figure 1.2.5.5.4.** 1D NOESY experiments of compounds **15** and **22** irradiating the  $sp^2$  protons of the cyclohexenone rings at 6.44 ppm and 6.02 ppm. *The spectra were taken with samples dissolved in MeOD.*

The data collected therefore supports the hypothesis that the substitution of a hydrogen in the meta position (related to the acid) by a larger substituent leads to a less strongly conjugated molecule, which has an increased inter-ring angle. Although the molecule was originally thought to be planar due to the conjugated system, the torsional strain increase in this eclipsed conformation is highly unfavorable and increasingly so as the nearby substituents become larger. The conjugated  $\pi$  system itself seems unnecessary for the activity, however addition of electron withdrawing substituents along this system have an important negative effect on the bioavailability of the compound.

The results from the second set of analogs, **28-30**, are shown below. This set of analogs was prepared to investigate the importance of the carbonyl group and its position relative to the aryl ring.

**Table 1.2.5.5.2.** After-discharge duration (ADD) after electrical stimulus in amygdala of kindled rats treated with analogs **28-30** and compared to **18**. A lower after-discharge duration is correlated to a stronger reduction in neuron firing from the administered compound. Results were obtained from OB Pharma, sample size information of the tests was not provided.

Compound	ADD at 5 mg/kg (s)	ADD at 20 mg/kg (s)
<b>18</b>	37.2 +/- 7.0	3.2 +/- 4.4
<b>28</b>	53.4 +/- 5.2	34.8 +/- 6.1
<b>29</b>	54.2 +/- 6.8	14.4 +/- 5.6
<b>30</b>	57.8 +/- 4.1	23.0 +/- 8.0

The analog **28** was prepared to bring the two oxygens in the molecule closer together. Based on the *In vivo* activity results, having the acid as a para substituent to the first ring is crucial as this simple position change increased the after-discharge duration by a factor of ten. While substituents of various sizes were added at this position, they all had the carbonyl at the same position. This supports an important interaction between this particular carbonyl and the target receptor.

The analog **29** was prepared to extend the distance between both  $sp^2$  oxygens by one bond, while isolating the carboxylic acid from the conjugated  $\pi$  system to increase its pKa. As seen above, the acid at the C4 position of the aryl ring was significantly more active than when at C3 such as in compound **28**. Phenylacetic acid has a pKa only 0.1 higher than that of benzoic acid, however it would also diminish the effects of conjugated electron-withdrawing groups on the aryl ring. Despite this, results from the bioassays of **29** showed that the decrease in acidity from the addition of an  $sp^3$  carbon between the acid and the conjugated system did not have an effect sufficient enough to counter the reduction in activity from having the acid displaced from its optimal position. Compound **30** showed similar results, with activity significantly poorer than that of **18**, after having the conjugated chain extended by two additional bonds.

The results obtained from analogs **28** to **30** consistently show that changing the position of the 4-carboxy substituent is detrimental to the activity *In vivo*. While previous analogs demonstrated that there is a decently large pocket of space available to increase the size of the compounds, this set of results strongly supports that the oxygen at the position mentioned above is responsible for a crucial interaction in binding to its receptor.

The last set of results represents the activity of the compounds, **34**, **37** and **42-43**, with varying substitutions at the cyclohexenone C5 position. These results are shown below.

**Table 1.2.5.5.3.** After-discharge duration (ADD) after electrical stimulus in amygdala of kindled rats treated with analogs **34**, **37**, **42** and **43**, and compared to **18**. A lower after-discharge duration is correlated to a stronger reduction in neuron firing from the administered compound. Results were obtained from OB Pharma, sample size information of the tests was not provided.

\*Data for compound **43** was not sent by OB Pharma, it was only mentioned that the compound is equivalent in activity to **18**.

Compound	ADD at 5 mg/kg (s)	ADD at 20 mg/kg (s)
<b>18</b>	37.2 +/- 7.0	3.2 +/- 4.4
<b>34</b>	60.8 +/- 5.7	27.6 +/- 7.8
<b>37</b>	32.4 +/- 4.6	4.0 +/- 3.8
<b>42</b>	37.6 +/- 5.6	5.3 +/- 3.3
<b>43</b>	N/A*	N/A*

The C5-substituted analogs were once again found to be potent inhibitors of epileptic activity. The importance of the C5 substituent is immediately evident when considering the results from compound **34**. The replacement of the C5 dimethyl of compounds **15** and **18** by hydrogens led to an almost complete loss of antiepileptic activity from compounds that were otherwise very potent. On the other hand, the substitution by a bulky phenyl ring instead exhibited the same activity as **18**. A difference in activity between **37** and **18** was harder to assess, as both compounds completely prevented stage 1 seizures and above at the concentrations tested. However, they both displayed nearly identical activities when concentrations were administered below effective dose. Compound **42** was slightly less active than its 5-phenyl analog, showing that the p-Cl group did not have a strong influence on the bioavailability or activity of the compound. Unsurprisingly, compound **43** also had comparable activity to **18**.

While the analogs shown above demonstrated a potency statistically identical activity to that of **18**, it is important to note that these 5-substituted analogs are racemic mixtures. Depending on the receptor binding site, it is therefore possible that the activity of one enantiomer could be higher than the other. If that was the case, the potency of this pure enantiomer would then be expected to be higher than that of **18**. Chiral resolution of the mixture was attempted by forming a chiral salt of **37** with quinine to utilize potential differences in solubility between the enantiomers to separate them by serial recrystallizations. However, while NMR analysis seemed to suggest that enantiomerically enriched samples were obtained, analytical methods needed to confirm the ratio of the isomers were unavailable. Furthermore, it would likely have been difficult to obtain a pure sample of either enantiomer without the means to perform a chiral column chromatography.

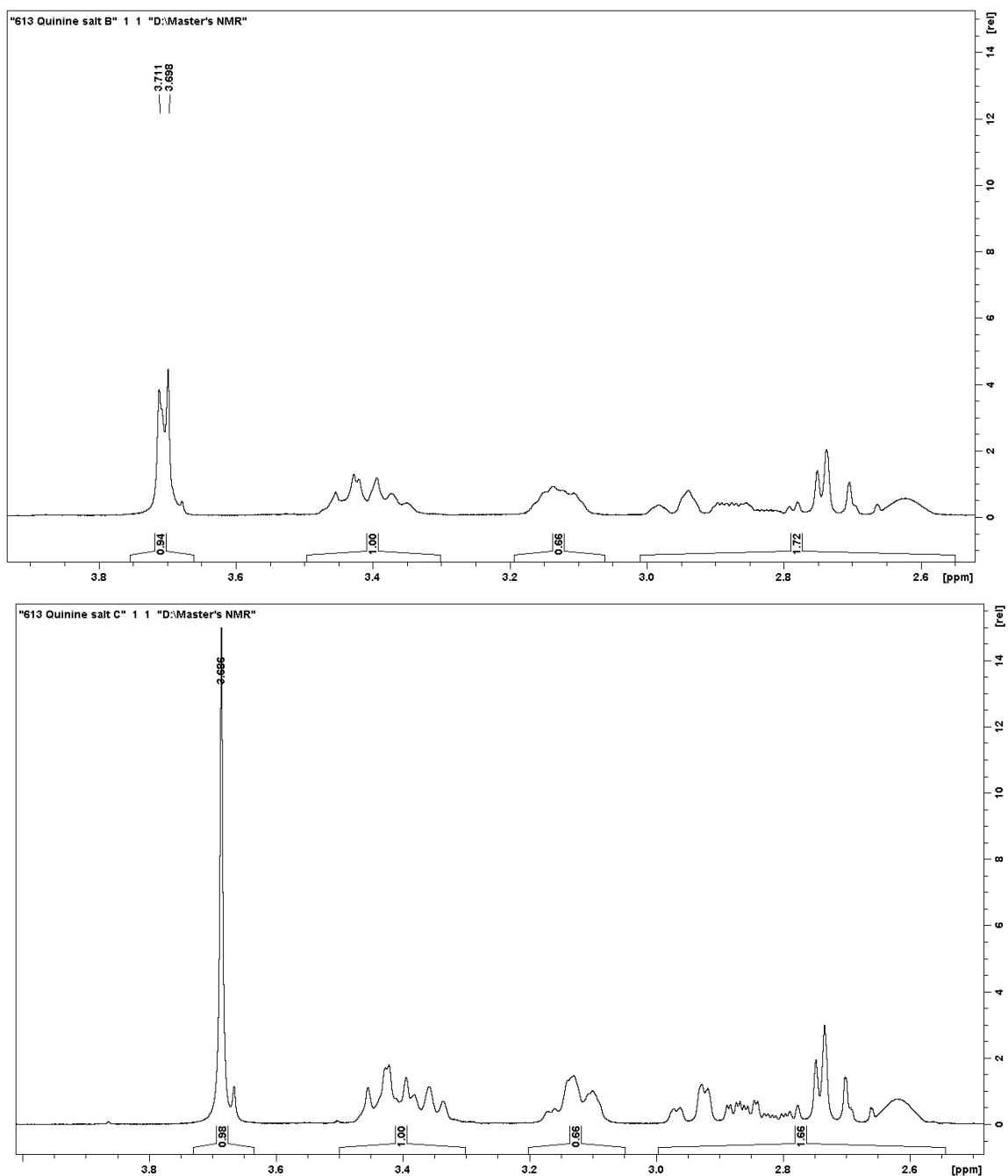


**Figure 1.2.5.5.5.**  $^1\text{H}$  NMR comparison between the initial quinine salt mixture of compound **37** and the recrystallised product. The peaks at  $\delta$  3.71 ppm and 3.69 ppm are thought to represent the methyl ether peak of quinone for the two diastereoisomers of the salt. The spectra seem to clearly show the removal of one isomer after recrystallisation, however the rest of the spectra would have been expected to exhibit similar changes on the rest of the chiral protons, which was not observed.

Within the constraints of the available data on the three compounds carrying hydrogen and or alkyl groups at C5 it appears that the activity increases as log P increases. A 5-phenyl group further increases logP compared to **18**.

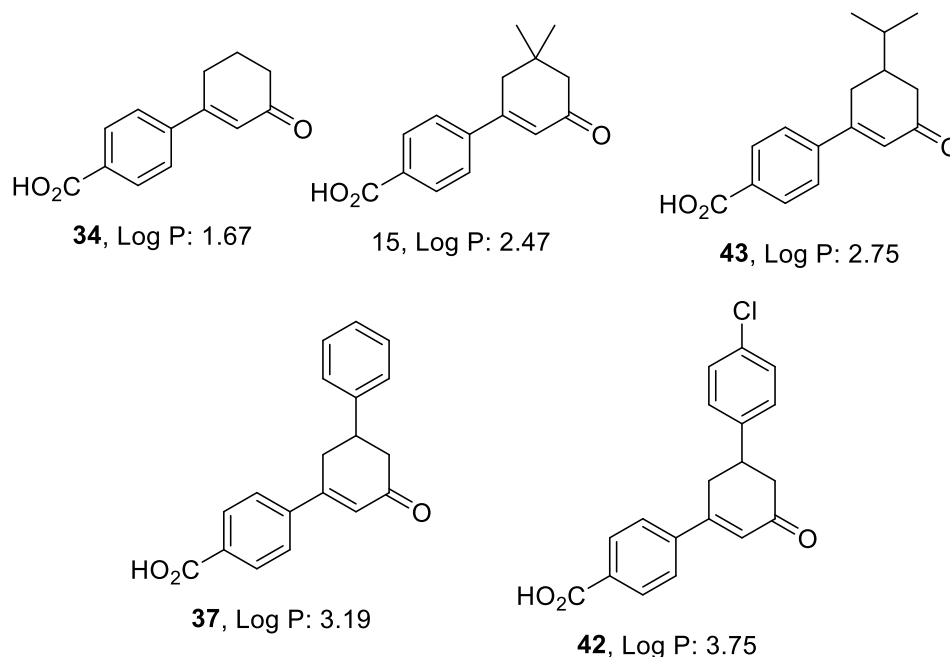


**Figure 1.2.5.5.6.** Structures and LogP of the various analogs with C5 modifications. *The estimated logP values are calculated by ChemDraw Prime version 19.*

Although these chiral monosubstituted derivatives have comparable, or possibly better, activity than **18**, they are less desirable as drug candidates since they are only available in racemic form at this stage. A synthesis leading to enantiomerically pure material or a resolution of the racemic compounds would need to be developed and the more active enantiomer would need to be identified. The synthesis would need to be completely different from the current one, as it starts with symmetrical cyclohexane-1,3-diones. Resolution might be possible via the generation and separation of diastereomeric salts with chiral amines such as quinine or a chiral  $\alpha$ -methylbenzyl amine. This would be costly and time consuming even beyond the obvious loss of half the material as the second enantiomer being removed. Isomer separation on a preparative and eventually commercial scale would also likely be prohibitively expensive.

Despite this flaw, the identification of these compounds as potent analogs does suggest some potential achiral structures which would not require enantiomeric resolution. It would be important to prepare and evaluate a number of compounds carrying two identical C5 alkyl substituents, such as the 5,5-diethyl derivative **44**. Also intriguing would be the spiro compounds **45** and **46**. All of these compounds are more hydrophobic than **18** and could potentially have a better bioavailability.

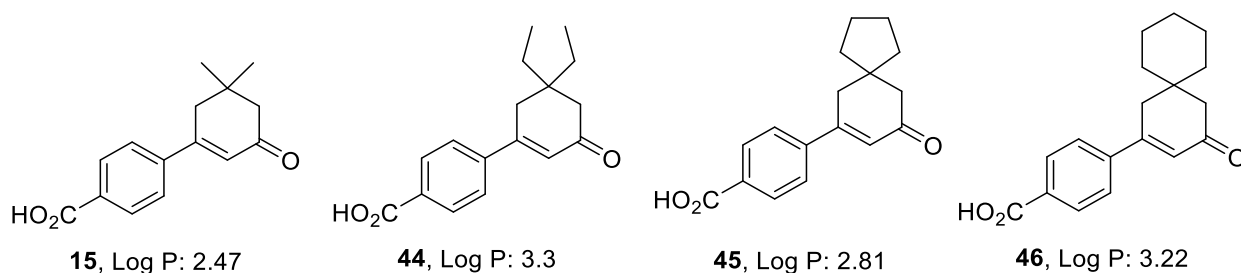


**Figure 1.2.5.5.7.** Structures and LogP of potential analogs **44-46**. The LogP values are calculated by ChemDraw.

The synthesis of these compounds could be approached by first preparing the requisite cyclohexane-1,3-diones. Such compounds including the precursor to the isopropyl derivative vi have been prepared from diethyl malonate and a corresponding  $\alpha,\beta$ -unsaturated ketone, as shown below. The  $\alpha,\beta$ -unsaturated ketones can be purchased or prepared from the corresponding aldehydes by aldol condensation with acetone, or from reaction with an acetone phosphonium ylide.

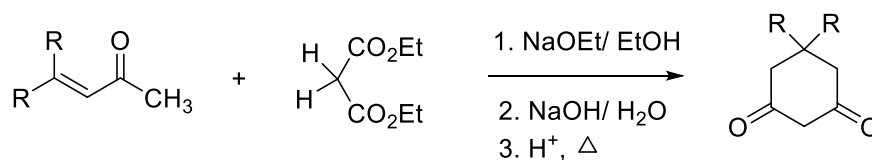


**Figure 1.2.5.5.8.** Reaction scheme for the preparation of the various cyclohexane-1,3-dione starting materials.

### 1.2.6 Conclusion and future work

In working towards the primary goal of the project, expanding the library of analogs, 22 new analogs were synthesized although not all were used for bioassay results. Several of the new analogs prepared showed promising results, such as **22** and **37**, with activity matching that of the lead compound **15** and suggesting additional possible improvements.

Based on the SAR studies described in this work, an updated pharmacophore can be proposed. While the skeleton of the molecule has not been changed, the importance of the aryl ring carbonyl has been confirmed, as well as the possibility of large pockets of space with potential for introducing additional receptor binding interactions.

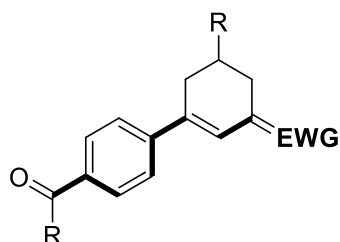


**Figure 1.2.6.1.** Revised proposed pharmacophore of the ISOX analogs family of antiepileptic compounds. *The distance and relative position of the two EWGs to each other appears to have a strong effect on antiepileptic activity. The labelled R groups indicate a pocket of space in the target receptor.*

In the near future, the next set of analogs to be prepared will continue to investigate C5 substituent modifications to increase the size, or add different EWGs or EDGs. These compounds were selected due to easy to procure starting materials.

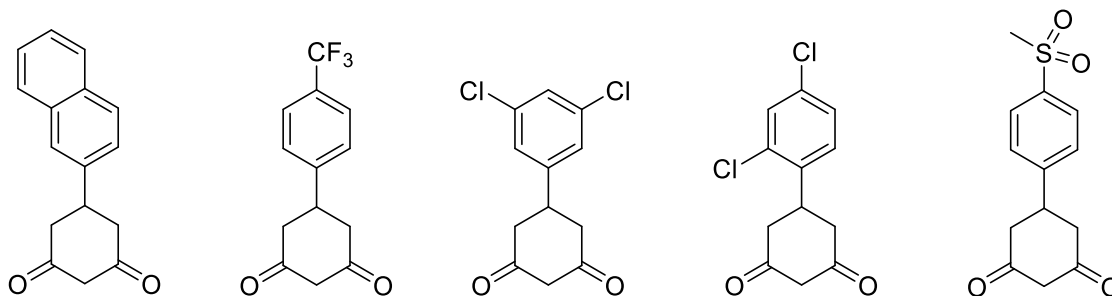


**Figure. 1.2.6.1.** Structures of analogs to be completed.

From the core structure presented above, there remain several interesting questions to answer to better understand the structure-activity relationship of this family of compounds. Some examples of analogs that could be prepared to investigate these questions are shown below.

The first changes to investigate should be addition of electron donating groups on the aryl ring. As the addition of electron withdrawing groups ortho to the acid severely impaired *In vivo* activity, it would not be unreasonable to expect the activity to improve if those were replaced by EDGs. Larger electron donating groups could also be added to the meta position, to determine whether the differences in activity between **18** and **22** were mainly caused by the addition of a meta EWG, or by the decrease in  $\pi$  system coordination. These analogs could be easily prepared via the current method by obtaining the appropriate phenylboronic acids.

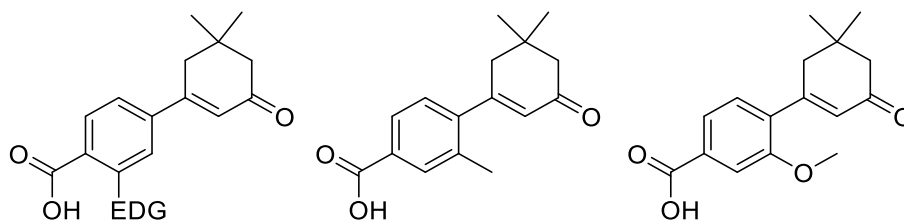


**Figure. 1.2.6.2.** Examples of analogs containing aryl electron donating groups.

The investigation of C5 substituent variations demonstrated the space available and the potential for new receptor interactions in this region of the molecule. While the

prepared analogs were successful, the ones prepared so far primarily had hydrophobic aromatic C5 substituents. Valuable information could be obtained from introducing various electron withdrawing or donating groups. The starting cyclohexanediones for these analogs could be prepared via the method mentioned in the previous section (see **Figure 1.2.5.5.8.**) from the corresponding aldehydes

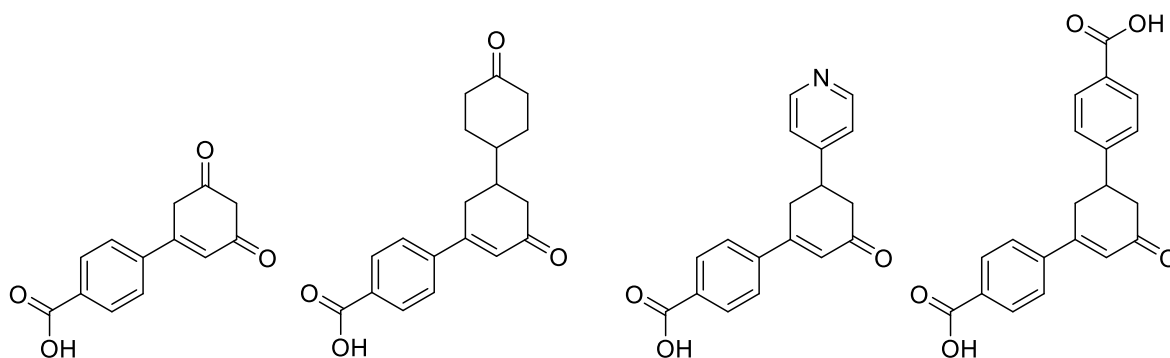


**Figure 1.2.6.2.** Examples of analogs containing polar C5 substituents.

The secondary goals of further developing compound **15** were met by completing a number of stability studies, characterizing the structure further via NOE NMR, UV-vis spectrometry and X-ray crystallography, and optimizing the synthesis. In addition, a large amount of material was prepared for use in animal toxicity studies. All the data obtained during this project supports the candidacy of this analog as an important AED. This compound is thermally stable and suitable for long term storage at room conditions, is not a chiral compound, and is easily prepared and purified from inexpensive starting materials. Based on the animal model bioassay results obtained until now, **15** and **18** have activity better than current standard of care AEDs, without the common associated side effects. The effective dose of **15** and **18** are significantly lower than that of competitors in *in vitro* models, however similar doses need to be used in animal models, due to the lower bioavailability of the compounds<sup>19,54</sup>. Future development and structure optimization should therefore focus on improving membrane permeability and bioavailability.

As mentioned previously, epilepsy is a broad spectrum of seizure disorders, that arise from various brain dysfunctions or injuries. Due to the various causes of, not all epilepsy drugs are equally effective at treating the different syndromes. While the results so far have been excellent with **15** and **18** preventing epilepsy in all testing models used, human efficacy trials on patients suffering from a range of seizure disorders would be important in the future to have an accurate idea of the antiepileptic activity spectrum of the compound.

Finally, around half of patients undergoing successful antiepileptic treatment can eventually discontinue treatment, after being seizure free for a few years. In addition, the results from **18** in traumatic brain injury models showed that a 4 week treatment with the compound greatly reduced the severity of seizures occurring after discontinuation of the treatment<sup>54</sup>. This drug candidate therefore has potential to be extremely useful in the prevention of TBI-induced epilepsy syndromes, when used as short term preventive treatment for a few months immediately following the injury. The most important step remaining in this project to bring an ISOX analog to the drug market, is for the compound to successfully undergo the human safety and efficacy clinical trials, which were planned to begin in 2020.

## 1.3 Experimental Data

### 1.3.1 General information

The work presented in this chapter was done for and in collaboration with OB Pharma. As such, only the compounds that they deemed important were fully characterized, and in those cases the characterization would be restricted to the minimum required to support future patent applications. Some intermediates or minor compounds that did not end up being used for bioassays were only identified via  $^1\text{H}$  NMR.

#### TLC

Thin layer chromatography was used to analyze product formation during reactions, assess purity of final products, determine appropriate solvent mixtures for column chromatography where required and detect the desired fractions to combine after elution. The samples to analyze were deposited on aluminum-backed thin layers silica plates and eluted with an appropriate solvent mixture, typically composed of DCM, ethyl acetate and/or hexanes. As most of the compounds in this project contained aromatic rings or  $\pi$  systems, the eluted plates were only visualized under UV light (254 nm).

#### Column chromatography

When required, the finished products were purified via column chromatography if other purification methods were unsuccessful or not appropriate. SiliaFlash F60 (230-400 mesh) silica powder was used. The columns were packed with dry silica, before adding the sample in a minimal amount of solvent and fully drying the column. The elution solvent system used was an ethyl acetate and hexane mixture. In all columns performed, the elution started with a small volume of pure hexanes, followed by a steady increase in ethyl acetate ratio. The gradients and solvent ratios used varied depending on the compounds being purified.

## NMR

The  $^1\text{H}$  and  $^{13}\text{C}$  NMR spectra were obtained on a Bruker Avance 400 MHz spectrometer, while NOE experiment spectra were obtained on a Bruker Avance II 300MHz spectrometer. The samples were prepared in  $\text{CDCl}_3$ , MeOD or  $\text{D}_2\text{O}$ . The solvent used for each sample is indicated with their respective spectra. The chemical shift values for all spectra are reported in parts per million (ppm) relative to tetramethylsilane (TMS) ( $\delta$  0.00 ppm). Coupling constants are reported in Hz where appropriate. Spectral information was processed using the TopSpin 4.06 software.

## 1.3.2 General procedures

### 1.3.2.1 Preparation of enol tosylates in acetone and water

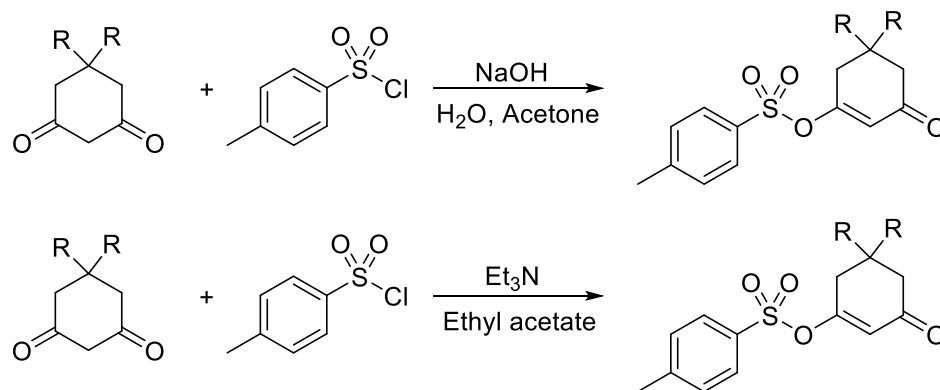


**Figure 1.3.2.1.1.** Two methods of preparation of dimesone enol tosylates.

Sodium hydroxide pellets (1.50 eq.) were fully dissolved in distilled water (1.0 mL per mmol of diketone). The diketone starting material (1.00 eq.) was added and a clear solution was obtained. A solution of p-toluenesulfonyl chloride (1.10 eq.) in acetone (2.0 mL per mmol of diketone) was then added. The mixture was sealed and stirred at room temperature overnight.

The following day, the acetone was evaporated in vacuo. The enol tosylate product was extracted from the aqueous solution three times with 20 mL of dichloromethane. The organic extract was dried with magnesium sulfate, the filtered by gravity to remove the deposits. The solvent was evaporated in vacuo to obtain the product as a clear, light yellow oil. The oil quickly solidified when hexanes were added to the flask. The solid product was obtained from the solution by suction filtration and characterized by  $^1\text{H}$  and  $^{13}\text{C}$  NMR.

The reaction was also performed in ethyl acetate (2.0 mL per mmol of diketone) by replacing the sodium hydroxide with triethylamine (1.50 eq). Both methods were equally effective.

### 1.3.2.2 Palladium-catalyzed Suzuki cross-coupling

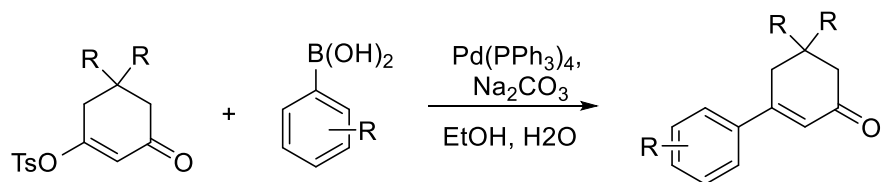


**Figure 1.3.2.2.1.** Preparation of 3-aryl cyclohexenones.

The enol tosylate obtained from the previous procedure (1.10 eq.), the boronic acid (1.00 eq.), the sodium carbonate (2.00 eq.) and the palladium catalyst (0.5 mol%), were all weighed separately on weighing paper and placed in a dry flask. The solvent mixture of ethanol (2.5 mL per mmol of boronic acid) and distilled water (1.25 mL per mmol of boronic acid) was prepared in a graduated cylinder and poured in the flask to dissolve most of the solids. A clear yellow solution with small amounts of sodium carbonate deposits was obtained. The solution was stirred at reflux in an oil bath at 100°C for 6 hours.

After the reflux, remaining solids were filtered out and the reaction mixture was concentrated in vacuo, removing most of the ethanol. The solution was diluted with additional water, then washed three times with 20 mL dichloromethane to remove any excess enol tosylate. The aqueous phase obtained, a clear yellow solution, was then acidified by dropwise addition of concentrated HCl. The flask was placed in a freezer for 15 minutes to promote crystallization. A small amount of concentrated HCl was added afterwards, to ensure no product remained in solution. The solid product was then recovered by suction filtration, and washed thoroughly with water. As the suction filtration was not usually sufficient for the product to be dried properly, the solid product obtained was dried further in a petri dish of appropriate size, placed in an oven at 70°C or at room temperature overnight. The product was then characterized by <sup>1</sup>H and <sup>13</sup>C NMR.

### 1.3.2.3 Conversion of carboxylic acids into sodium salts

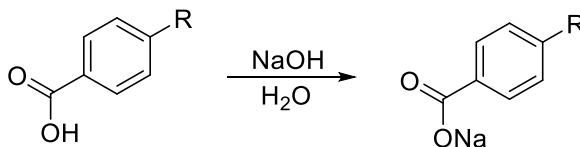
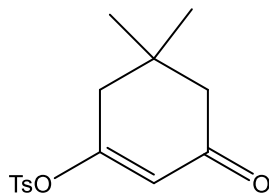


**Figure 1.3.2.3.1.** Preparation of the sodium salts.

A 10% NaOH solution was prepared by dissolving sodium hydroxide pellets in an appropriate amount of distilled water. The solution was standardized by titration against a solution of dry potassium hydrogen phthalate. The carboxylic acid starting material (1.00 eq.) was then dissolved in this NaOH solution (0.95 eq.). An excess of acid was used to ensure no unreacted sodium hydroxide remained in the finished product. The solution was filtered by gravity through filter paper to remove any undissolved starting material, and transferred into an appropriately sized petri dish. Water was then evaporated by leaving the solution in the petri dish out in the open until the salt crystals formed were fully dry. The product was characterized by <sup>1</sup>H and <sup>13</sup>C NMR by dissolving a sample in Deuterium oxide, with a few small grains of sodium carbonate to allow the compound to dissolve.

### 1.3.3 Experimental procedures and product characterization

#### Preparation of the enol tosylate of dimedone, **12**.

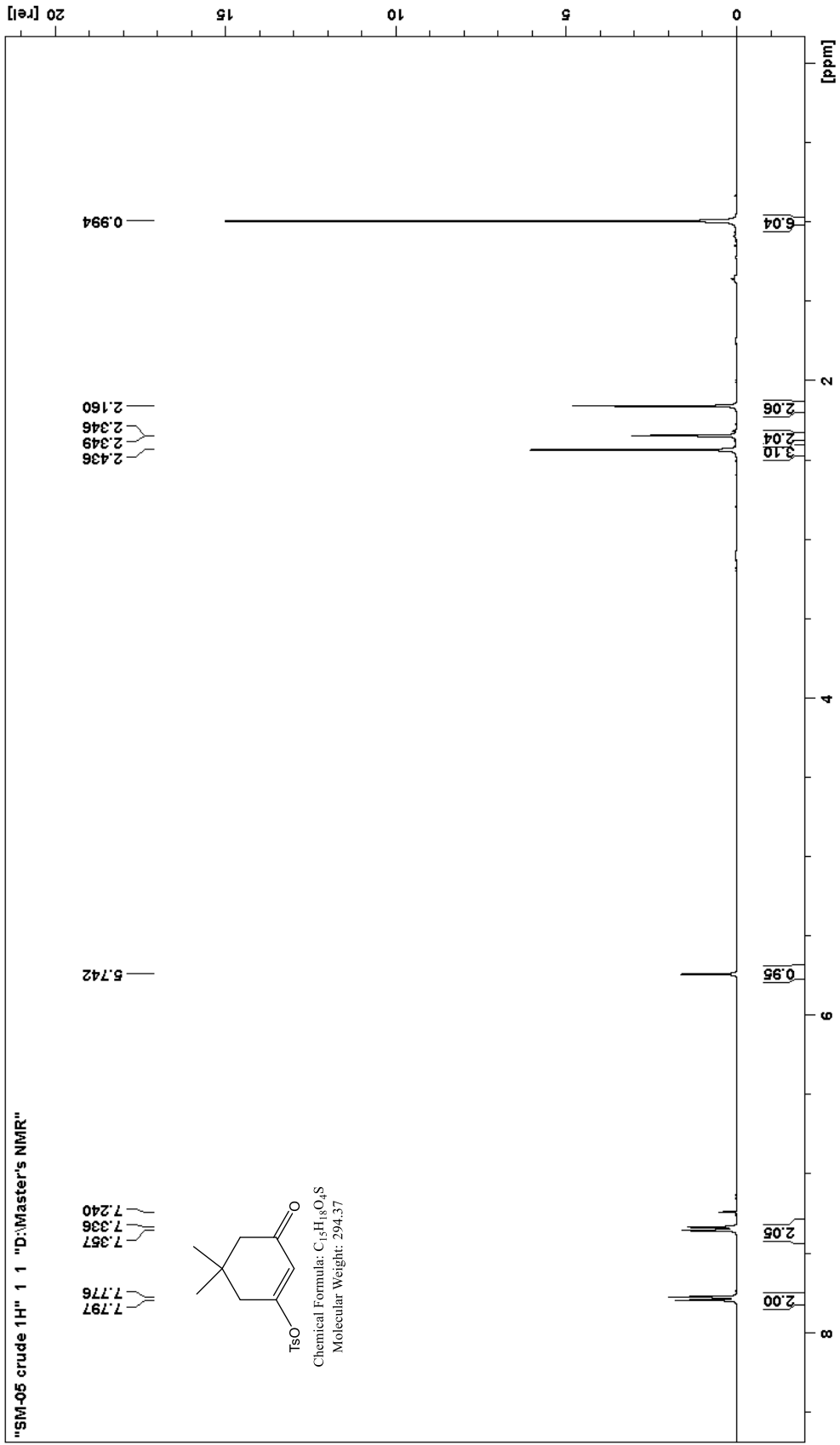


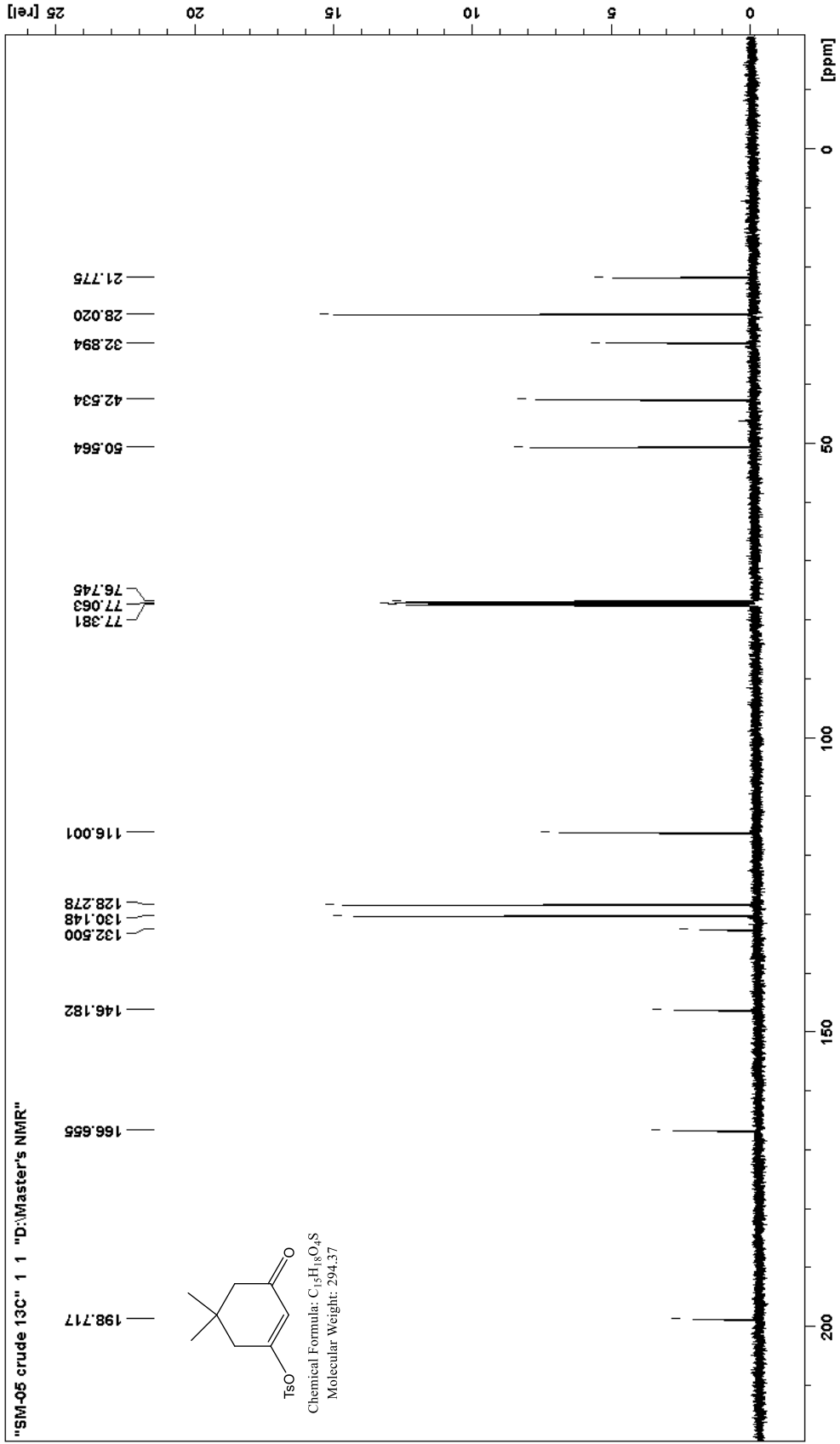
**12**

5,5-Dimethylcyclohexane-1,3-dione **8** (2.22 g, 15.8 mmol) was partially dissolved in ethyl acetate (40.0 mL). Triethylamine (2.48 g, 24.5 mmol) was added next, followed by p-toluenesulfonyl chloride (3.32 g, 17.4 mmol) which immediately caused the precipitation of triethylamine hydrochloride as a white solid. The mixture was stirred at room temperature overnight. The solution was washed once with distilled water (30 mL). The organic layer was dried with magnesium sulfate, filtered and evaporated to yield **12** as a yellow oil, which rapidly crystallized upon addition of hexanes. The final product was obtained by suction filtration as a white powder (3.90 g, 84%, mp: 54,8 – 56.0°C).

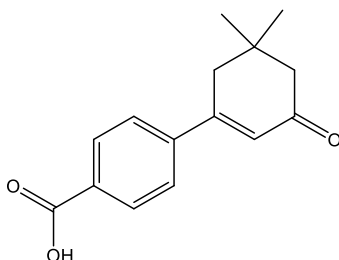
<sup>1</sup>H NMR (400 MHz, CDCl<sub>3</sub>) δ, ppm: 7.79 (d, J = 8.4 Hz, 2H), 7.35 (d, J = 8.4 Hz, 2H), 5.74 (s, 1H), 2.44 (s, 3H), 2.35 (d, J = 1.2 Hz, 2H), 2.16 (s, 2H), 0.99 (s, 6H).

<sup>13</sup>C NMR (400 MHz, CDCl<sub>3</sub>) δ, ppm: 198.72, 166.66, 146.18, 135.50, 130.15 (2C), 128.8 (2C), 116.00, 50.56, 42.53, 32.89, 28.02 (2C), 21.78.





### Preparation of 4-carboxyphenyl-5,5-dimethylcyclohex-2-enone, **15**.

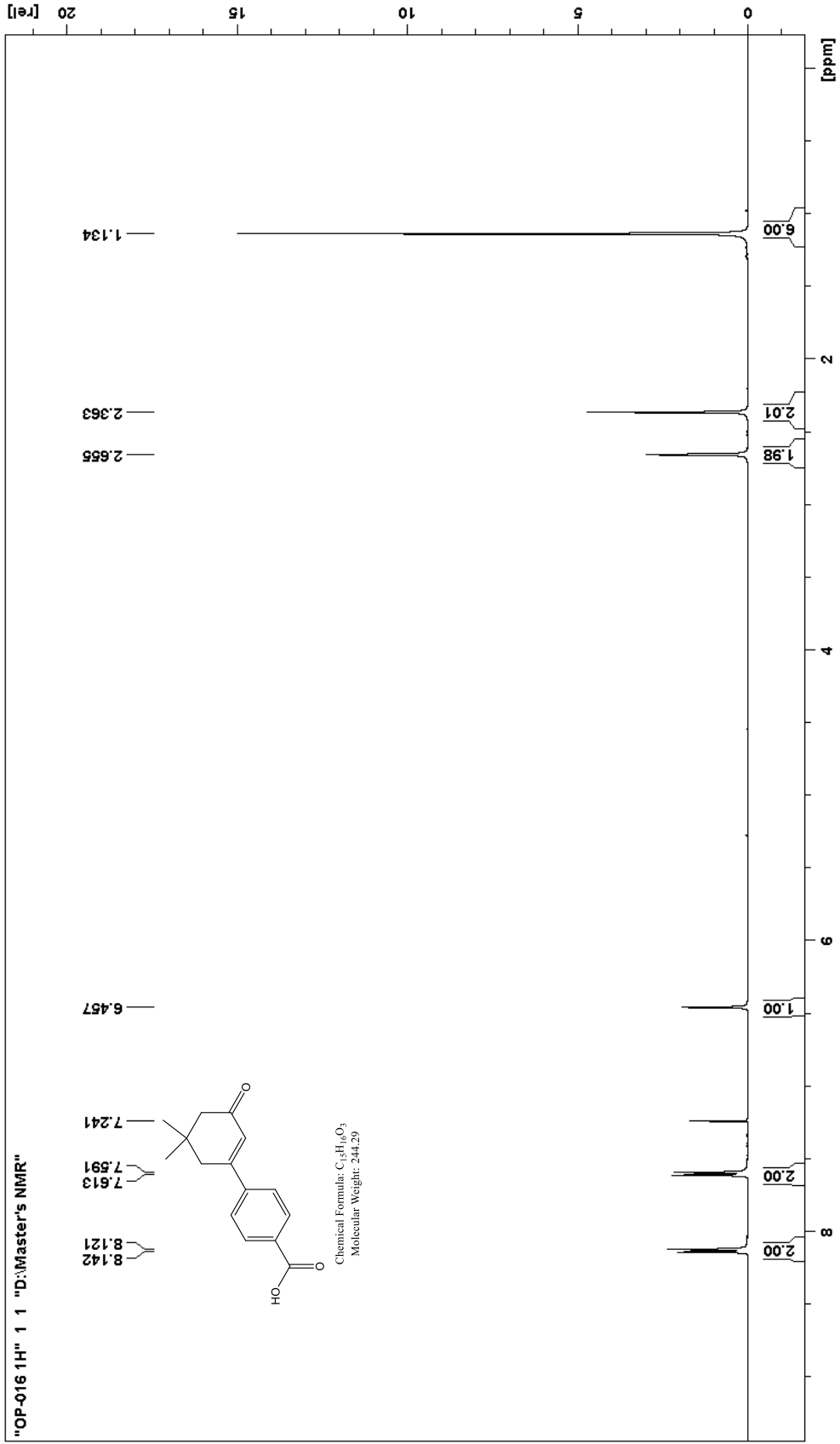


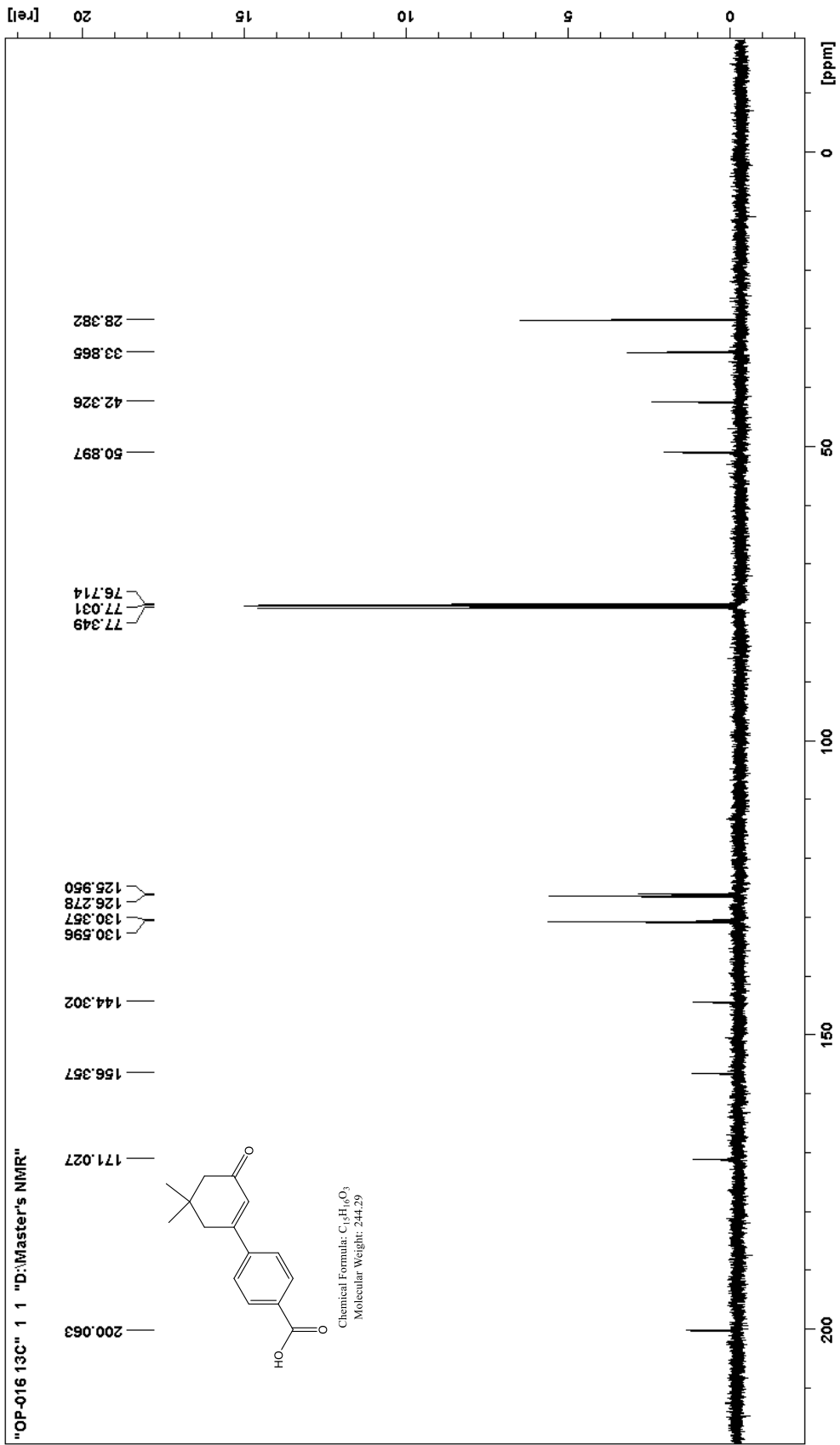
**15**

4-carboxyphenyl boronic acid (1.54 g, 9.28 mmol), the dimedone enol tosylate **12** (3.02 g, 9.28 mmol), sodium carbonate (2.07 g, 19.6 mmol) and tetrakis(triphenylphosphine)-palladium(0) (59 mg, 0.051 mmol, 0.55 mol%) were dissolved in 33 mL of a 2:1 mixture of 95% ethanol and distilled water. The mixture was refluxed in an oil bath at 100°C for six hours, after which the solution was filtered through cotton into a larger flask. The solution was concentrated on the rotary evaporator by removing most of the ethanol. The solution was diluted with an additional 40 mL of water, and washed three times with 20 mL of dichloromethane. The aqueous layer was acidified by slow addition of concentrated HCl and chilled to induce precipitation. The solid formed was isolated by suction filtration and rinsing with water, and dried for two hours in an oven at 70°C. The product was obtained as a white dry solid (3.31 g, 86%, mp: 181.1 – 182.7°C).

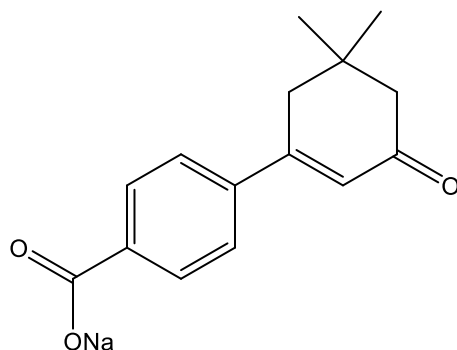
**<sup>1</sup>H NMR (400 MHz, CDCl<sub>3</sub>) δ, ppm:** 8.13 (d, J = 8.4 Hz, 2H), 7.60 (d, J = 8.4 Hz, 2H), 6.46 (s, 1H), 2.66 (d, J = 1.6 Hz, 2H), 2.36 (s, 2H), 1.13 (s, 6H).

**<sup>13</sup>C NMR (400 MHz, CDCl<sub>3</sub>) δ, ppm:** 200.06, 171.03, 156.36, 144.30, 130.60 (2C), 130.36, 126.28 (2C), 125.95, 50.90, 42.33, 33.87, 28.38 (2C).





### Preparation of compound 18.



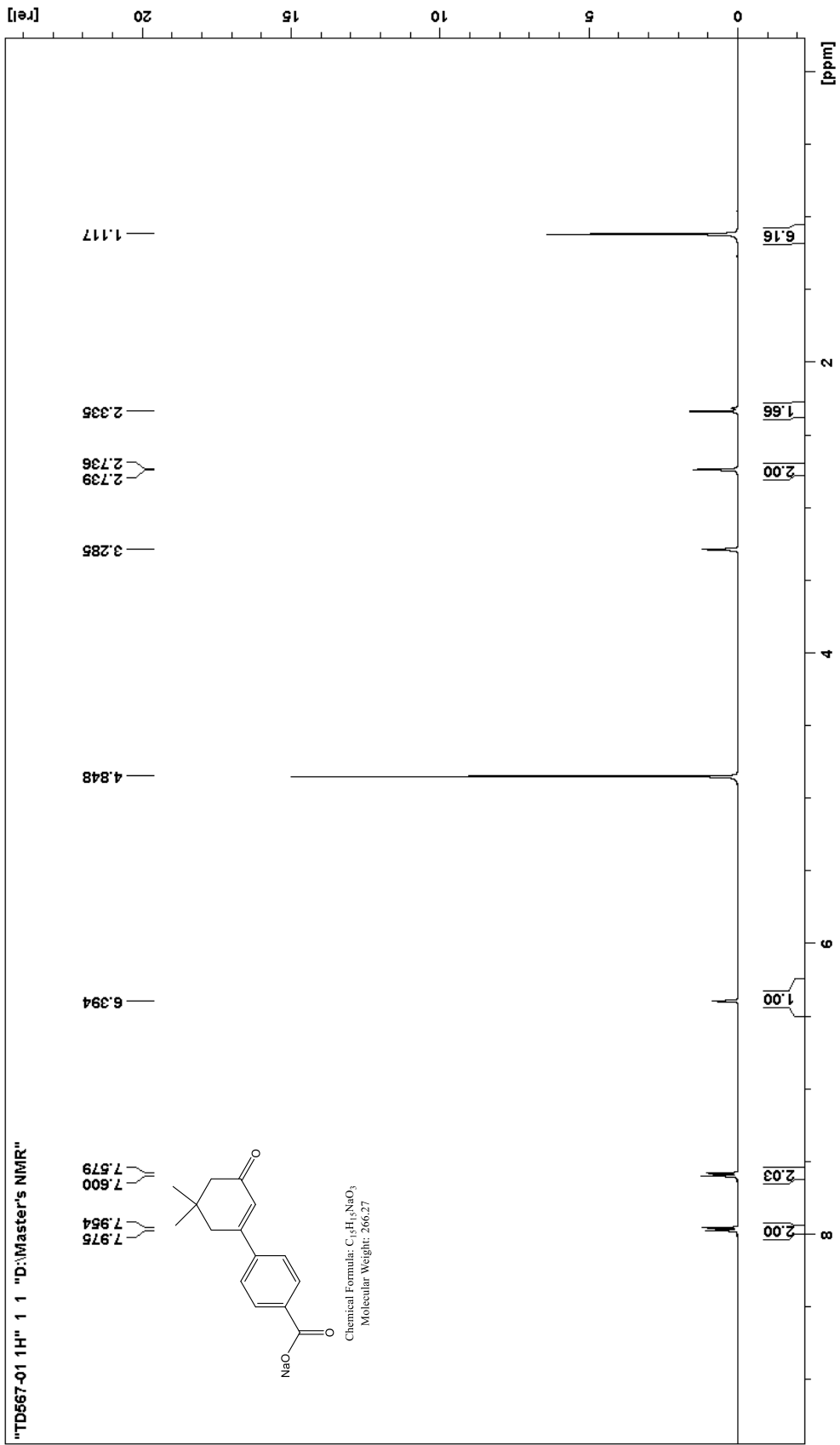
**18**

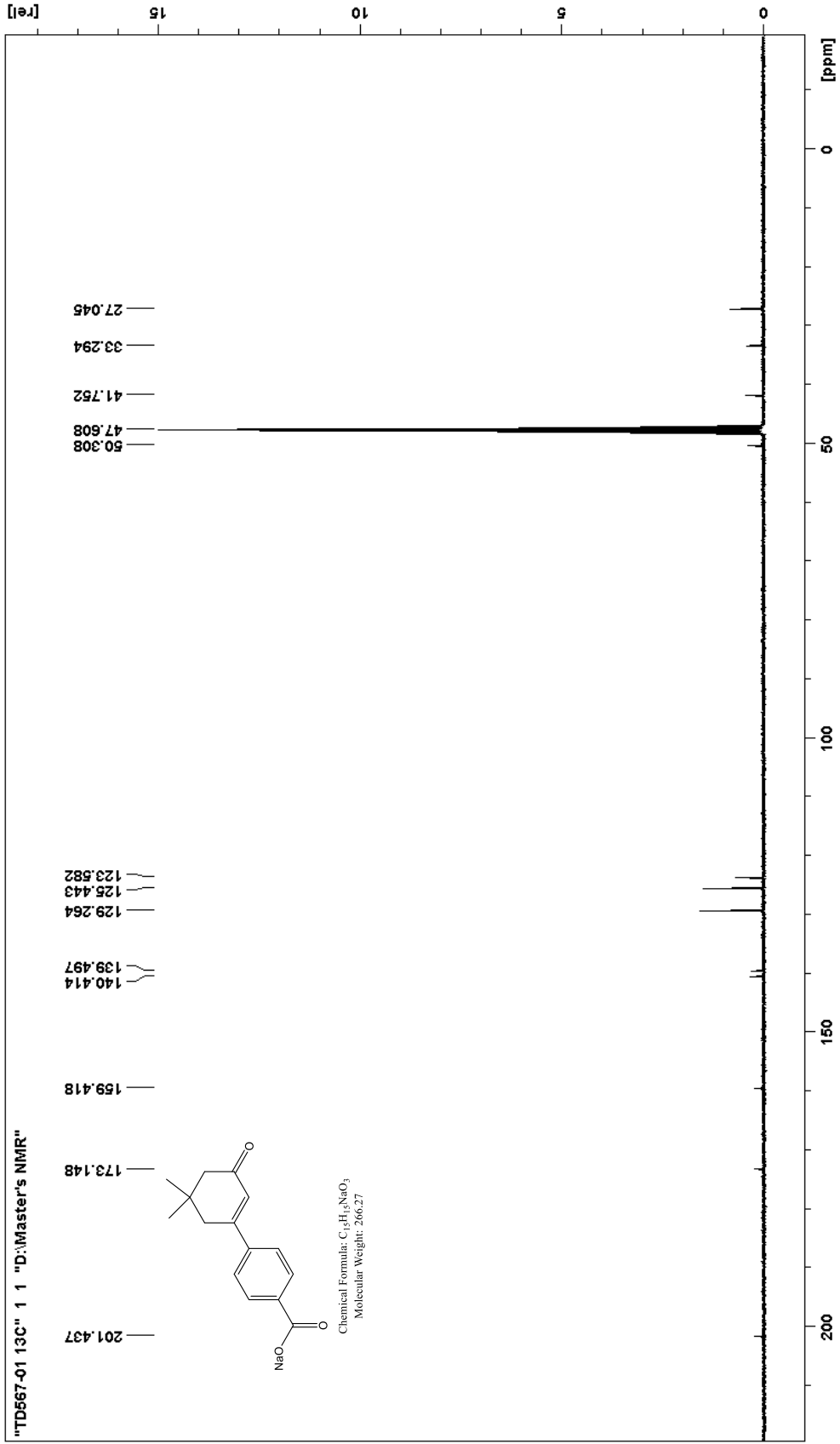
3-(4-carboxyphenyl)-5,5-dimethylcyclohexen-2-one **15** (2.41 g, 9.86 mmol) was stirred in a 0.102 M solution of sodium hydroxide (95 mL, 9.69 mmol). Once the solid was fully dissolved, the solution was transferred to a wide 3 L glass container, and was left to sit at 40°C overnight to fully evaporate. The product was obtained as slightly transparent, light beige crystals (2.64 g, 100%).

**<sup>1</sup>H NMR (400 MHz, MeOD) δ, ppm:** 7.96 (d, J = 8.4 Hz, 2H), 7.59 (d, J = 8.4 Hz, 2H), 6.39 (s, 1H), 2.73 (d, J = 1.2 Hz, 2H), 2.34 (s, 1.7H\*), 1.12 (s, 6H).

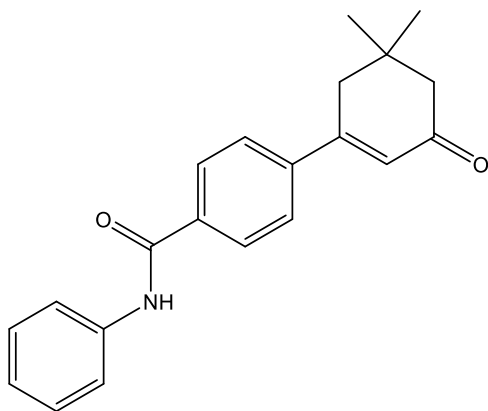
\*This peak integrates lower than the expected 2, due to the proton being slightly acidic and exchanging with deuterium from the solvent.

**<sup>13</sup>C NMR (400 MHz, MeOD) δ, ppm:** 201.44, 173.15, 159.42, 140.41, 139.50, 129.26 (2C), 125.44 (2C), 123.58, 50.30, 41.75, 33.29, 27.05 (2C).





### Preparation of compound 14.



14

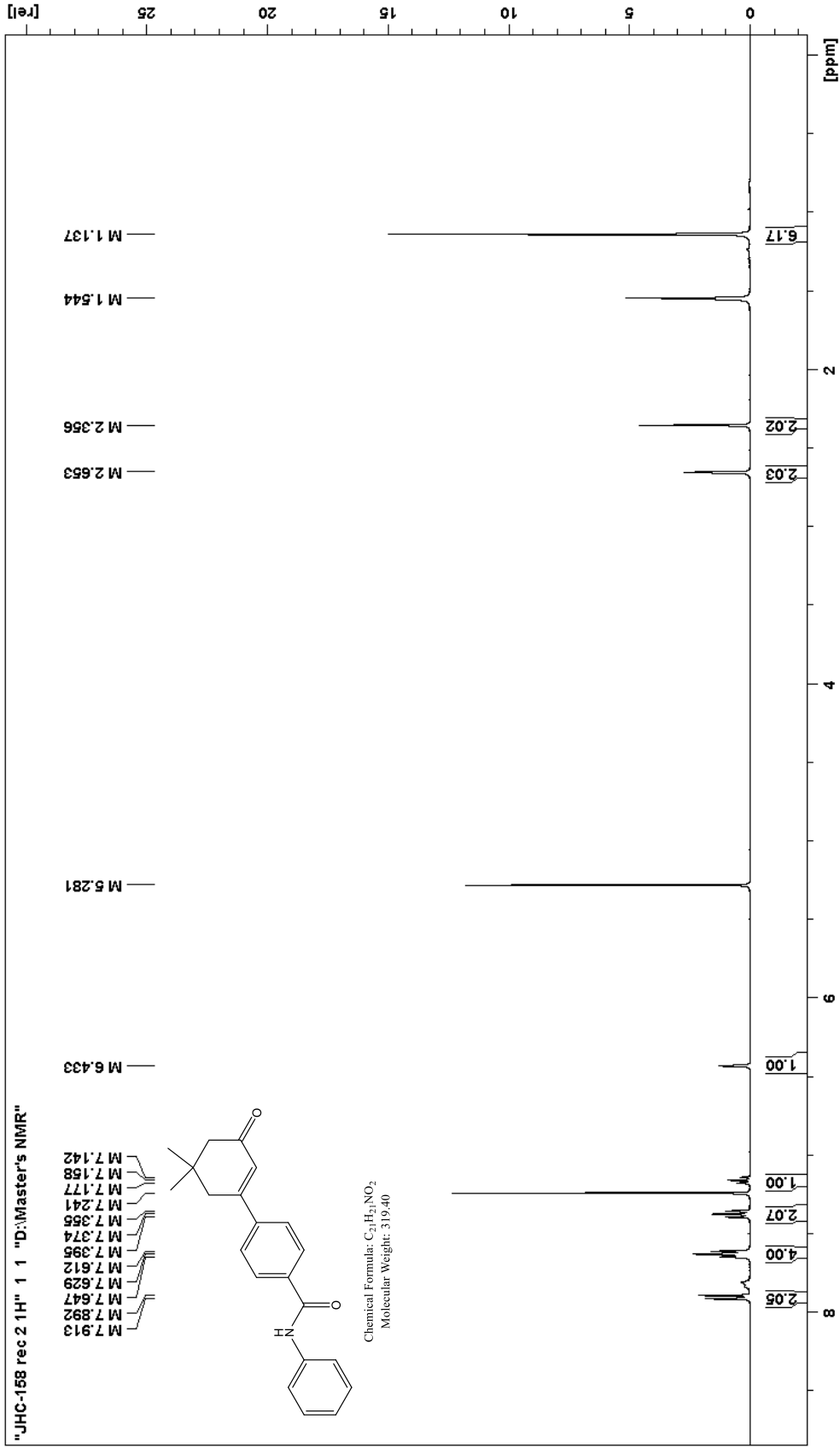
3-(4-Carboxyphenyl)-5,5-dimethylcyclohexen-2-one **15** (0.49 g, 2.00 mmol) was dissolved in DCM (15.0 mL). Aniline (0.20 mL, 2.19 mmol), DMAP (0.31 g, 2.54 mmol) and EDCI (0.49 g, 2.56 mmol) were subsequently added, forming a cloudy white solution. The mixture was refluxed in an oil bath at 70°C for 4h 30min. After the reflux and cooling to room temperature, the solution was washed once with 15 mL of 10% NaOH<sub>(aq)</sub>, and twice with 15 mL of 5% HCl<sub>(aq)</sub>. The organic layer was filtered through a filter paper to remove a white solid in suspension in the solution, dried with MgSO<sub>4</sub> and filtered, and then evaporated in vacuo. The crude product was purified by recrystallisation in a mixture of dichloromethane and hexanes. The purified product was obtained as a white powder (0.33 g, 52%).

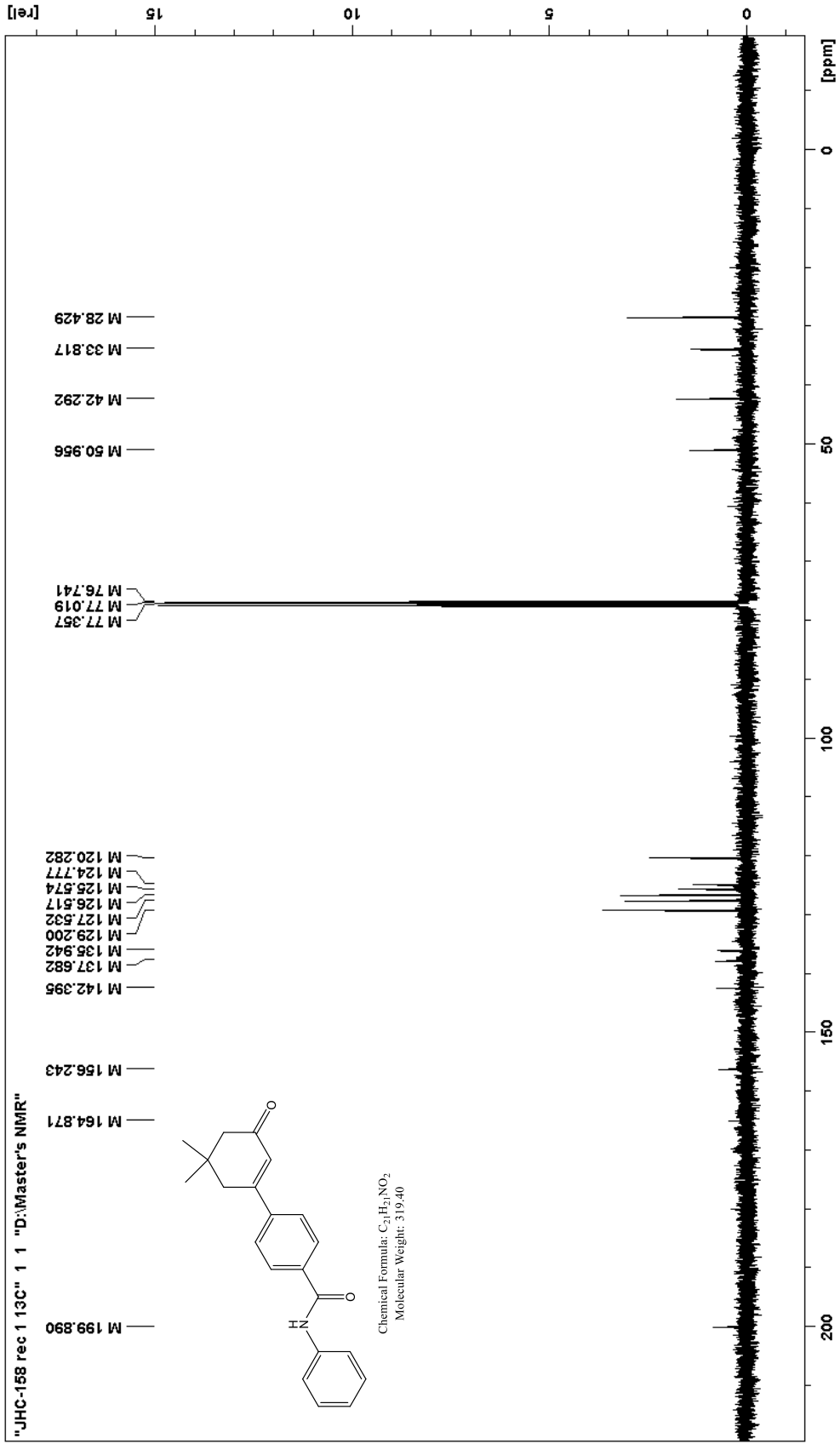
\*Despite drying with magnesium sulfate, evaporating the solvents under vacuum for an appropriate duration, and letting the sample rest under air flow before preparing the sample, presence of water and DCM was still observed by <sup>1</sup>H NMR.

**<sup>1</sup>H NMR (400 MHz, CDCl<sub>3</sub>) δ, ppm:** 7.90 (d, J = 8.4 Hz, 2H), 7.63 (dd, J = 7.2 Hz, 4H), 7.37 (t, J = 8.4 Hz, 2H), 7.158 (t, J = 7.6 Hz, 1H), 2.65 (s, 2H), 2.36 (s, 2H), 1.14 (s, 6H).

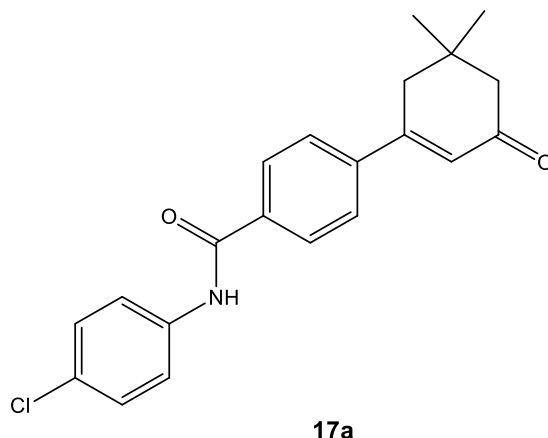
\*The amide proton was not visible in this spectrum.

**<sup>13</sup>C NMR (400 MHz, CDCl<sub>3</sub>) δ, ppm:** 199.89, 164.87, 156.24, 142.40, 137.68, 135.94, 129.20 (2C), 127.53 (2C), 126.52 (2C), 125.57, 124.78, 120.28 (2C), 50.96, 42.29, 33.82, 28.43 (2C).





### Preparation of compound 17a.



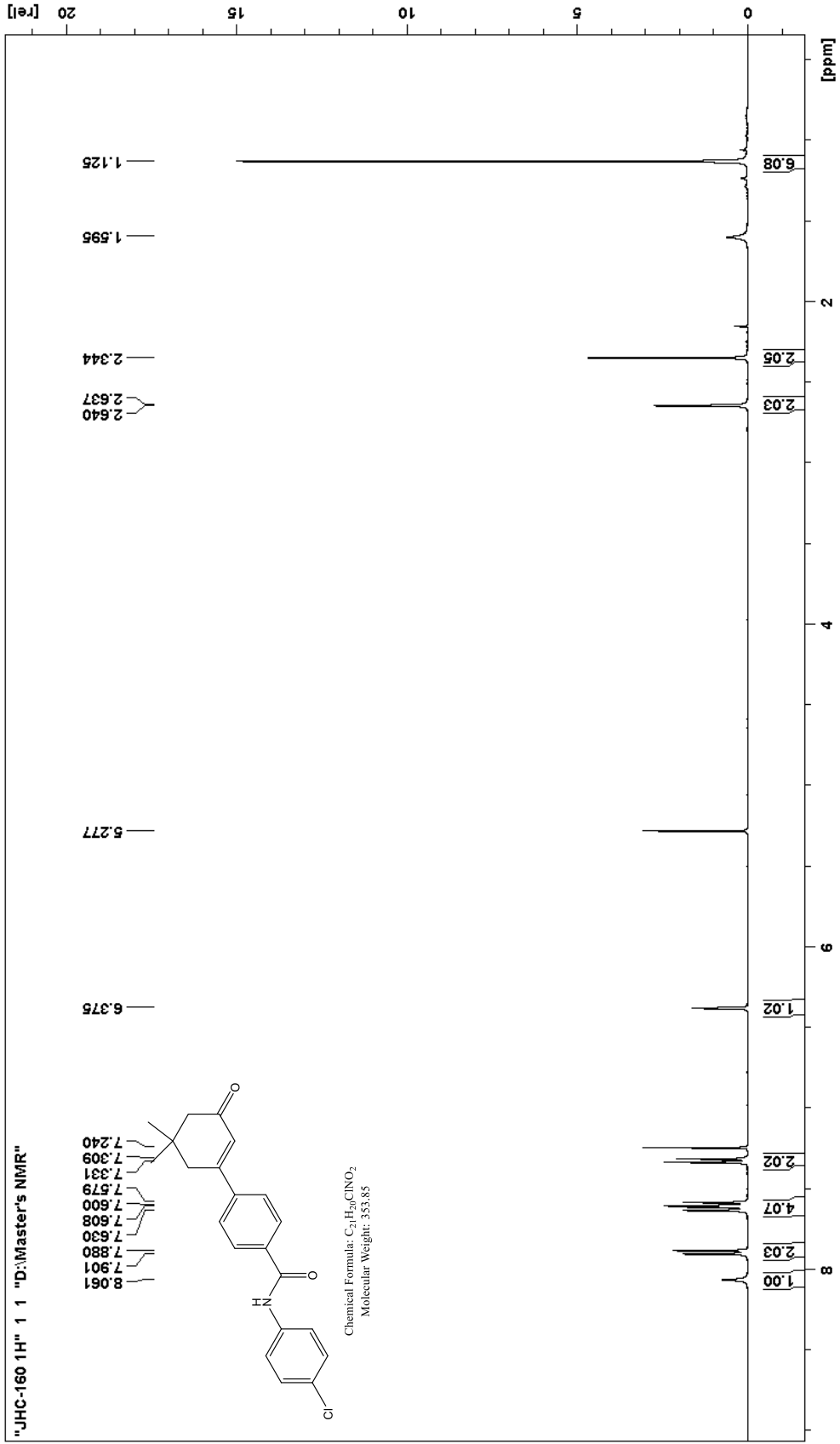
3-(4-carboxyphenyl)-5,5-dimethylcyclohexen-2-one **15** (0.22 g, 0.90 mmol) was dissolved in DCM (15.0 mL). 4-Chloroaniline (0.17 g, 1.33 mmol), DMAP (0.19 g, 1.56 mmol) and EDCI (0.33 g, 1.72 mmol) were subsequently added, forming a cloudy white solution. The mixture was stirred at room temperature for two days. Afterwards, the solution was washed once with 15 mL of 10% NaOH<sub>(aq)</sub> and twice with 15 mL of 5% HCl<sub>(aq)</sub>. The organic layer was filtered through a filter paper to remove a white solid in suspension in the solution, dried with MgSO<sub>4</sub> and filtered, and then evaporated in vacuo. The crude product was purified by recrystallisation in a mixture of dichloromethane and hexanes. The purified product was obtained as a white powder (46.9 mg, 15%).

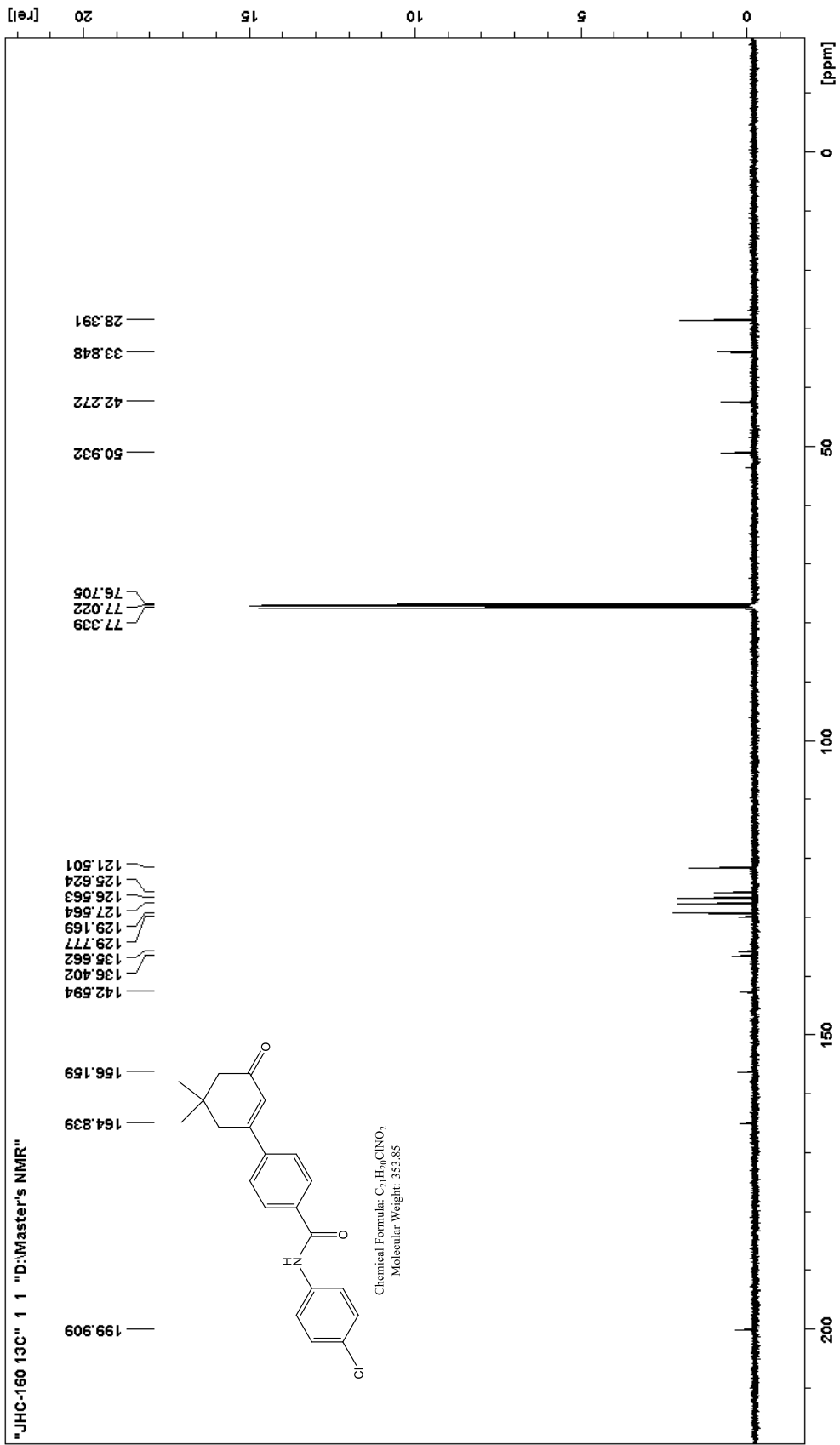
\*Despite drying with magnesium sulfate, evaporating the solvents under vacuum for an appropriate duration, and letting the sample rest under air flow before preparing the sample, presence of water and DCM was still observed by <sup>1</sup>H NMR.

**<sup>1</sup>H NMR (400 MHz, CDCl<sub>3</sub>) δ, ppm:** 8.06 (s, 1H), 7.89 (d, J = 8.4 Hz, 2H), 7.60 (dd, J<sub>1</sub> = 8.8 Hz, J<sub>2</sub> = 12.0 Hz, 4H), 7.32 (d, J = 8.4 Hz, 2H), 6.38 (s, 1H), 2.64 (d, J = 1.2 Hz, 2H), 2.34 (s, 2H), 1.13 (s, 6H).

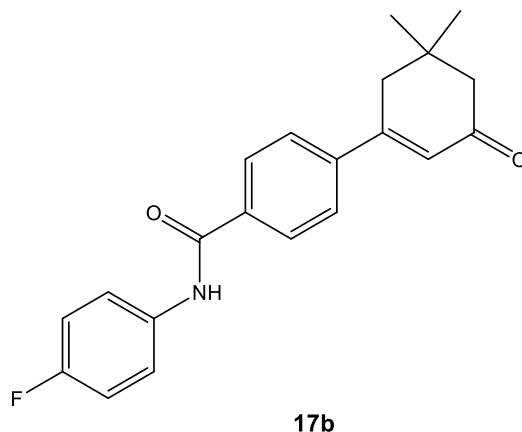
**<sup>13</sup>C NMR (400 MHz, CDCl<sub>3</sub>) δ, ppm:** 199.91, 164.84, 156.16, 142.59, 136.40, 135.66, 129.78, 129.17 (2C), 127.56 (2C), 126.56 (2C), 125.62, 121.50 (2C), 50.93, 42.27, 33.85, 28.39 (2C).

**HRMS-EI m/z:** M<sup>+</sup> calcd for C<sub>21</sub>H<sub>20</sub>ClNO<sub>2</sub>, 353.1183; found, 353.1182.





### Preparation of compound 17b.



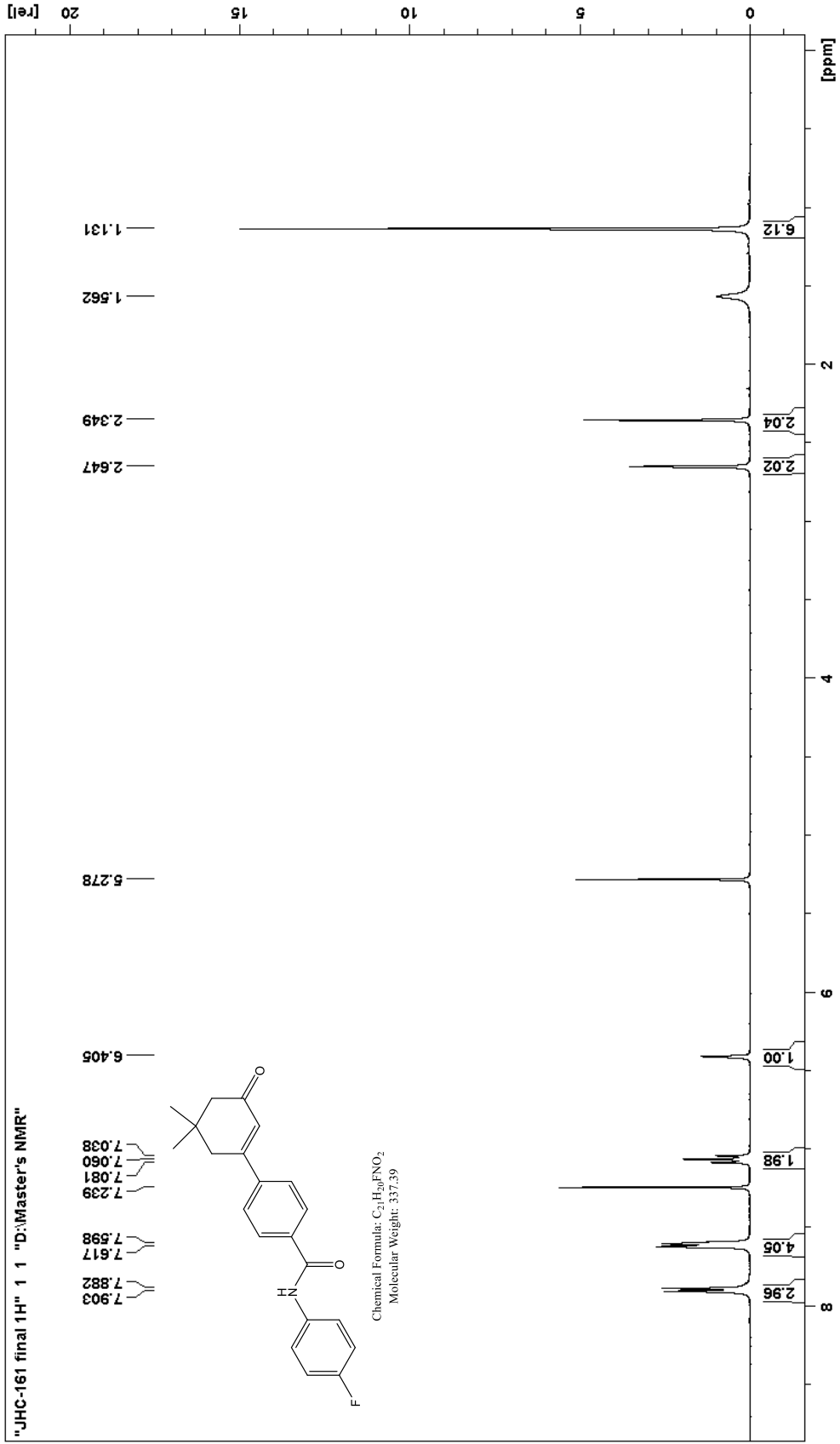
3-(4-carboxyphenyl)-5,5-dimethylcyclohexen-2-one **15** (0.17 g, 0.70 mmol) was dissolved in DCM (15.0 mL). 4-Fluoroaniline (0.08 mL, 0.84 mmol), DMAP (0.12 g, 0.98 mmol) and EDCI (0.20 g, 1.04 mmol) were subsequently added, forming a cloudy white solution. The mixture was stirred at room temperature for two days. Afterwards, the solution was washed once with 15 mL of 10% NaOH<sub>(aq)</sub> and twice with 15 mL of 5% HCl<sub>(aq)</sub>. The organic layer was filtered through a filter paper to remove a white solid in suspension in the solution, dried with MgSO<sub>4</sub> and filtered, and then evaporated in vacuo. The crude product was purified by recrystallisation in a mixture of dichloromethane and hexanes. The purified product was obtained as a white powder (50.4 mg, 21%).

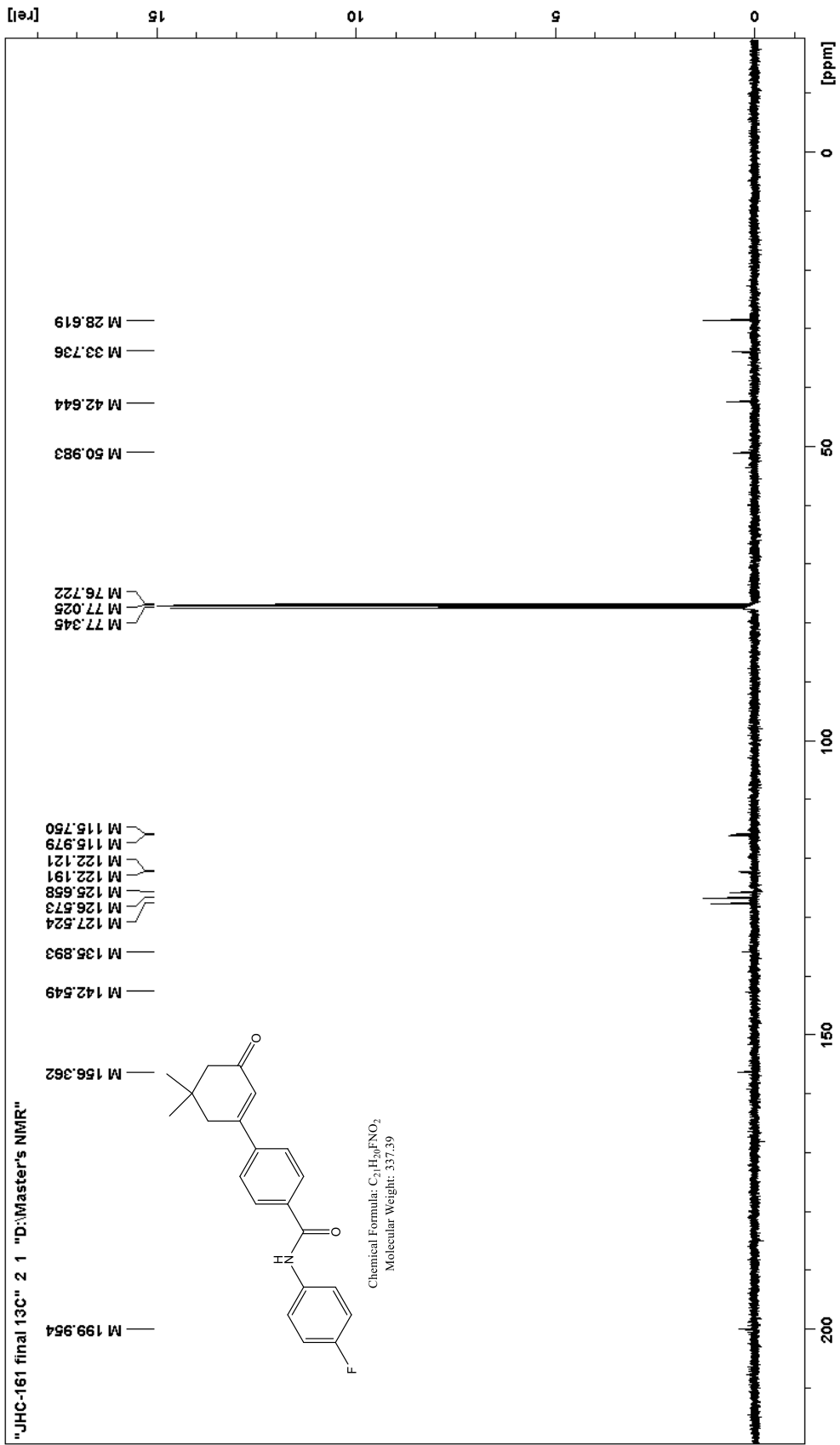
\*Despite drying with magnesium sulfate, evaporating the solvents under vacuum for an appropriate duration, and letting the sample rest under air flow before preparing the sample, presence of water and DCM was still observed by <sup>1</sup>H NMR.

**<sup>1</sup>H NMR (400 MHz, CDCl<sub>3</sub>) δ, ppm:** 7.89 (d, J = 8.4 Hz, 3H), 7.61 (m, J = 7.6 Hz, 4H), 7.06 (t, J = 8.4 Hz, 2H), 6.41 (s, 1H), 2.65 (s, 2H), 2.35 (s, 2H), 1.13 (s, 6H).

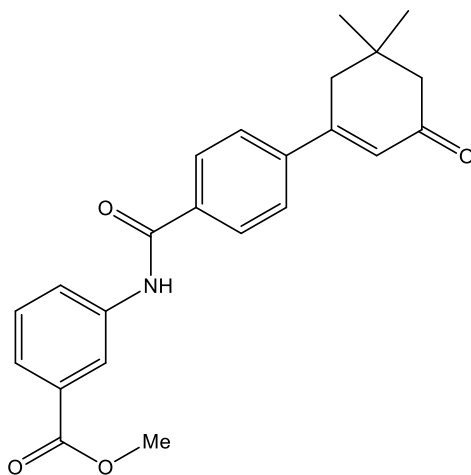
**<sup>13</sup>C NMR (400 MHz, CDCl<sub>3</sub>) δ, ppm:** 199.95, 156.36, 142.55, 135.89, 127.52 (2C), 126.57 (2C), 125.66 (2C), 122.19, 122.12, 11.98, 115.75, 50.98, 42.64, 33.74, 28.62 (2C).

\*The quaternary carbons were difficult to locate due to the low concentration of the sample.





### Preparation of compound 17c.



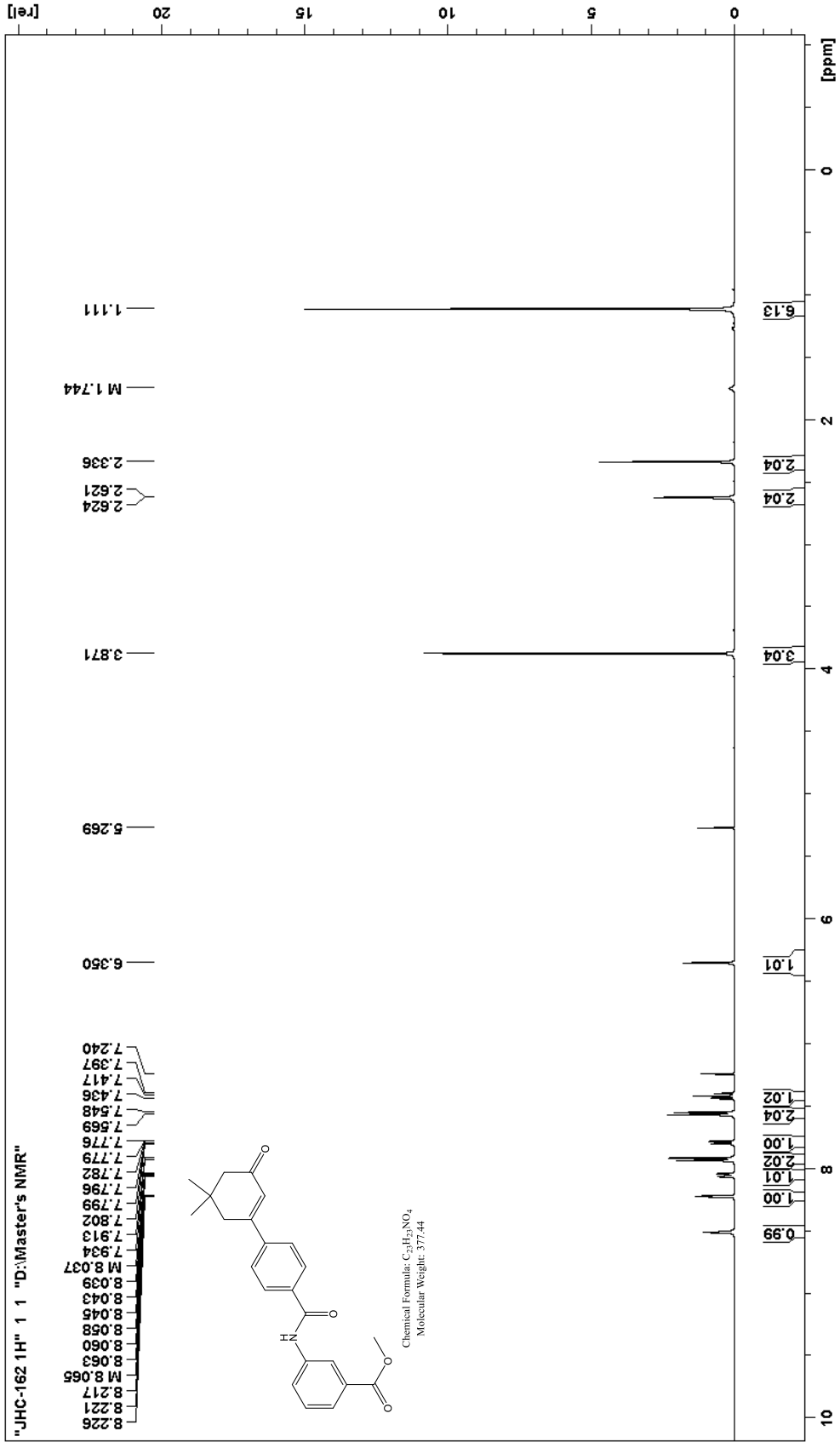
17c

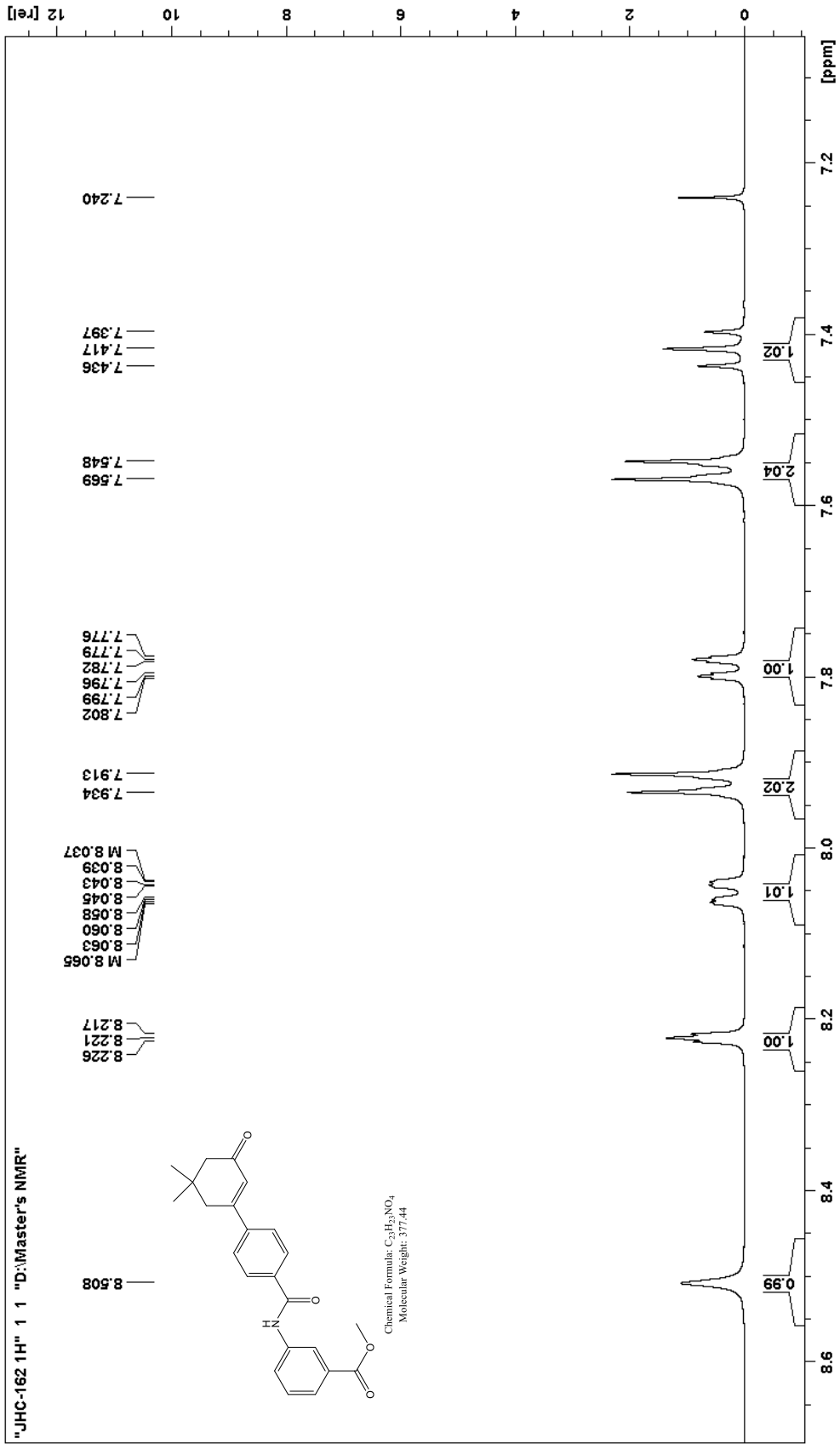
3-(4-Carboxyphenyl)-5,5-dimethylcyclohexen-2-one **15** (0.14 g, 0.57 mmol) was dissolved in DCM (15.0 mL). Methyl 3-aminobenzoate (0.12 g, 0.79 mmol), DMAP (0.12 g, 0.98 mmol) and EDCI (0.16 g, 0.84 mmol) were subsequently added, forming a cloudy white solution. The mixture was stirred at room temperature for two days. Afterwards, the solution was washed once with 15 mL of 10% NaOH<sub>(aq)</sub> and twice with 15 mL of 5% HCl<sub>(aq)</sub>. The organic layer was filtered through a filter paper to remove a white solid in suspension in the solution, dried with MgSO<sub>4</sub> and filtered, and then evaporated in vacuo. The product was obtained as a white powder (0.25 g, 116%), without additional purification steps.

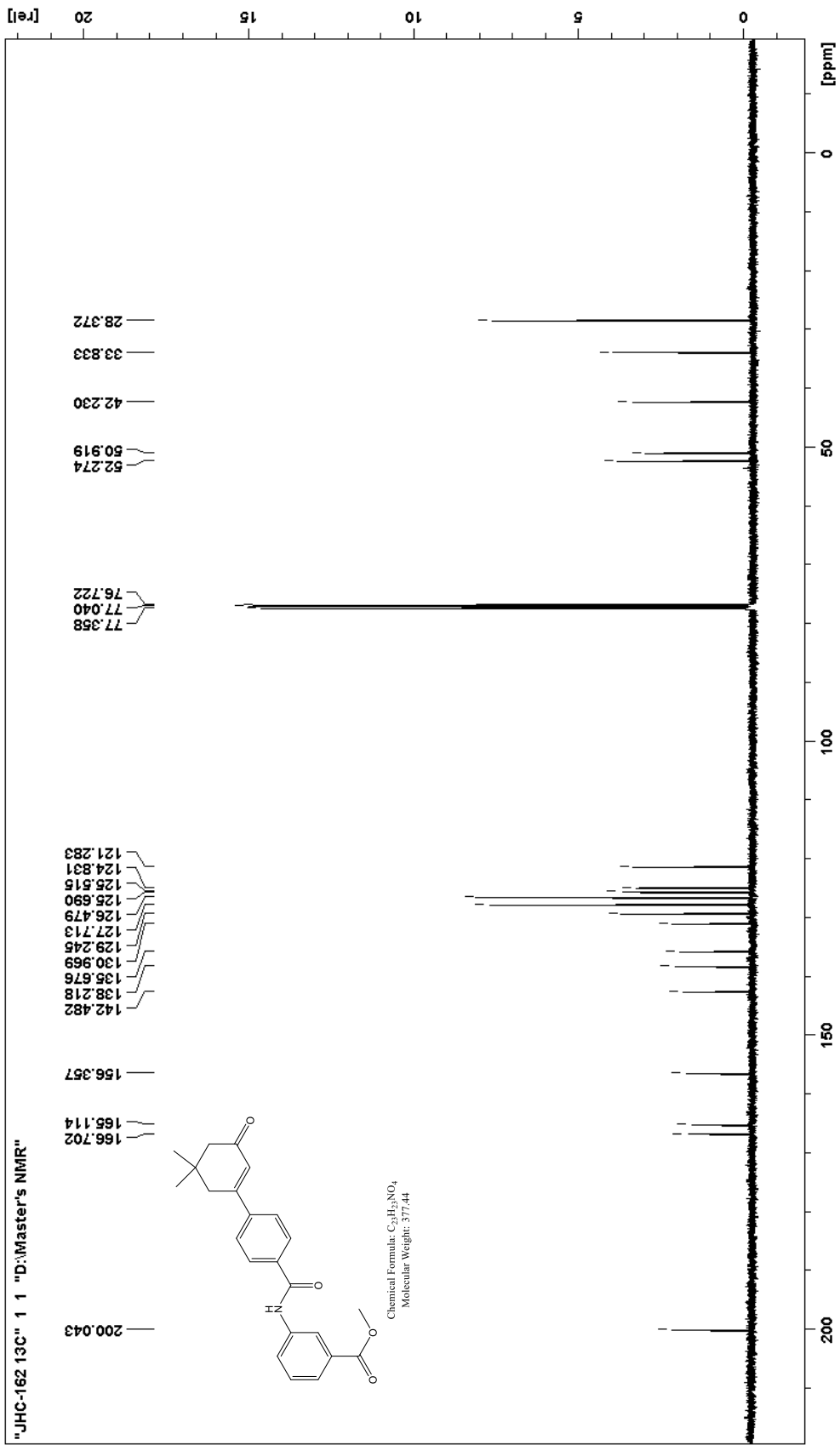
\*A small amount of DCM and water remained in the sample. The impurity causing the yield above 100% was possibly due to residues of MgSO<sub>4</sub> improperly filtered, as no additional impurities were detected by <sup>1</sup>H and <sup>13</sup>C NMR or by TLC.

**<sup>1</sup>H NMR (400 MHz, CDCl<sub>3</sub>) δ, ppm:** 8.51 (s, 1H), 8.22 (t, J = 2.0 Hz, 1H), 8.05 (dq, J<sub>1</sub> = 8.4 Hz, J<sub>2</sub> = 0.8 Hz, 1H), 7.92 (d, J = 8.4 Hz, 2H), 7.789 (dt, J<sub>1</sub> = 8.0 Hz, J<sub>2</sub> = 1.2 Hz), 7.55 (d, J = 8.4 Hz), 7.42 (t, J = 8.0 Hz, 1H), 6.35 (s, 1H), 3.87 (s, 3H), 2.62 (d, J = 1.2 Hz, 2H), 2.34 (s, 2H), 1.11 (s, 6H)

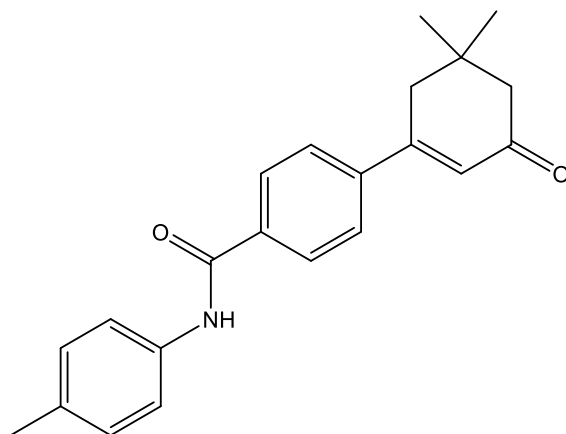
**<sup>13</sup>C NMR (400 MHz, CDCl<sub>3</sub>) δ, ppm:** 200.04, 166.70, 165.11, 156.36, 142.48, 138.22, 135.68, 130.97, 129.25, 127.71 (2C), 126.48 (2C), 125.69, 125.52, 124.83, 121.28, 52.27, 50.92, 42.23, 33.83, 28.37 (2C).







### Preparation of compound 17d.



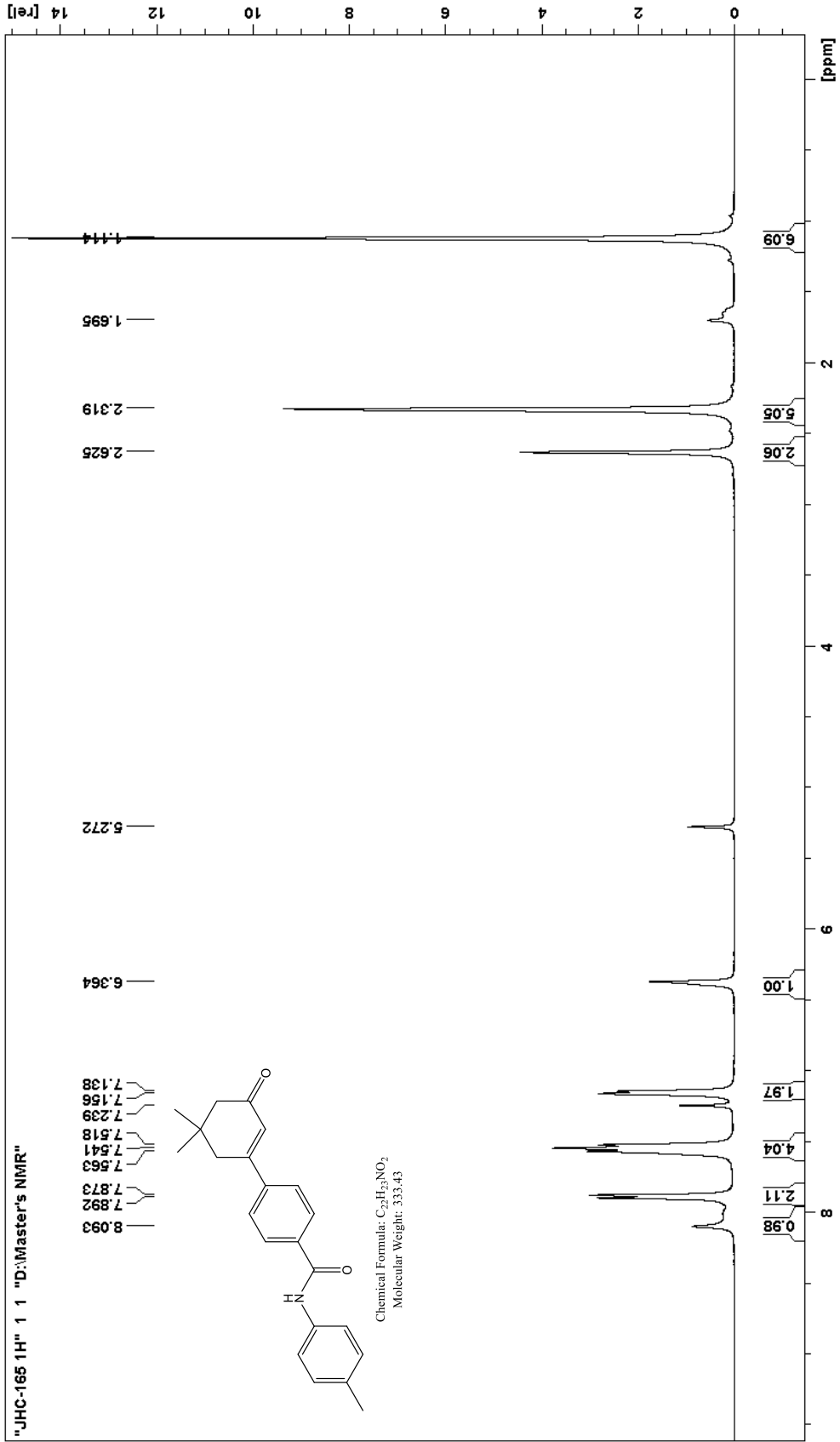
**17d**

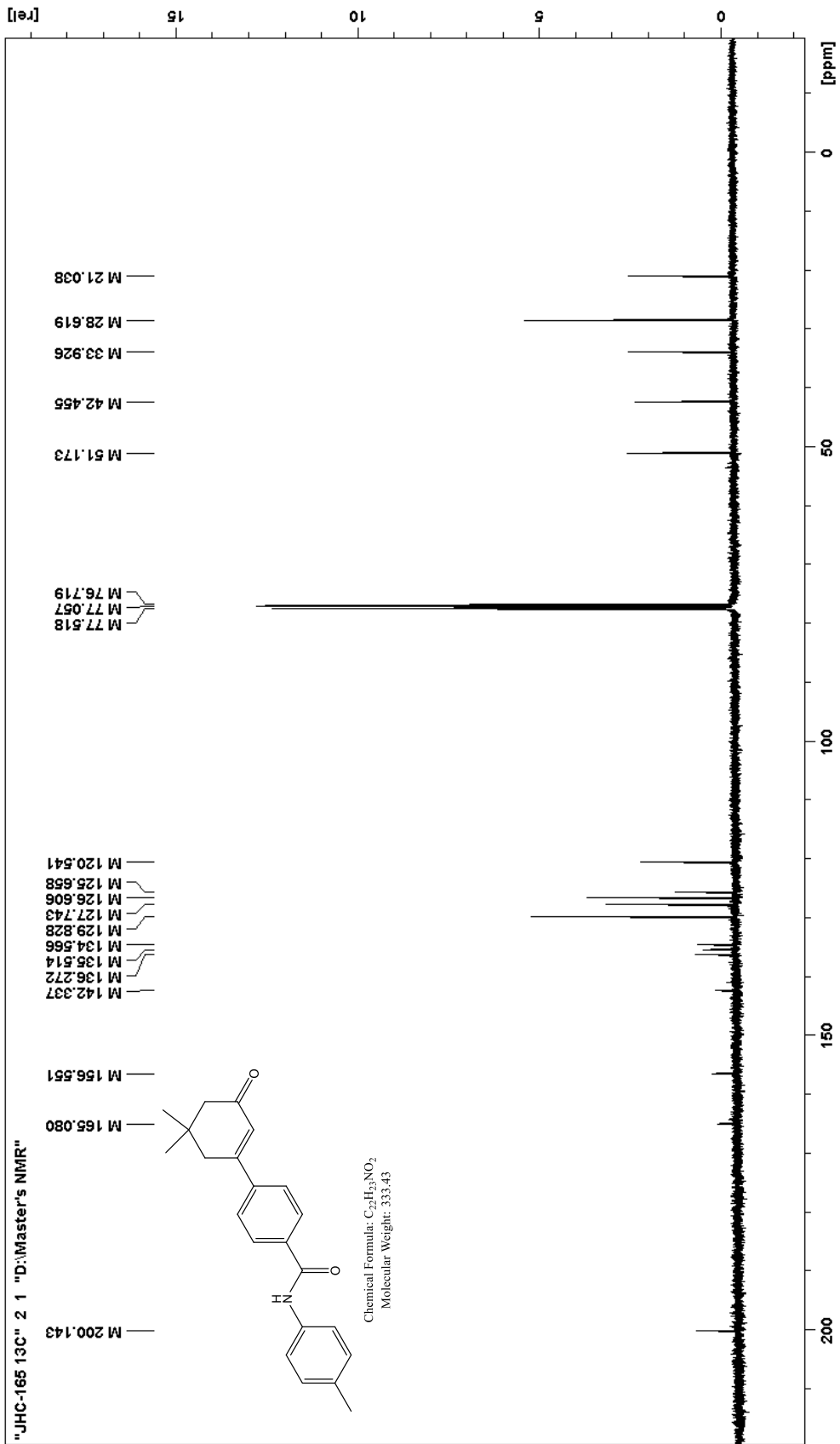
3-(4-carboxyphenyl)-5,5-dimethylcyclohexen-2-one **15** (0.19 g, 0.78 mmol) was dissolved in DCM (15.0 mL). p-Toluidine (0.11 g, 1.02 mmol), DMAP (0.15 g, 1.23 mmol) and EDCI (0.25 g, 0.1.30 mmol) were subsequently added, forming a cloudy white solution. The mixture was stirred at room temperature overnight. Afterwards, the solution was washed once with 15 mL of 10% NaOH<sub>(aq)</sub> and twice with 15 mL of 5% HCl<sub>(aq)</sub>. The organic layer was dried with MgSO<sub>4</sub> and filtered, then evaporated under reduced pressure. The product was dissolved in dichloromethane and partially recrystallized by addition of hexanes, yielding a white solid (95 mg, 37%).

\*A small amount of DCM and water remained in the sample.

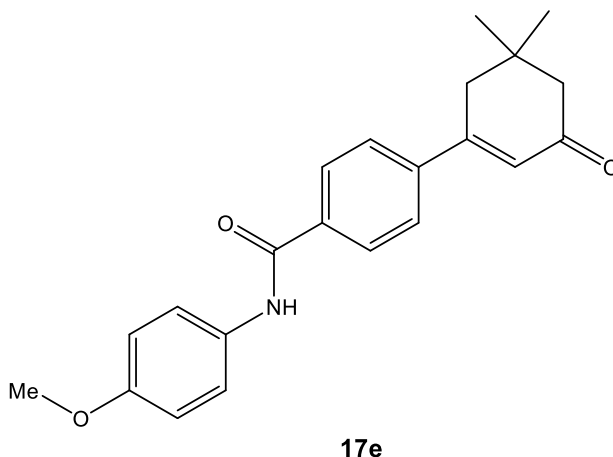
**<sup>1</sup>H NMR (400 MHz, CDCl<sub>3</sub>) δ, ppm:** 8.09 (s, 1H), 7.88 (d, J = 7.6 Hz, 2H), 7.54 (m, J = 8.8 Hz, 4H), 7.15 (d, J = 7.2 Hz, 2H), 6.36 (s, 1H), 2.63 (s, 2H), 2.32 (s, 5H), 1.11 (s, 6H).

**<sup>13</sup>C NMR (400 MHz, CDCl<sub>3</sub>) δ, ppm:** 200.14, 165.08, 156.55, 142.34, 136.27, 135.51, 134.57, 129.83 (2C), 127.74 (2C), 126.61 (2C), 125.66, 120.54 (2C), 51.17, 42.46, 33.93, 28.62 (2C), 21.04.





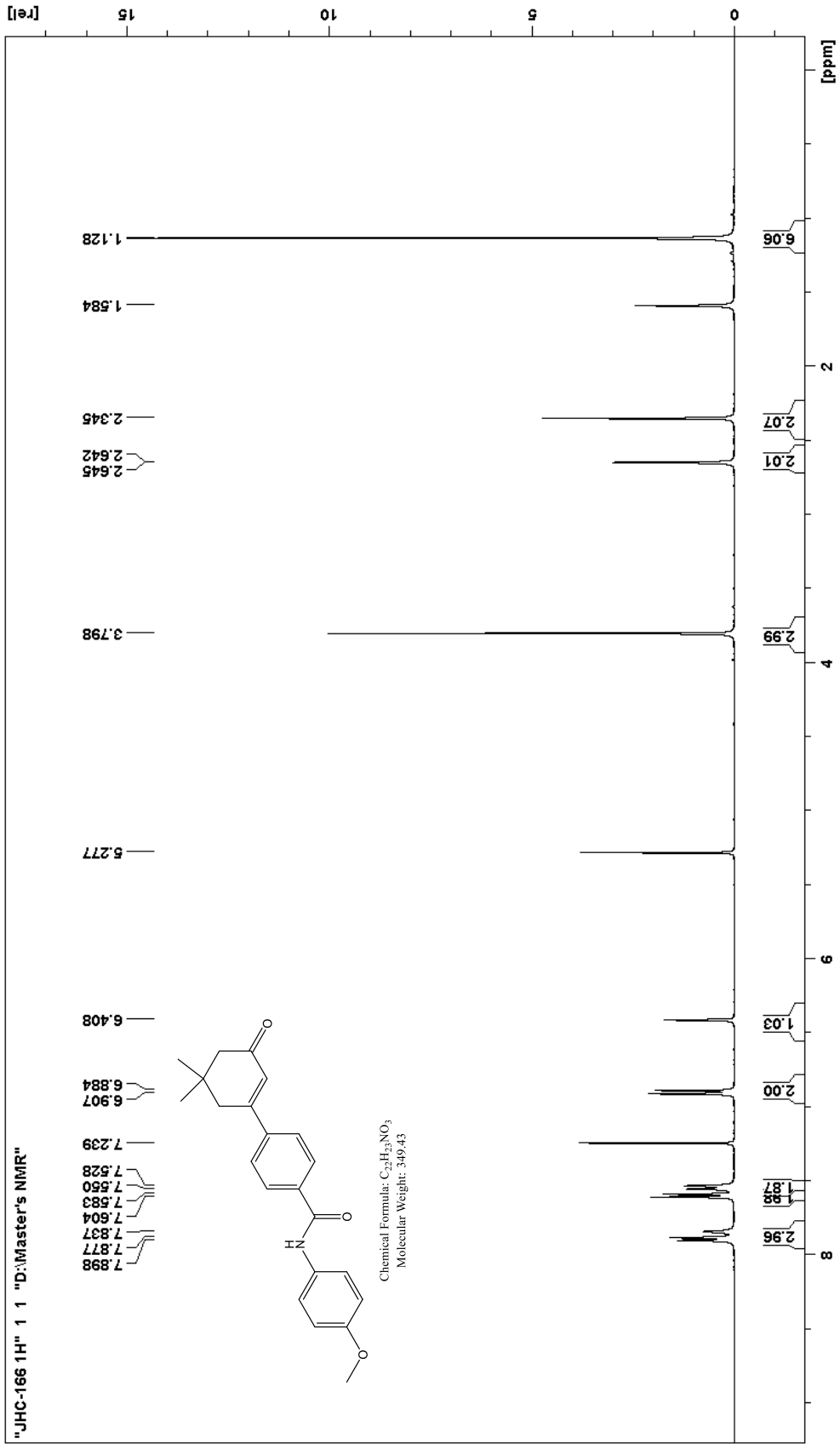
### Preparation of compound 17e.

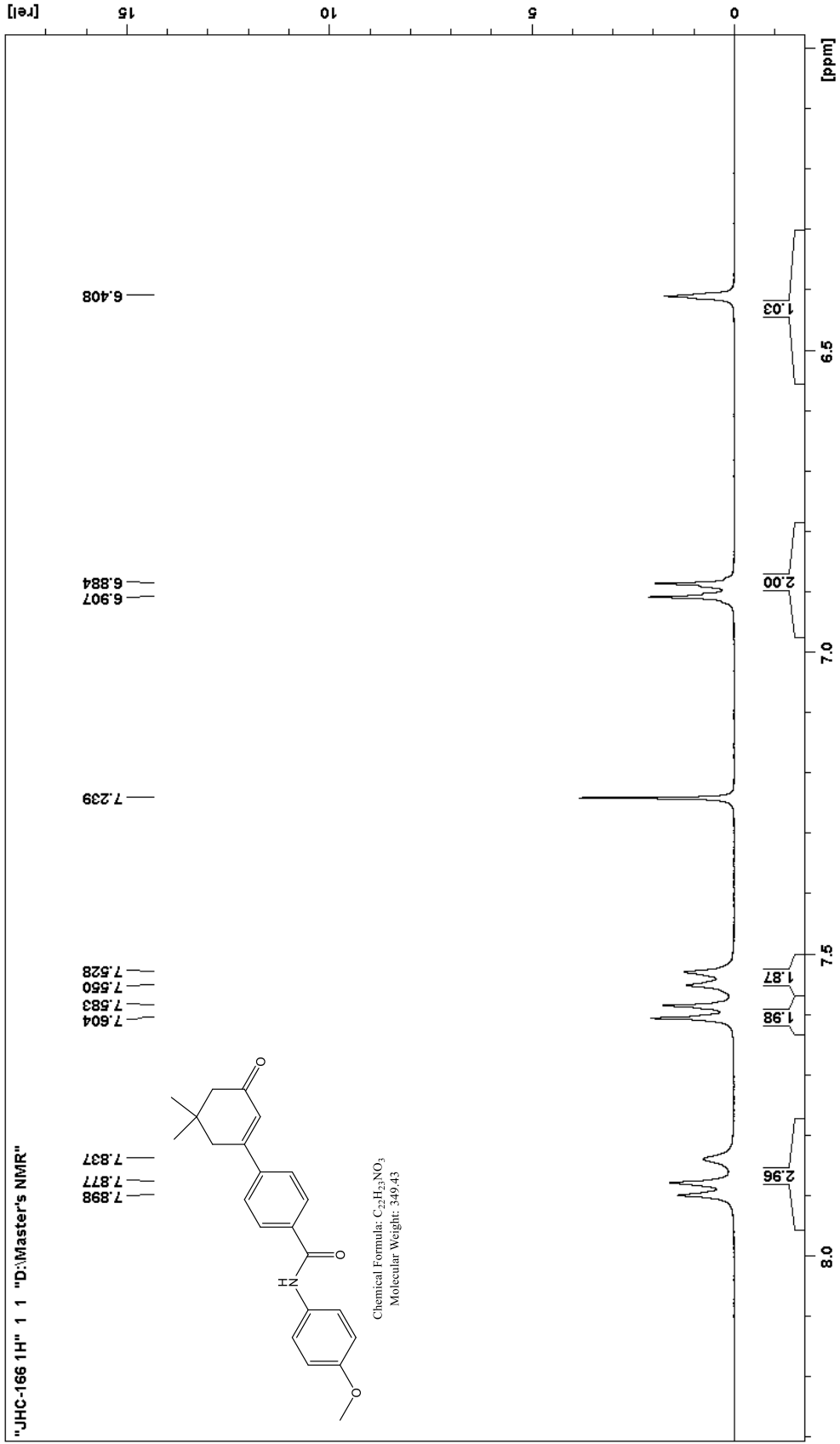


3-(4-carboxyphenyl)-5,5-dimethylcyclohexen-2-one **15** (0.22 g, 0.90 mmol) was dissolved in DCM (15.0 mL). p-Anisidine (0.16 g, 1.29 mmol), DMAP (0.16 g, 1.31 mmol) and EDCI (0.26 g, 0.1.36 mmol) were subsequently added, forming a cloudy white solution. The mixture was stirred at room temperature overnight. Afterwards, the solution was washed once with 15 mL of 10% NaOH<sub>(aq)</sub> and twice with 15 mL of 5% HCl<sub>(aq)</sub>. The organic layer was dried with MgSO<sub>4</sub> and filtered, then evaporated under reduced pressure. The product was dissolved in dichloromethane and partially recrystallized by addition of hexanes, yielding a white solid (0.139 g, 44%).

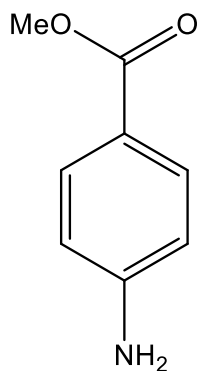
\*A small amount of DCM and water remained in the sample.

**<sup>1</sup>H NMR (400 MHz, CDCl<sub>3</sub>) δ, ppm:** 7.89 (d, J = 8.4 Hz, 2H), 7.84 (s, 1H), 7.59 (d, J = 8.4 Hz, 2H), 7.54 (d, J = 8.8 Hz, 2H), 6.90 (d, J = 9.2 Hz, 2H), 6.41 (s, 1H), 3.80 (s, 3H), 2.64 (d, J = 1.2 Hz, 2H), 2.35 (s, 2H), 1.13 (s, 6H).



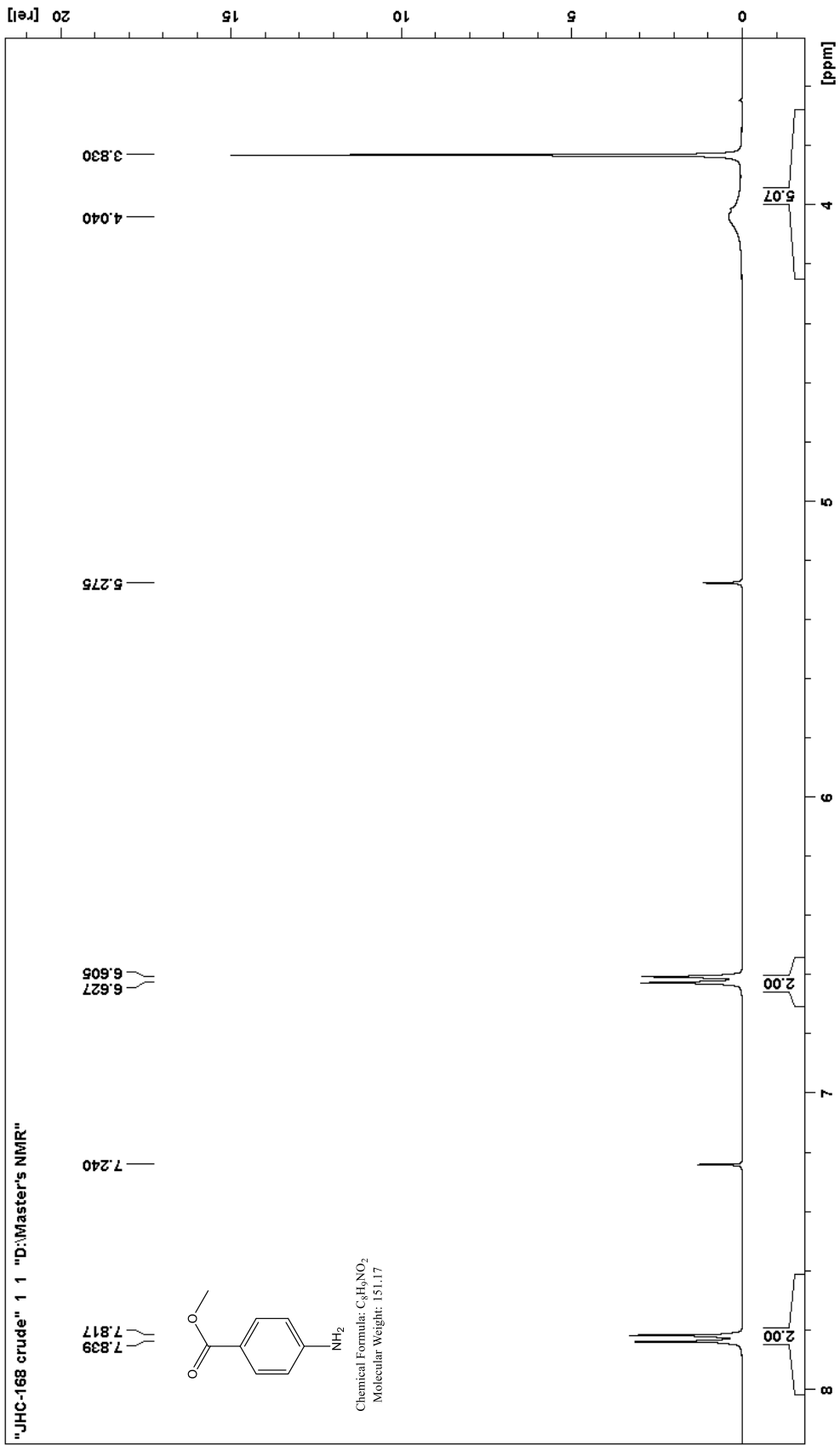


### Preparation of methyl 4-aminobenzoate

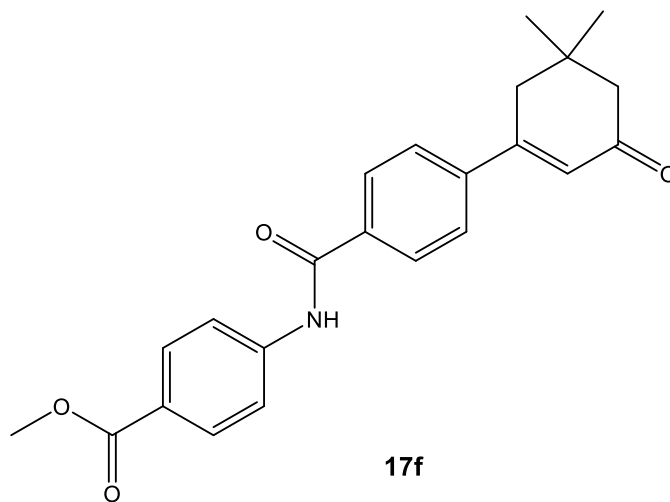


p-Aminobenzoic acid (1.26 g, 9.19 mmol) was dissolved partially in methanol (10 mL). Concentrated sulfuric acid was added to the solution, which was then refluxed in an oil bath at 70°C for three hours, then stirred at 50°C overnight. No undissolved solids remained in solution at the end of the reaction. The solution was diluted with a large volume of water and extracted to DCM. The organic layer was washed once with a 5% NaOH solution, then dried over MgSO<sub>4</sub> and filtered. The solvent was evaporated under reduced pressure, yielding the product as a white powder (0.31 g, 22%).

<sup>1</sup>H NMR (400 MHz, CDCl<sub>3</sub>) δ, ppm: 7.83 (d, J = 8.8 Hz, 2H), 6.62 (d, J = 8.8 Hz, 2H), 4.04 (s, 2H), 3.83 (s, 3H).



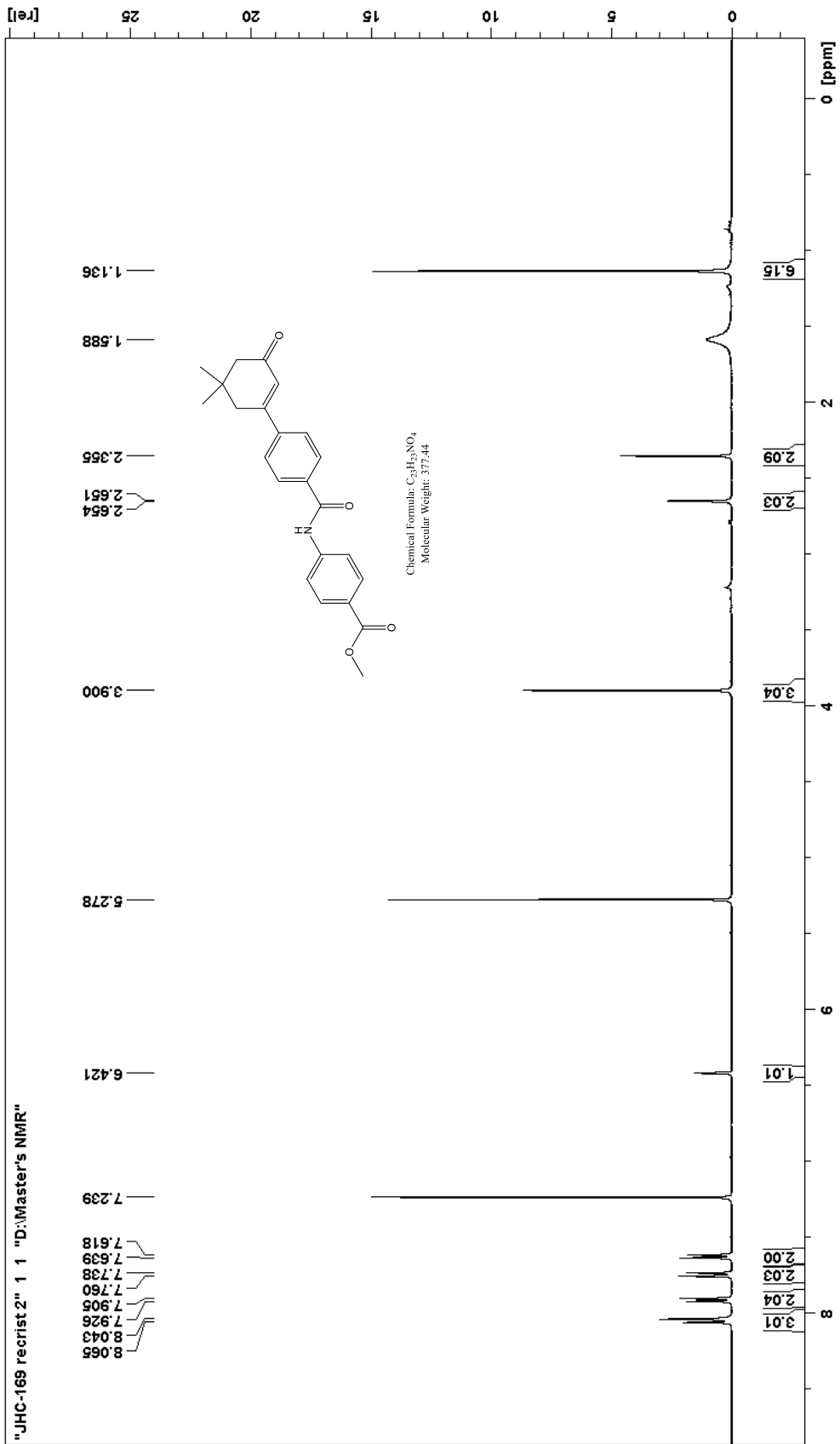
### Preparation of compound 17f.



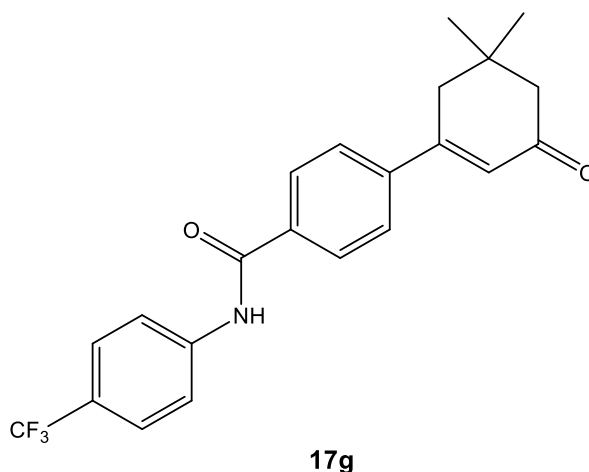
Methyl 4-aminobenzoate (0.31 g, 2.05 mmol) was mixed with 3-(4-carboxyphenyl)-5,5-dimethylcyclohexen-2-one **15** (0.35 g, 1.43 mmol) in DCM. DMAP (0.26 g, 2.13 mmol) and EDCI (0.44 g, 2.29 mmol) were added to the mixture, which was stirred at room temperature overnight. As product crystals started forming over the course of the reaction, the mixture was chilled in the freezer to promote the crystallization. The solid was then filtered out by gravity. Further product was obtained from the filtered solution by partially evaporating the solvent under air flow, and addition of hexanes. Both crops were combined. The crystals of product were obtained in the form of long white needles (315.6 mg, 58%).

\*A significant amount of DCM and water were still in the sample at the time the NMR were taken.

**<sup>1</sup>H NMR (400 MHz, CDCl<sub>3</sub>) δ, ppm:** 8.05 (d, J = 8.8 Hz, 2H), 7.92 (d, J = 8.4 Hz, 2H), 7.75 (d, J = 8.8 Hz, 2H), 7.63 (d, J = 8.4 Hz, 2H), 6.42 (s, 1H), 3.90 (s, 3H), 2.65 (d, J = 1.2 Hz, 2H), 2.36 (s, 2H), 1.14 (s, 6H).



### Preparation of compound 17g.



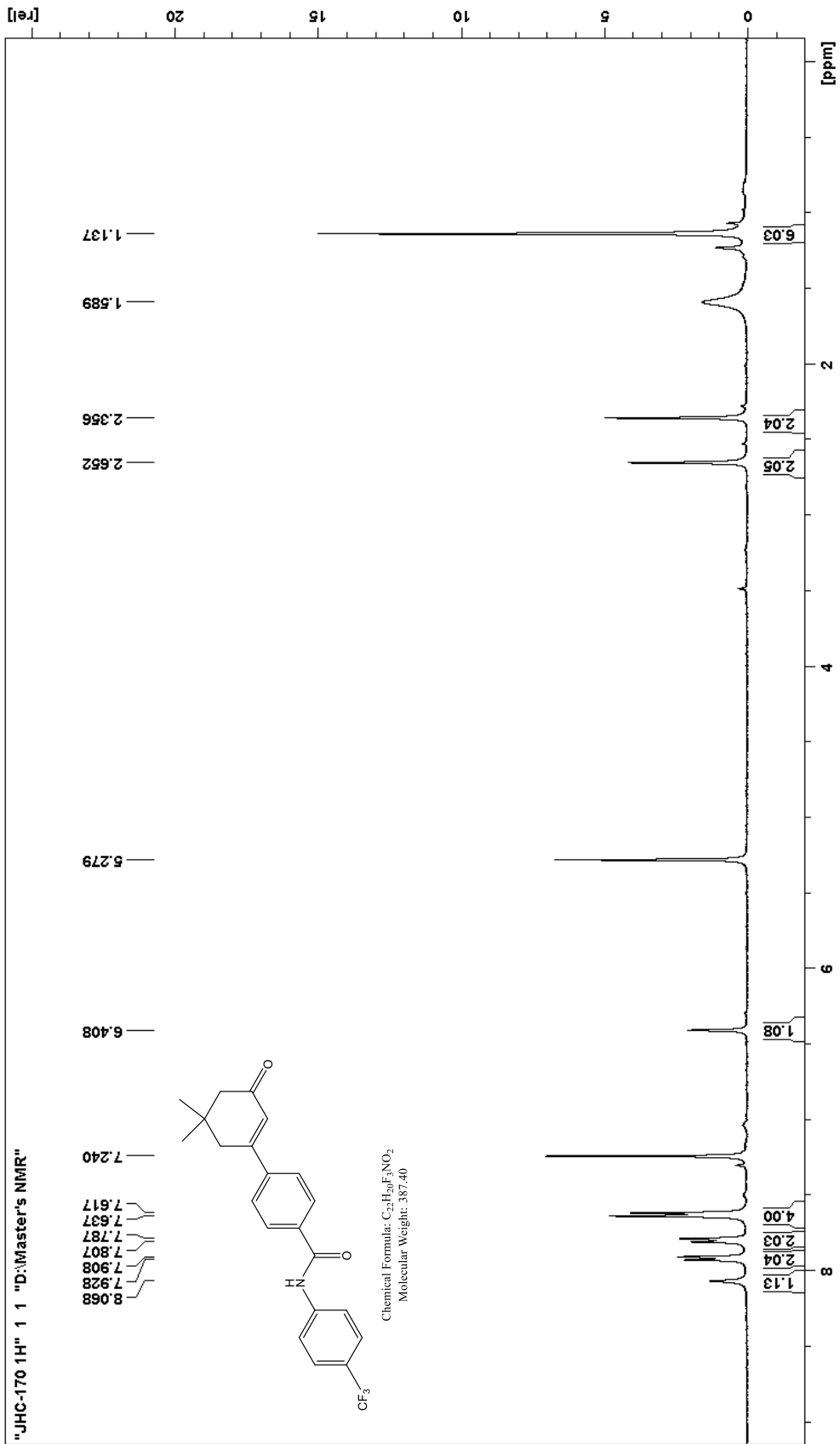
3-(4-carboxyphenyl)-5,5-dimethylcyclohexen-2-one **15** (0.17 g, 0.70 mmol) was dissolved in DCM. 4-trifluoromethylaniline (0.25 mL, 1.99 mmol), DMAP (0.21 g, 1.72 mmol) and EDCI (0.44 g, 2.29 mmol) were added to the mixture, which was stirred at room temperature overnight. The product was quite insoluble and crystallized naturally over the course of the reaction. The product (127 mg, 47%) was obtained as a white powder by a simple suction filtration from the reaction mixture. An additional quantity of product was obtained from concentrating the filtered solution further, however this second crop was contaminated with traces of 4-fluoromethylaniline. This second amount of product (0.09 g, 33%) was not kept, as enough clean product had already been obtained for bioassays.

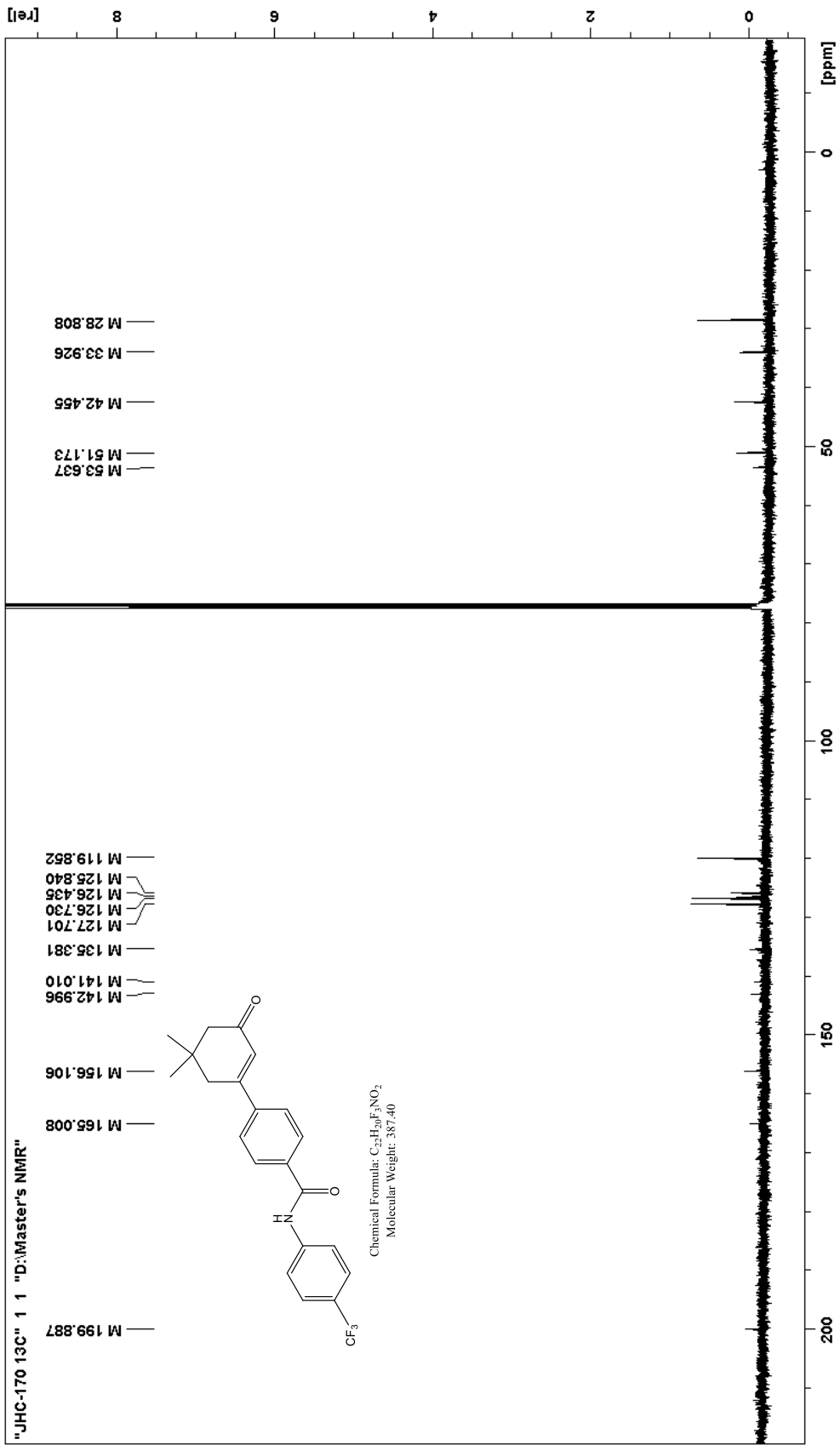
\*A significant amount of DCM and water were still in the sample at the time the NMR were taken.

**<sup>1</sup>H NMR (400 MHz, CDCl<sub>3</sub>) δ, ppm:** 8.07 (s, 1H), 7.92 (d, J = 8.0 Hz, 2H), 7.80 (d, J = 8.0 Hz, 2H), 7.63 (d, J = 8.0 Hz, 4H), 6.41 (s, 1H), 2.65 (s, 2H), 2.36 (s, 2H), 1.14 (s, 6H).

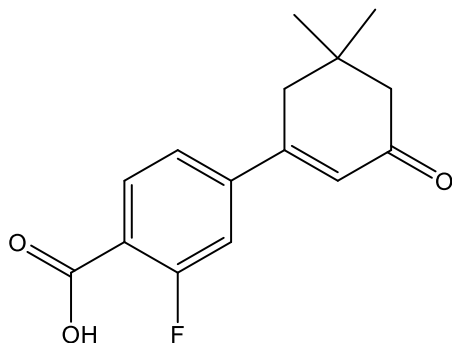
**<sup>13</sup>C NMR (400 MHz, CDCl<sub>3</sub>) δ, ppm:** 199.89, 165.01, 156.11, 143.00, 141.01, 135.38, 127.70 (2C), 126.73 (2C), 126.45, 126.41, 125.84 (2C), 119.85 (2C), 53.64, 51.17, 42.46, 33.93, 28.81 (2C).

\*The quaternary carbons were very difficult to detect due to the low solubility of the compound.





**Preparation of 3-(4-carboxy-2-fluorophenyl)-5,5-dimethylcyclohex-2-enone, 20.**

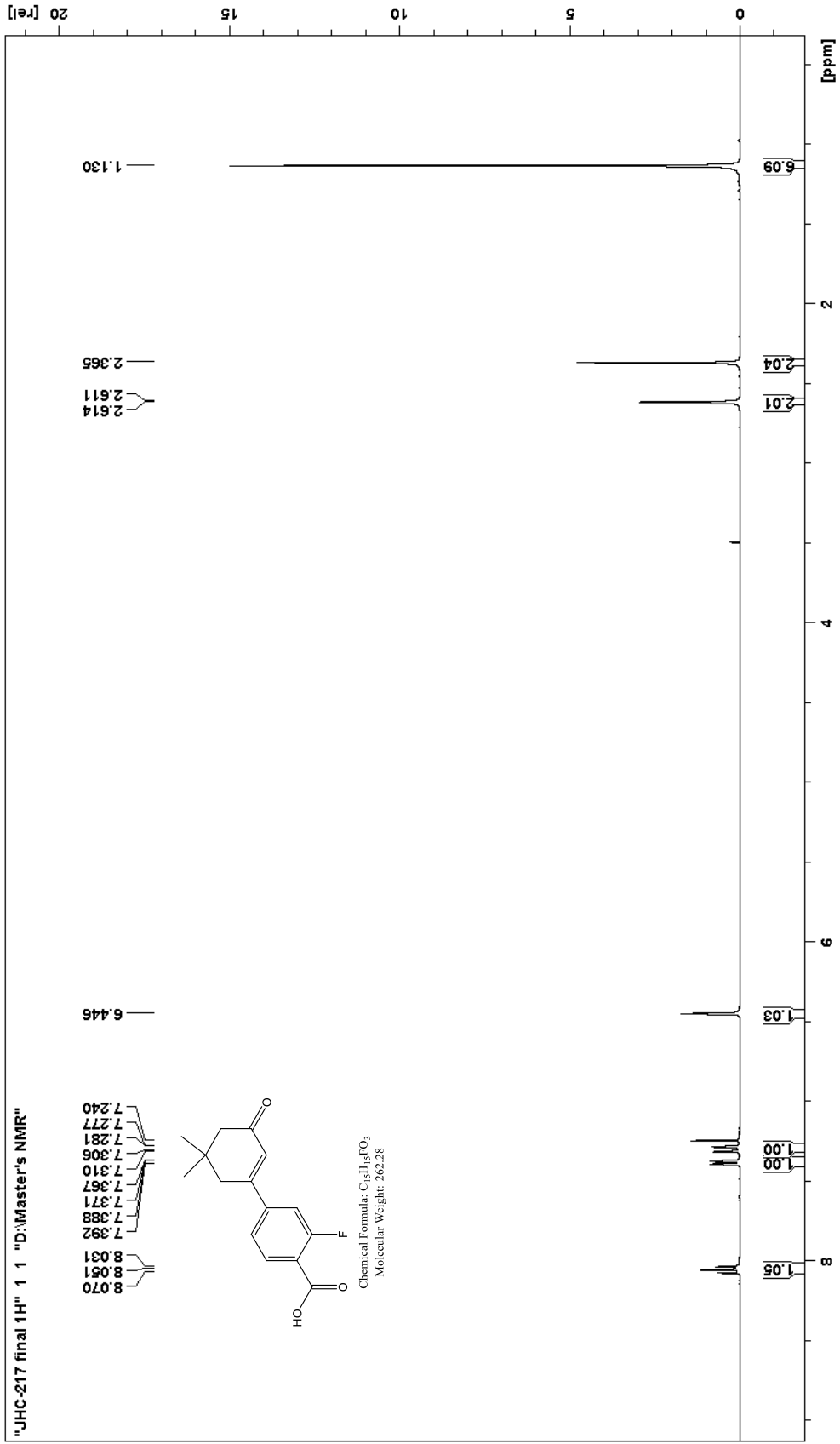


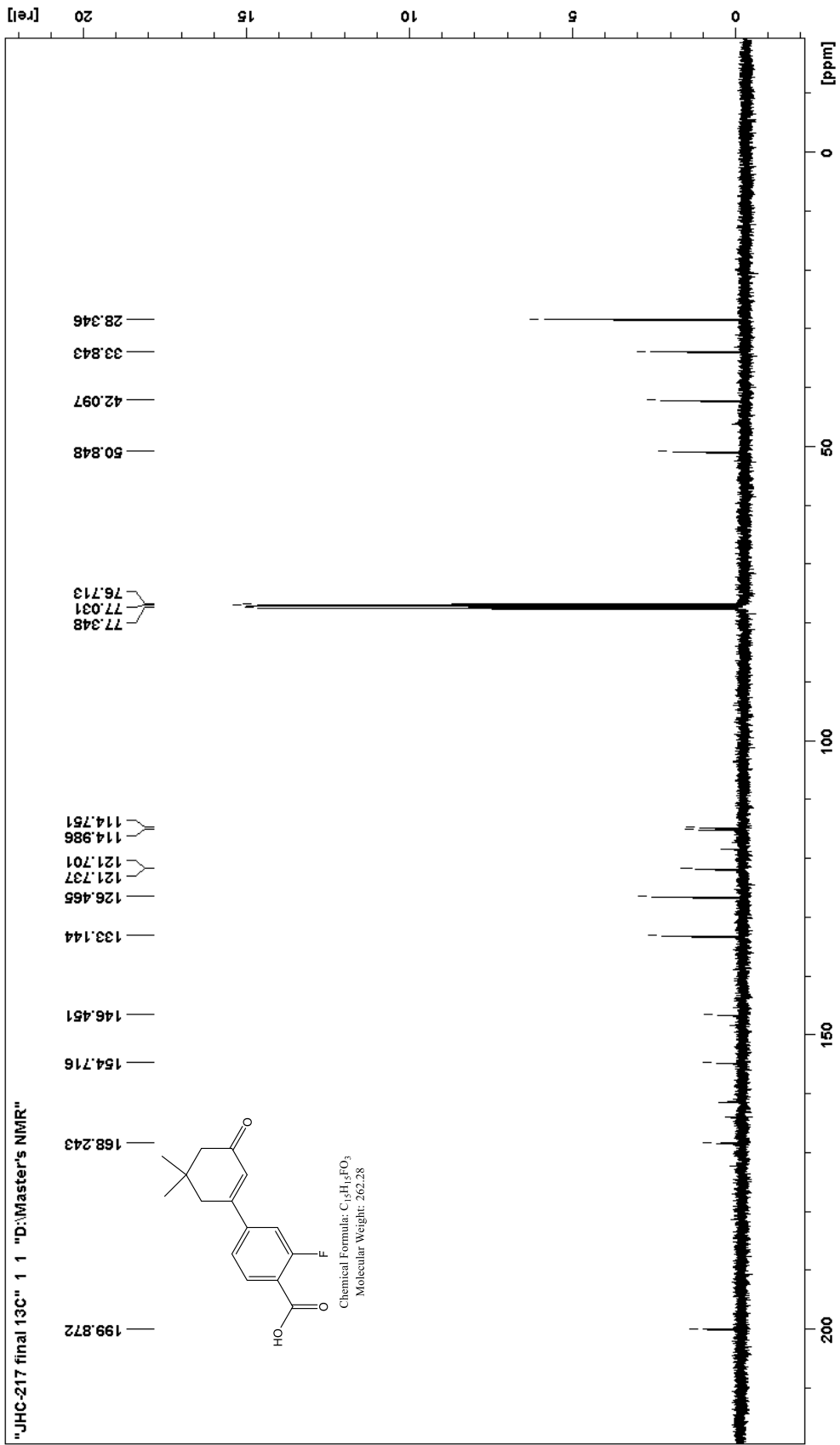
**20**

4-carboxy-3-fluorophenyl boronic acid (0.51 g, 2.77 mmol), the dimedone enol tosylate **12** (0.78 g, 2.64 mmol), sodium carbonate (0.83 g, 7.83 mmol) and tetrakis(triphenylphosphine)-palladium(0) (0.03 g, 0.026 mmol, 1.0 mol%) were dissolved in a 2:1 mixture of 95% ethanol and distilled water. The mixture was refluxed in an oil bath at 100°C for three hours, after which the solution was placed on the rotary evaporator to remove the ethanol. The solution was then diluted with water, and washed three times with DCM. The aqueous layer was acidified by slow addition of concentrated HCl and chilled to induce precipitation. The solid formed was isolated by suction filtration, rinsed with distilled water, and dried overnight at 40°C. The product was obtained as a white dry solid (0.54 g, 78%, mp: 164.8 – 166.2°C).

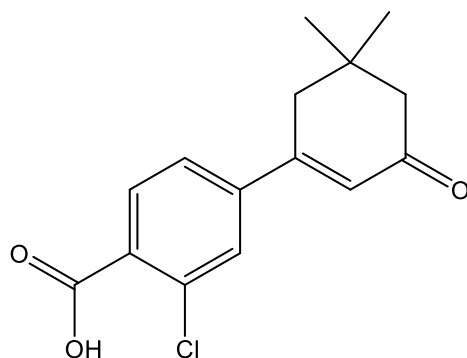
**<sup>1</sup>H NMR (400 MHz, CDCl<sub>3</sub>) δ, ppm:** 8.05 (t, J = 8.0 Hz, 1H), 7.380 (dd, J = 8.4 Hz, J<sub>2</sub> = 1.6 Hz, 1H), 7.29 (dd, J<sub>1</sub> = 11.6 Hz, J<sub>2</sub> = 1.6 Hz, 1H), 6.45 (s, 1H), 2.61 (d, J = 1.2 Hz, 2H), 2.37 (s, 2H), 1.13 (s, 6H).

**<sup>13</sup>C NMR (400 MHz, CDCl<sub>3</sub>) δ, ppm:** 199.87, 168.24, 154.72, 146.45, 133.14, 126.47, 121.74, 121.70, 114.99, 114.75, 50.85, 42.10, 33.84, 28.35 (2C).





**Preparation of 3-(4-carboxy-2-chlorophenyl)-5,5-dimethylcyclohex-2-enone, 21.**



**21**

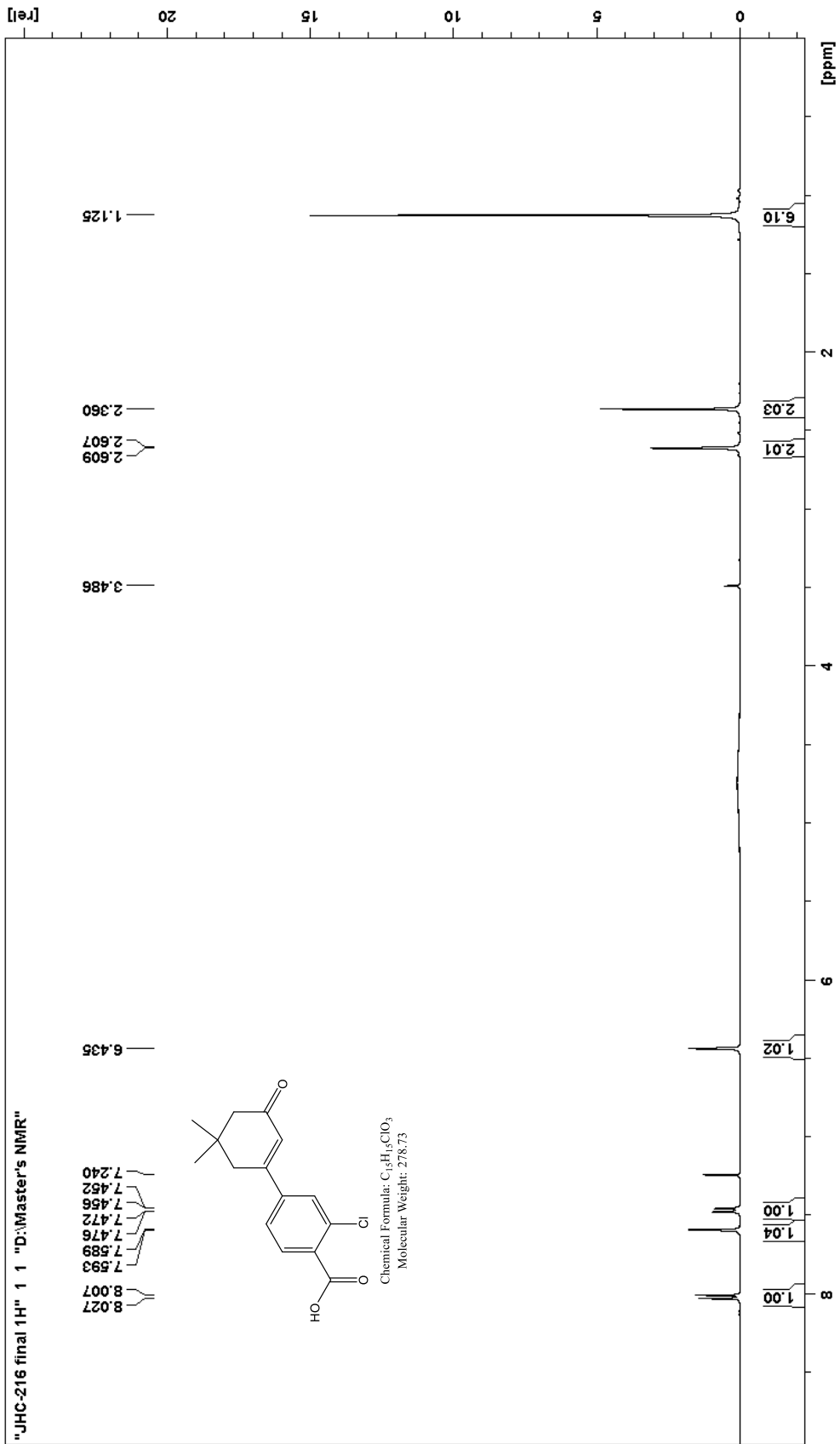
4-Carboxy-3-chlorophenyl boronic acid (0.46 g, 2.29 mmol), the dimedone enol tosylate **12** (0.79 g, 2.68 mmol), sodium carbonate (2.00 g, 18.9 mmol, the unnecessarily high amount was accidentally poured in) and tetrakis(triphenylphosphine)-palladium(0) (0.11 g, 0.095 mmol, 3.8 mol%) were dissolved in a 2:1 mixture of 95% ethanol and distilled water. The mixture was refluxed in an oil bath at 100°C for three hours, after which the solution was placed on the rotary evaporator to remove the ethanol. The solution was then diluted with water, and washed three times with DCM. The aqueous layer was acidified by slow addition of concentrated HCl and chilled to induce precipitation. The solid formed was isolated by suction filtration and dried overnight at 40°C. The product was obtained as a white dry solid (0.42 g, 66%, mp: 156.9 – 158.4°C).

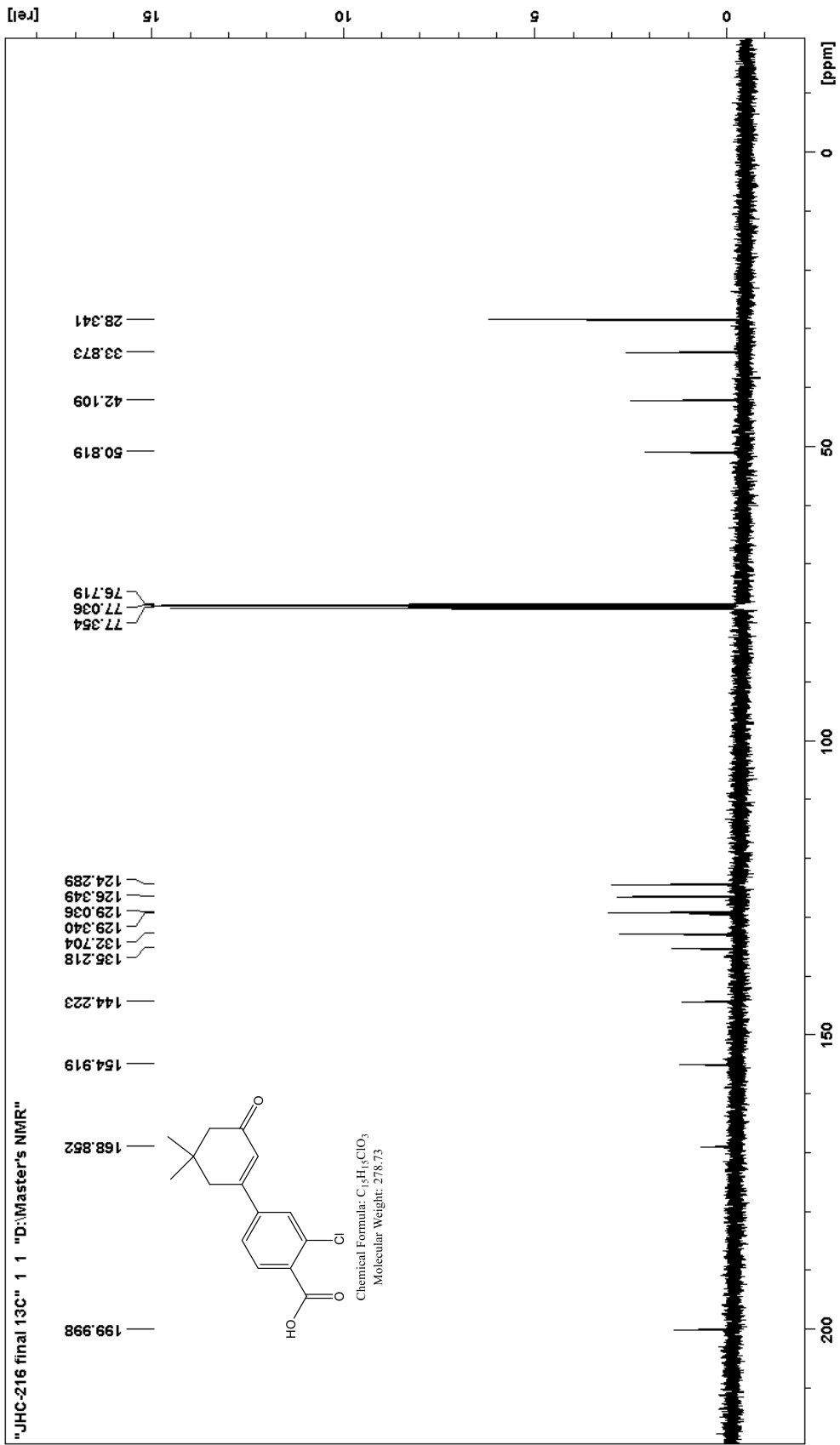
\*Ethanol and water were present in the NMR sample due to not having rinsed the solution with clear water during the final filtration.

**<sup>1</sup>H NMR (400 MHz, CDCl<sub>3</sub>) δ, ppm:** 8.02 (d, J = 8.0 Hz, 1H), 7.59 (d, J = 1.6 Hz, 1H), 7.46 (dd, J<sub>1</sub> = 8.0 Hz, J<sub>2</sub> = 1.6 Hz, 1H), 6.44 (s, 1H), 2.61 (d, J = 0.8 Hz, 2H), 2.36 (s, 2H), 1.13 (s, 6H).

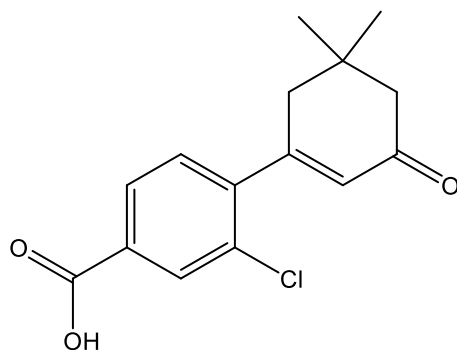
**<sup>13</sup>C NMR (400 MHz, CDCl<sub>3</sub>) δ, ppm:** 200.00, 168.85, 154.82, 144.22, 135.22, 132.70, 129.32, 129.04, 126.35, 124.29, 50.82, 42.11, 33.87, 28.34 (2C).

**HRMS-EI m/z:** M<sup>+</sup> calcd for C<sub>15</sub>H<sub>15</sub>ClO<sub>3</sub>, 278.0710; found, 278.0725.





**Preparation of 3-(4-carboxy-3-chlorophenyl)-5,5-dimethylcyclohex-2-enone, 22.**



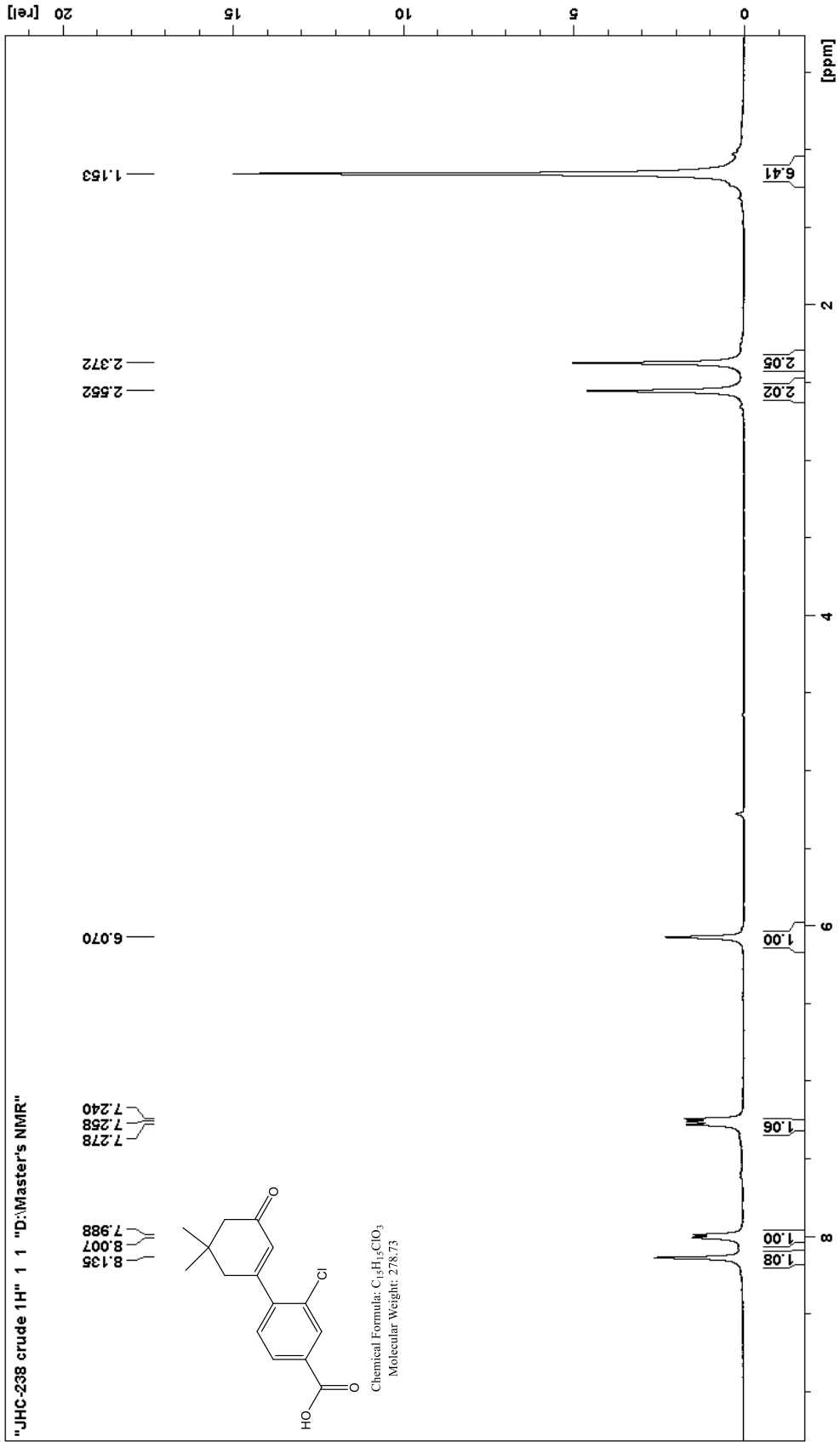
**22**

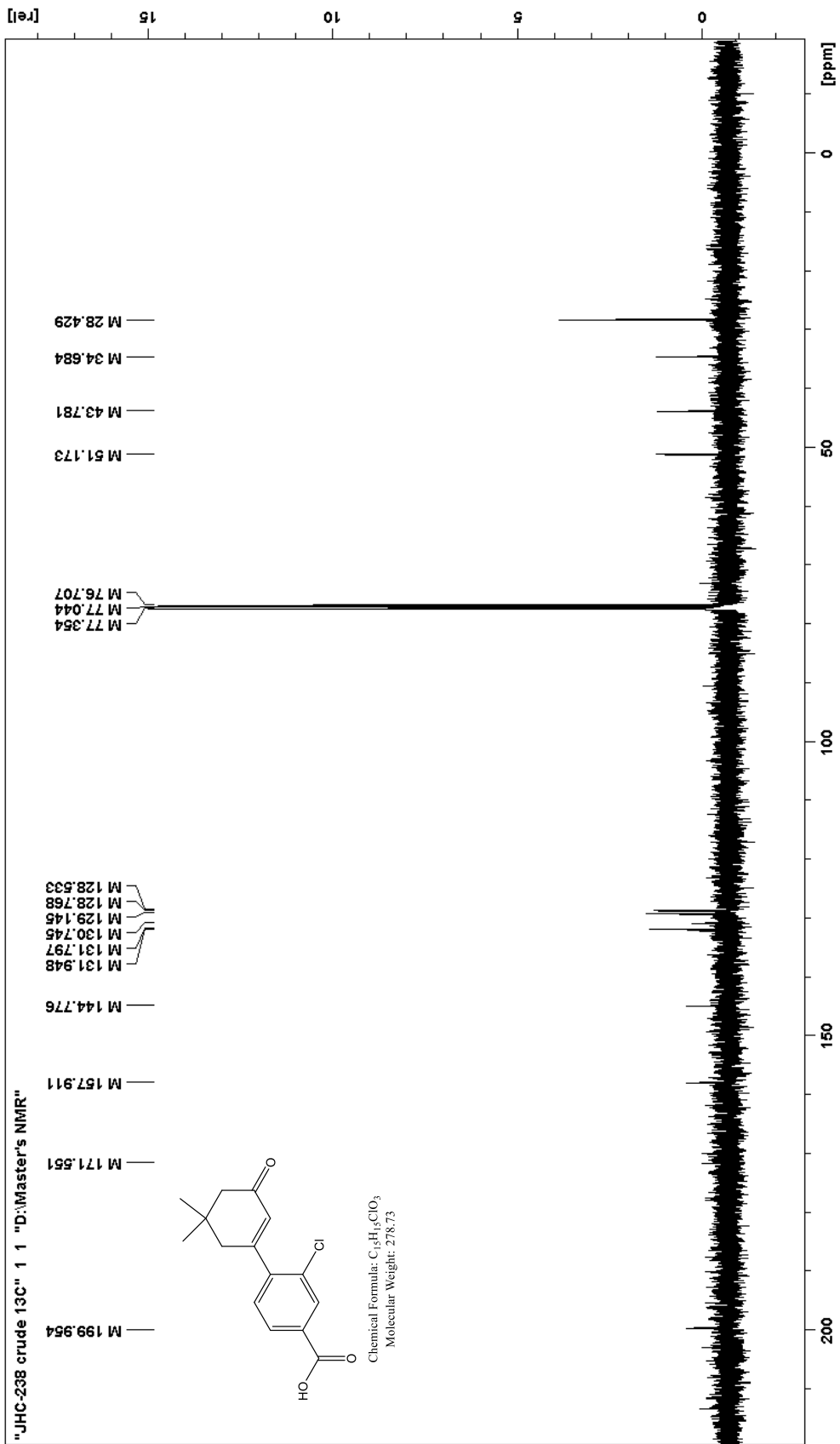
4-carboxy-2-chlorophenyl boronic acid (0.55 g, 2.74 mmol), the dimedone enol tosylate **12** (0.89 g, 3.02 mmol), sodium carbonate (0.70 g, 6.60 mmol) and tetrakis(triphenylphosphine)-palladium(0) (0.03 g, 0.025 mmol, 0.9 mol%) were dissolved in 30 mL of a 2:1 mixture of 95% ethanol and distilled water. The mixture was refluxed in an oil bath at 100°C for four hours, after which the solution was placed on the rotary evaporator to remove the ethanol. The solution was then diluted with water, and washed three times with DCM. The aqueous layer was acidified by slow addition of concentrated HCl and chilled to induce precipitation. The solid formed was isolated by suction filtration and dried overnight at 40°C. The crude product obtained was a brown powder (0.59 g, 77%). This crude product was dissolved in a small amount of DCM, and filtered to remove solid impurities. Purified product was crystallized by addition of a small amount of hexanes, and leaving the solution under light air flow to let crystals form slowly. The final product obtained was a much lighter beige powder (0.27 g, 35%, mp: 181.5 – 183.9°C).

**<sup>1</sup>H NMR (400 MHz, CDCl<sub>3</sub>) δ, ppm:** 8.14 (s, 1H), 8.00 (d, J = 7.6 Hz, 1H), 7.27 (d, J = 8.0 Hz, 1H), 6.07 (s, 1H), 2.55 (s, 2H), 2.37 (s, 2H), 1.15 (s, 6H).

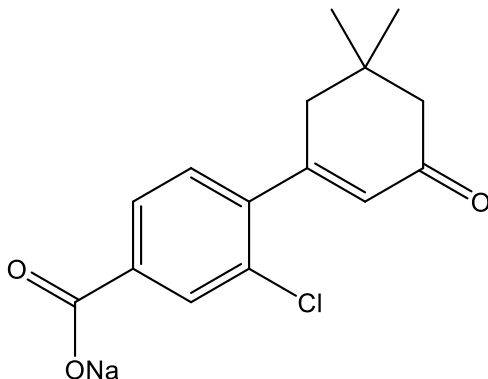
**<sup>13</sup>C NMR (400 MHz, CDCl<sub>3</sub>) δ, ppm:** 199.95, 171.55, 157.91, 144.78, 131.95, 131.80, 130.75, 129.15, 128.77, 128.53, 51.17, 43.78, 34.68, 28.43 (2C).

**HRMS-EI m/z:** M<sup>+</sup> calcd for C<sub>15</sub>H<sub>15</sub>ClO<sub>3</sub>, 278.0710; found, 278.0711.



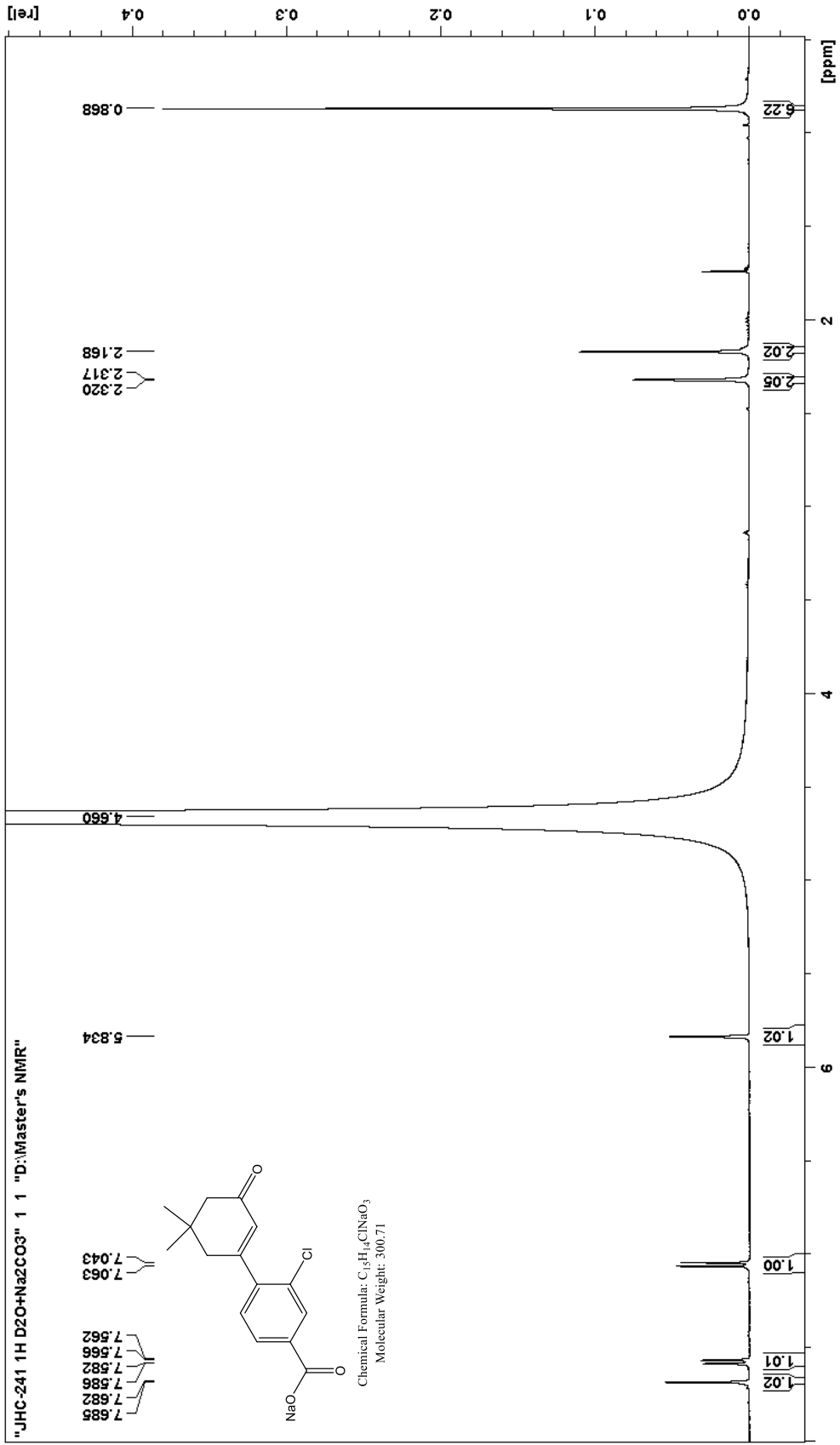


**Preparation of the sodium salt of 3-(4-carboxy-3-chlorophenyl)-5,5-dimethylcyclohex-2-enone.**

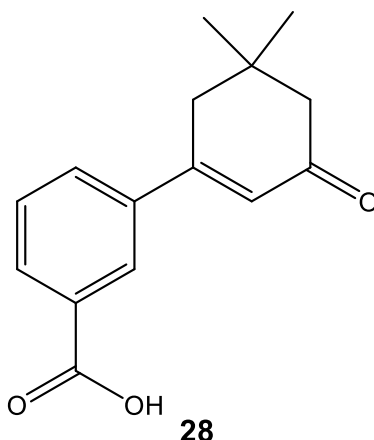


3-(4-carboxy-2-chlorophenyl)-5,5-dimethylcyclohex-2-enone (0.13 g, 0.47 mmol) was dissolved in a 10% NaOH<sub>aq</sub> solution added dropwise until only a few grains of the starting material remained visible as solids. The undissolved acid was filtered out by gravity. The aqueous solution was evaporated overnight at 40°C in a petri dish, leaving behind a hard, semi-transparent solid (0.12 g, 86%).

**<sup>1</sup>H NMR (400 MHz, D<sub>2</sub>O+Na<sub>2</sub>CO<sub>3</sub>) δ, ppm:** 7.68 (d, J = 1.2 Hz, 1H), 7.57 (dd, J<sub>1</sub> = 8.0 Hz, J<sub>2</sub> = 1.6 Hz, 1H), 7.05 (d, J = 8.0 Hz, 1H), 5.83 (s, 1H), 2.32 (d, J = 1.2 Hz, 2H), 2.17 (s, 2H), 0.89 (s, 6H).



**Preparation of 3-(3-carboxyphenyl)-5,5-dimethylcyclohex-2-enone, 28.**

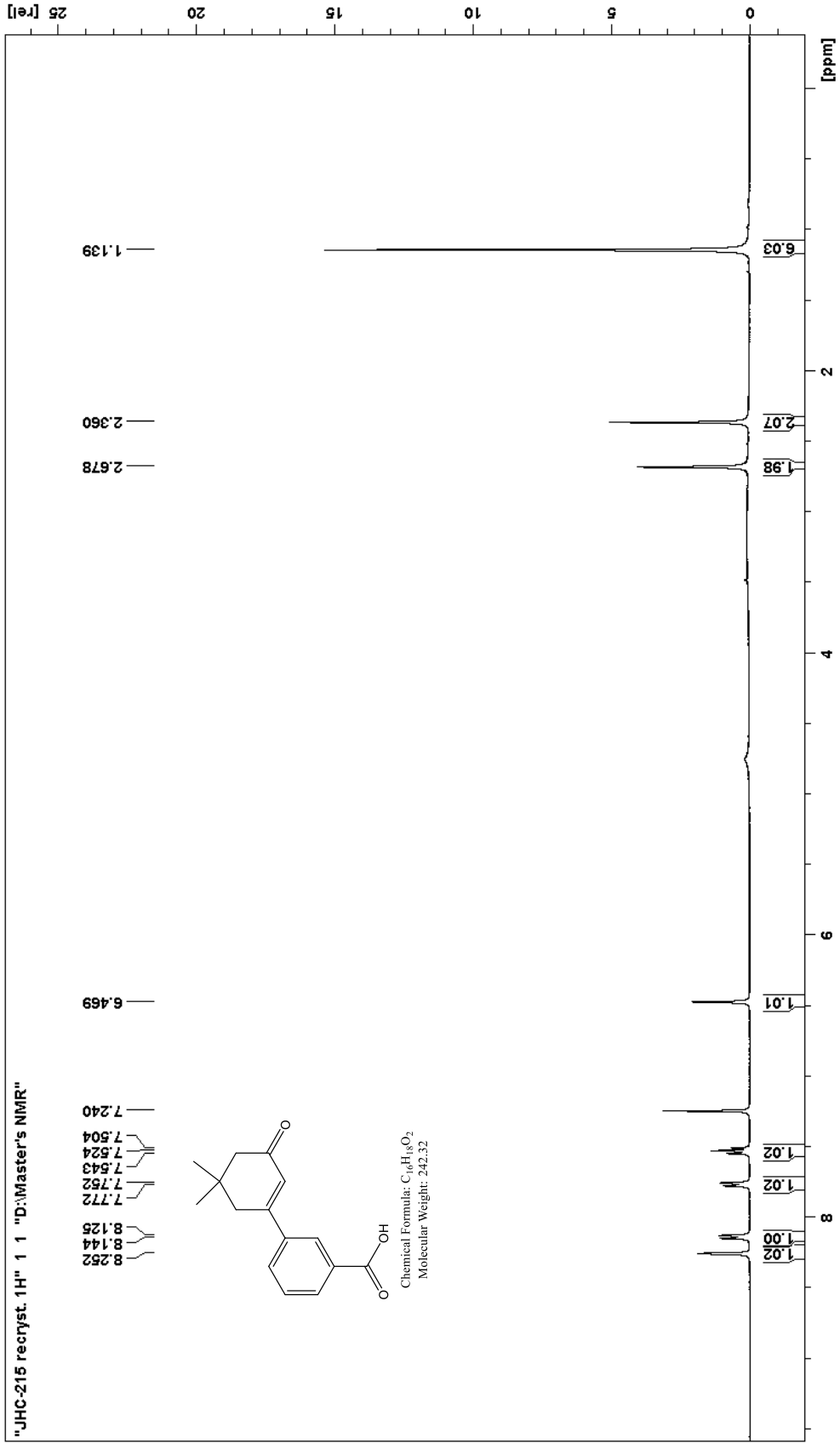


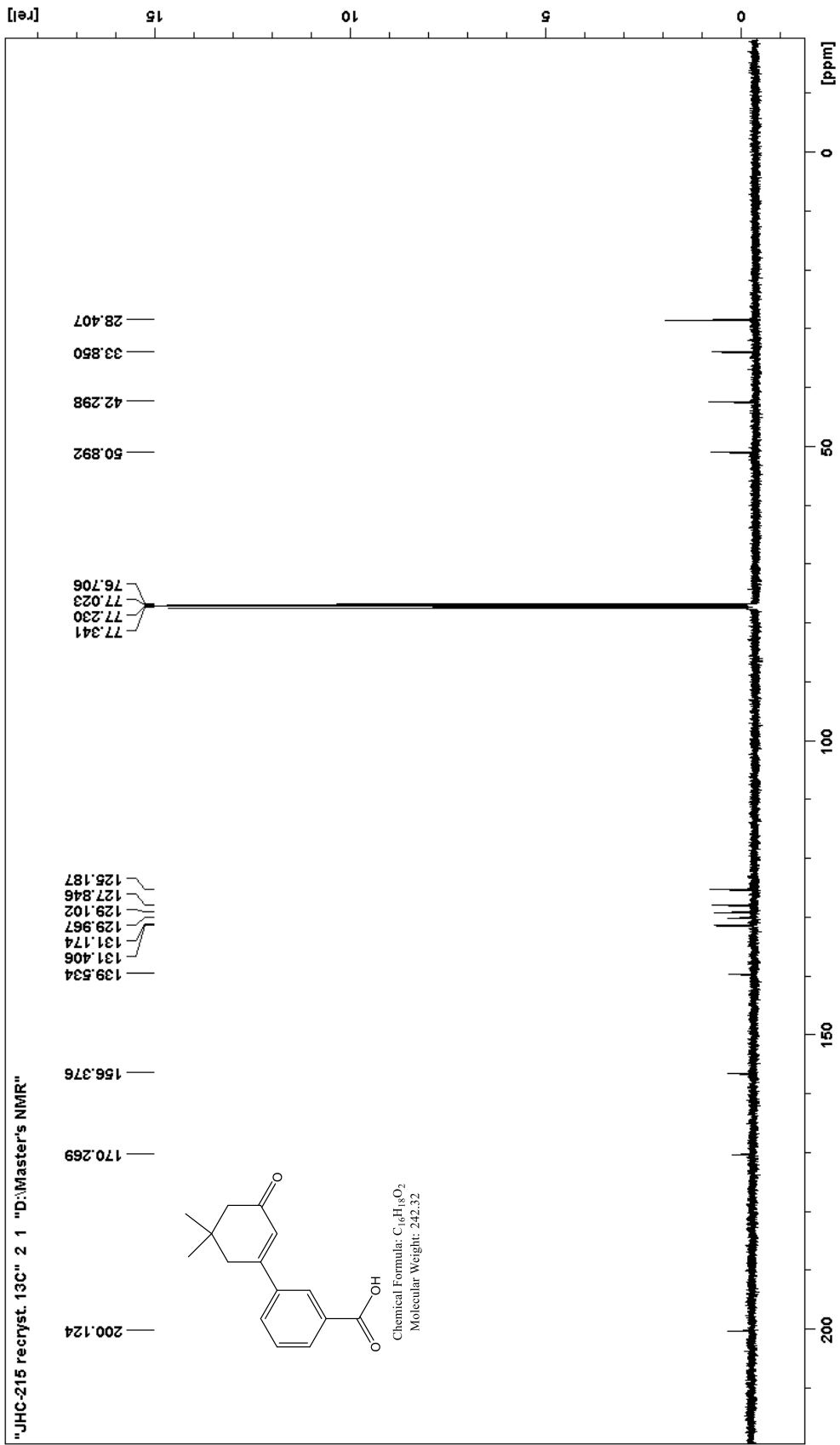
3-carboxyphenyl boronic acid (0.41 g, 2.47 mmol), the dimedone enol tosylate **12** (0.76 g, 2.58 mmol), sodium carbonate (0.80 g, 7.55 mmol) and tetrakis(triphenylphosphine)-palladium(0) (0.03 g, 0.025 mmol, 0.9 mol%) were dissolved in 30 mL of a 2:1 mixture of 95% ethanol and distilled water. The mixture was refluxed in an oil bath at 100°C for three hours, after which the solution was placed on the rotary evaporator to remove the ethanol. The solution was then diluted with water, and washed three times with DCM. The aqueous layer was acidified by slow addition of concentrated HCl and chilled to induce precipitation. The solid formed was isolated by suction filtration. The crude product obtained (0.49 g, 81%) was recrystallized in a mixture of DCM and hexanes. The purified product was obtained as a clean white powder (0.26 g, 43%).

**<sup>1</sup>H NMR (400 MHz, CDCl<sub>3</sub>) δ, ppm:** 8.25 (s, 1H), 8.14 (d, J = 7.6 Hz, 1H), 7.56 (d, J = 8.0 Hz, 1H), 7.52 (t, J = 8.0 Hz, 1H), 6.47 (s, 1H), 2.68 (s, 2H), 2.36 (s, 2H), 1.14 (s, 6H).

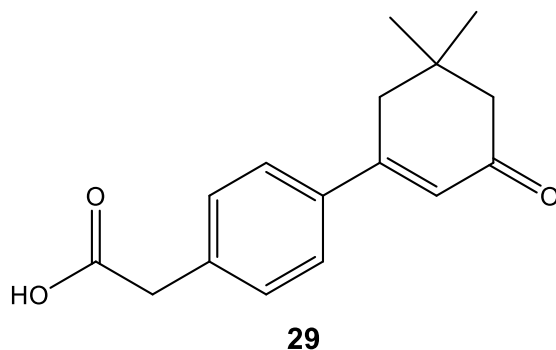
**<sup>13</sup>C NMR (400 MHz, CDCl<sub>3</sub>) δ, ppm:** 200.12, 170.27, 156.38, 139.53, 131.40, 131.17, 129.97, 129.10, 127.85, 125.19, 50.89, 42.30, 33.85, 28.41 (2C).

**HRMS-EI m/z:** M<sup>+</sup> calcd for C<sub>15</sub>H<sub>16</sub>O<sub>3</sub>, 244.1099; found, 244.1121.





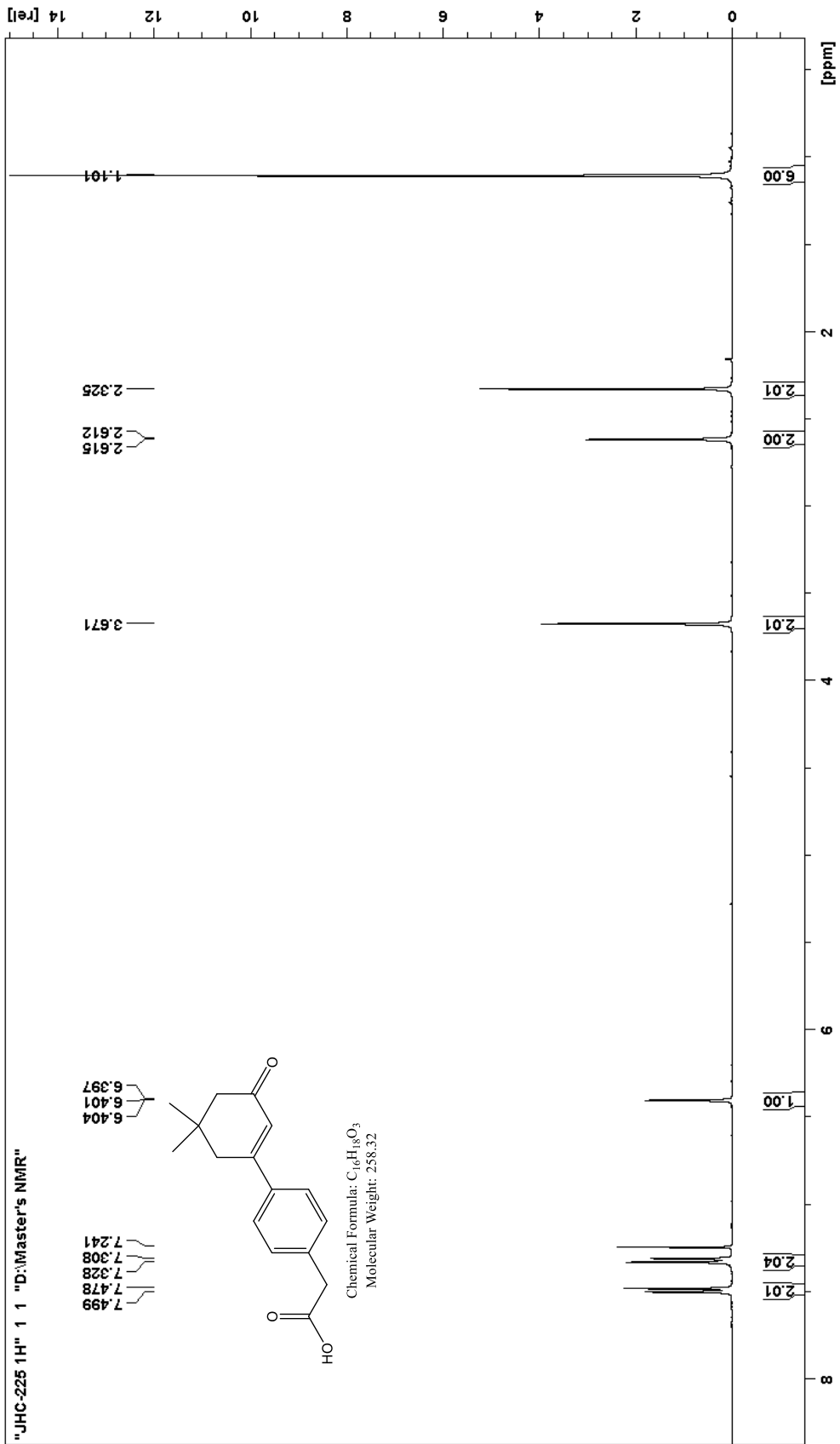
**Preparation of 3-(4-carboxymethylphenyl)-5,5-dimethylcyclohex-2-enone, 29.**

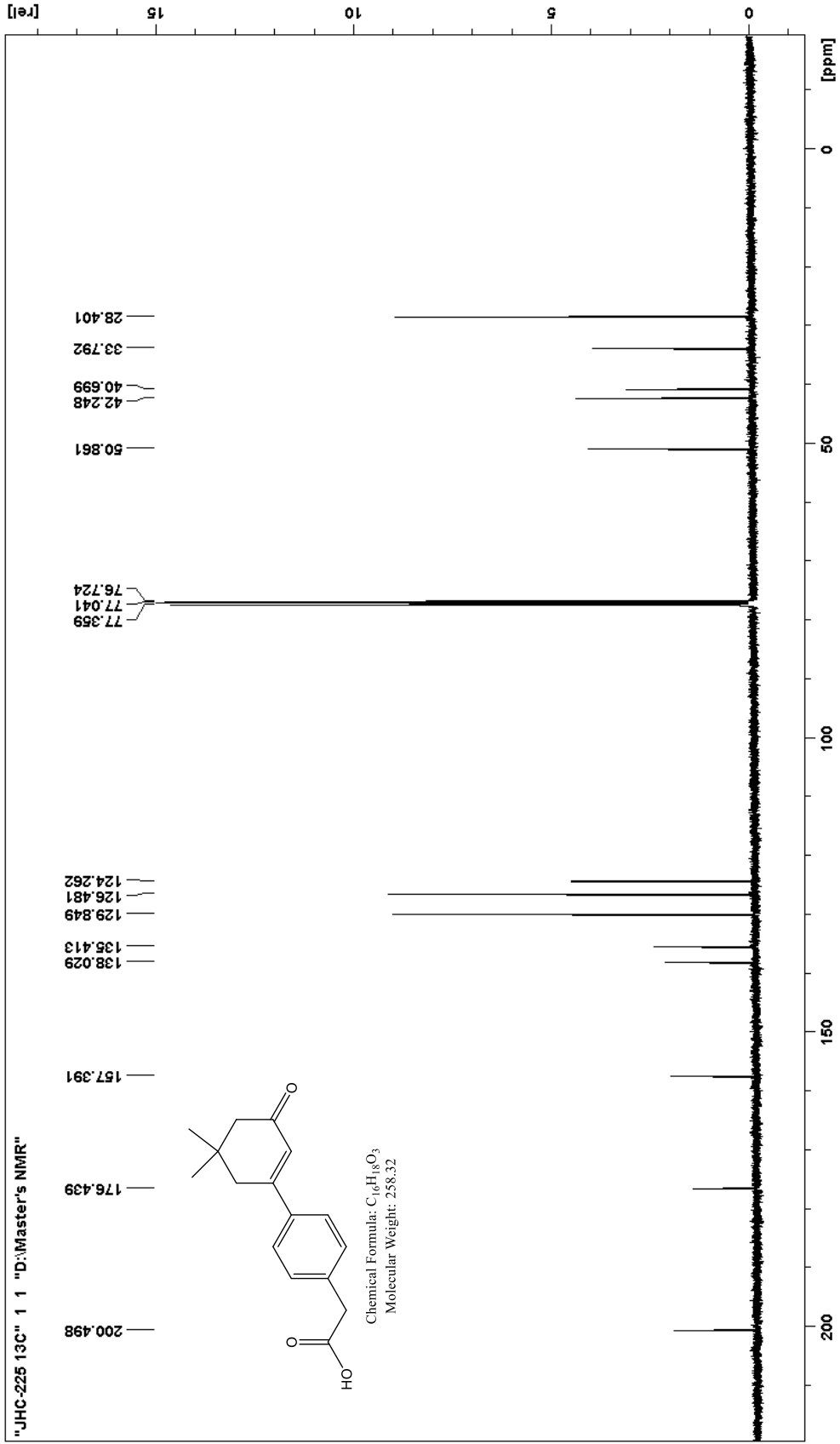


4-(Carboxymethyl)phenyl boronic acid (0.45 g, 2.50 mmol), the dimedone enol tosylate **12** (0.88 g, 2.99 mmol), sodium carbonate (0.55 g, 5.19 mmol) and tetrakis(triphenylphosphine)-palladium(0) (0.02 g, 0.017 mmol, 0.7 mol%) were dissolved in 27 mL of a 2:1 mixture of 95% ethanol and distilled water. The mixture was refluxed in an oil bath at 100°C for three hours, after which the solution was placed on the rotary evaporator to remove the ethanol. The solution was then diluted with water, and washed three times with DCM. The aqueous layer was acidified by slow addition of concentrated HCl and chilled to induce precipitation. The solid formed was isolated by suction filtration and rinsed with water. The product was obtained as a grayish dry solid (0.11 g, 17%).

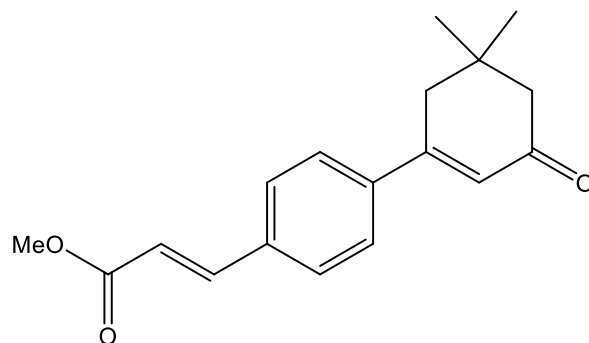
**<sup>1</sup>H NMR (400 MHz, CDCl<sub>3</sub>) δ, ppm:** 7.49 (d, J = 8.4 Hz, 2H), 7.32 (d, J = 8.0 Hz, 2H), 6.40 (t, J = 1.2 Hz, 1H), 3.67 (s, 2H), 2.61 (d, J = 1.2 Hz, 2H), 2.33 (s, 2H), 1.10 (s, 6H).

**<sup>13</sup>C NMR (400 MHz, CDCl<sub>3</sub>) δ, ppm:** 200.50, 176.44, 157.39, 138.03, 135.41, 129.85 (2C), 126.48 (2C), 124.26, 50.86, 42.25, 40.70, 33.79, 28.40 (2C).





**Preparation of 3-(4-(E-2-carboxyvinyl)phenyl)-5,5-dimethylcyclohex-2-enone, 30.**



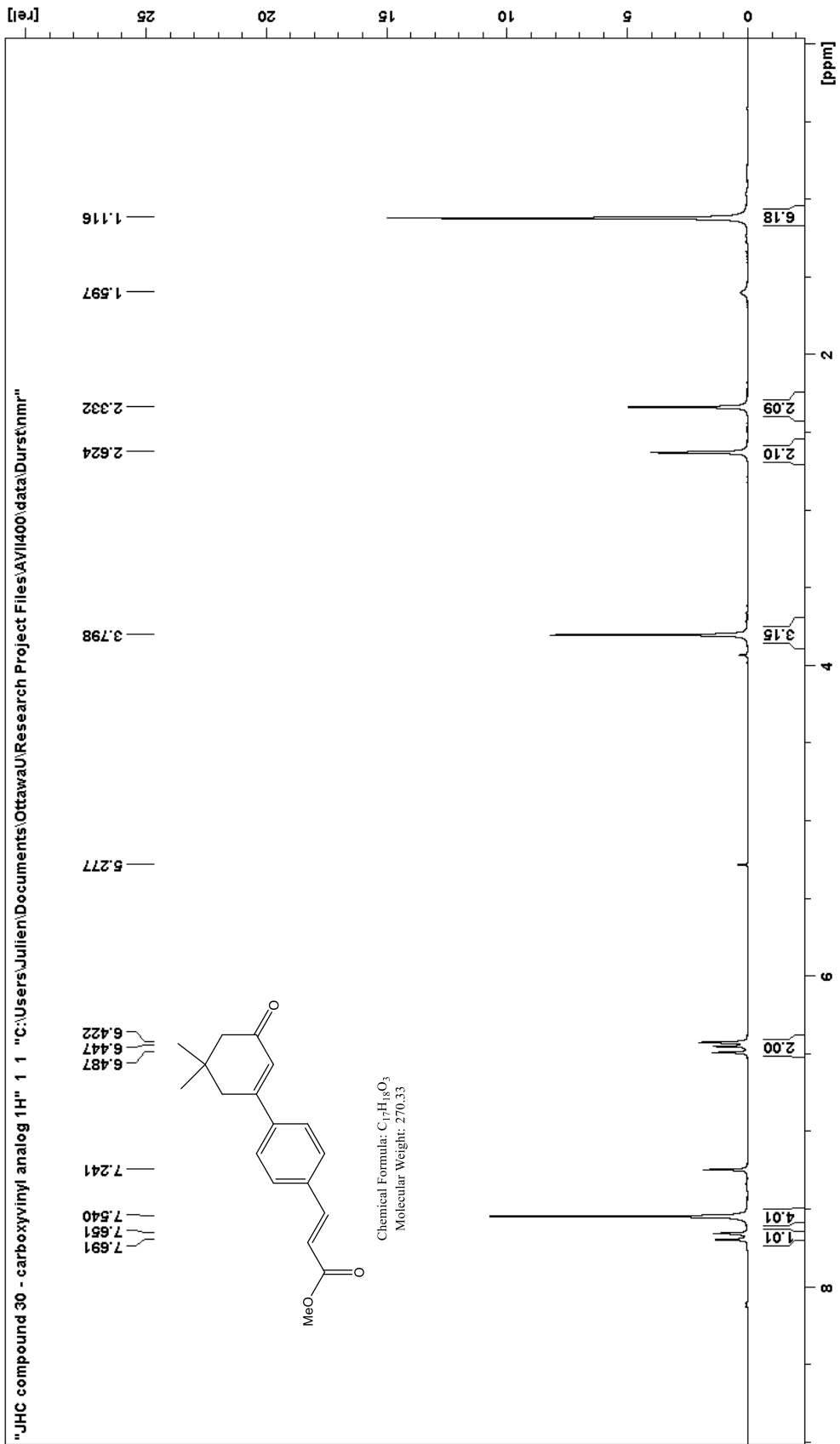
**30**

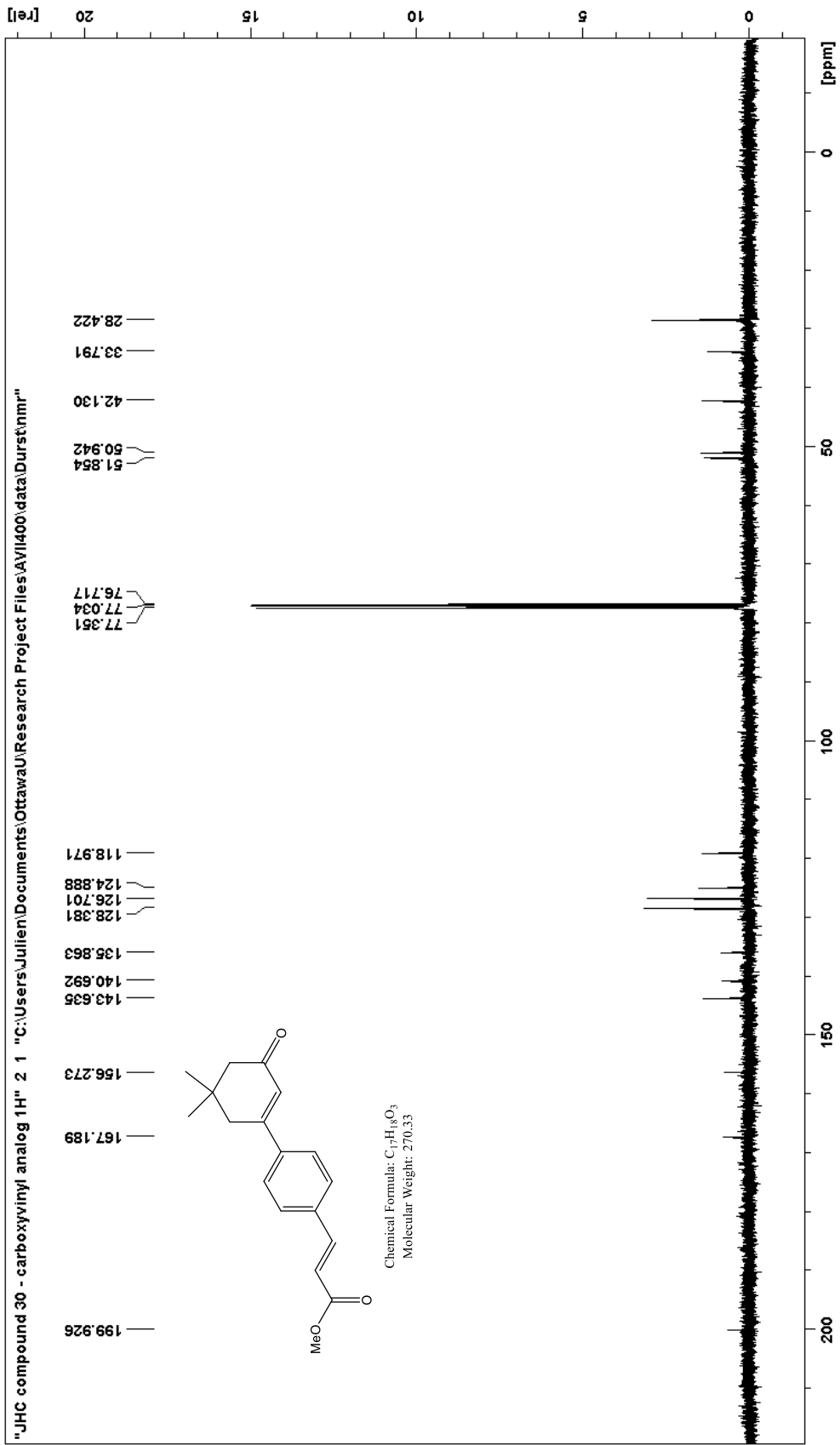
4-(E-2-carboxyvinyl)phenyl boronic acid (0.27 g, 1.40 mmol), the dimedone enol tosylate **12** (0.49 g, 1.66 mmol), sodium carbonate (0.36 g, 3.40 mmol) and tetrakis(triphenylphosphine)-palladium(0) (0.02 g, 0.017 mmol, 1.2 mol%) were dissolved in 20 mL of a 2:1 mixture of 95% ethanol and distilled water. The mixture was refluxed in an oil bath at 100°C for five hours, after which the solution was placed on the rotary evaporator to remove the ethanol. The solution was then diluted with water, and washed three times with DCM. The aqueous layer was acidified by slow addition of concentrated HCl and chilled to induce precipitation. The solid formed was isolated by suction filtration and rinsed with water. The product was obtained as a gray powder (0.34 g, 89%), which was recrystallized afterwards in a mixture of DCM and hexanes. This product was further purified by converting the acid to the methyl ester by refluxing it in methanol (40 mL) with concentrated sulfuric acid (5 mL) for 3 hours. The purified product (0.15 g, 38%) was obtained by extracting the solution with DCM and evaporating this organic layer, then recrystallizing in a DCM and hexanes mixture again.

**<sup>1</sup>H NMR (400 MHz, CDCl<sub>3</sub>) δ, ppm:** 7.67 (d, J = 16.0 Hz, 1H), 7.54 (s, 4H), 6.47 (d, J = 16.0 Hz, 1H), 6.42 (s, 1H), 3.80 (s, 3H), 2.62 (s, 2H), 2.33 (s, 2H), 1.12 (s, 6H).

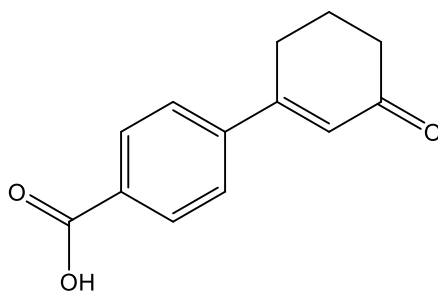
**<sup>13</sup>C NMR (400 MHz, CDCl<sub>3</sub>) δ, ppm:** 199.93, 167.19, 156.27, 143.64, 140.69, 135.86, 128.38 (2C), 126.70 (2C), 124.89, 118.97, 51.85, 50.94, 42.13, 33.79, 28.42 (2C).

**HRMS-EI m/z:** M<sup>+</sup> calcd for C<sub>18</sub>H<sub>20</sub>O<sub>3</sub>, 284.1412; found, 284.1440.





### Preparation of 3-(4-carboxyphenyl)-cyclohex-2-enone, **34**.



**34**

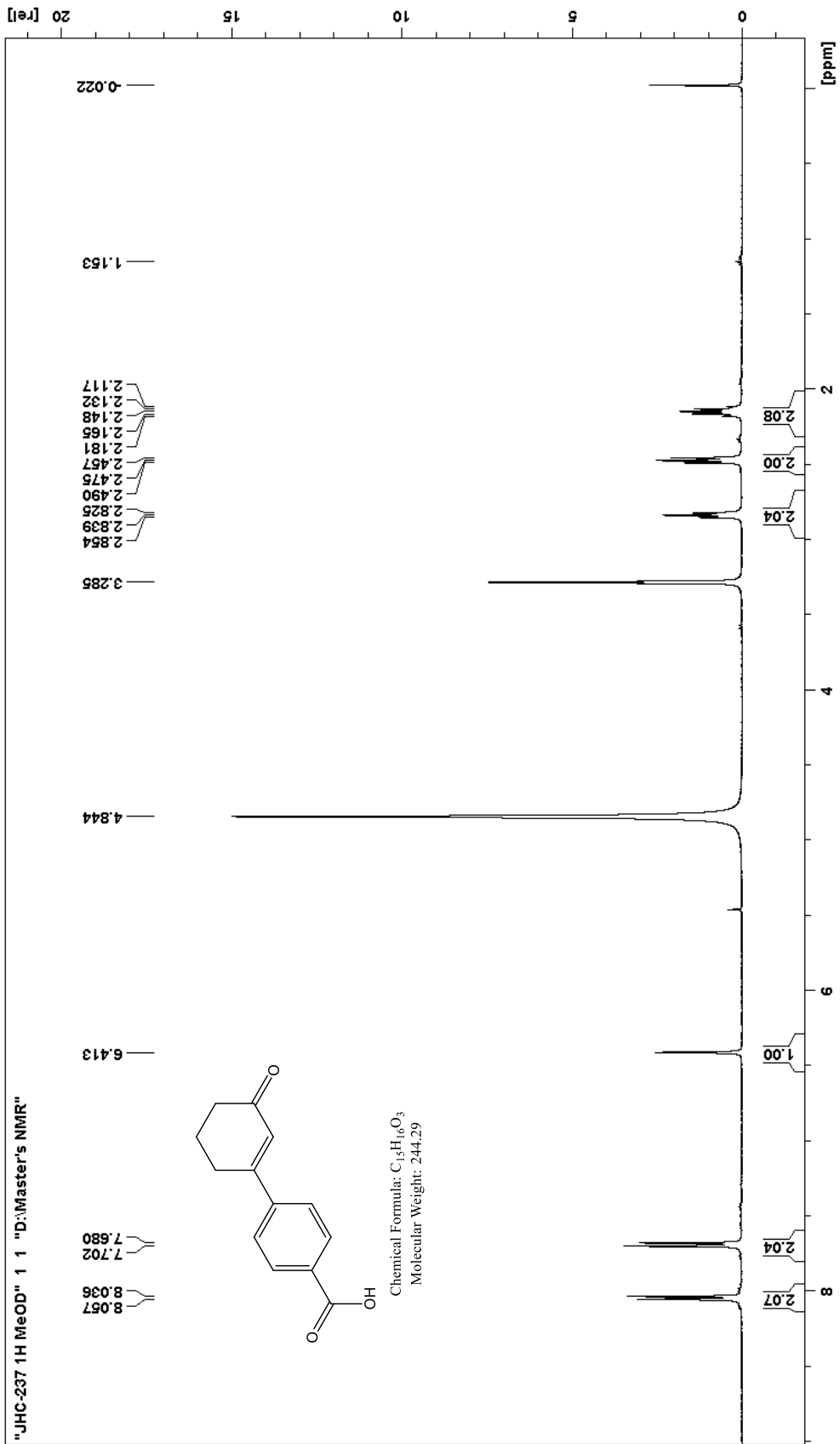
4-carboxyphenyl boronic acid (1.88 g, 11.3 mmol), cyclohexane-1,3-dione enol tosylate (3.1 g, 11.7 mmol) previously prepared by an undergraduate student, sodium carbonate (2.40 g, 3.40 mmol) and tetrakis(triphenylphosphine)-palladium(0) (0.09 g, 0.08 mmol, 0.7 mol%) were dissolved in 45 mL of a 2:1 mixture of 95% ethanol and distilled water. The mixture was refluxed in an oil bath at 100°C for six hours, after which the solution was placed on the rotary evaporator to remove the ethanol. The solution was then diluted with water, and washed three times with DCM. The aqueous layer was acidified by slow addition of concentrated HCl and chilled to induce precipitation. The solid formed was isolated by suction filtration and rinsed with water. The product was obtained as a white solid (1.89 g, 77%).

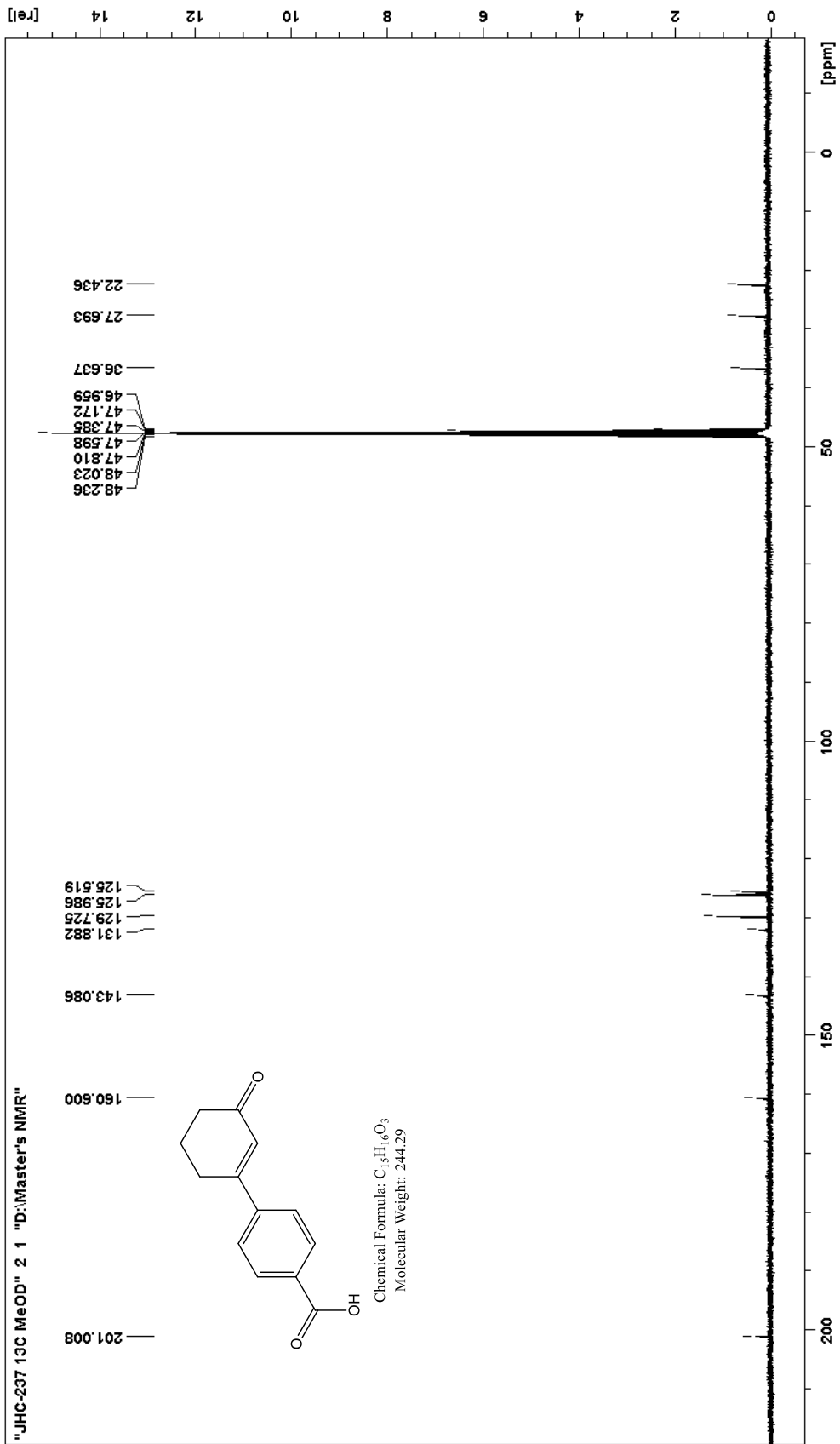
**<sup>1</sup>H NMR (400 MHz, MeOD)  $\delta$ , ppm:** 8.05 (d,  $J$  = 8.4 Hz, 2H), 7.69 (d,  $J$  = 8.8 Hz, 2H), 6.41 (s, 1H), 2.84 (t,  $J$  = 6.0 Hz, 2H), 2.47 (t,  $J$  = 6.0 Hz, 2H), 2.15 (q,  $J$  = 6.4 Hz, 2H).

\*A large amount of water is visible in the spectrum, in addition to the MeOD residual peak and TMS.

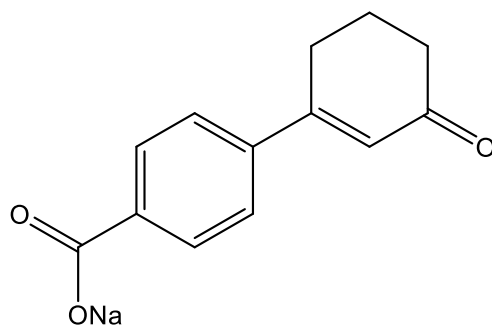
**<sup>13</sup>C NMR (400 MHz, MeOD)  $\delta$ , ppm:** 201.00, 160.60, 143.09, 131.88, 129.73 (2C), 125.99 (2C), 125.52, 36.64, 27.69, 22.44.

**HRMS-EI  $m/z$ :**  $M^+$  calcd for  $C_{13}H_{12}O_3$ , 216.0786; found, 216.0785.





**Preparation of the sodium salt of 3-(4-carboxyphenyl)-cyclohex-2-enone.**

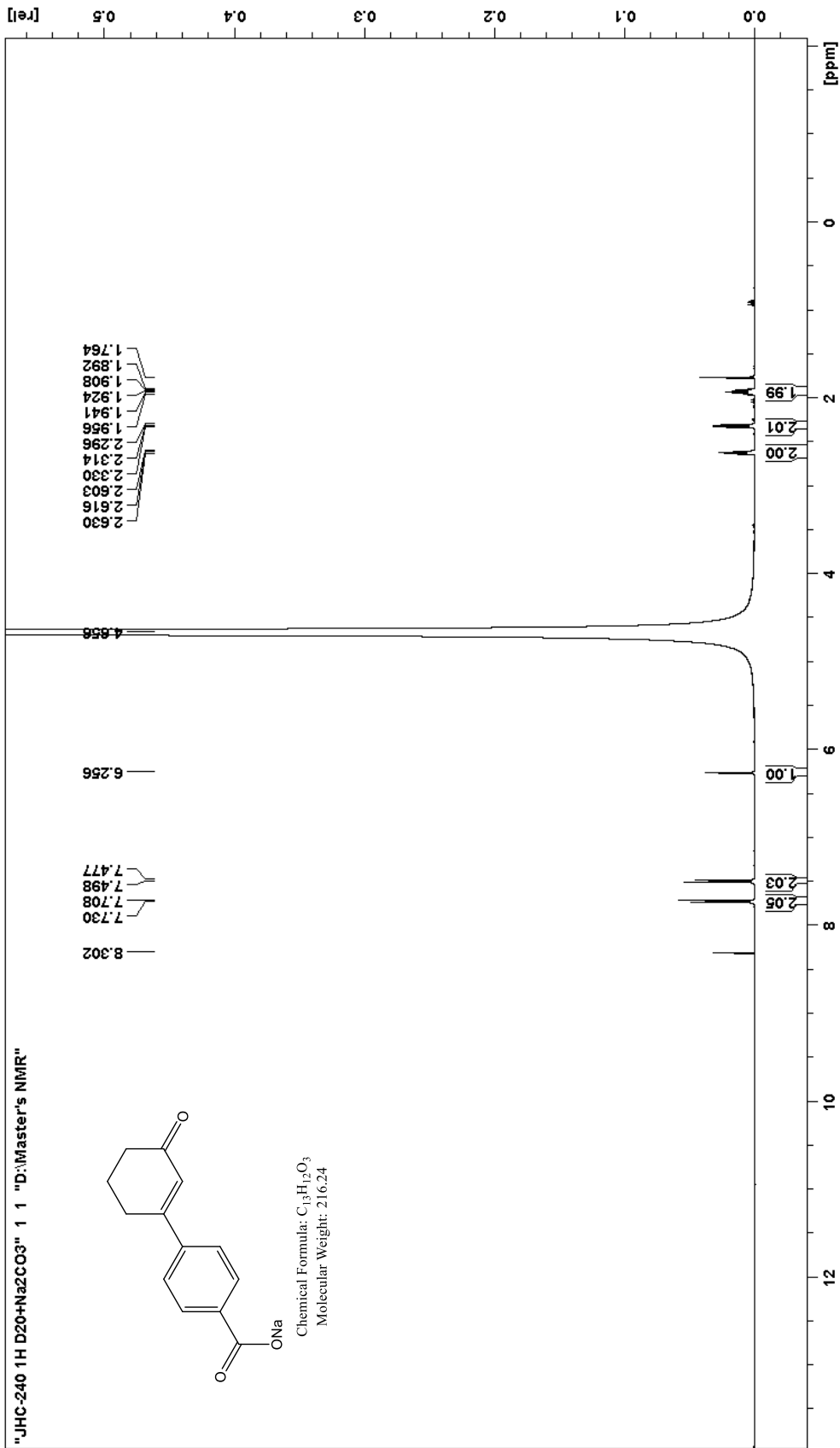


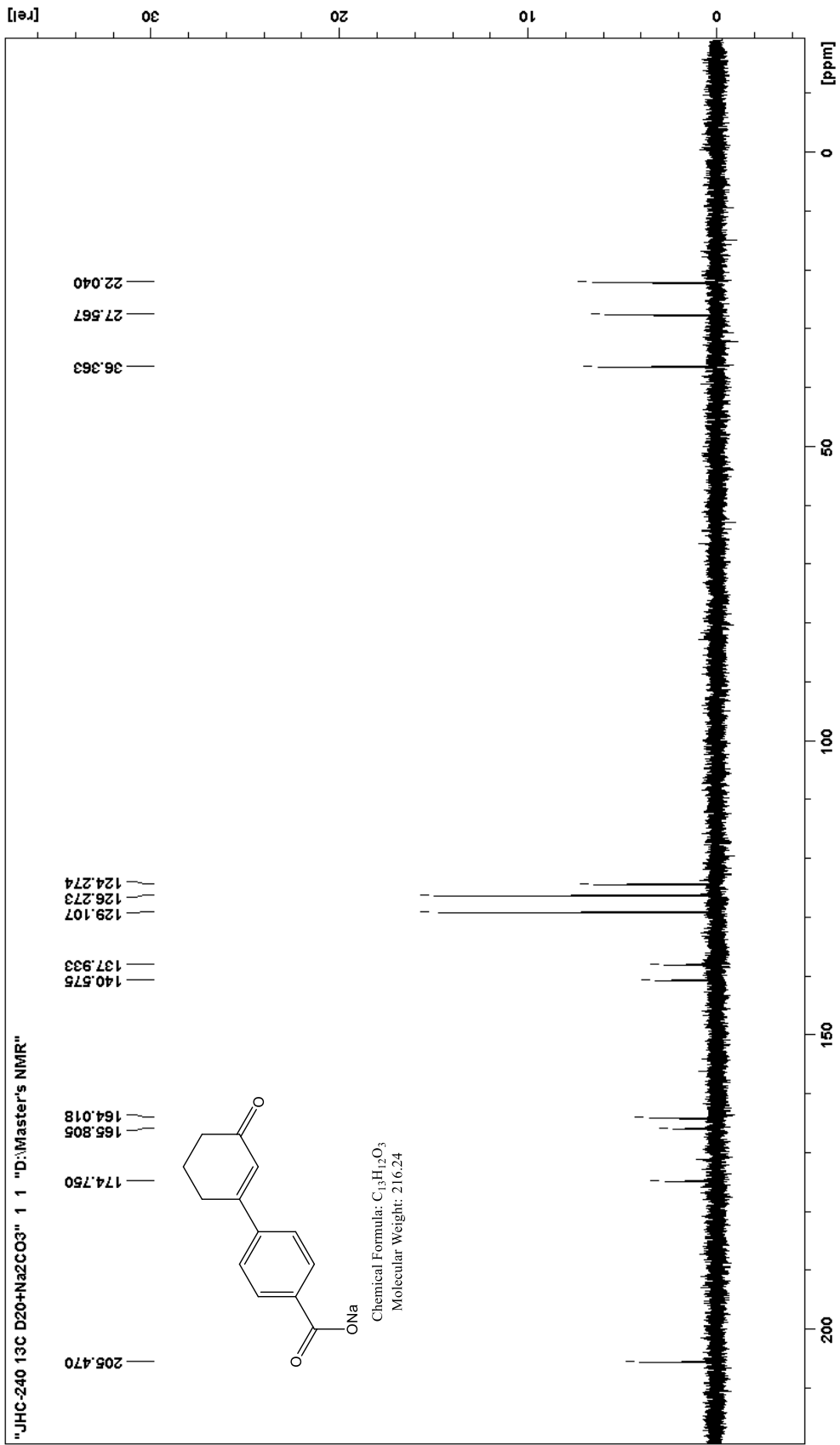
3-(4-carboxyphenyl)cyclohex-2-enone (0.36 g, 1.66 mmol) was dissolved in a 10% NaOH<sub>aq</sub> solution (0.5 mL, 1.25 mmol) added dropwise, to ensure the starting material was not fully dissolved. The undissolved acid was filtered out by gravity. The aqueous solution was evaporated overnight at 40°C in a petri dish, leaving behind a hard, semi-transparent solid (0.22 g, 74%).

**<sup>1</sup>H NMR (400 MHz, D<sub>2</sub>O+Na<sub>2</sub>CO<sub>3</sub>) δ, ppm:** 7.72 (d, J = 8.8 Hz, 2H), 7.49 (d, J = 8.4 Hz, 2H), 6.26 (s, 1H), 2.62 (t, J = 5.6 Hz, 2H), 2.31 (t, J = 6.4 Hz, 2H), 1.92 (m, J = 5.6 Hz, 2H).

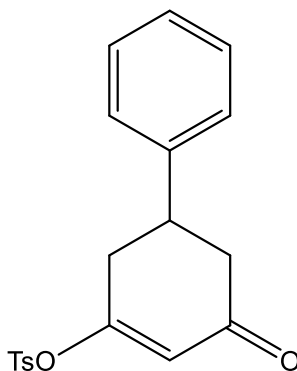
**<sup>13</sup>C NMR (400 MHz, D<sub>2</sub>O+Na<sub>2</sub>CO<sub>3</sub>) δ, ppm:** 205.47, 165.81, 164.02, 140.58, 137.93, 129.11 (2C), 126.27 (2C), 124.27, 36.36, 27.57, 22.04.

\*Na<sub>2</sub>CO<sub>3</sub> carbon peak at 174





**Preparation of the enol tosylate of 5-phenylcyclohexane-1,3-dione, 36.**



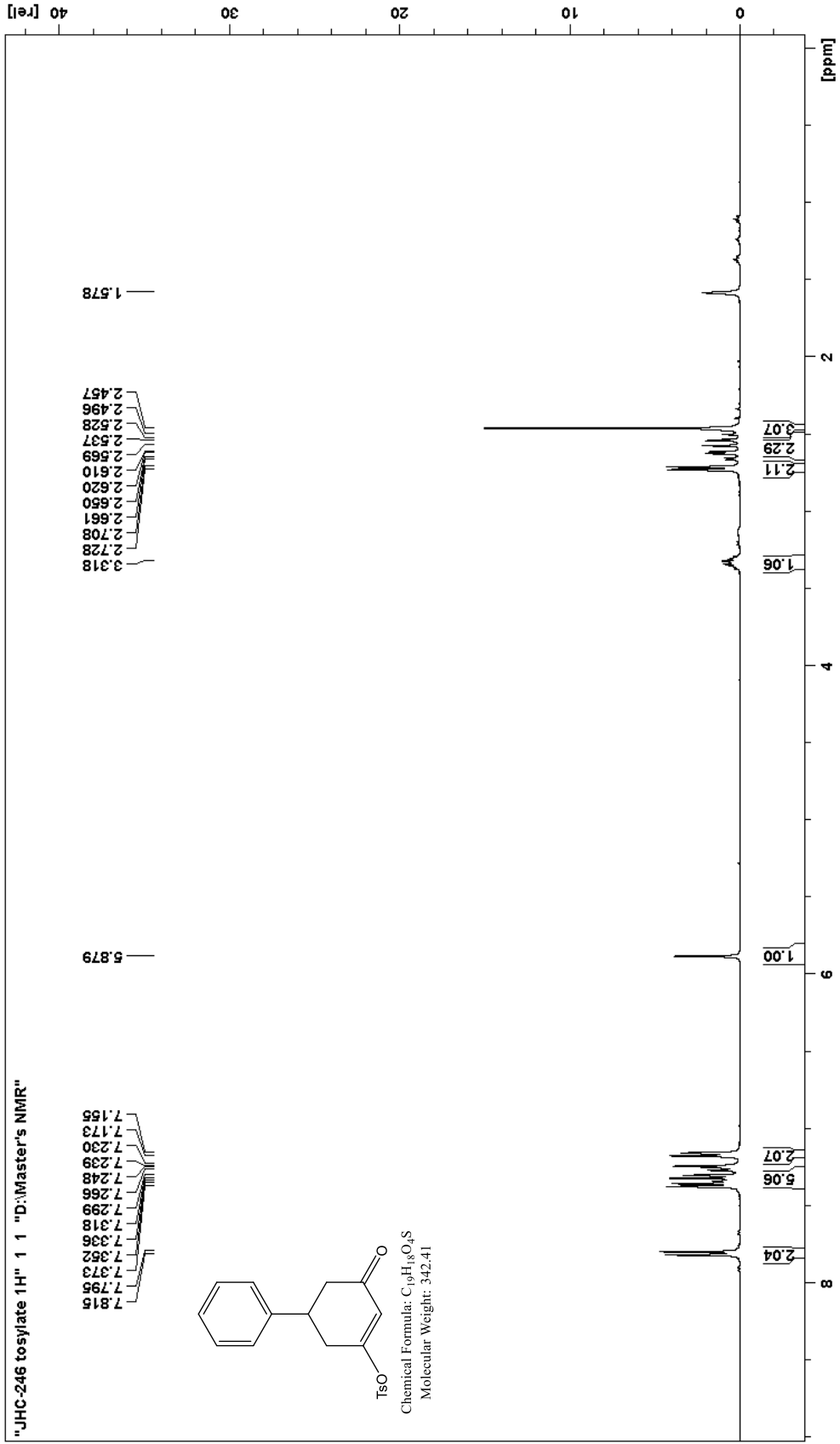
**36**

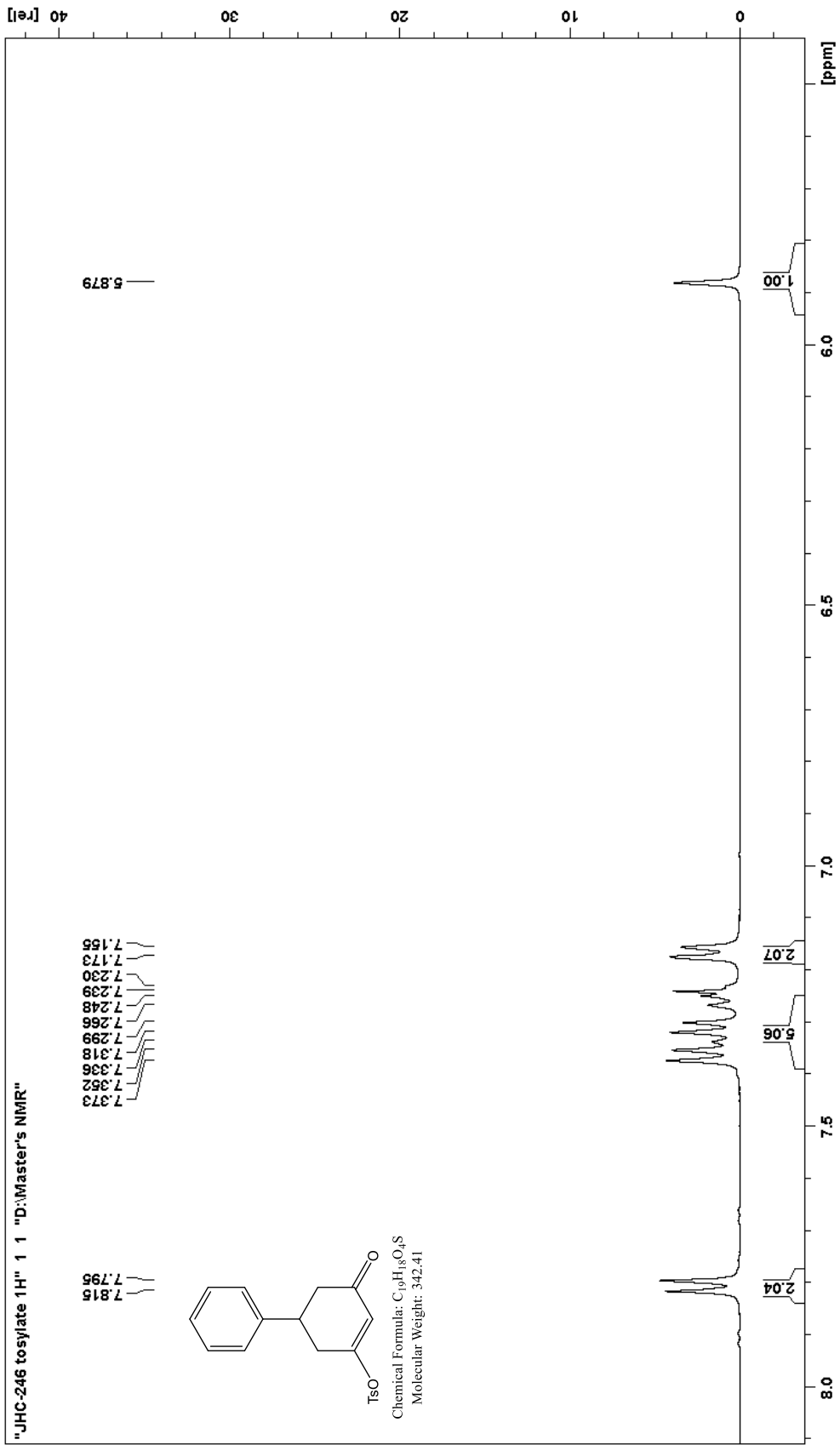
5-phenylcyclohexane-1,3-dione **8** (5.06 g, 26.9 mmol) was partially dissolved in ethyl acetate (50.0 mL). Triethylamine (4.16 g, 41.1 mmol) was added next, which immediately caused the precipitation of triethylamine hydrochloride as a white solid. then p-toluenesulfonyl chloride (6.23 g, 32.7 mmol). The solution was stirred at room temperature for 24 hours. The solution was washed once with a 10% NaOH<sub>aq</sub> (75 mL). The organic layer was dried with magnesium sulfate, filtered and evaporated to yield an oil, which rapidly crystallized in hexanes and filtered by suction. This product was recrystallized in a DCM and hexanes mixture. The final product was obtained as a white clumpy solid (5.75 g, 62%).

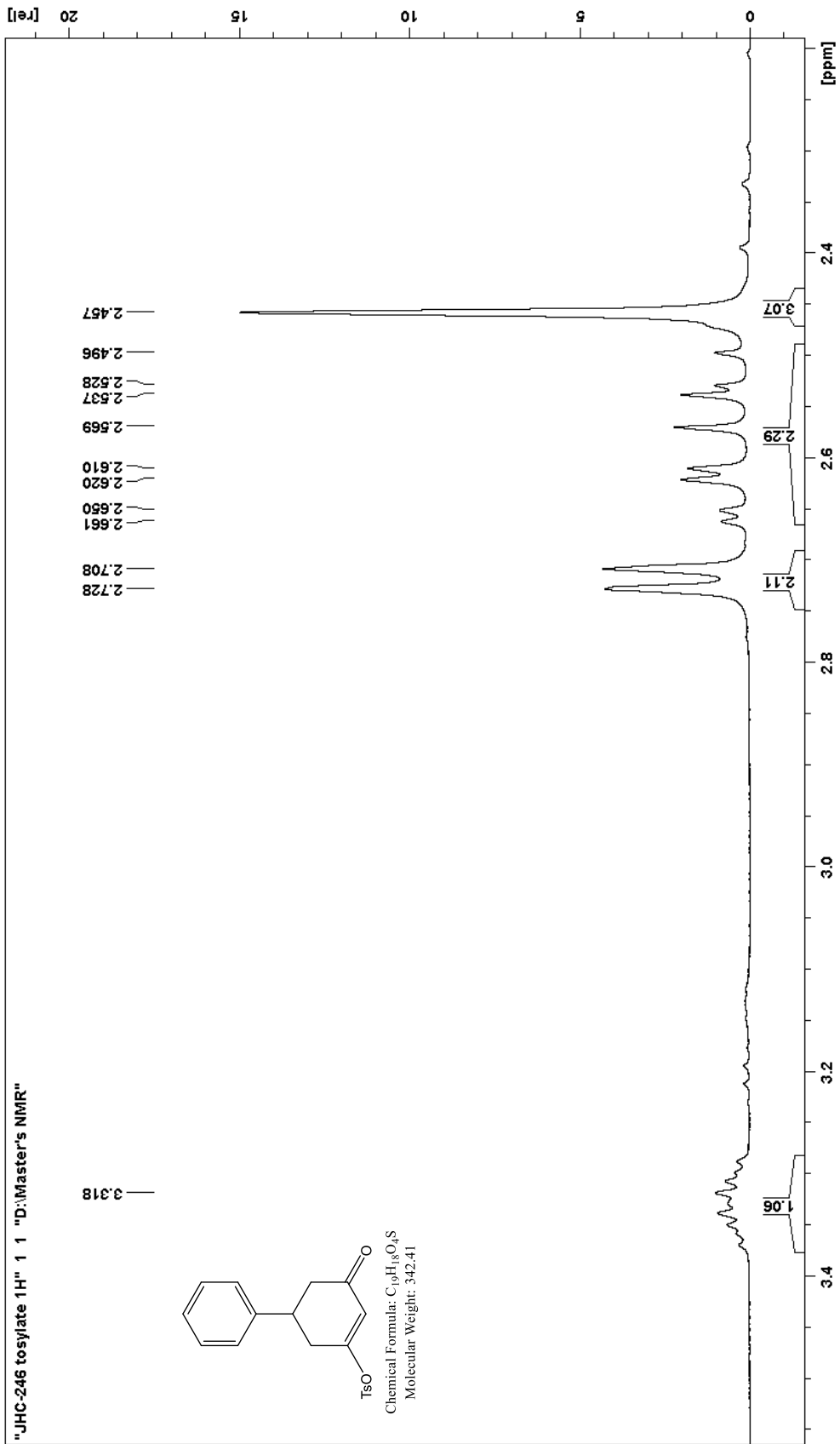
**<sup>1</sup>H NMR (400 MHz, CDCl<sub>3</sub>) δ, ppm:** 7.81 (d, J = 8.0 Hz, 2H), 7.37-7.23 (m, 5H), 7.17 (d, J = 7.2 Hz, 2H), 5.88 (s, 1H), 3.32 (m, 1H), 2.72 (d, 8.0 Hz, 2H), 2.66-2.50 (ddd, J<sub>1</sub> = 16.4 Hz, J<sub>2</sub> = 12.8 Hz, J<sub>3</sub> = 4.4 Hz, 2H), 2.46 (s, 3H).

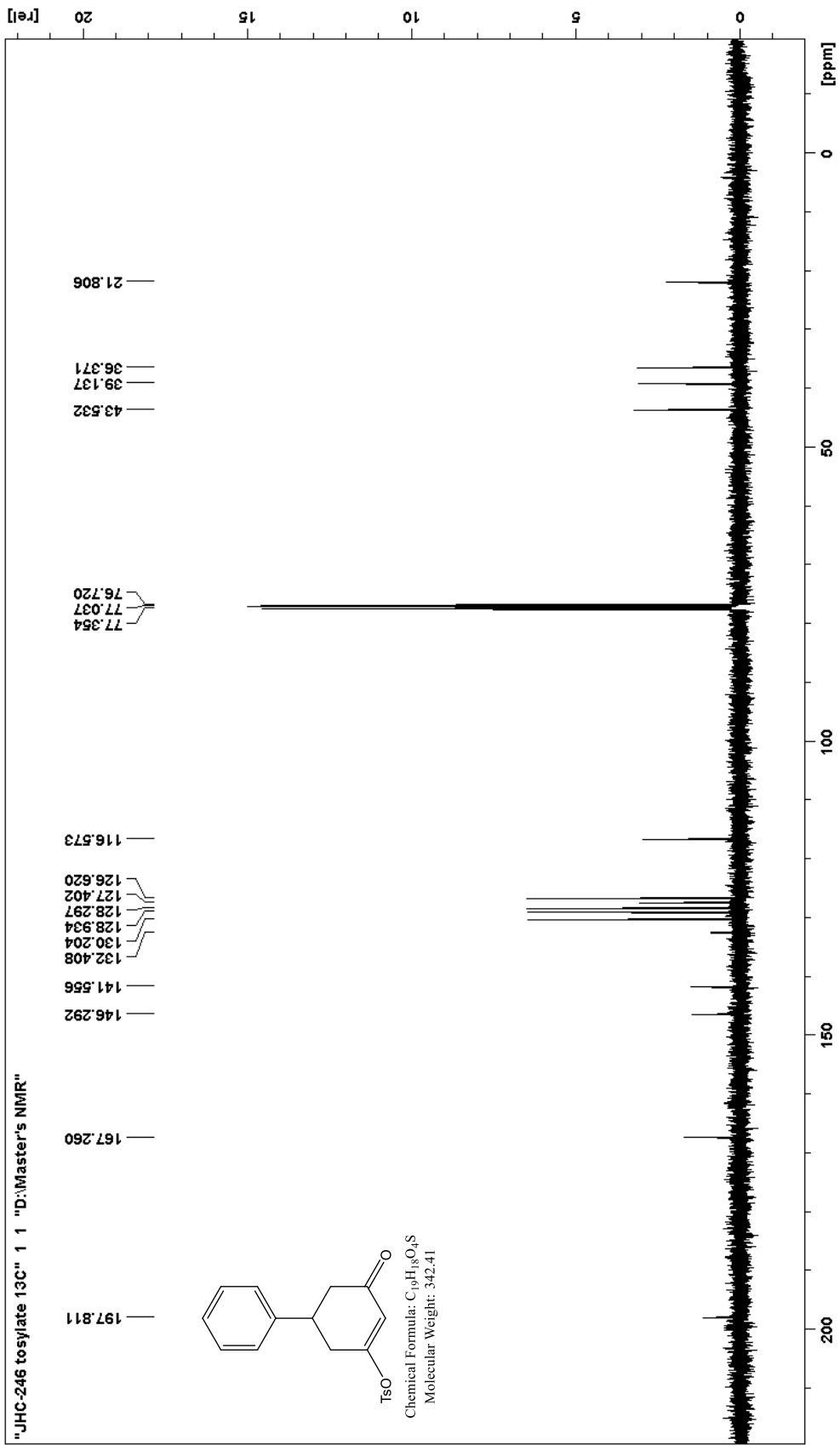
\*presence of water and grease from evaporation of hexanes was detected in the sample.

**<sup>13</sup>C NMR (400 MHz, CDCl<sub>3</sub>) δ, ppm:** 197.81, 167.26, 146.29, 141.56, 132.41, 130.20 (2C), 128.93 (2C), 128.30 (2C), 127.40, 126.62 (2C), 116.67, 43.53, 39.14, 36.37, 21.81.

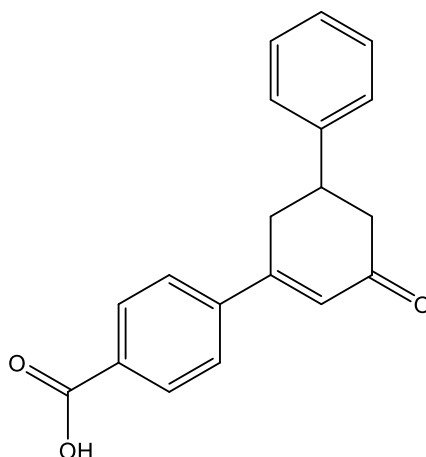








**Preparation of 3-(4-carboxyphenyl)-5-phenylcyclohex-2-enone, 37.**



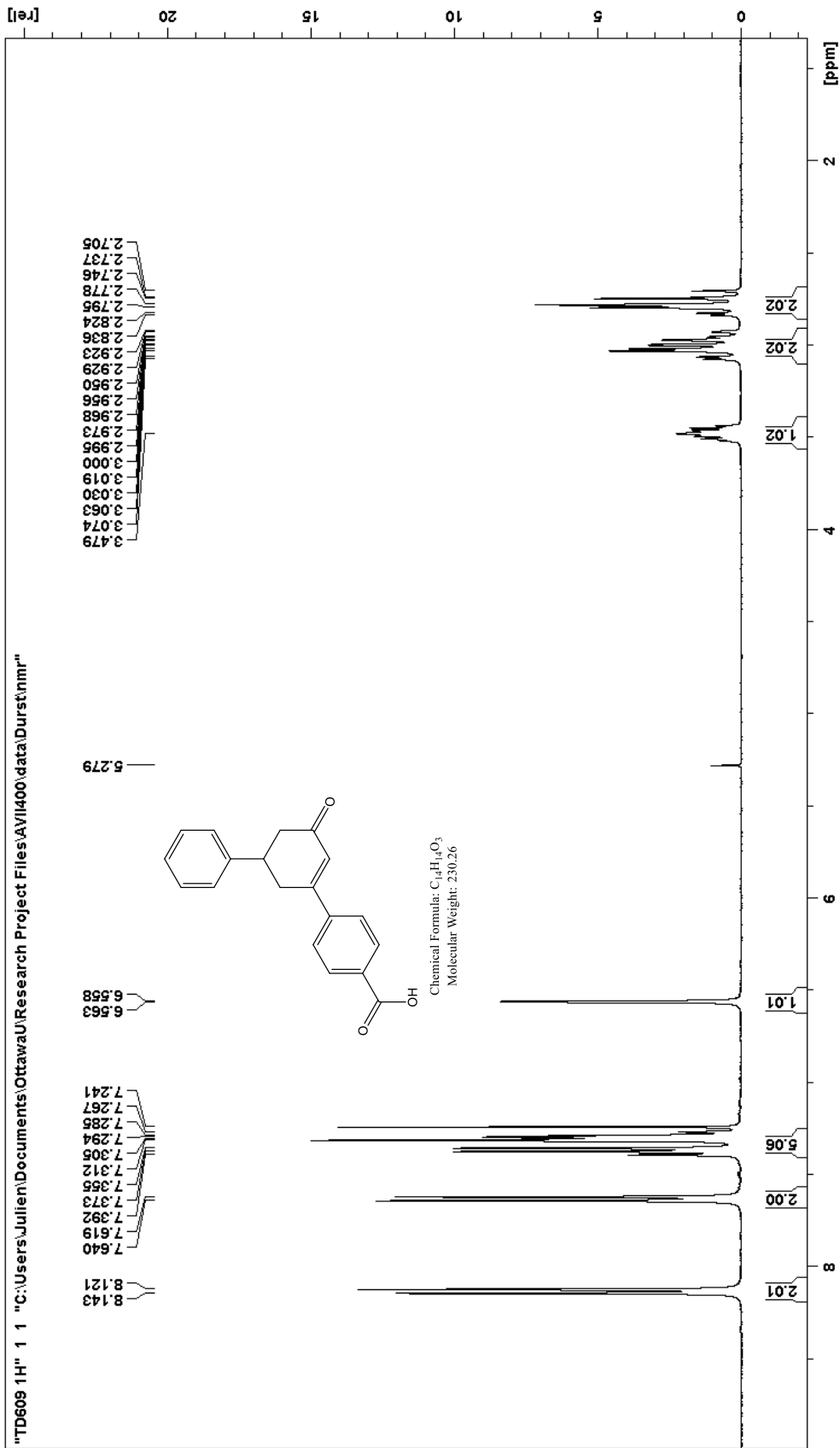
**37**

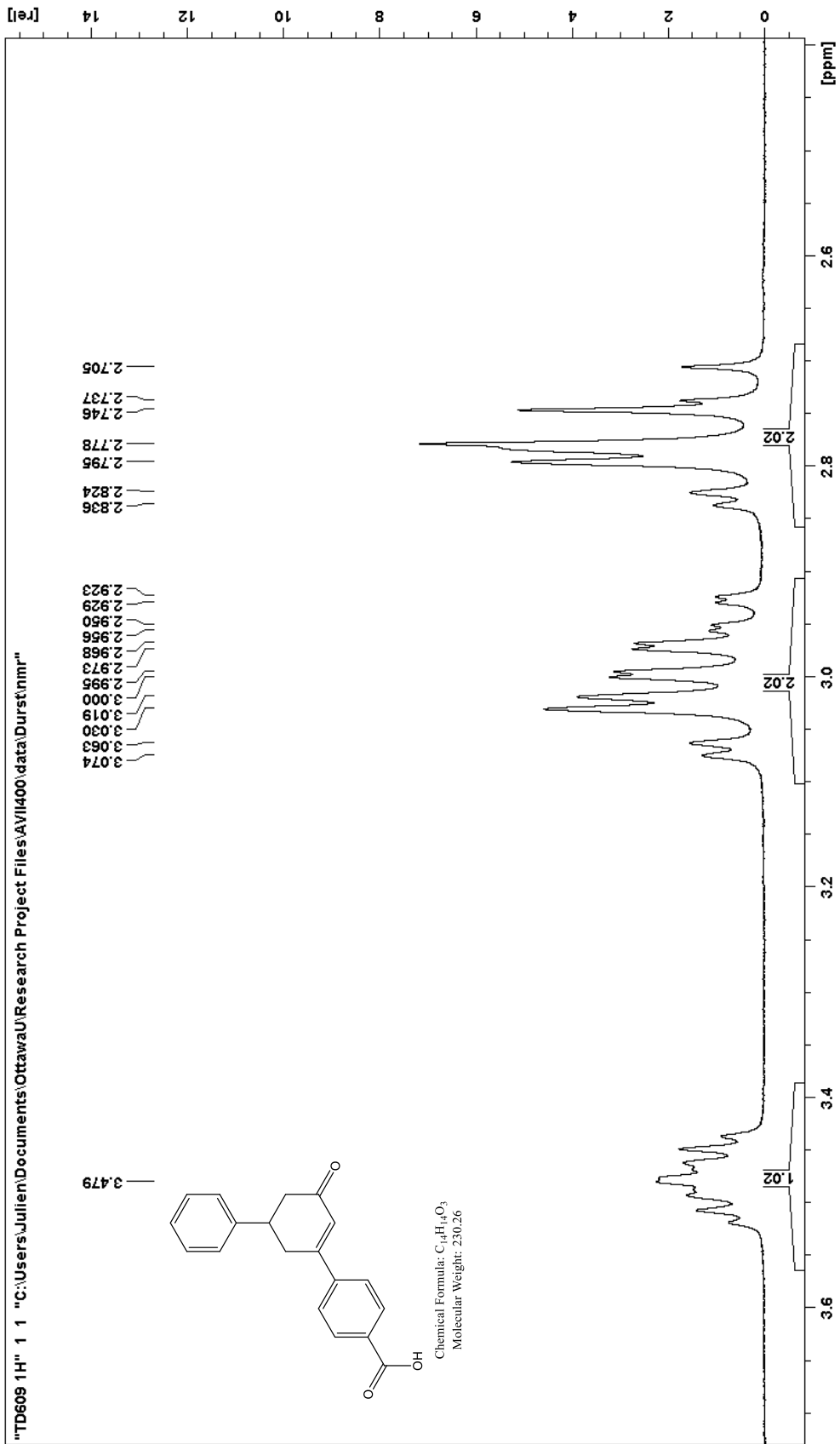
4-carboxyphenyl boronic acid (1.37 g, 8.25 mmol), the 5-phenylcyclohexane-1,3-dione enol tosylate (3.08 g, 8.99 mmol), sodium carbonate (1.81 g, 17.1 mmol) and tetrakis(triphenylphosphine)-palladium(0) (0.06 g, 0.05 mmol, 0.6 mol%) were dissolved in 45 mL of a 2:1 mixture of 95% ethanol and distilled water. The mixture was refluxed in an oil bath at 100°C for four hours, after which the solution was placed on the rotary evaporator to remove the ethanol. The solution was then diluted with water, and washed three times with DCM. The aqueous layer was acidified by slow addition of concentrated HCl and chilled to induce precipitation. The solid formed was isolated by suction filtration and rinsed with water. The product was obtained as a white solid (1.87 g, 78%, mp: 217.6 – 222.0°C).

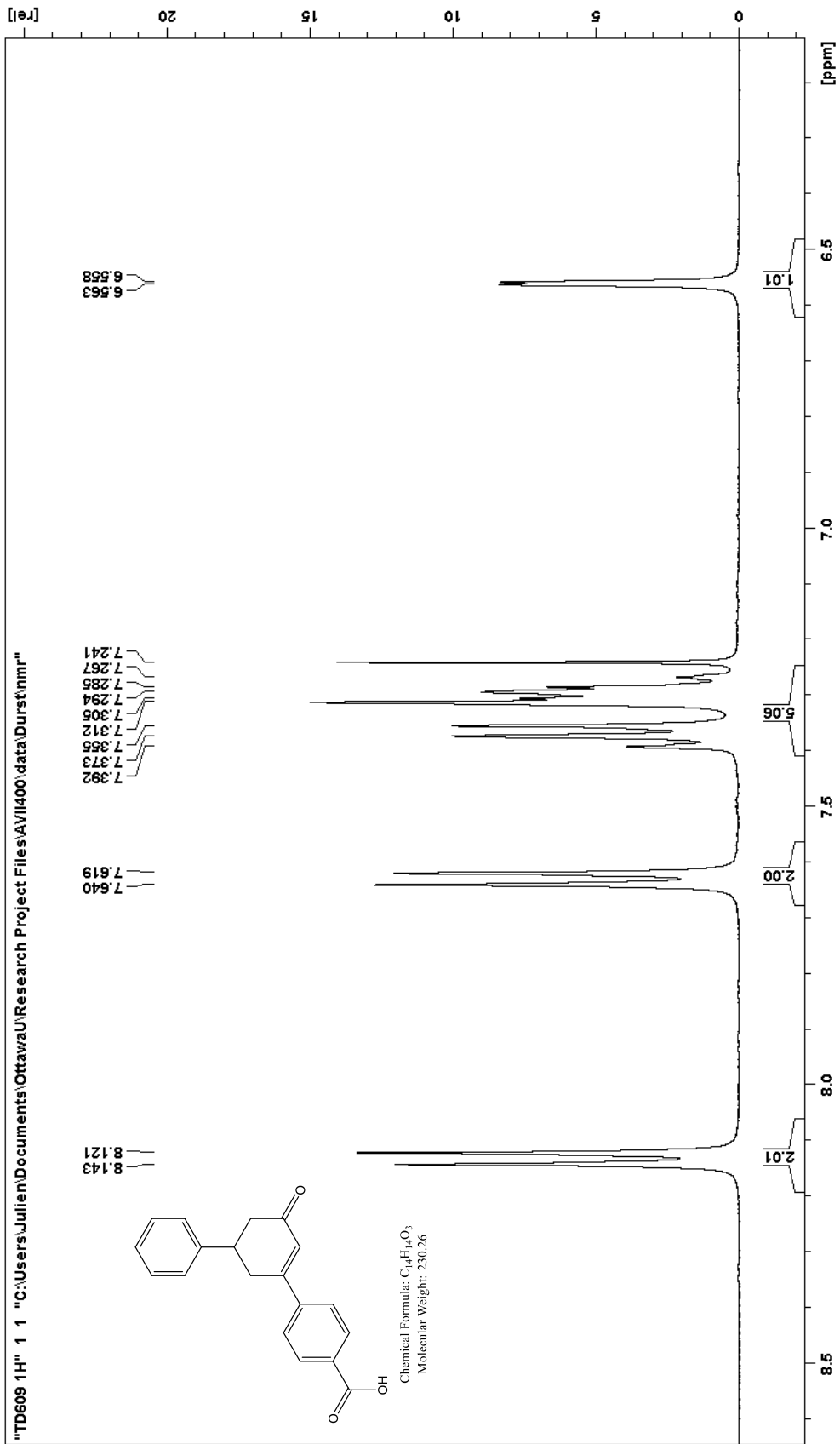
**<sup>1</sup>H NMR (400 MHz, CDCl<sub>3</sub>) δ, ppm:** 8.13 (d, J = 8.8 Hz, 2H), 7.63 (d, J = 8.4 Hz, 2H), 7.39-7.27 (m, 5H), 6.56 (d, J = 2.0 Hz, 1H), 3.48 (m, 1H), 3.07-2.92 (m, J<sub>1</sub> = 17.6 Hz, J<sub>2</sub> = 10.8 Hz, J<sub>3</sub> = 4.4 Hz, J<sub>4</sub> = 2.0 Hz, 2H), 2.84-2.71 (ddd, J<sub>1</sub> = 16.4 Hz, J<sub>2</sub> = 12.8 Hz, J<sub>3</sub> = 4.8 Hz, 2H).

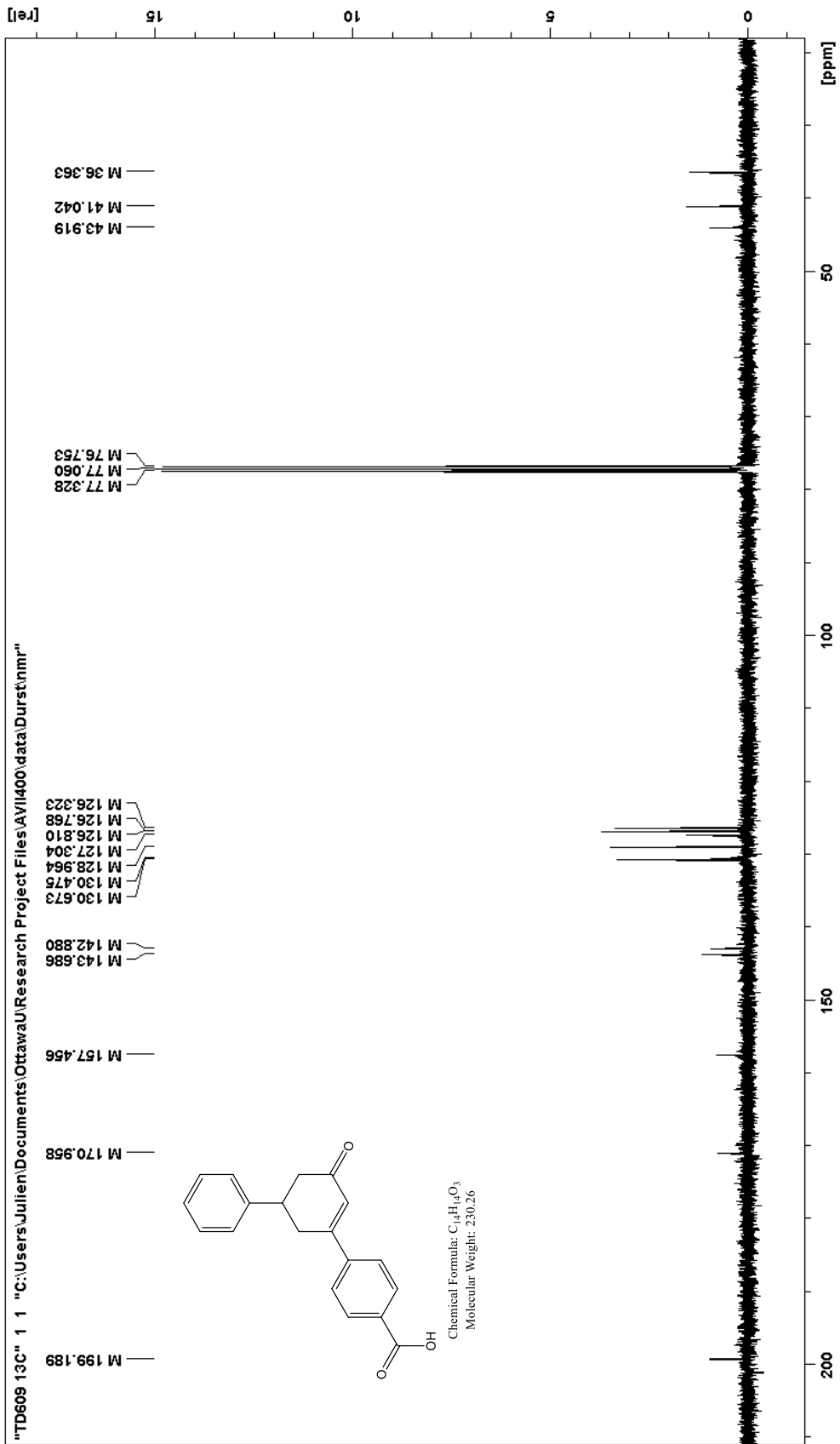
**<sup>13</sup>C NMR (400 MHz, CDCl<sub>3</sub>) δ, ppm:** 199.19, 170.96, 157.46, 143.69, 142.88, 130.67 (2C), 130.48, 128.96 (2C), 127.30, 126.81 (2C), 126.77, 126.32 (2C), 43.92, 41.04, 36.36.

**HRMS-EI m/z:** M<sup>+</sup> calcd for C<sub>19</sub>H<sub>16</sub>O<sub>3</sub>, 292.1099; found, 292.1129.

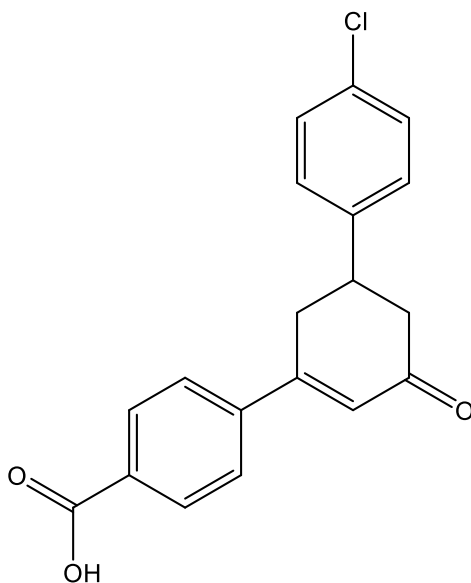








**Preparation of 3-(4-carboxyphenyl)-5-(4-chlorophenyl)cyclohex-2-enone, 42.**

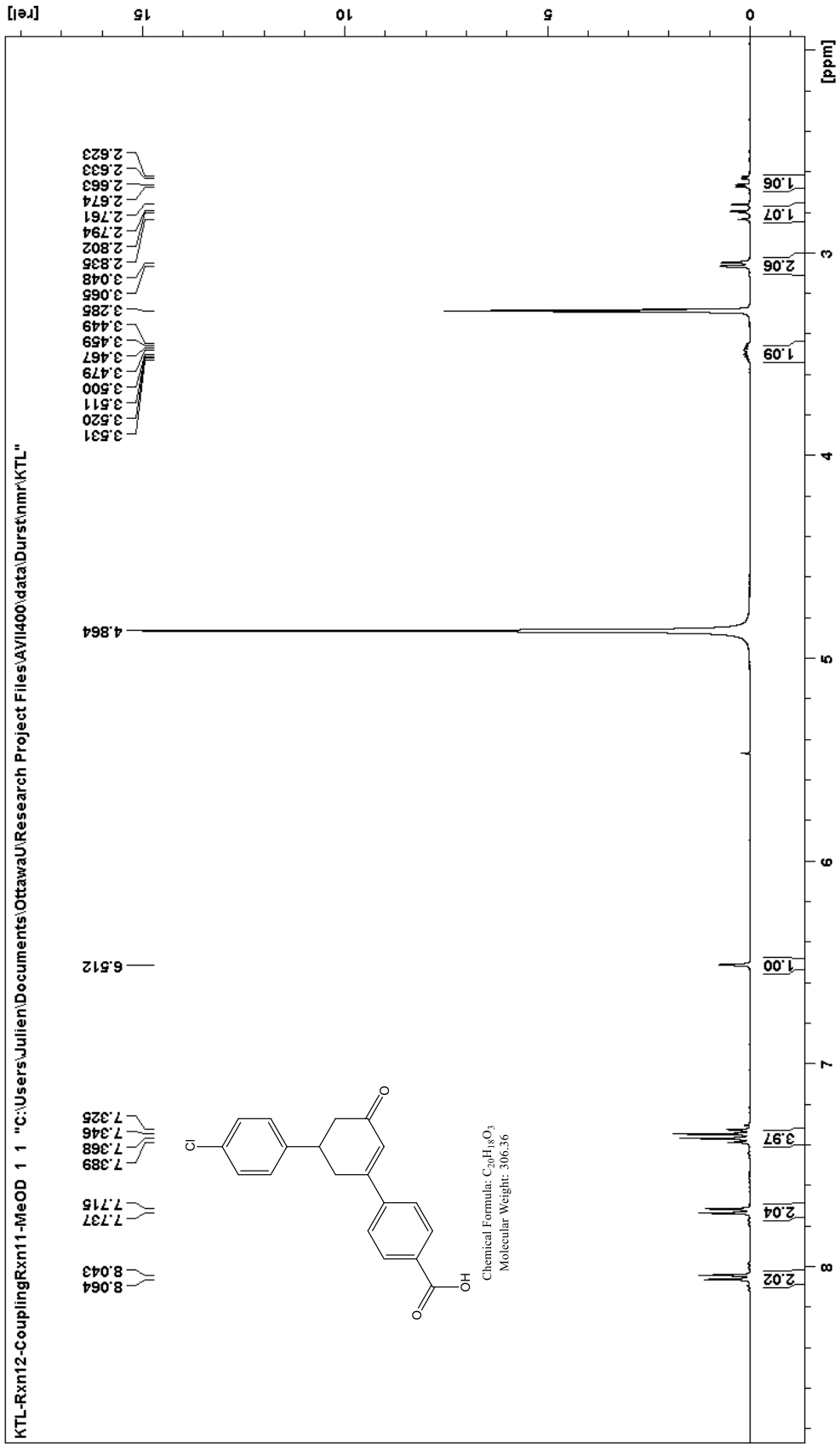


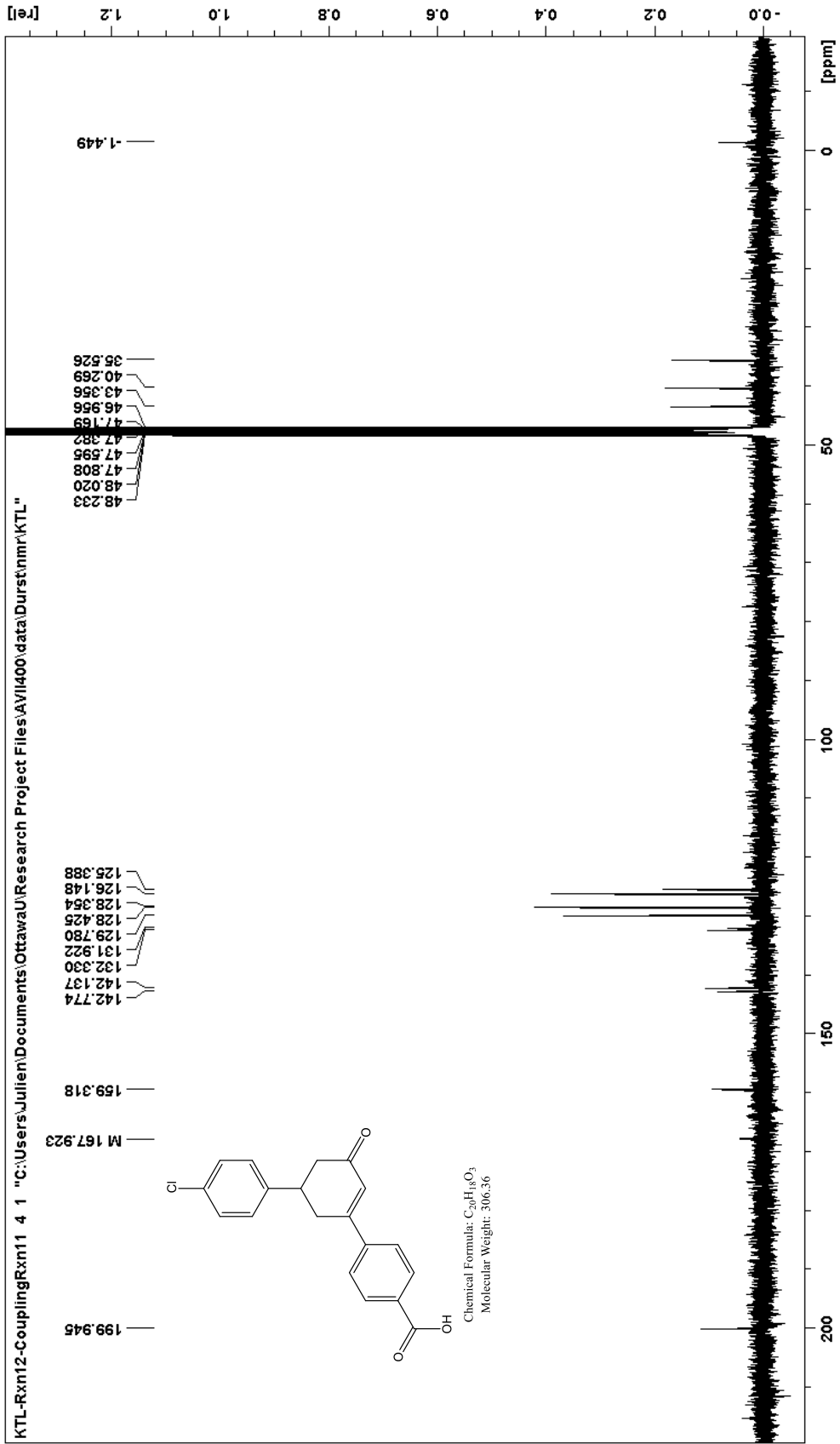
**42**

This compound was prepared via the usual two-step process from starting 5-(4-chlorophenyl) cyclohexane-1,3-dione by visiting student researcher Sofi Liu, but is included due to its importance in this work. The lab book containing the experimental data for this compound was unfortunately unavailable.

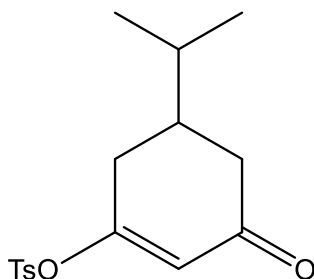
**<sup>1</sup>H NMR (400 MHz, CDCl<sub>3</sub>) δ, ppm:** 8.05 (d, J = 8.4 Hz, 2H), 7.73 (d, J = 8.8 Hz, 2H), 7.39 – 7.33 (m, J = 8.4 Hz, 4H), 6.51 (s, 1H), 3.53-3.45 (m, J = 4.4 Hz, 1H), 3.06 (d, J = 6.8 Hz, 2H), 2.80 (dd, J<sub>1</sub> = 16.4 Hz, J<sub>2</sub> = 13.2 Hz, 1H), 2.65 (dd, J<sub>1</sub> = 16.4 Hz, J<sub>2</sub> = 4.4 Hz, 1H).

**<sup>13</sup>C NMR (400 MHz, CDCl<sub>3</sub>) δ, ppm:** 199.95, 167.92, 159.32, 142.77, 142.14, 132.33, 131.92, 129.78 (2C), 128.43 (2C), 128.35 (2C), 126.15 (2C), 125.39, 43.57, 40.27, 35.53.





**Preparation of the enol tosylate of 5-isopropylcyclohexane-1,3-dione, 41.**

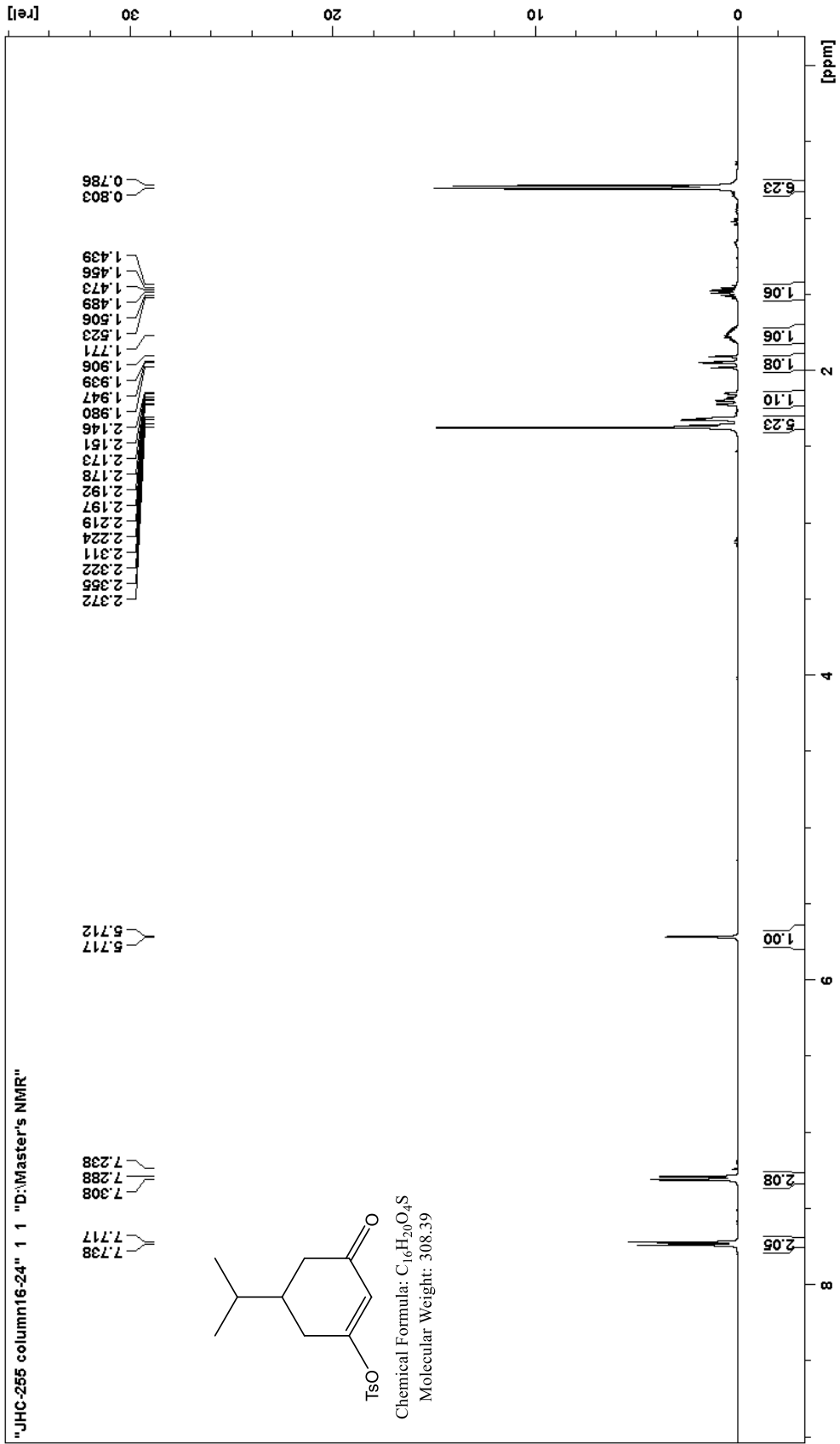


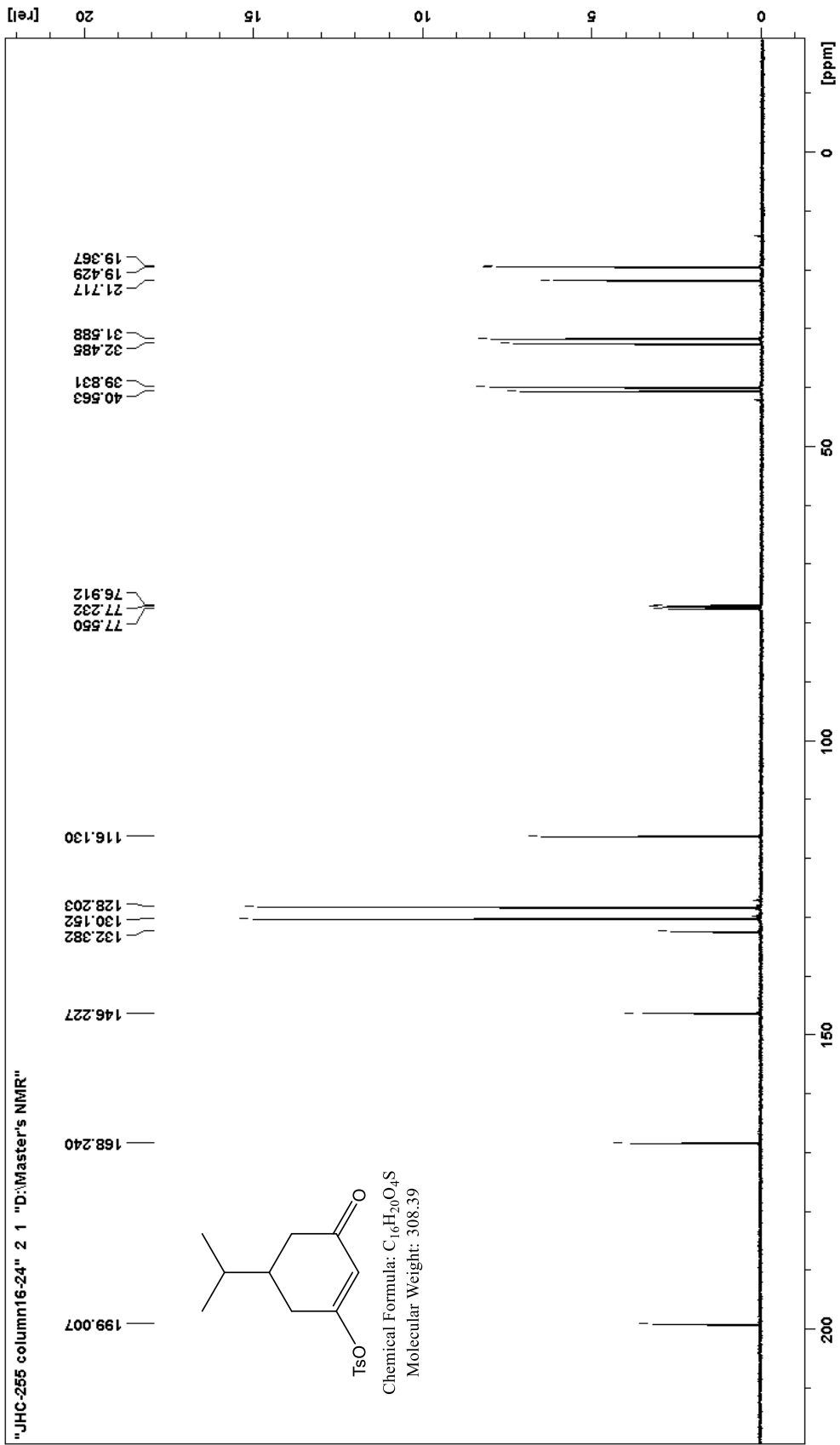
**41**

5-isopropylcyclohexane-1,3-dione (0.45 g, 2.91 mmol) and p-toluenesulfonyl chloride (0.94 g, 4.93 mmol) were dissolved in ethyl acetate (10 mL). Triethylamine (0.45 g, 4.44 mmol) was added to the mixture, which caused precipitation of triethylamine hydrochloride as a white solid. The solution was stirred at room temperature overnight, then washed twice with 10% NaOH<sub>aq</sub> and once with distilled water. The aqueous phases were combined and acidified but no starting material appeared to be recovered. The organic layer was dried over MgSO<sub>4</sub>, filtered, and evaporated under reduced pressure. The crude product obtained was passed quickly through a silica column, using a 5% to 20% ethyl acetate in hexanes solvent gradient, to separate remaining p-toluenesulfonyl chloride that was detected by TLC. The appropriate fractions were combined and evaporated, to yield to product as a pale yellow solid (0.64 g, 71%).

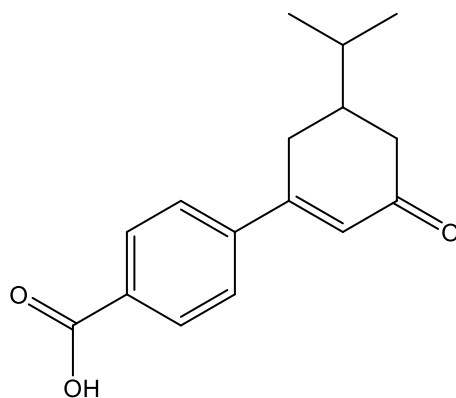
**<sup>1</sup>H NMR (400 MHz, CDCl<sub>3</sub>) δ, ppm:** 7.73 (d, J = 8.4 Hz, 2H), 7.30 (d, J = 8.0 Hz, 2H), 5.17 (s, 1H), 2.37 (s, 3H), 2.34 (dd, J<sub>1</sub> = 17.6 Hz, J<sub>2</sub> = 4.4 Hz, 2H), 2.19 (ddd, J<sub>1</sub> = 18.4 Hz, J<sub>2</sub> = 10.8 Hz, J<sub>3</sub> = 2.0 Hz, 1H), 1.94 (dd, J<sub>1</sub> = 16.4 Hz, J<sub>2</sub> = 13.2 Hz, 1H), 1.77 (m, 1H), 1.48 (m, J = 6.8 Hz, 1H), 0.80 (d, J = 6.8 Hz, 6H).

**<sup>13</sup>C NMR (400 MHz, CDCl<sub>3</sub>) δ, ppm:** 199.00, 168.24, 146.23, 132.38, 130.15 (2C), 128.20 (2C), 116.13, 40.56, 39.83, 32.49, 31.59, 21.71, 19.43, 19.37.





**Preparation of 3-(4-carboxyphenyl)-5-isopropylcyclohex-2-enone, 43.**

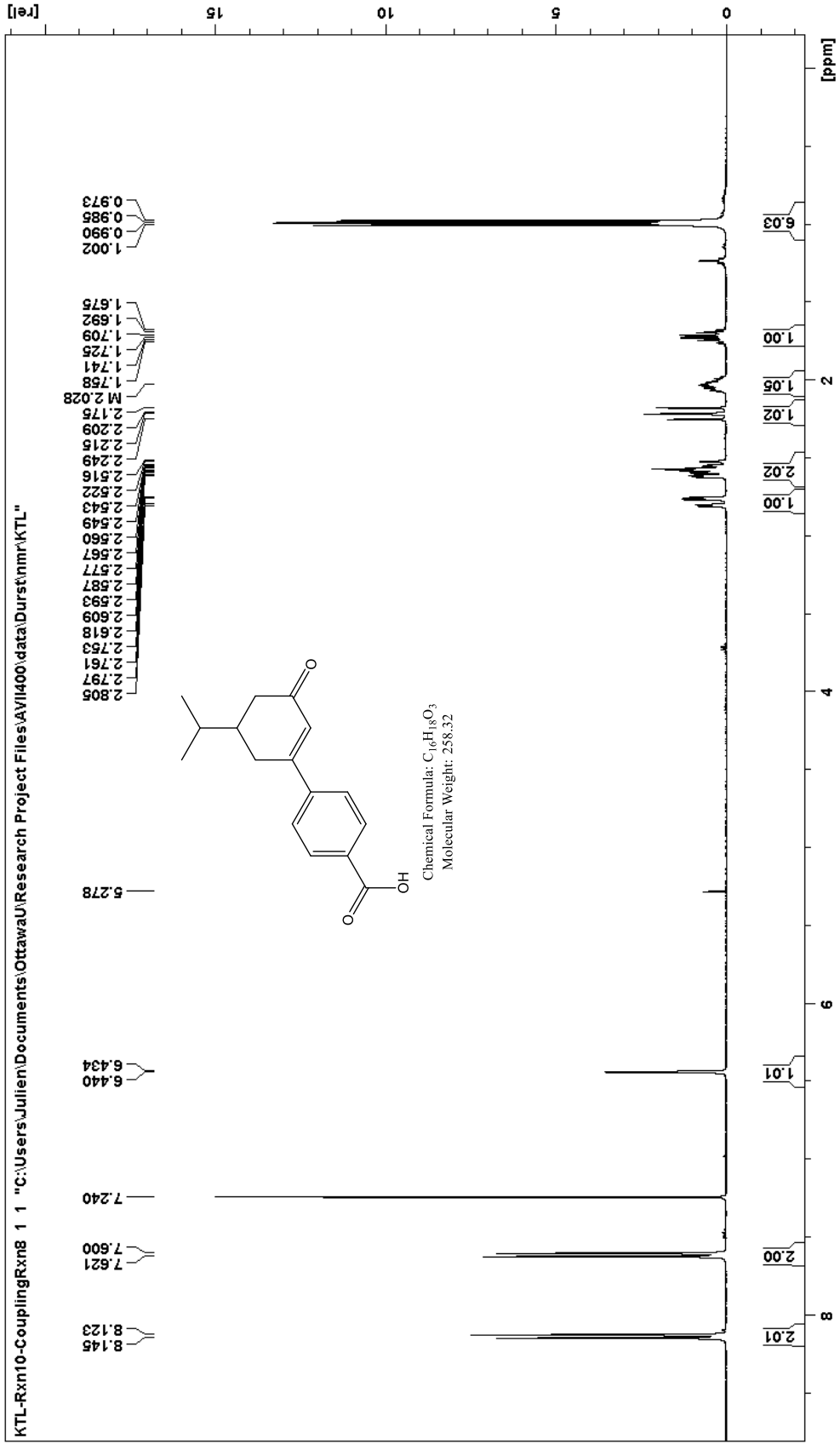


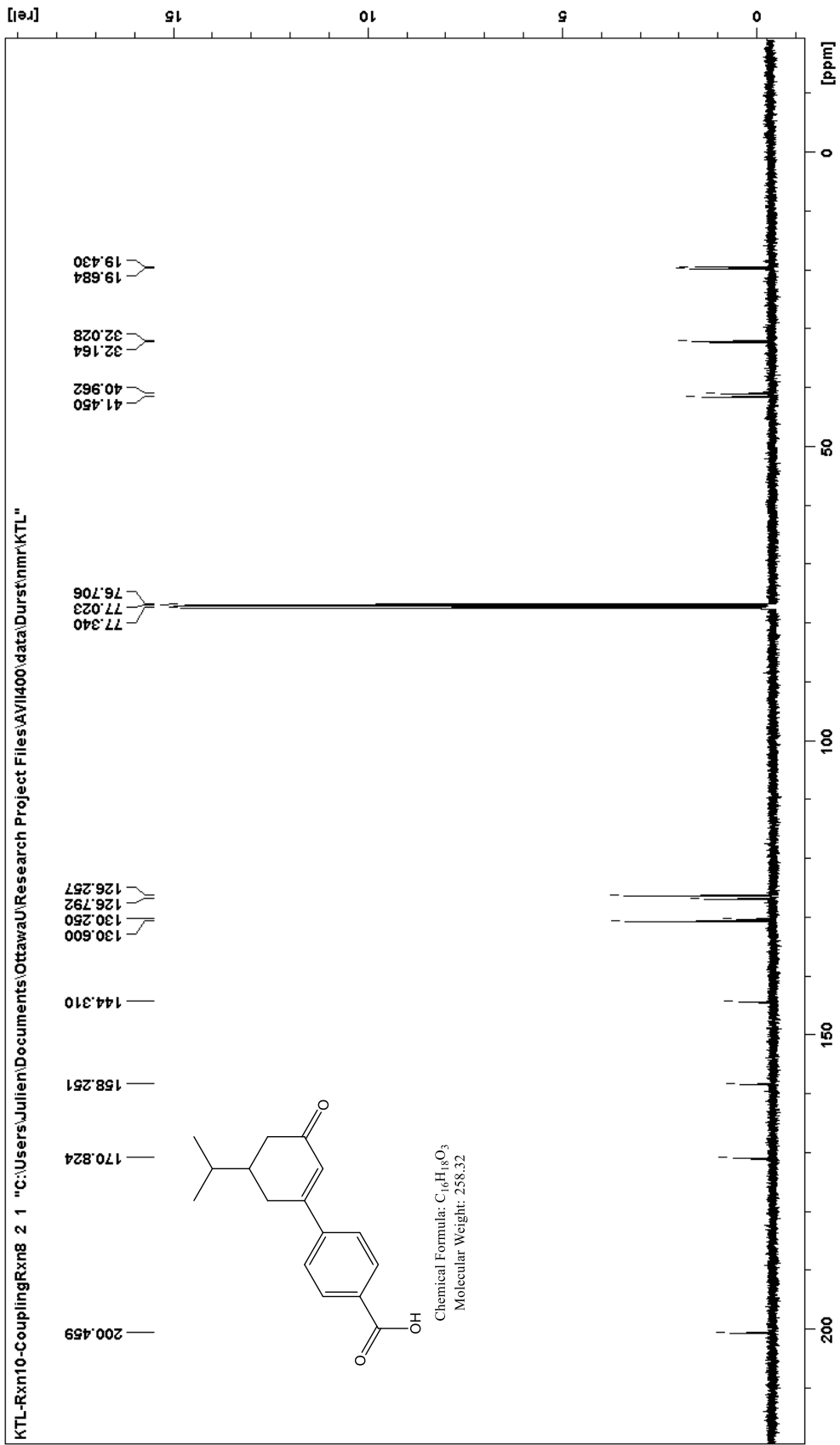
**43**

4-carboxyphenyl boronic acid (0.24 g, 1.45 mmol), the 5-phenylcyclohexane-1,3-dione enol tosylate (0.47 g, 1.60 mmol), sodium carbonate (0.32 g, 3.02 mmol) and tetrakis(triphenylphosphine)-palladium(0) (17 mg, 0.015 mmol, 1.0 mol%) were dissolved in 20 mL of a 2:1 mixture of 95% ethanol and distilled water. The mixture was refluxed in an oil bath at 100°C for four hours, after which the solution was placed on the rotary evaporator to remove the ethanol. The solution was then diluted with water, and washed three times with DCM. The aqueous layer was acidified by slow addition of concentrated HCl and chilled to induce precipitation. The solid formed was isolated by suction filtration and rinsed with water. The product was obtained as a white solid (0.26 g, 69%, mp: 195.0 – 196.8°C).

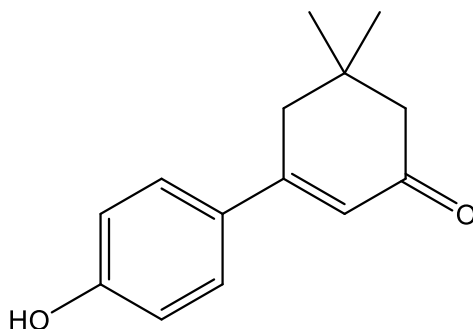
**<sup>1</sup>H NMR (400 MHz, CDCl<sub>3</sub>) δ, ppm:** 8.12 (d, J = 8.8 Hz, 2H), 7.61 (d, J = 8.4 Hz, 2H), 6.44 (d, J = 2.4 Hz, 1H), 2.78 (dd, J<sub>1</sub> = 17.6 Hz, J<sub>2</sub> = 3.2 Hz, 1H), 2.62-2.52 (m, 2H), 2.21 (dd, J<sub>1</sub> = 16.0 Hz, J<sub>2</sub> = 13.6 Hz, 1H), 2.03 (m, 1H), 1.72 (m, J = 6.8 Hz, 1H), 0.99 (dd, J<sub>1</sub> = 6.8 Hz, J<sub>2</sub> = 4.8 Hz, 6H).

**<sup>13</sup>C NMR (400 MHz, CDCl<sub>3</sub>) δ, ppm:** 200.46, 170.82, 158.25, 144.31, 130.60 (2C), 130.25, 126.79, 126.26 (2C), 41.45, 40.96, 32.16, 32.03, 19.68, 19.43.





### Preparation of 3-(4-hydroxyphenyl)-cyclohex-2-enone.



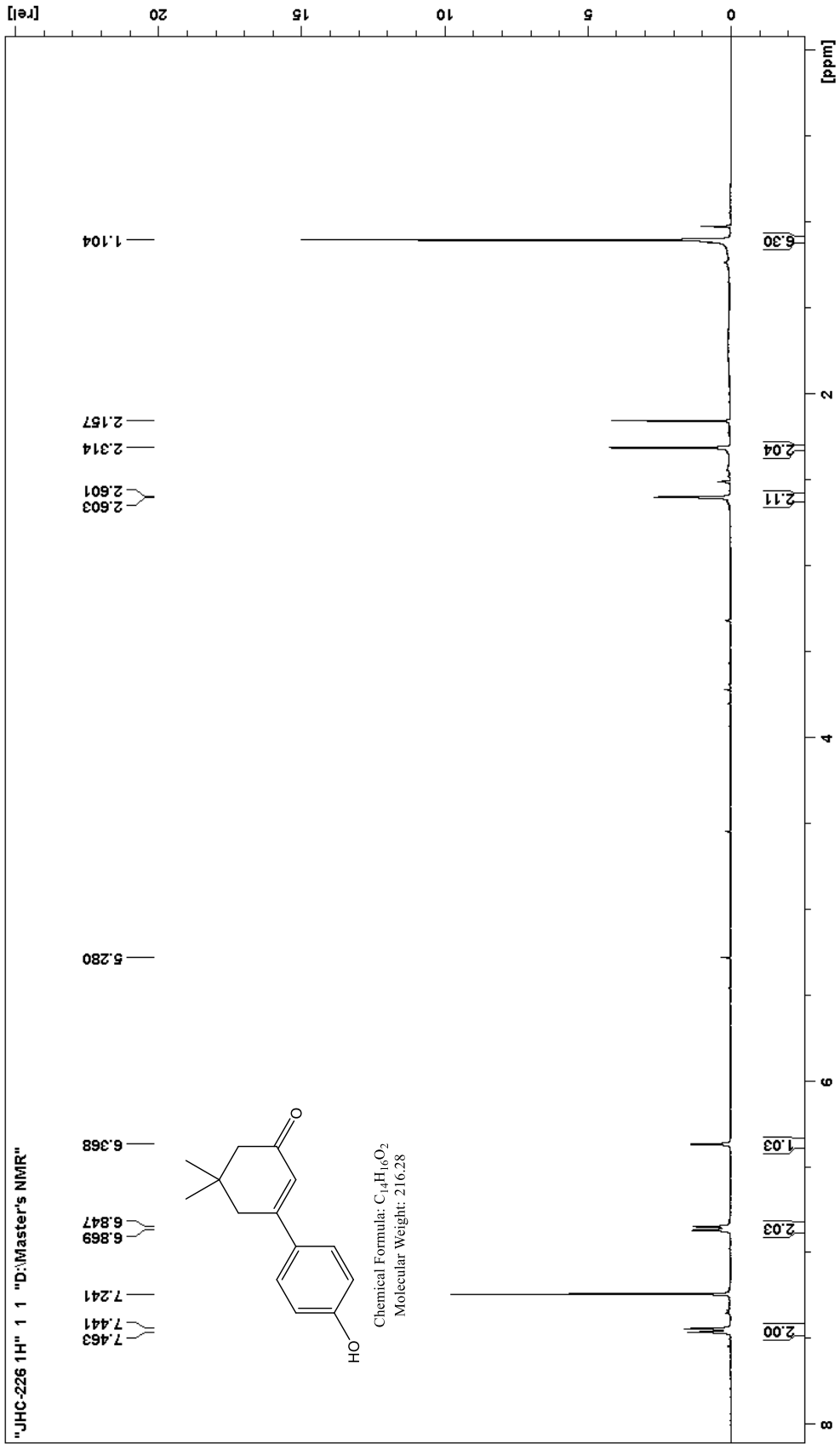
4-hydroxyphenylboronic acid (1.52 g, 11.0 mmol), dimedone enol tosylate (3.68 g, 12.5 mmol), sodium carbonate (2.43 g, 22.9 mmol) and tetrakis(triphenylphosphine)palladium(0) (0.07 g, 0.06 mmol, 0.55 mol%) were dissolved in a 2:1 solution of 95% ethanol and water (45 mL). The solution was refluxed for 6 hours in an oil bath at 100°C, then placed on the rotary evaporator to remove most of the ethanol. The solution remaining was diluted with an additional small amount of water, before washing three times with DCM. The aqueous layer was acidified with concentrated HCl added dropwise, then left in the freezer to promote crystallization. The precipitate was recovered via suction filtration, yielding the product as a light yellow solid with flakes of brown impurities (1.15 g, 48%)

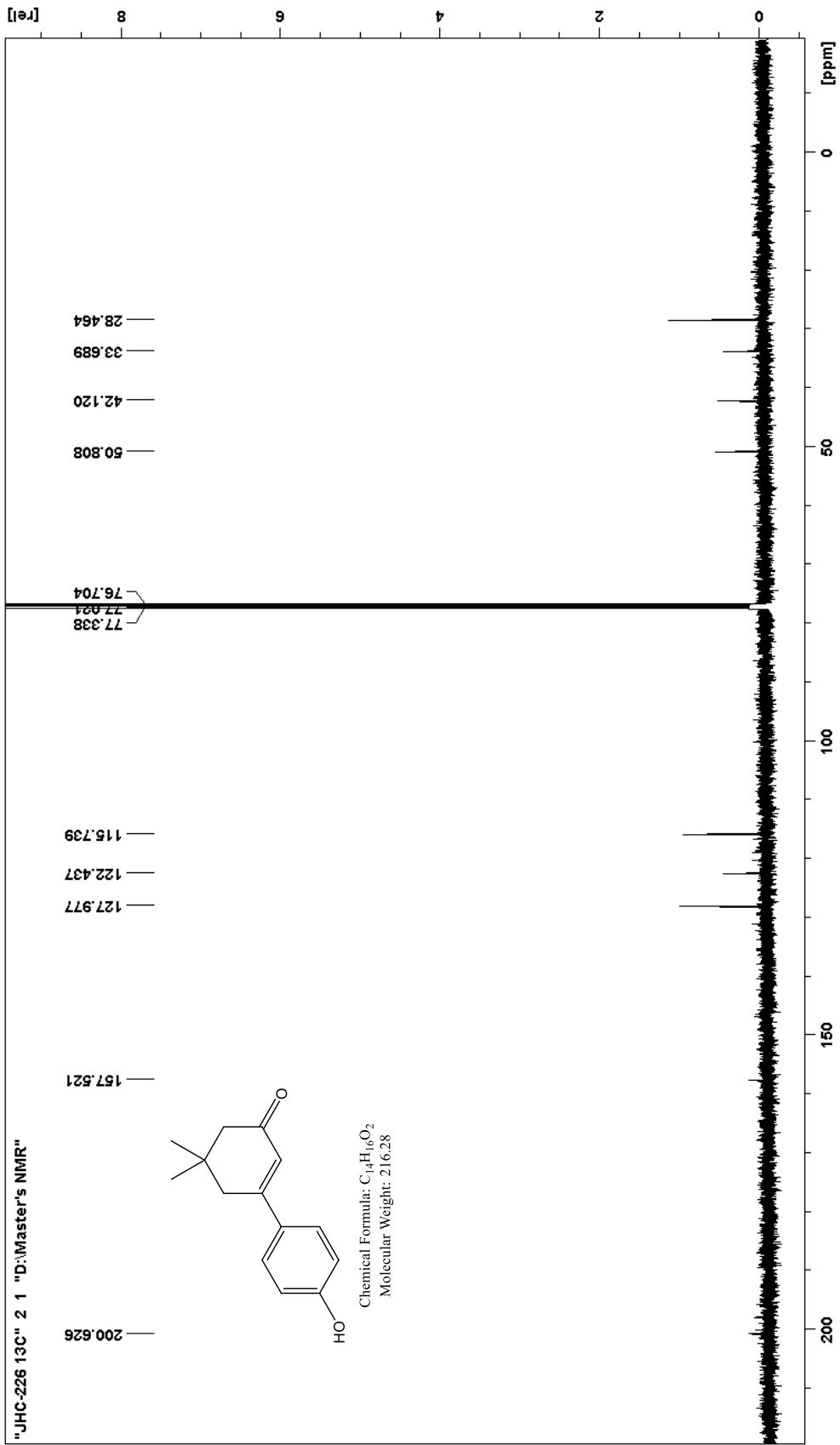
**<sup>1</sup>H NMR (400 MHz, CDCl<sub>3</sub>) δ, ppm:** 7.45 (d, J = 8.8 Hz, 2H), 6.86 (d, J = 8.8 Hz, 2H), 6.37 (s, 1H), 2.60 (d, J = 0.8 Hz, 2H), 2.31 (s, 2H), 1.10 (s, 6H).

\*presence of acetone is detected by NMR, likely due to the NMR tube itself rather than in the sample.

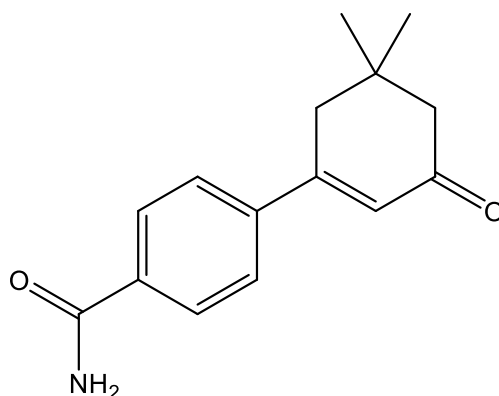
**<sup>13</sup>C NMR (400 MHz, CDCl<sub>3</sub>) δ, ppm:** 200.63, 157.52, 127.98 (2C), 122.44, 115.74 (2C), 50.81, 42.12, 33.69, 28.46 (2C).

\*The peaks of the quaternary carbons are difficult to locate due to the low solubility of the sample in CDCl<sub>3</sub>. Two of the peaks could not be detected from the signal noise, however <sup>1</sup>H NMR data was deemed sufficient for this compound.





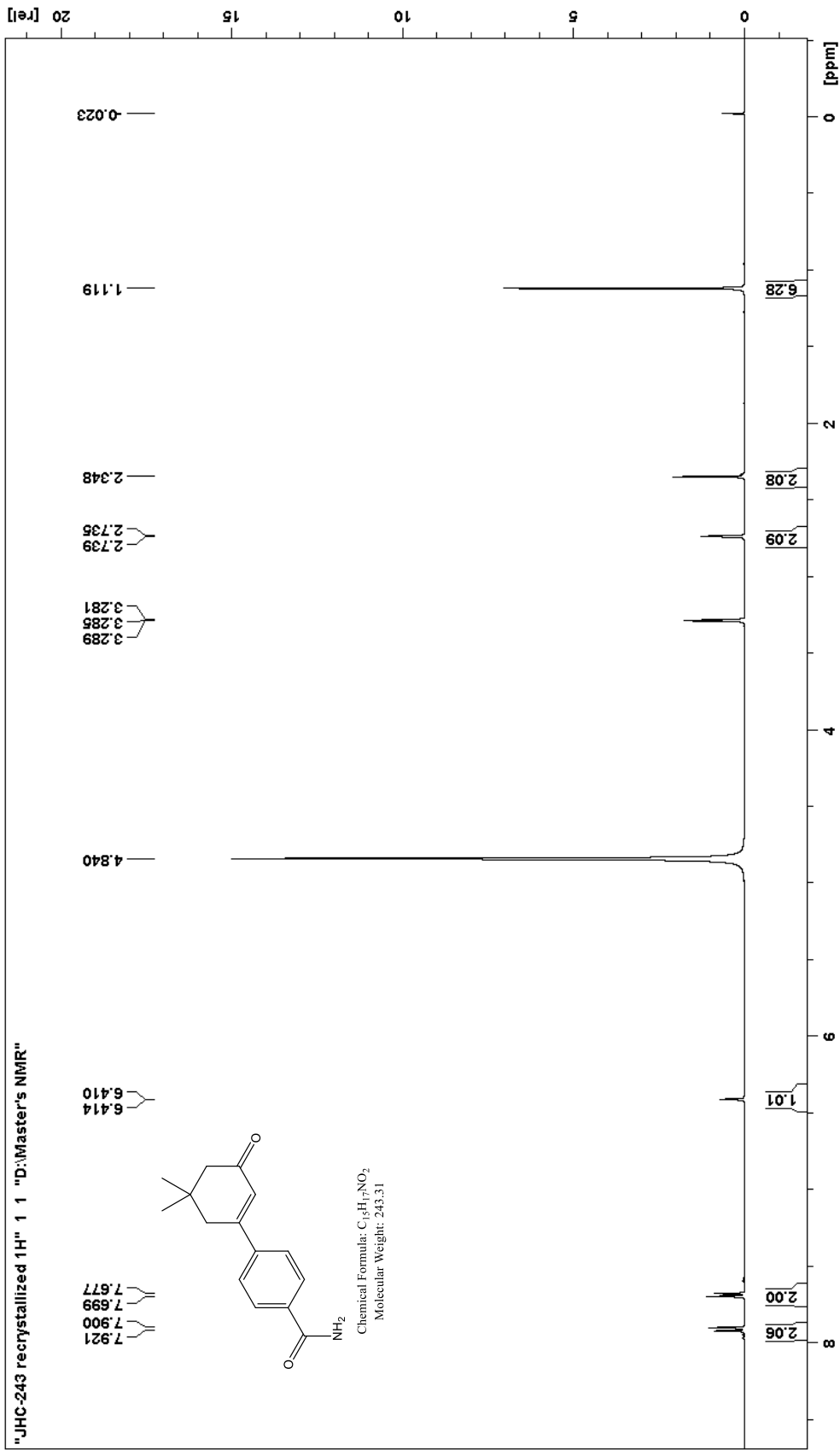
### Preparation of 4-(5,5-dimethylcyclohexen-3-one)-benzamide

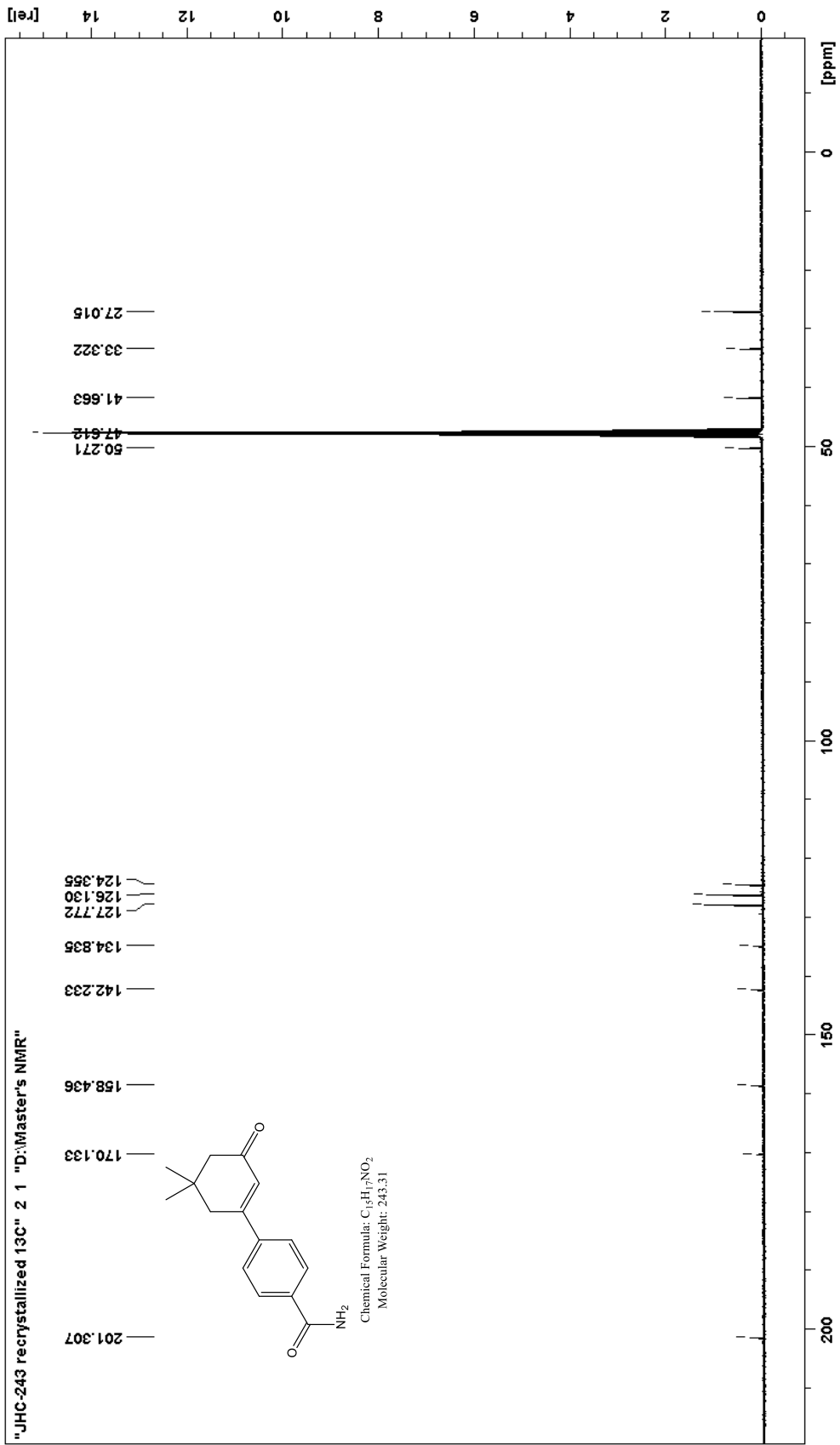


3-(4-carboxyphenyl)-5,5-dimethylcyclohex-2-enone (0.98 g, 4.01 mmol) was dissolved in 20 mL DCM. Oxalyl chloride (0.69 g, 5.43 mmol) was added slowly via syringe. The solution was heated gently for 5 minutes to bring the reaction close to reflux, then 3 drops of catalytic DMF were added. The mixture started to reflux immediately, and was left to react for 2 hours. Afterwards, the solvent was evaporated under reduced pressure, leaving behind a red oil which solidified in the freezer. This solid (0.77 g, 73%, mp: 99.6 – 103.2°C) was recrystallized in a mixture of DCM and hexanes before the next step. A small amount of this acid chloride was set aside. The rest (0.57 g, 2.17 mmol) was dissolved in THF (20 mL), and a second solution of 30%  $\text{NH}_4\text{OH}_{\text{aq}}$  (2.0 mL, 17 mmol) in THF (10 mL) was prepared. Both solutions were chilled in ice baths, then the acid chloride mixture was slowly added to the ammonia solution. The combined solution was left to warm up to room temperature for 30 minutes, after which the solvent was evaporated. 50 mL of a 10%  $\text{Na}_2\text{CO}_3_{\text{aq}}$  solution was added to the flask. The product was extracted three times with DCM, dried over  $\text{MgSO}_4$ , filtered and evaporated. The crude product (0.35 g, 66%) was purified by recrystallization in DCM and hexanes to obtain the purified product as a white powder (0.23 g, 44%, mp: 229.9 – 232.2°C).

$^1\text{H NMR}$  (400 MHz, MeOD)  $\delta$ , ppm: 7.91 (d,  $J = 8.4$  Hz, 2H), 6.69 (d,  $J = 8.8$  Hz, 2H), 6.41 (d,  $J = 1.6$  Hz, 1H), 2.74 (d,  $J = 1.6$  Hz, 2H), 2.44 (s, 2H), 1.12 (s, 6H)

$^{13}\text{C NMR}$  (400 MHz, MeOD)  $\delta$ , ppm: 201.31, 170.13, 158.44, 142.23, 134.84, 127.77 (2C), 126.13 (2C), 124.36, 50.27, 41.66, 33.32, 27.02 (2C).





## 1.4 References

- (1) Feigin, V. L. et al. Global, Regional, and National Burden of Neurological Disorders during 1990–2015: A Systematic Analysis for the Global Burden of Disease Study 2015. *Lancet Neurol.* **2017**, *16* (11), 877–897. [https://doi.org/10.1016/S1474-4422\(17\)30299-5](https://doi.org/10.1016/S1474-4422(17)30299-5).
- (2) World Health Organization. Epilepsy Facts Sheet. <https://www.who.int/news-room/fact-sheets/detail/epilepsy>.
- (3) *An Introduction to Epilepsy*; Bromfield, E. B., Cavazos, J. E., Sirven, J. I., Eds.; American Epilepsy Society: West Hartford (CT), 2006.
- (4) Fisher, R. S.; Cross, J. H.; French, J. A.; Higurashi, N.; Hirsch, E.; Jansen, F. E.; Lagae, L.; Moshé, S. L.; Peltola, J.; Roulet Perez, E.; Scheffer, I. E.; Zuberi, S. M. Operational Classification of Seizure Types by the International League Against Epilepsy: Position Paper of the ILAE Commission for Classification and Terminology. *Epilepsia* **2017**, *58* (4), 522–530. <https://doi.org/10.1111/epi.13670>.
- (5) Epilepsy foundation. Types Of Seizures. <https://www.epilepsy.com/learn/types-seizures>.
- (6) Tellez-Zenteno, J. F.; Patten, S. B.; Jetté, N.; Williams, J.; Wiebe, S. Psychiatric Comorbidity in Epilepsy: A Population-Based Analysis. *Epilepsia* **2007**, *48* (12). <https://doi.org/10.1111/j.1528-1167.2007.01222.x>.
- (7) Comorbidity in Adults with Epilepsy — United States, 2010 <https://www.cdc.gov/mmwr/preview/mmwrhtml/mm6243a2.htm> (accessed 2020 -01 -08).
- (8) Gaitatzis, A.; Johnson, A. L.; Chadwick, D. W.; Shorvon, S. D.; Sander, J. W. Life Expectancy in People with Newly Diagnosed Epilepsy. *Brain J. Neurol.* **2004**, *127* (Pt 11), 2427–2432. <https://doi.org/10.1093/brain/awh267>.
- (9) Epilepsies, I. of M. (US) C. on the P. H. D. of the; England, M. J.; Liverman, C. T.; Schultz, A. M.; Strawbridge, L. M. *Epilepsy Across the Spectrum: Promoting Health and Understanding.*; National Academies Press (US), 2012.
- (10) Baker, G. A.; Hargis, E.; Hsieh, M. M.-S.; Mounfield, H.; Arzimanoglou, A.; Glauser, T.; Pellock, J.; Lund, S.; International Bureau for Epilepsy. Perceived Impact of Epilepsy in Teenagers and Young Adults: An International Survey. *Epilepsy Behav. EB* **2008**, *12* (3), 395–401. <https://doi.org/10.1016/j.yebeh.2007.11.001>.
- (11) Epilepsy Foundation. Meeting News: Do Seizures Damage the Brain? <https://www.epilepsy.com/article/2014/3/meeting-news-do-seizures-damage-brain> (accessed 2020 -01 -08).
- (12) Magiorkinis, E.; Sidiropoulou, K.; Diamantis, A. Hallmarks in the History of Epilepsy: Epilepsy in Antiquity. *Epilepsy Behav.* **2010**, *17* (1), 103–108. <https://doi.org/10.1016/j.yebeh.2009.10.023>.
- (13) Arzimanoglou, A.; Ben-Menachem, E.; Cramer, J.; Glauser, T.; Seeruthun, R.; Harrison, M. The Evolution of Antiepileptic Drug Development and Regulation. *Epileptic. Disord.* **2010**, *12* (1), 3–15. <https://doi.org/10.1684/epd.2010.0303>.
- (14) Olson, K. R. *Poisoning & Drug Overdose*; Lange Medical Books/McGraw-Hill, 2004.
- (15) Galanter, M.; Kleber, H. D. *The American Psychiatric Publishing Textbook of Substance Abuse Treatment*; American Psychiatric Pub., 2008.

- (16) Putnam, T. J.; Merritt, H. H. Experimental determination of the anticonvulsant properties of some phenyl derivatives. *Science* **1937**, *85* (2213), 525–526. <https://doi.org/10.1126/science.85.2213.525>.
- (17) Hodgkin, A. L.; Huxley, A. F. A Quantitative Description of Membrane Current and Its Application to Conduction and Excitation in Nerve. *J. Physiol.* **1952**, *117* (4), 500–544. <https://doi.org/10.1113/jphysiol.1952.sp004764>.
- (18) Jefferys, J. G. R. Advances in Understanding Basic Mechanisms of Epilepsy and Seizures. *Seizure* **2010**, *19* (10), 638–646. <https://doi.org/10.1016/j.seizure.2010.10.026>.
- (19) Lang, D. G.; Wang, C. M.; Cooper, B. R. Lamotrigine, Phenytoin and Carbamazepine Interactions on the Sodium Current Present in N4TG1 Mouse Neuroblastoma Cells. *J. Pharmacol. Exp. Ther.* **1993**, *266* (2), 829–835.
- (20) FDA. Lamictal Prescribing Information.
- (21) Stafstrom, C. E.; Carmant, L. Seizures and Epilepsy: An Overview for Neuroscientists. *Cold Spring Harb. Perspect. Med.* **2015**, *5* (6). <https://doi.org/10.1101/cshperspect.a022426>.
- (22) Madsen, K. K.; White, H. S.; Schousboe, A. Neuronal and Non-Neuronal GABA Transporters as Targets for Antiepileptic Drugs. *Pharmacol. Ther.* **2010**, *125* (3), 394–401. <https://doi.org/10.1016/j.pharmthera.2009.11.007>.
- (23) Löscher, W.; Rogawski, M. A. How Theories Evolved Concerning the Mechanism of Action of Barbiturates. *Epilepsia* **2012**, *53* (s8), 12–25. <https://doi.org/10.1111/epi.12025>.
- (24) Perucca, P.; Carter, J.; Vahle, V.; Gilliam, F. G. Adverse Antiepileptic Drug Effects: Toward a Clinically and Neurobiologically Relevant Taxonomy. *Neurology* **2009**, *72* (14), 1223–1229. <https://doi.org/10.1212/01.wnl.0000345667.45642.61>.
- (25) Perucca P.; Gilliam F. G. Adverse effects of antiepileptic drugs. *Lancet Neurol.* **2012**, *11* (9), 746. DOI: 10.1016/S1474-4422(12)70153-9.
- (26) Lobectomy (Frontal & Temporal) Surgery | Children’s Pittsburgh <https://www.chp.edu/our-services/brain/neurosurgery/epilepsy-surgery/services/lobectomy> (accessed 2020 -01 -27).
- (27) EPIDIOLEX (Cannabidiol) Oral Solution Prescribing Information. Greenwich biosciences. [https://www.epidiolex.com/sites/default/files/pdfs/1021/EPX-03633-1021\\_EPIDIOLEX\\_\(cannabidiol\)\\_USPI.pdf](https://www.epidiolex.com/sites/default/files/pdfs/1021/EPX-03633-1021_EPIDIOLEX_(cannabidiol)_USPI.pdf).
- (28) Perucca, E. Cannabinoids in the Treatment of Epilepsy: Hard Evidence at Last? *J. Epilepsy Res.* **2017**, *7* (2), 61–76. <https://doi.org/10.14581/jer.17012>.
- (29) Kaur, H.; Kumar, B.; Medhi, B. Antiepileptic Drugs in Development Pipeline: A Recent Update. *eNeurologicalSci* **2016**, *4*, 42–51. <https://doi.org/10.1016/j.ensci.2016.06.003>.
- (30) Carter, R. B.; Wood, P. L.; Wieland, S.; Hawkinson, J. E.; Beelli, D.; Lambert, J. J.; White, H. S.; Wolf, H. H.; Mirsadeghi, S.; Tahir, S. H.; Bolger, M. B.; Lan, N. C.; Gee, K. W. Characterization of the Anticonvulsant Properties of Ganaxolone (CCD 1042; 3alpha-Hydroxy-3beta-Methyl-5alpha-Pregnan-20-One), a Selective, High-Affinity, Steroid Modulator of the Gamma-Aminobutyric Acid(A) Receptor. *J. Pharmacol. Exp. Ther.* **1997**, *280* (3), 1284–1295.
- (31) Luszczki, J. J. Third-Generation Antiepileptic Drugs: Mechanisms of Action, Pharmacokinetics and Interactions. *Pharmacol. Rep. PR* **2009**, *61* (2), 197–216. [https://doi.org/10.1016/s1734-1140\(09\)70024-6](https://doi.org/10.1016/s1734-1140(09)70024-6).

- (32) American Epilepsy Society. FACTS AND FIGURES [https://www.aesnet.org/for\\_patients/facts\\_figures](https://www.aesnet.org/for_patients/facts_figures) (accessed 2020 -01 -08).
- (33) Epilepsy Foundation. Refractory Seizures. <https://www.epilepsy.com/learn/types-seizures/refractory-seizures> (accessed 2020 -01 -27).
- (34) Rahman, S.; Ali Khan, R.; Kumar, A. Experimental Study of the Morphine De-Addiction Properties of Delphinium Denudatum Wall. *BMC Complement. Altern. Med.* **2002**, *2* (1), 6. <https://doi.org/10.1186/1472-6882-2-6>.
- (35) Raza, M.; Shaheen, F.; Choudhary, M. I.; Sombati, S.; Rafiq, A.; Suria, A.; Rahman, A.-; DeLorenzo, R. J. Anticonvulsant Activities of Ethanolic Extract and Aqueous Fraction Isolated from Delphinium Denudatum. *J. Ethnopharmacol.* **2001**, *78* (1), 73–78. [https://doi.org/10.1016/S0378-8741\(01\)00327-0](https://doi.org/10.1016/S0378-8741(01)00327-0).
- (36) Raza, M.; Shaheen, F.; Choudhary, M. I.; Rahman, A.; Sombati, S.; DeLorenzo, R. J. In Vitro Inhibition of Pentylentetrazole and Bicuculline-Induced Epileptiform Activity in Rat Hippocampal Pyramidal Neurons by Aqueous Fraction Isolated from Delphinium Denudatum. *Neurosci. Lett.* **2002**, *333* (2), 103–106. [https://doi.org/10.1016/s0304-3940\(02\)01027-3](https://doi.org/10.1016/s0304-3940(02)01027-3).
- (37) Raza, M.; Shaheen, F.; Choudhary, M. I.; Rahman, A.; Sombati, S.; Suria, A.; Rafiq, A.; DeLorenzo, R. J. Anticonvulsant Effect of FS-1 Subfraction Isolated from Roots of Delphinium Denudatum on Hippocampal Pyramidal Neurons. *Phytother. Res. PTR* **2003**, *17* (1), 38–43. <https://doi.org/10.1002/ptr.1072>.
- (38) Raza, M.; Shaheen, F.; Choudhary, M. I.; Sombati, S.; Rahman, A.; DeLorenzo, R. J. Inhibition of Sustained Repetitive Firing in Cultured Hippocampal Neurons by an Aqueous Fraction Isolated from Delphinium Denudatum. *J. Ethnopharmacol.* **2004**, *90* (2–3), 367–374. <https://doi.org/10.1016/j.jep.2003.10.017>.
- (39) Rahman, A.; Choudhary, M. I.; Shaheen, F.; Ganesan, A.; Simjee, S. U.; Raza, A. M. United States Patent Application: 0080004353 - New Anticonvulsant Compounds. 20080004353, A1.
- (40) Simjee, S. U.; Shaheen, F.; Choudhary, M. I.; Rahman, A.; Jamall, S.; Shah, S. U. A.; Khan, N.; Kabir, N.; Ashraf, N. Suppression of C-Fos Protein and mRNA Expression in Pentylentetrazole-Induced Kindled Mouse Brain by Isoxylitones. *J. Mol. Neurosci.* **2012**, *47* (3), 559–570. <https://doi.org/10.1007/s12031-011-9674-4>.
- (41) Rahman, A.; Choudhary, M. I.; Shaheen, F.; Simjee, S. U.; Kahn, N.; Malhi, S. M.; Shah, S. U. A.; Ashraf, M. N. United States Patent Application: 0140221682 - SYNTHESIS AND BIOLOGICAL STUDIES OF AN ISOMERIC MIXTURE OF (E/Z) ISOXYLITONES AND ITS ANALOGUES. 20140221682, A1.
- (42) Ashraf, M. N.; Gavrilovici, C.; Ali Shah, S. U.; Shaheen, F.; Choudhary, M. I.; Rahman, A.; Fahnestock, M.; Simjee, S. U.; Poulter, M. O. A Novel Anticonvulsant Modulates Voltage-Gated Sodium Channel Inactivation and Prevents Kindling-Induced Seizures. *J. Neurochem.* **2013**, *126* (5), 651–661. <https://doi.org/10.1111/jnc.12352>.
- (43) The roots of an unlikely hope for epilepsy | The Star [https://www.thestar.com/news/insight/2014/04/12/the\\_roots\\_of\\_an\\_unlikely\\_hope\\_for\\_epilepsy.html](https://www.thestar.com/news/insight/2014/04/12/the_roots_of_an_unlikely_hope_for_epilepsy.html) (accessed 2020 -01 -13).
- (44) Grinvald, A.; Hildesheim, R. VSDI: A New Era in Functional Imaging of Cortical Dynamics. *Nat. Rev. Neurosci.* **2004**, *5* (11), 874–885. <https://doi.org/10.1038/nrn1536>.

- (45) Macefield, V. G.; Rundqvist, B.; Sverrisdottir, Y. B.; Wallin, B. G.; Elam, M. Firing Properties of Single Muscle Vasoconstrictor Neurons in the Sympathoexcitation Associated with Congestive Heart Failure. *Circulation* **1999**, *100* (16), 1708–1713. <https://doi.org/10.1161/01.cir.100.16.1708>.
- (46) Hermes, D.; Kasteleijn-Nolst Trenité, D. G. A.; Winawer, J. Gamma Oscillations and Photosensitive Epilepsy. *Curr. Biol. CB* **2017**, *27* (9), R336–R338. <https://doi.org/10.1016/j.cub.2017.03.076>.
- (47) Goddard, G. V. Development of Epileptic Seizures through Brain Stimulation at Low Intensity. *Nature* **1967**, *214* (5092), 1020–1021. <https://doi.org/10.1038/2141020a0>.
- (48) Bertram, E. The Relevance of Kindling for Human Epilepsy. *Epilepsia* **2007**, *48* (s2), 65–74. <https://doi.org/10.1111/j.1528-1167.2007.01068.x>.
- (49) Seizure Clusters <https://www.epilepsy.com/learn/professionals/refractory-seizures/potentially-remediable-causes/seizure-clusters> (accessed 2020 -01 -13).
- (50) Delgado, JoséM. R.; Sevillano, M. Evolution of Repeated Hippocampal Seizures in the Cat. *Electroencephalogr. Clin. Neurophysiol.* **1961**, *13* (5), 722–733. [https://doi.org/10.1016/0013-4694\(61\)90104-3](https://doi.org/10.1016/0013-4694(61)90104-3).
- (51) Cela, E.; McFarlan, A. R.; Chung, A. J.; Wang, T.; Chierzi, S.; Murai, K. K.; Sjöström, P. J. An Optogenetic Kindling Model of Neocortical Epilepsy. *Sci. Rep.* **2019**, *9* (1), 5236. <https://doi.org/10.1038/s41598-019-41533-2>.
- (52) Saikaley, A. I. Preparation of  $\beta$ -Amino Sulfoxides as Potential Selective Connexin Inhibitors II. Synthesis of Isoxylitone Analogues for the Treatment of Epilepsy. Thesis, Université d'Ottawa / University of Ottawa, 2015. <http://dx.doi.org/10.20381/ruor-3997>.
- (53) Fluet-Chouinard, Adrien. Synthesis of Analogs of a Potential Drug for Treatment of Epilepsy. Thesis, Université d'Ottawa / University of Ottawa, 2019.
- (54) OB Pharma. OB Pharma Confidential Overview. 2019.
- (55) Michael Poulter, Private Communication.
- (56) Cheval, N. P.; Dikova, A.; Blanc, A.; Weibel, J.-M.; Pale, P. Vinyl Nosylates: An Ideal Partner for Palladium-Catalyzed Cross-Coupling Reactions. *Chem. – Eur. J.* **2013**, *19* (27), 8765–8768. <https://doi.org/10.1002/chem.201300127>.
- (57) Khalaf, J.; Estrella-Jimenez, M. E.; Shashack, M. J.; Phatak, S. S.; Zhang, S.; Gilbertson, S. R. Design, Synthesis, and Diversification of 3,5-Substituted Enone Library. *ACS Comb. Sci.* **2011**, *13* (4), 351–356. <https://doi.org/10.1021/co200070m>.
- (58) Zhang, Z.; Tang, W. Drug Metabolism in Drug Discovery and Development. *Acta Pharm. Sin. B* **2018**, *8* (5), 721–732. <https://doi.org/10.1016/j.apsb.2018.04.003>.
- (59) Carbodiimide Crosslinker Chemistry - CA <https://www.thermofisher.com/ca/en/home/life-science/protein-biology/protein-biology-learning-center/protein-biology-resource-library/pierce-protein-methods/carbodiimide-crosslinker-chemistry.html> (accessed 2020 -01 -29).
- (60) Osier, N.; Dixon, C. E. The Controlled Cortical Impact Model of Experimental Brain Trauma: Overview, Research Applications, and Protocol. *Methods Mol. Biol. Clifton NJ* **2016**, *1462*, 177–192. [https://doi.org/10.1007/978-1-4939-3816-2\\_11](https://doi.org/10.1007/978-1-4939-3816-2_11).
- (61) Bowes, J.; Brown, A. J.; Hamon, J.; Jarolimek, W.; Sridhar, A.; Waldron, G.; Whitebread, S. Reducing Safety-Related Drug Attrition: The Use of in Vitro Pharmacological Profiling. *Nat. Rev. Drug Discov.* **2012**, *11* (12), 909–922. <https://doi.org/10.1038/nrd3845>.

- (62) Sanguinetti, M. C.; Tristani-Firouzi, M. HERG Potassium Channels and Cardiac Arrhythmia. *Nature* **2006**, *440* (7083), 463–469. <https://doi.org/10.1038/nature04710>.
- (63) ICH. Guideline for Elemental Impurities Q3D (R1). 2019.
- (64) Blangetti, M.; Rosso, H.; Prandi, C.; Deagostino, A.; Venturello, P. Suzuki-Miyaura Cross-Coupling in Acylation Reactions, Scope and Recent Developments. *Molecules* **2013**, *18* (1), 1188–1213. <https://doi.org/10.3390/molecules18011188>.
- (65) Ennis, D. S.; McManus, J.; Wood-Kaczmar, W.; Richardson, J.; Smith, G. E.; Carstairs, A. Multikilogram-Scale Synthesis of a Biphenyl Carboxylic Acid Derivative Using a Pd/C-Mediated Suzuki Coupling Approach. *Org. Process Res. Dev.* **1999**, *3* (4), 248–252. <https://doi.org/10.1021/op980079g>.
- (66) Home Page- AK Scientific <https://aksci.com/index.php> (accessed 2020 -01 -30).
- (67) Jacks, T. E.; Belmont, D. T.; Briggs, C. A.; Horne, N. M.; Kanter, G. D.; Karrick, G. L.; Krikke, J. J.; McCabe, R. J.; Mustakis, J. G.; Nanninga, T. N.; Risedorph, G. S.; Seamans, R. E.; Skeean, R.; Winkle, D. D.; Zennie, T. M. Development of a Scalable Process for CI-1034, an Endothelin Antagonist. *Org. Process Res. Dev.* **2004**, *8* (2), 201–212. <https://doi.org/10.1021/op034104g>.
- (68) World Health Organization. Stability Testing of Active Pharmaceutical Ingredients and Finished Pharmaceutical Products. <https://apps.who.int/medicinedocs/en/m/abstract/Js19133en/> (accessed 2020 -03 -12).

Part II. Synthesis of SOX9 inhibitors as promoters of recovery from spinal cord injury.

## 2.1 Introduction

### 2.1.1 Overview on spinal cord injuries

As a part of the central nervous system, the spinal cord is a nervous structure responsible for transmitting information between the brain and the rest of the body. It begins right below the brain and extends along the spine below the ribcage. Any damage done to this structure is referred to as a spinal cord injury (SCI) regardless of whether this is due to an illness, physiological condition or physical trauma. According to the World Health Organization, 250 to 500 thousand people develop a spinal cord injury each year.<sup>1</sup> A large majority of these are a result of trauma, with over 70% of SCI cases in the united states being the result of falls or car accidents, without even taking into account other types of accidents.<sup>1,2</sup> There is therefore a higher prevalence of SCI in younger males, more at risk of car accidents, and the elderly, who are more prone to falls.<sup>1-3</sup> In addition to physical trauma, spinal cord damage can also be the result of various diseases that cause pressure on the spinal cord, or restrict incoming oxygen and/or blood flow. Non-traumatic SCI is often caused by tumors or inflammation growing next to the spinal cord, with other potential causes being infections or degenerative diseases such as multiple sclerosis.<sup>4-6</sup> The spread of prevalence of SCI due to the various causes varies depending on geography, with developed countries having higher rates of SCI caused by cancer and degenerative conditions whereas SCI caused by infections are more common in developing countries.<sup>7</sup>

Spinal cord injuries are classified based on the severity of the symptoms. A complete spinal cord injury refers to patients where the nerve damage resulted in a total loss of motor and sensory abilities below the site of injury whereas they are only partially diminished by an incomplete injury.<sup>8</sup>

### 2.1.2 Symptoms and effects of SCI on quality of life

Patients who survive the first 24 hours after the initial injury will generally recover and be able to live the rest of their lives, albeit with a decreased life expectancy and potential severe lingering effects.<sup>1,2,6</sup> More than half of patients suffering from spinal cord damage have tetraplegia, with most of them being an incomplete injury.<sup>2,9</sup> A number of physical complications can occur following paralysis of the lower body, such as bedsores or urinary tract infections due to lost bladder control. Most people affected by an SCI suffer from chronic pains. In addition, being bedridden can also easily lead to poor overall health due to lack to exercise, increasing the likelihood of other issues such as obesity or heart disease.<sup>10</sup> While organ function is retained even in patients with a complete SCI, breathing is often made more difficult due to the effect of the SCI on the respiratory muscles, causing a much higher risk of respiratory complications.<sup>11,12</sup> In fact, unlike in the general population, the leading causes of death for patients with spinal cord damage are septicemia and respiratory issues such as pneumonia.<sup>9,11</sup>

As a result of these physical issues, quality of life is often diminished for the patients. After the injury, most patients lose their jobs and only a small portion are eventually able to return to work due to physical disabilities, as well as it becoming much more difficult to find employment. In the long term, 60 to 70% of people with an SCI remain unemployed.<sup>1,9</sup> This is made worse by the costs of treatment, rehabilitation and adaptations needed, which are significantly higher than those associated with other long-term conditions. These costs can easily total up to over a million dollars during a patient's lifetime, even for the less severe injuries.<sup>9</sup> For patients with complete SCI and tetraplegia, the lifetime costs can reach as high as 3 millions.<sup>13</sup> These various factors take a heavy toll on the mental health of the patients and many develop depression, which can make it even harder to deal with the other issues.<sup>1</sup>

### **2.1.3 Current treatments for SCI**

Prompt treatment is essential in healing from a SCI, as additional damage to the spine can often occur if a patient is not, or poorly, treated due to inflammation at the site of injury or additional movement of the spine. While patients with a less severe incomplete injury can recover some function and some may eventually learn to walk again, this is unlikely and highly dependent on the severity of the injury. Unfortunately, people who suffering from a complete SCI do not typically recover.<sup>8</sup> The current existing treatments are thus focused on mitigating the initial damage, promoting rehabilitation and helping the patients to cope and learn to adapt to their disability. Although many options are being developed, no treatment currently exists to regrow severed spinal cords.<sup>14,15</sup>

### **2.1.4 Natural inhibition of neuronal regeneration by CSPGs**

The causes of SCI are varied, and so are the specific effects of the injury on the patient. A common result in all cases is damage and death of neurons and/or surrounding cells.<sup>14</sup> Surviving neurons can also become demyelinated, which can worsen over time in a manner reminiscent of Guillain-Barré syndrome. Usually, the injury will also result in inflammation, and formation of a structure called a glial scar.<sup>14,16</sup>

The common misconception that nerves cannot regrow has been disproved for some time. While in practice the damage from a fully severed spinal cord is permanent, it has been shown that nerves can in fact regenerate in healthy physiological conditions.<sup>14</sup> However, axonal growth and formation of new synapses is blocked physically and inhibited as a result of the damage.<sup>14,15</sup> The previously mentioned glial scar is a structure of various glial cells, primarily astrocytes, formed by the body to protect the injured area. To this end, the glial scar forms a physical barrier, as well as inhibiting neuroplasticity

around the injured neurons.<sup>15</sup> This chemical and physical blockage to axonal growth results in spinal cord injuries not healing over time.

A key structural component of the glial scar is the Chondroitin Sulfate Proteoglycans (CSPGs), produced naturally by astrocytes and upregulated in cases of SCI.<sup>15,17</sup> In normal conditions, CSPGs are found in perineuronal nets (PNNs).<sup>17</sup> PNNs are a stabilizing component of the brain extracellular matrix, that are thought to reduce neuroplasticity and regulate the junctions of neurons. Less present in children where the brain is still developing, the PNNs help control axon sprouting once the neuronal network is properly developed and prevent the number of new synapses from continuing to increase past this point.<sup>17</sup> While they are not the sole control for neuroplasticity, PNNs, CSPGs and synapse formation are intrinsically linked. Removal of CSPGs via enzymatic digestion or knock-out animal models showed increased axon sprouting, demonstrating that they can regrow in adults, long past the developmental stage.<sup>15,18</sup>

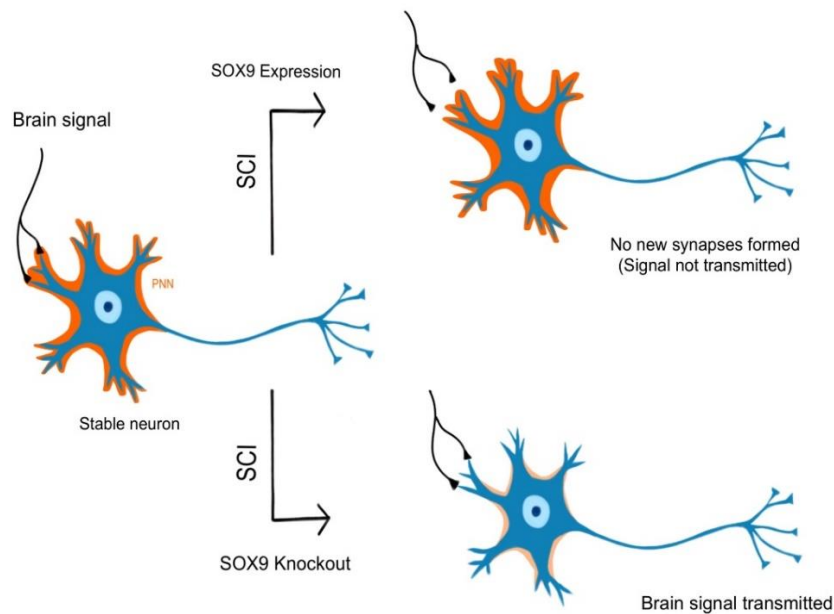


**Figure 2.1.4.1.** The CSPG-heavy perineuronal nets block axonal sprouting. *The axons are represented in blue, and the perineuronal nets in orange. SOX9 ablation diminishes the presence of the PNNs which results in increased axonal sprouting from uninjured neurons and improved recovery over an untreated SCI.*

## **2.1.5 Finding a lead structure**

### **2.1.5.1 The SOX9 gene plays a key role in the inhibition of recovery from SCI**

Arthur Brown and his group at the Robarts institute of Western University, have been researching CSPGs and means of lowering their expression after spinal cord injuries.<sup>15,18,19</sup> This led to the identification of the SOX9 transcription factor, coded by the gene of the same name, as a promoter of CSPG formation. The SOX9 transcription factor is an important regulator for a large number of genes active during the development, and astrocyte activation.<sup>18</sup> The Brown group confirmed this relationship through knock-out animal models, showing that ablation of SOX9 resulted in diminished presence of CSPGs and improved recovery from administered SCI.<sup>18</sup> Furthermore, they were able to demonstrate that a knock out of SOX9 one week post-SCI remained effective at improving recovery, although the therapeutic effect seemed to diminish as the delay between the injury and SOX9 ablation became longer.<sup>15</sup> While this project is focused on spinal cord injuries, SOX9 ablation is also beneficial for other types of brain damage.<sup>19</sup>

### **2.1.5.2 ZO2 as SOX9 inhibitor**

During this work, the Brown group tasked Critical Outcomes Technologies Inc. with designing a small molecule that would effectively bind a specific region of the SOX9 transcription factor, which prevents its dimerization and expression of the target genes.<sup>15</sup> Critical Outcomes Technologies used computer algorithms to screen small molecule databases. After multiple iterations, they proposed 10 potential small molecule inhibitors, which were tested in vitro. Of these ten candidates, compound **1**, which they designated as ZO2, was shown to inhibit SOX9 at 10 mM.<sup>15,20</sup> More importantly, they were able to show that mice with partially severed spinal cords when treated with ZO2 recovered more mobility than those treated with a placebo.<sup>15</sup>

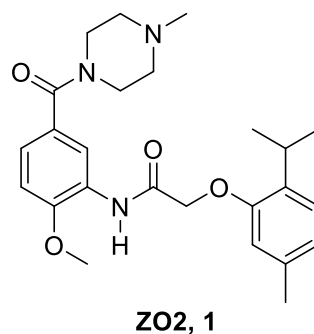


**Figure 2.1.5.2.1.** Chemical structure of the lead compound Z02 (1).

Professor Brown had become aware of our work with his colleague Professor Michael Poulter dealing with the preparation of close to one hundred anti-epilepsy compounds.<sup>21</sup> It was at this point he asked the Durst group to partner with him in this important research. The task was to assist with an SAR study by preparing analogs of the lead structure and sending them to the Brown group to be tested via luciferase gene expression bioassays.

The bioassays were performed by cloning ATDC5 cells with a reporter gene comprised of a promoter with four SOX9 transcription factor binding site sequences, followed by the luciferase gene.<sup>15</sup> These ATDC5 cells biosynthesize their own SOX9 peptide, which promotes the expression of luciferase.<sup>15</sup> This enzyme produces light as a product of their reaction, which can be measured with a luminometer and quantified. The cell clones treated with a diluted solution of the tested compound were compared to a control by observing the percentage by which light produced diminishes, which correlates to the percentage of inhibition of the SOX9 peptide.

### 2.1.6 Previous work by the Durst group

The Durst group's contribution to the project was started by Vikrant Raina as a section of his M. Sc. Thesis.<sup>22</sup> As part of this project, Raina developed an efficient method of synthesizing ZO2 analogs, and prepared 17 such compounds.

He recognized that ZO2 is composed of four units, referred to as A, B, C and D, and that these could be assembled relatively quickly. The only required reactions being the formation of two amide bonds and the alkylation of thymol with chloroacetic acid. A variety of methods are available to stitch the pieces together.

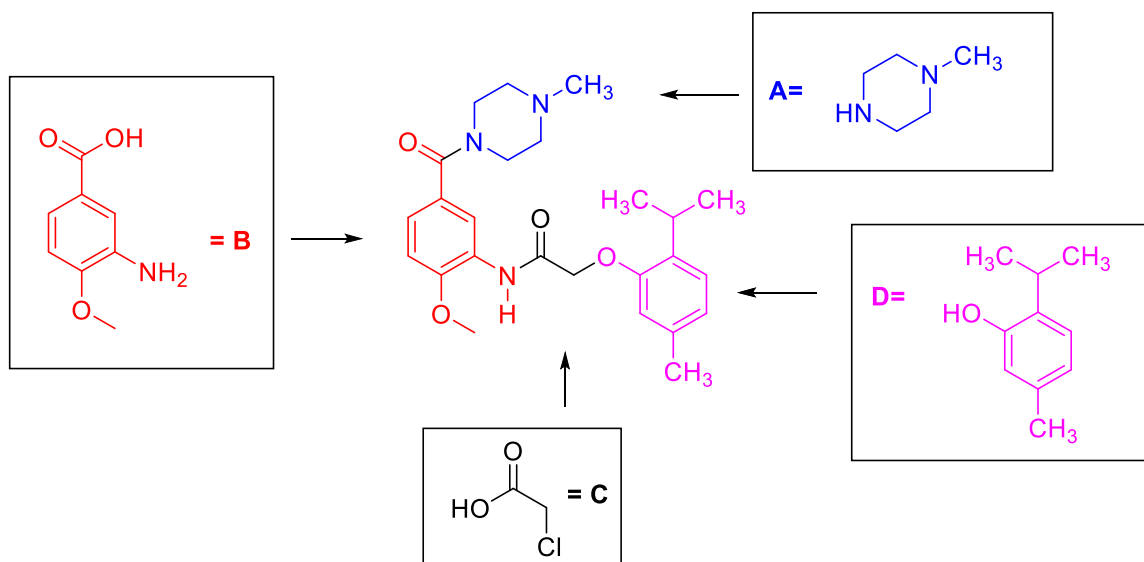
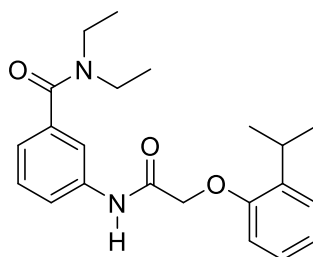


**Figure 2.1.6.1.** The four main units in the ZO2 (1) structure.

Raina was most successful by preparing separately the AB and CD units before combining them to obtain new ABCD compounds. A variety of commercially available nitrobenzoic acids served as B units, which were then converted to acid chlorides and coupled with amines. The 3-nitro substituents were then reduced to generate the AB units. The CD unit was prepared by heating a phenol, such as thymol, with chloroacetic acid for several days in a basic solution, then coupled with the AB unit to yield the desired final product. Once purified, these compounds were shipped to the Brown group to

undergo in vitro bioassays. The results were used to select the next sequence of analogs to prepare.

Rowan Swan continued the task of preparing analogs as part of her summer COOP work term. Prior to the start of her work, the group was informed by Brown that another lead structure designated as STL26 (**2**) had been identified and was significantly more active than any previous compound tested. The superior demonstrated activity of **2** over **1** was quite surprising since it had initially been assumed that the basic nitrogen present in the piperazine ring of compound **1** was crucial to activity. Swan's work therefore mainly targeted analogs of STL26 (**2**).



**STL26, 2**

**Figure 2.1.6.2.** Chemical structure of the compound STL26 (**2**).

The conclusions regarding possible structure-activity relationships presented below are based on bioassay results obtained from a combination of the compounds prepared by Raina and Swan. It should be pointed out that these are at times somewhat tentative, since none of the active compounds synthesized showed activity greater than that of compound **2**. Comparing the activity between compounds was also made complicated as there was sometimes more than one structural change in individual analogs.

### 2.1.6.1 Modifications of Unit A

Together, Raina and Swan produced a number of variations in unit A. Some of these analogs are shown in the figure below.

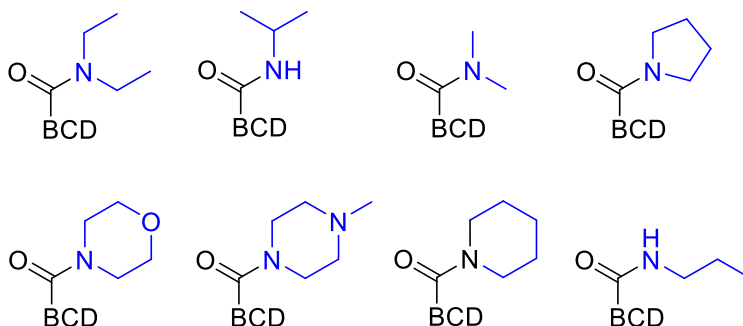


**Figure 2.1.6.1.1.** Structures of the various A units tested by Raina and Swan, sorted by decreasing potency.

Among the various A units tested, the diethylamide compounds consistently had the best activity compared to the others analogs, confirming the results from STL26. The isopropylamine, dimethylamine and pyrrolidine were somewhat less active, while the other four amines used made for generally poorly active compounds. In fact, rather than the targeted inhibition, some test results even returned a slightly increased value of SOX9 expression although this is likely to be due to standard variance in the bioassays. The assays were reportedly difficult to carry out due to the low solubility of the compounds.

While small, the difference in activity of the morpholine analog relative to the *N*-methylpiperazine in ZO2 was surprising since both compounds have a six membered ring and a hydrogen bond accepting atom at the same position.

The extent to which the diethyl groups improved the activity over the pyrrolidine or piperidine groups was surprising, and suggests that the A unit occupies a pocket of space that benefitted from the increased flexibility of the ethyl groups over the other groups tested. It was also a surprise that there was such a gap in activity between the

pyrrolidine and piperidine. The testing of isopropylamine and propylamine gave inconclusive results on whether or not a secondary amine was beneficial, as while the isopropylamine analog was roughly as active as ZO2, the analog made with propylamine showed no activity whatsoever.

In addition, a number of analogs were prepared containing a simple carboxylic acid, a methyl ester and a phenyl ketone as unit A. No significant SOX9 inhibition was observed for these compounds.

### 2.1.6.2 Modifications of Unit B

B unit analogs were not thoroughly investigated at the start of this project, and only a few different variations were used. On the other hand, this meant that each B unit analog was present in several prepared compounds, containing various modifications of the other units. This proved unhelpful however, as despite the large sample size for each of the three B rings shown below, none stood out above the other. None of the substituent tested at the C4 position in the ring seemed to noticeably improve or inhibit activity at this point in the project, which lead to not pursuing further modifications to this position. Due to the functional group tolerance observed at this position, it could be a good potential target later on when optimizing the pharmacokinetics, if the need to add additional polar or hydrophobic substituents arises.

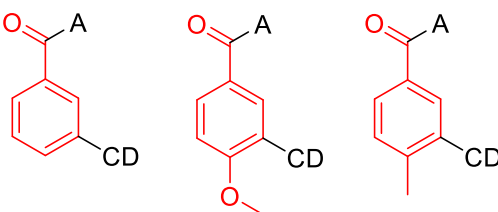


**Figure 2.1.6.2.1.** Structures of the B ring C4 analogs.

Despite underwhelming results from the other B ring analogs, valuable SAR information was obtained for this region nonetheless. Moving the A and CD units adjacent (ortho) to each other on the B ring led to very poor activity compared to the meta analogs. Due to the high impact on potency caused by this change, it would be interesting to prepare the para analog.

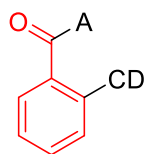


**Figure 2.1.6.2.2.** Structure of the ortho-CD analogs.

### 2.1.6.3 Modifications of unit C

As with the B ring, only a few analogs were prepared with modifications to this section of the structure. In each case, diethylamide was maintained as unit A. These analogs all showed poor to no SOX9 inhibition, especially when compared to compound **2**. The only ones showing a slight activity were the compounds containing the saturated carbon as a replacement for the oxygen. All in all, this proved that this portion of the lead structure plays an important role in binding its target. One could wonder what the effect of removing the amide carbonyl group would be, however this was not done at this stage, as it would complicate the synthesis.

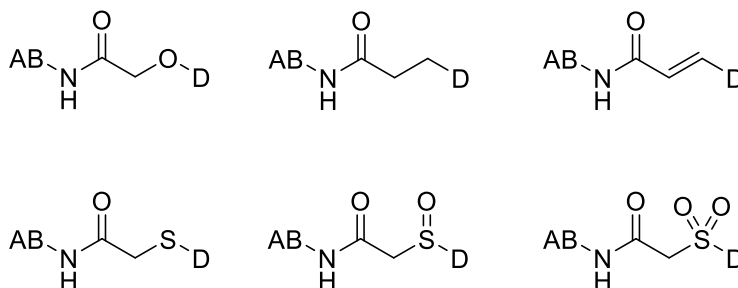


**Figure 2.1.6.3.1.** Structures of the unit C analogs.

#### 2.1.6.4 Modifications of unit D

Among the D ring analogs tested, the most potent compounds were those prepared from thymol and o-isopropyl phenol. The results were quite similar for both, but the thymol analogs tended to be slightly more active. The analogs made from the two methyl phenols had better activity when the methyl group was in the ortho position rather than meta, although both were not significantly active. Meanwhile, analogs made from simple phenol were generally inactive. These results suggested that the size and position of the alkyl chains are somewhat important, and that this section of the molecule is likely to occupy a decently sized hydrophobic pocket of space. Based on the results, it is possible that replacing the isopropyl group with larger substituents would improve activity. Surprisingly however, the lone p-methoxy phenol analog tested showed reasonable activity. While not potent enough that it would be worth pursuing, it would have been expected that the substituent in the para position would lead to a compound similarly inactive to the phenol analogs.

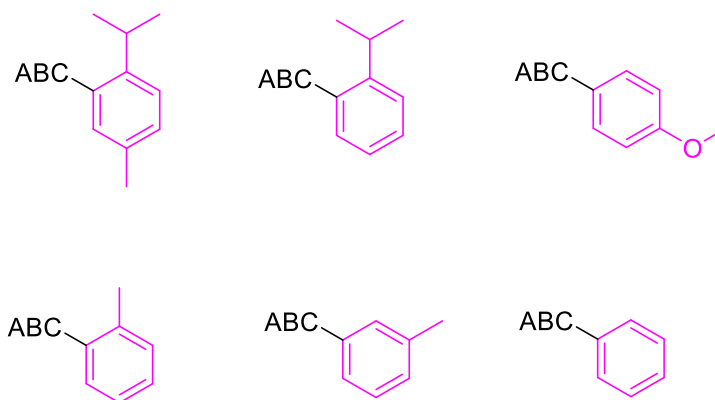


**Figure 2.1.6.4.1.** Structures of the unit D analogs, ordered by decreasing potency.

In conclusion, a preliminary SAR study was performed to identify regions of interest in the structure of Z02 (**1**). Most analogs tested had poor activity, but a select few were effective SOX9 inhibitors. Overall, the initial SAR data confirmed the validity of the lead compound suggested by Critical Outcomes Technologies, as most of the Z02 structure could not be significantly altered without a loss of activity.

## 2.2 Discussion and results

### 2.2.1 Introduction

The goal for this project was to continue preparing analogs of Z02 (**1**) and STL26 (**2**) and gain further understanding of the key structural features necessary for a potent SOX9 inhibitor.

The experiments carried out as part of this work investigated amide groups larger than those in STL26 (**2**) as part of unit A, additional B ring substituents and substituents larger than the *o*-isopropyl on ring D. Each of these will be covered in their own section.

Some effort was put into obtaining an accurate three-dimensional structure of an active STL26 (**2**) analog, and information on its primary conformation in solution. Achieving these goals required the use of NOE NMR experiments and X-ray crystallography. Subsequently, a small number of additional analogs were prepared containing modifications that would strongly favor or hinder the preferred conformation, in order to better understand its role in the inhibitory activity.

### 2.2.2 Synthesis of the Z02 analogs

#### 2.2.2.1 General synthetic process

The first series of analogs were prepared using the procedures developed by Raina and Swan. Their synthesis is summarized below, and the detailed procedures can be found in in the experimental data section.

The starting point of the synthesis for each analog was an appropriate nitrobenzoic acid which would become unit B. The first step was the formation of the amide bond between units A and B. This was carried out by first converting the benzoic

acid into the corresponding acyl chloride by refluxing the acid with oxalyl chloride and a catalytic amount of *N,N*-dimethylformamide (DMF). The acyl chloride was isolated and then added slowly to a solution containing the desired amine. The cooling and slow addition were important due to the reaction being quite exothermic. Because of their reactivity with water the acyl chlorides were preferably used quickly, although they could be stored temporarily in the freezer if sealed properly. Finally, triethylamine was often added to the amine solution to neutralize the HCl produced by the reaction, when the amine substrate was too expensive to be used in excess. There is no risk of forming a by-product with a tertiary amine.

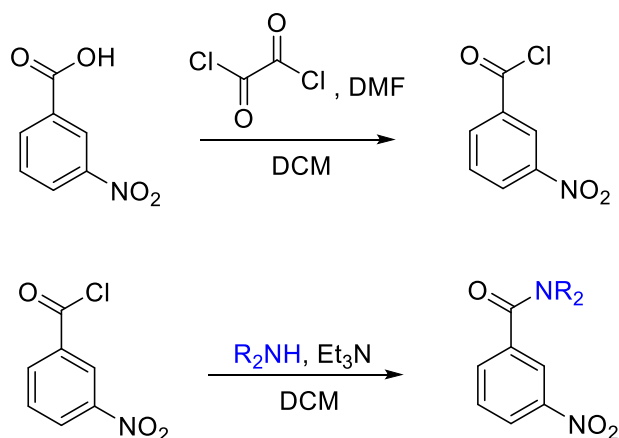


**Figure 2.2.2.1.1.** Formation of the AB amide bond via acyl chloride intermediate.

Once the first amide bond was formed, the nitro group was reduced to NH<sub>2</sub> and thus ready to be coupled with the CD unit. This reduction was carried out by heating the AB nitro compound in a solution of ethanol and water, with iron powder and ammonium chloride.

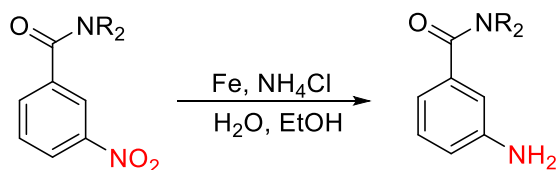


**Figure 2.2.2.1.2.** Reduction of the 3-nitro protecting group.

The second half of the molecule, the CD unit, was prepared next. A substituted phenol appropriate for the desired unit D was used as starting material. For a majority of the compounds prepared, the starting material used was thymol (shown below). The phenol was refluxed with chloroacetic acid in water and sodium hydroxide, to allow the phenol to act as nucleophile. The rates of reaction were quite slow, and the solution had to be refluxed at least two days before acceptable amounts of product was formed. Some analogs could not be prepared by this method, yielding only minimal amounts of product form after being heated for a week. While this is not ideal and could be improved upon, the reaction yielded pure and thermally stable CD intermediates. This made it possible for thymol acetic acid (**3**) to be prepared on a large scale to avoid the need to perform this reaction regularly. This intermediate was stored as the acid, and converted to the acyl chloride, in small amounts and as needed, by the method described previously.

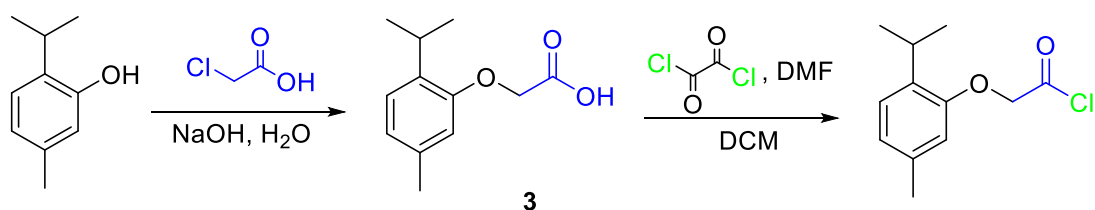


**Figure 2.2.2.1.3.** Preparation of the CD unit, thymol acetic acid (**3**), and its conversion to the acyl chloride.

The last step was the coupling of both halves of the molecule, using the same amide bond formation reaction as the coupling between units A and B. The reaction was reliable, although in yields typically lower than that of the first reaction.

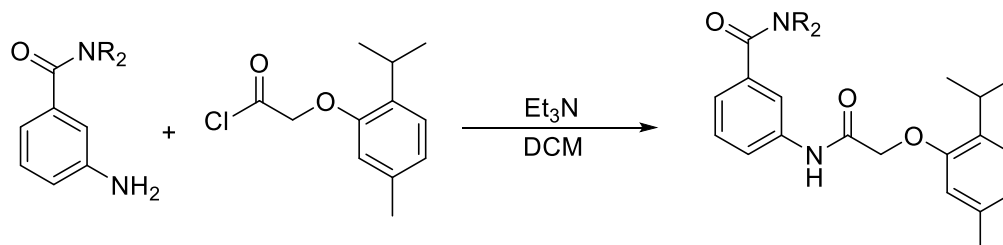


**Figure 2.2.2.1.4.** Amide bond formation between the AB and CD units.

### 2.2.2.2 Using EDCI as coupling reagent for a cleaner amide bond formation

Later in the project, an alternate method of amide bond formation was tested, in an attempt to improve yields and reduce the time spent on each reaction. A reaction procedure was developed based on using the coupling reagent *N*-ethyl-*N'*-(3-dimethylaminopropyl) carbodiimide hydrochloride (EDCI). *N,N*-Dimethylaminopyridine (DMAP) was also used, to accelerate the reaction and reduce the risk of forming byproducts.

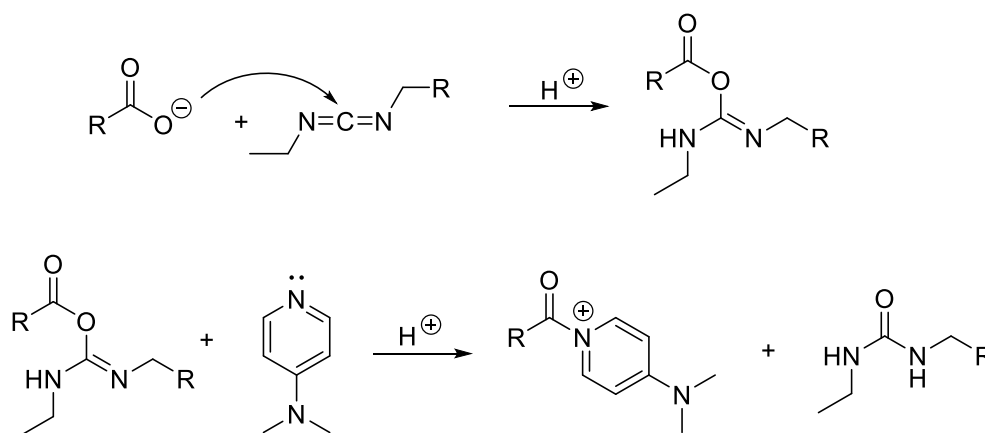


**Figure 2.2.2.2.1.** Formation and reaction of an active ester intermediate.

This reaction occurs by in situ formation of a reactive *O*-acyl isourea intermediate. The amines present in solution then quickly react with this intermediate, forming the respective amides. DMAP is included as a better nucleophile to form a second, more stable, active intermediate before the *O*-acyl isourea can decompose or react intramolecularly to form the more stable *N*-acylurea.<sup>23,24</sup> The reaction then proceeds by seeing the acyl substrate transferred from the DMAP to the secondary amine substrate, forming the more thermodynamically favoured product. The only by-product should be the EDCI being converted to an urea after reacting, which is water soluble and easily removed as a salt.

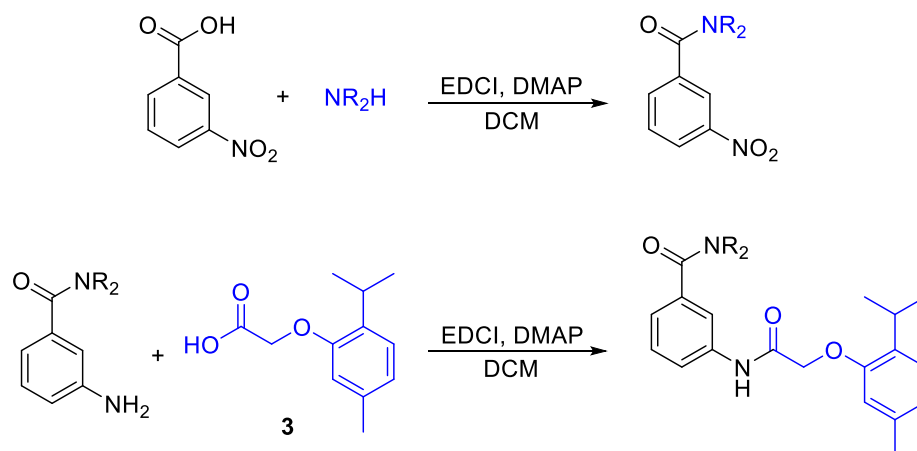


**Figure 2.2.2.2.1.** Amide bond formation using EDCI.

This reaction made use of the same substrates as the acyl chloride method, however the manipulations were significantly simpler and the product was obtained in a single step. An amine substrate, either unit A or a reduced AB intermediate, was dissolved in DCM alongside the acid substrate. EDCI and *N,N*-dimethylaminopyridine (DMAP) were then added to the mixture. All reagents dissolved readily and the reaction occurred at room conditions in as little as two hours, although it was typically prepared in the late afternoon and left to react overnight.

While easier to carry out, this new procedure did not significantly improve the coupling yields. It did however result in substantial time savings. While both reactions could be carried out and the product purified in under three hours, the active preparation time of the EDCI/DMAP method was significantly lower, and the slightly longer reaction time could be performed safely overnight due not requiring heat or water flow for a reflux. The purification of the products obtained was also significantly easier, all undesirable compounds being removed by base then acid washes. After validating the method with several examples, subsequent analogs were prepared using the EDCI coupling unless the required acyl chloride was already available.

### 2.2.2.3 Using EDCI to circumvent the nitro reduction step

Towards the end of this project, it was thought that the EDCI/DMAP amide coupling could be used to prepare reduced AB units directly, thus eliminating one out of the three steps. This hypothesis was tested by performing the reaction with 3-aminobenzoic acid and diethylamine. The reaction was successful, although a large amount of DMAP remained in the product mixture. The excess DMAP was not removed as it would have been wasteful to do so, only to add it again during the next step. Based on the NMR data, a DMAP to product ratio of 2.8:1.0 was obtained, resulting in a 48% yield of desired 3-amino-*N,N*-diethylbenzamide.

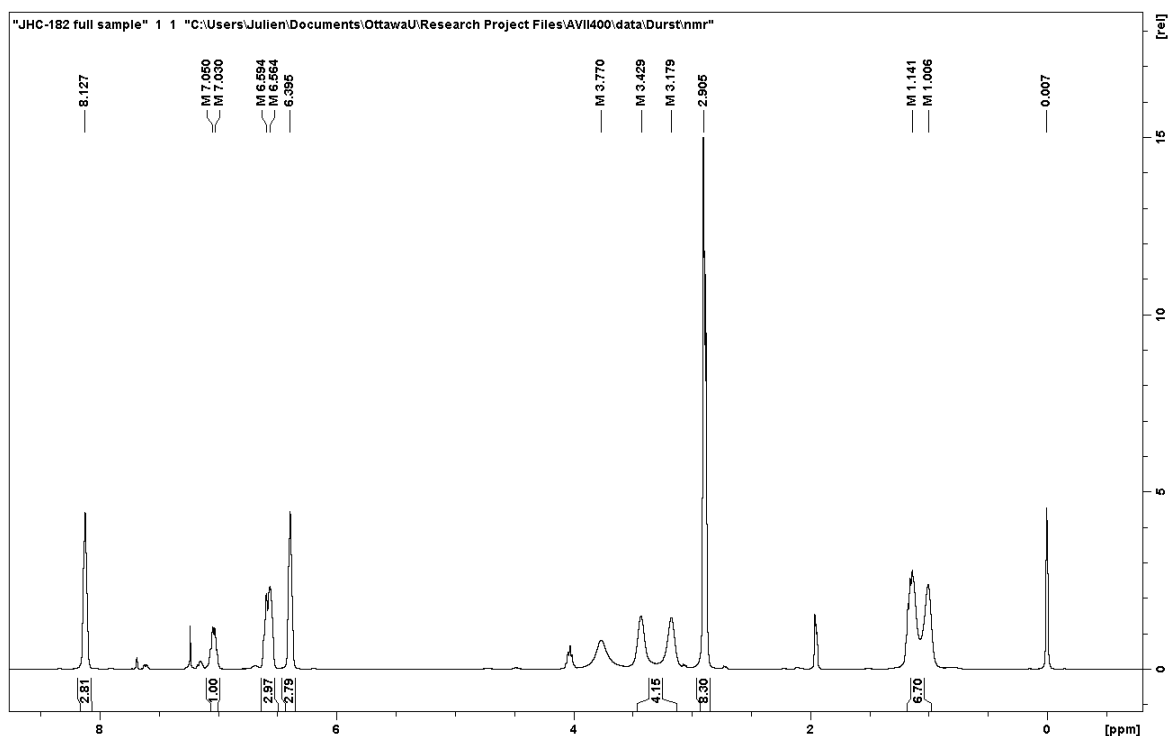


**Figure 2.2.2.3.1.**  $^1\text{H}$  NMR spectrum of the EDCI/DMAP coupling on 3-aminobenzoic acid. The peaks at 8.12 ppm, 6.40 ppm and 2.90 ppm correspond to those of DMAP. The sample was dissolved in  $\text{CDCl}_3$  spiked with TMS. Additional peaks of water and ethyl acetate can be seen.

After this success, the next step was to attempt the two-step one-pot synthesis of an entire ABCD analog. Since the first reaction was successful, it should be likely that adding an appropriate amount of thymol acetic acid (**3**) and necessary additional equivalents of EDCI and DMAP would lead to a second successful amide coupling. The compounds in solution after the first reaction should only include a small amount of leftover starting materials and intermediates, the product and the urea by-product of EDCI. As they were evidently not an issue in the first amide coupling, none of these should interfere with the second reaction.

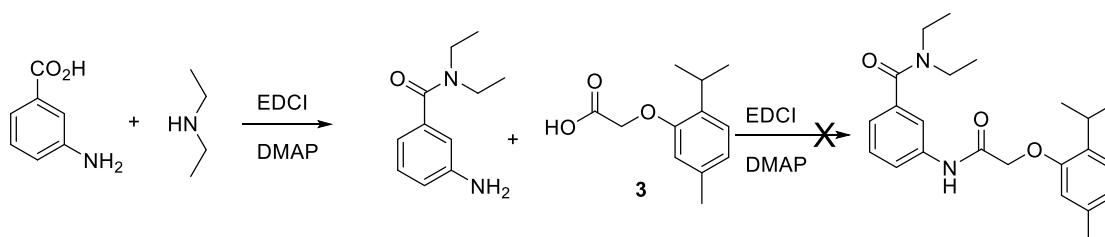


**Figure 2.2.2.2.2.** Attempted one pot formation of an ABCD analog.

Unfortunately, the one-pot reaction test was not successful, and no ABCD product was detected in the final mixture. As this occurred near the end of the project and was not among the original goals, the one-pot synthesis was not investigated further.

### 2.2.3 Analogs containing unit A modifications

As outlined previously, one of the goals of this project was to investigate the activity of amides in unit A featuring amines larger than diethylamine. ABCD analogs prepared from smaller amines such as dimethylamine or pyrrolidine have been previously shown to be less active than STL26 (**2**) featuring diethylamide. Based on the previous results, the priority was placed on testing acyclic substituents. Four analogs were prepared using dipropylamine and diisopropylamine, in addition to the diethylamine analogs containing the equivalent BCD units. The activity of these analogs was compared

to that of compound **7** which was the most potent compound prepared by Swan. It is important to note that the bioassay results used to draw conclusions regarding these compounds varied significantly, possibly because of different cell cultures used between assays, or due to the cells aging between different series of compounds. It is not known whether a control assay was performed for every analog tested. Results received from the Brown group were thus rounded to the nearest decimal value. Differences in activity between analogs were considered significant if they were observed consistently across multiple analogs, or if the difference was larger than one decimal point.

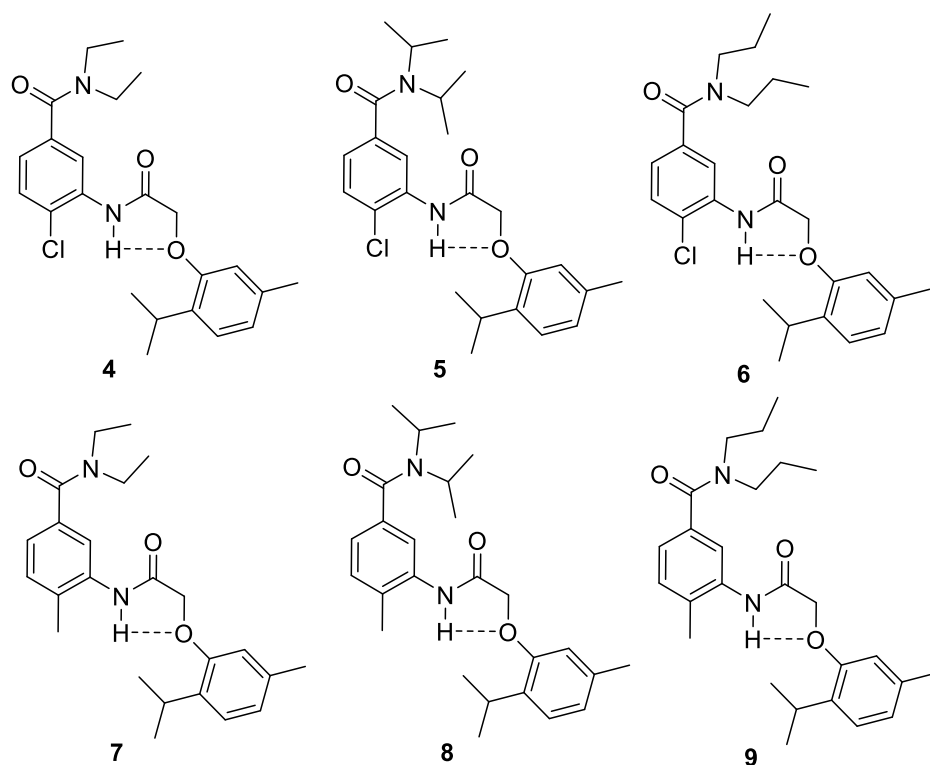


**Figure 2.2.3.1.** Chemical structure of compounds **4** to **9**.

As the replacement of the diethylamide unit A by sterically smaller groups had been shown to result in less potent compounds, it was expected that larger units would lead to an increase in potency. However, for both series of analogs, the compounds prepared from dipropylamine or diisopropylamine showed less than half the inhibitory activity of their diethylamine counterpart. While these analogs were prepared as a preliminary test before moving on to larger amines, the results showed that further enlarging the carbon chains of unit A was unlikely to be helpful in any way. Interestingly, the dimethylamide and dipropylamide analogs had roughly similar activities.

It appears based on the available data that the ideal size of unit A is that of diethylamine, with both larger and smaller groups showing lower activity. This suggests the presence of a well-defined pocket for this unit on the target. The relative activities of analogs containing many different A units prepared by Raina and Swan, which covered primary amines, cyclic and heterocyclic amines as well as the dipropyl and diisopropyl compounds reported in this work were all lower than analogs containing a diethylamide unit A. Considering this, as well as the high impact on potency observed from seemingly small changes to unit A, discovering a superior structure seems unlikely.

The relative activity between the dipropylamine and diisopropylamine analogs cannot be assessed with the results obtained. There was no statistically significant difference between the inhibitory activities of analogs **8** and **9**. Bioassay results from compound **6** could potentially clarify which structure is more active, however results from this analog were not received.

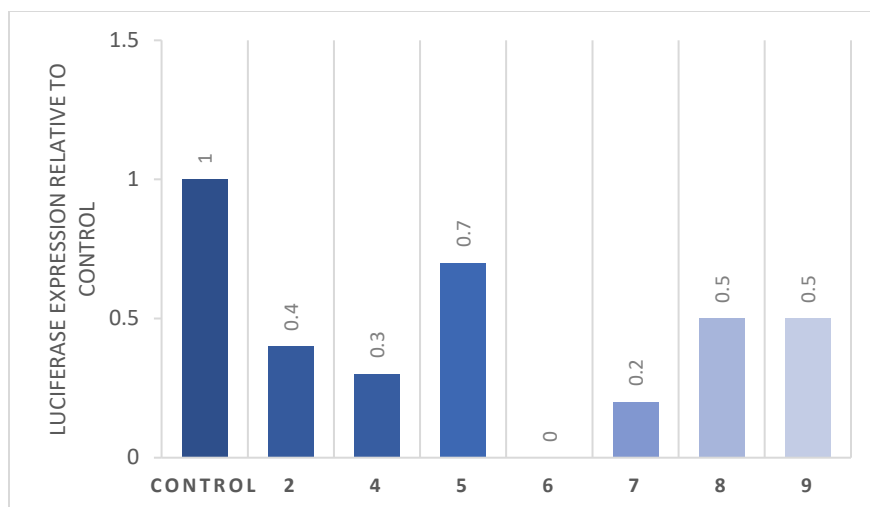


**Figure 2.2.3.2.** Luciferase expression assay results of compounds **4** to **9**. Compound **6** was prepared and sent, but not tested.

#### 2.2.4 Analogs containing unit B modifications

Among the changes to unit B, one priority was to confirm the previous findings regarding the preferred meta conformation. The quality of the data used for this conclusion could be improved by preparing the alternative conformations, using the most active units A, C and D. The para (**11**) and ortho (**12**) analogs were prepared from the respective para and ortho benzoic acids, diethylamine and thymol acetic acid (**3**). Unfortunately, no bioassay results were returned for either of the two compounds.

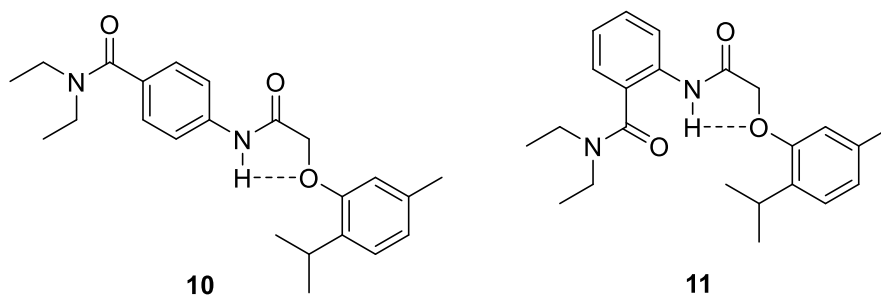


**Figure 2.2.4.1.** Chemical structure of the unit B para (**11**) and ortho (**12**) conformations.

The C4 substituents on unit B were shown to have a negligible effect in previous work from our group.<sup>22</sup> However, the scope of analogs prepared lacked electron withdrawing substituents. To remedy this, analogs were prepared with the readily available 4-chloro-3-nitro benzoic acid as starting material. Three new analogs (**4**, **12-13**) were prepared with various 4-substituted 3-nitrobenzoic acids, with identical units A, C and D. These can be used to determine preferred qualities of unit B substituents.

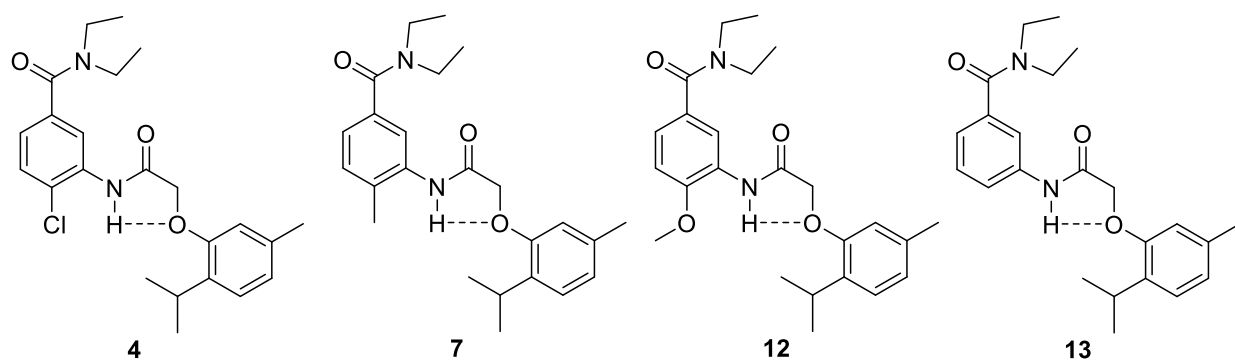


**Figure 2.2.4.2.** Chemical structure of the analogs containing various C4 substituents on unit B.

While most of the compounds prepared were difficult to dissolve in common solvents, the solubility issues of compound **12** were significant enough to cause the bioassays to be unsuccessful. The results from compound **13** were also not received, potentially for the same reason. Based on the results of previous work by our group<sup>22</sup>, the 4-methyl and 4-methoxy analogs had roughly similar activities, neither showing significant improvement over the other in the pairs tested and can be considered to be equal.

The results of compounds **4** and **7** show a slightly reduced activity by substituting the methyl group by a chlorine. While not sufficient on their own, this is further supported by the analogs **5** and **8** shown in the previous section. Electron-withdrawing substituents at C4 in unit B are therefore likely to be slightly less favored.

Lastly, the results of **7** compared to STL26 (**2**) show improved activity from the presence of a 4-methyl substituent on ring B. The D ring of compound **7** also has an additional methyl over that of STL26 however, which could be slightly beneficial. One other appropriate comparison between a methyl group and a hydrogen was found in compounds from the Raina thesis which supported this hypothesis. All other potential comparisons between these two groups had too many additional modifications in other regions of the structure, making any data gathered from them unreliable.

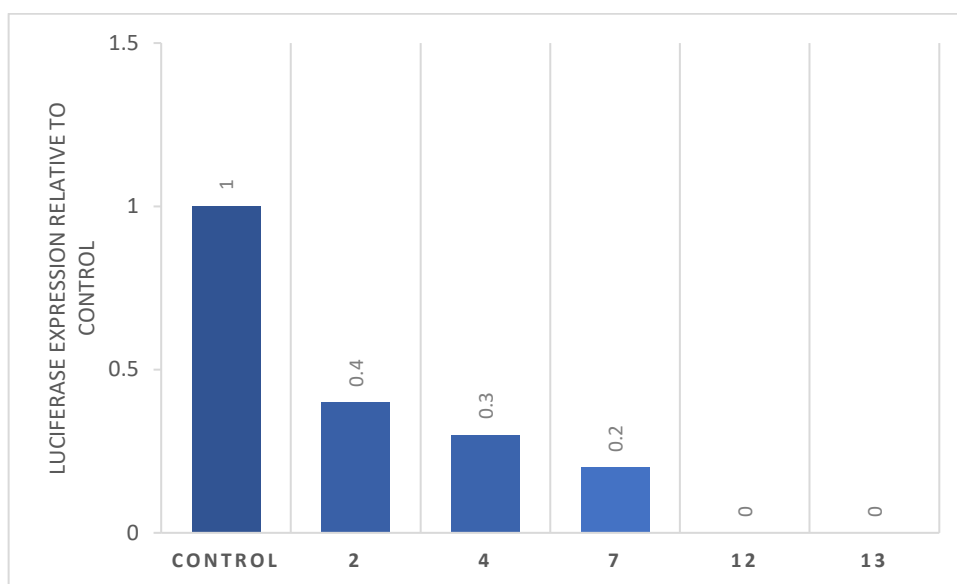


**Figure 2.2.4.3.** Luciferase expression assay results of ring B C4-modified analogs. Compounds **12** and **13** were prepared and sent, but results were not received.

The possible conclusions above are a best attempt at interpreting the results. Due to the quality of the data, the only certain conclusion that can be drawn is that the impact on potency of the small C4 substituents tested is low. If pharmacokinetic or bioavailability issues arise in the future, this could be a good position to introduce modifications targeting these problems.

The preparation of two B units containing SPh or SCH<sub>2</sub>Ph at the C4 position was attempted via aromatic nucleophilic substitution from the 4-chloro substituent of the AB unit in compound **4**. Such reactions should be mechanically feasible since the aromatic ring carries strong electron-withdrawing substituents both ortho and para to the chlorine.

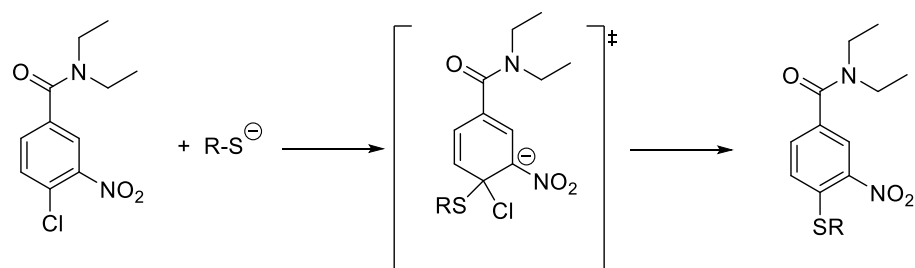


**Figure 2.2.4.4.** Preparation of C4 thioether analogs.

These reactions were low yielding and extremely difficult to purify, only to have the product fail to be coupled to the desired CD units. These were not investigated further, although the information from the use of larger substituents would have been interesting.

#### 2.2.4.1 Structural and conformational analysis

Following the encouraging results from compounds **4** and **7**, it was deemed a good point to try and obtain information regarding the tridimensional structure of these analogs. X-ray crystallography is a powerful tool to visualize this structure for the compounds in their crystalline form, and was used as a starting point. To obtain appropriately sized crystals, a sample of compound **4** was dissolved in methanol in a small Erlenmeyer flask, and sealed with parafilm. Small holes were pierced in the seal, and the sample was left at room temperature to let the solvent evaporate slowly over two weeks. The method was very successful and large crystals were obtained. A single crystal X-ray diffraction analysis was performed by the X-Ray core facility of the university of Ottawa, who processed the data and returned the results shortly afterwards. The images below

were generated from the data with the CDCC's Mercury crystal structure visualisation tool.

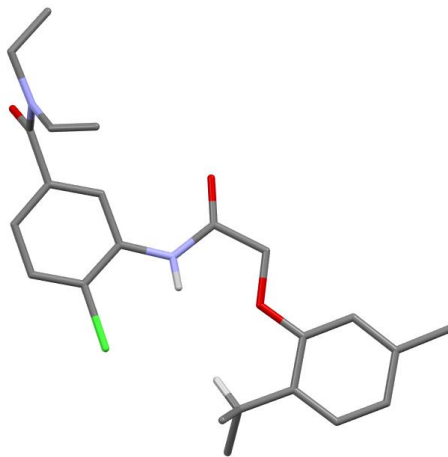


**Figure 2.2.4.3.1.** Tridimensional structure of compound **4** in a crystal lattice, obtained by single crystal X-ray diffraction.

In the crystal state, the BCD portion of the molecule is almost fully planar. It was expected that unit A would be perpendicular, or nearly so, to ring B. Hydrogen bonding between the oxygen atom of ring D and the amide hydrogen of unit B defined the spatial relationship of the B, C and D units. It is interesting to note that the isopropyl group adopts a position relatively close the amide involved in the hydrogen bond. Based on this crystal structure, the depiction of the analogs in the introduction of this work was modified to reflect this new knowledge. The unit A perpendicular to the B ring is drawn as if being planar for simplicity.

As this structure was only applicable to the compound in its solid form, the next step was to use  $^1\text{H}$  NMR NOE experiments to gather further data on its conformation in solution. 1D experiments were used, to see clearly the other protons interacting with a single targeted peak. A primary question to be answered was whether or not the aforementioned intramolecular hydrogen bond is retained in solution. Methanol- $d_4$  was chosen as solvent, since it would be more likely to disrupt the intramolecular hydrogen

bond due to the formation of hydrogen bonds between the compound **4** and the solvent. The following information was obtained by using a specific pulse sequence to irradiate only a single target proton on the molecule, which would allow any other proton in physical proximity to the target to be detected on the resulting NMR spectrum.

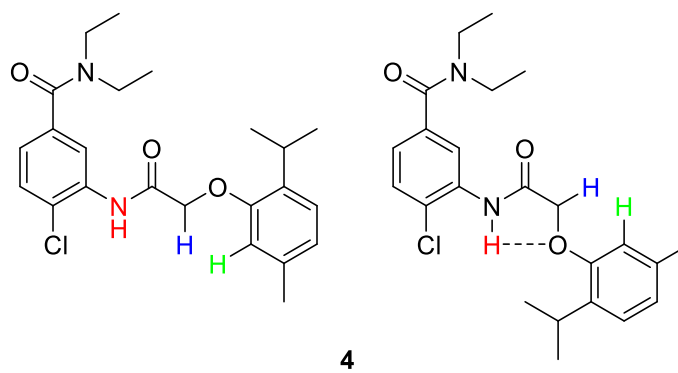


**Figure 2.2.4.3.2.** Relevant protons in the NOE experiment on compound **4** in both possible major conformations. The irradiated protons are in blue, the nearby interacting protons in green and the amide proton forming the hydrogen bond is in red.

First, the unit C CH<sub>2</sub> peak at 4.71 ppm of **4** was irradiated with a highly selective pulse, which proved to be difficult to do while also avoiding irradiation of the residual methanol peak at 4.86 ppm. The irradiation of a solvent peak would ruin the experiment by showing the protons in proximity to solvent, which would then show every single proton on the compound. The spectrum obtained is shown below. The only visible interaction is with the C6 hydrogen of ring D (6.87 ppm), which is near the irradiated CH<sub>2</sub> whether or not the intramolecular hydrogen bond is present. The primary method of assessing the presence of the hydrogen bond would be to determine the distance between the target CH<sub>2</sub> and the amide proton. In the conformation of the molecule when the hydrogen bond is present, the distance between the amide and the target CH<sub>2</sub> is at its maximum, whereas one of the two protons would be close enough to the amide to be detected by NOE in any other conformation. The BC amide proton cannot be seen in a regular <sup>1</sup>H NMR experiment due to exchanging with the solvent, and is not a suitable irradiation target. However, it can appear when interacting with a different target proton as was shown in a second NOE experiment. In this experiment, the CH of the isopropyl

group was irradiated and the resulting spectrum showed two peaks indicating spatial proximity to the two adjacent methyl groups, as well as the amide NH. This supports the idea that the conformation observed in crystals via X-ray, is also the conformation of the molecule in solution. The fact that the amide proton was observed by irradiation of the isopropyl CH, but not the unit C CH<sub>2</sub> are a strong indication that the intramolecular hydrogen bond is present even in protic solvents such as methanol.

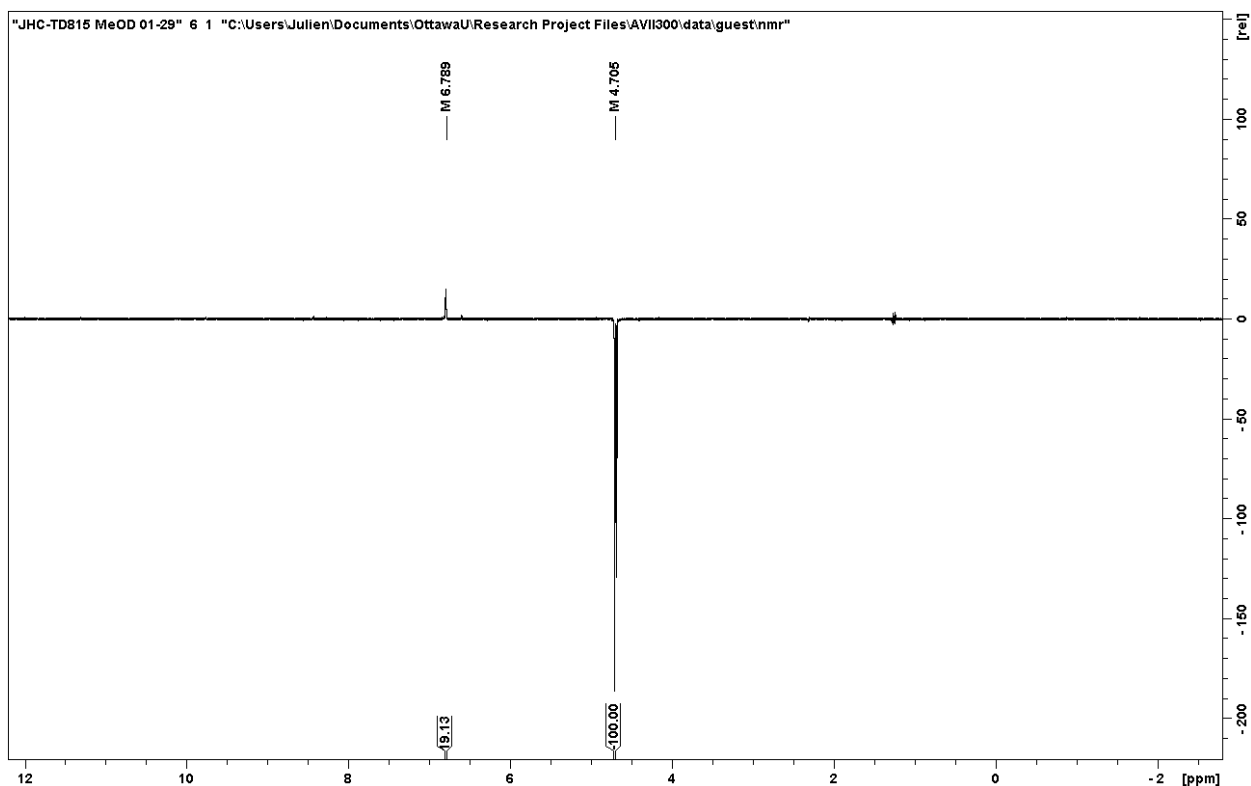


**Figure 2.2.4.3.3.** 1D <sup>1</sup>H NOE spectrum of compound **4**, with irradiation of the 4.71ppm CH<sub>2</sub> peak. The spectrum was obtained on a Bruker Avance II 300MHz, from a selnogh experiment. A 65.5 db gaussian shaped pulse of 60 000 us duration was used, centered at 4.71 ppm. A mixing time (d8) of 1.5 s was used.

### 2.2.4.2 Additional unit B analogs

With the conformation of the crystalline structure being known, four analogs were prepared to lock the conformation of the molecule, or force it to change via steric bulk between neighboring groups. Compounds **14** and **16** were designed to force units B and C out of alignment, while compound **15** prevented any rotation from occurring. The amide linking units B and C was methylated in the pair **16-17**, to observe the result of an absence of the intramolecular hydrogen bond found previously.

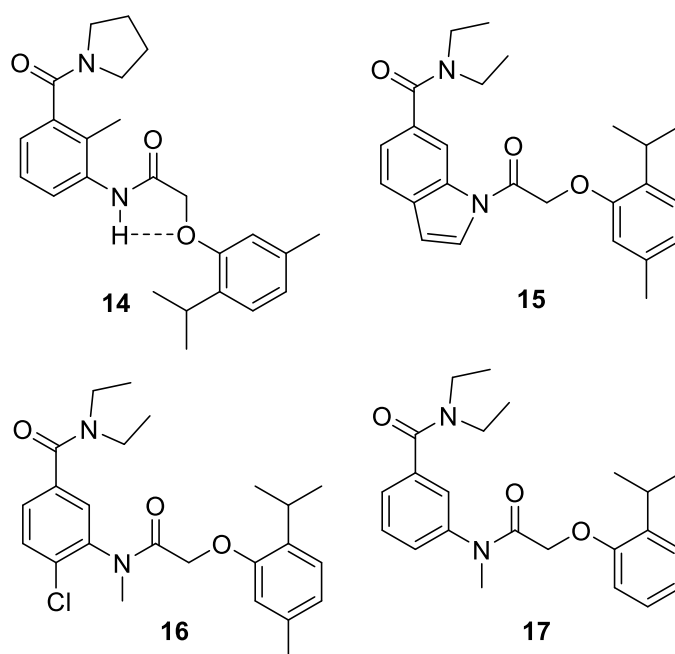


**Figure 2.2.4.2.1.** Chemical structure of the conformation-altering analogs **14-17**.

The analog **14** was prepared using the previously described methods starting with commercially available 2-methyl-3-nitrobenzoic acid **I**. The starting material for **15**, indole-6-carboxylic acid **II**, was first converted into the amide **III** and then coupled to thymol acetic acid (**3**). Finally, the diethylamides of the 3-aminobenzoic acids **IV** and **V** were methylated by treatment with dimethyl sulfate and then coupled to **3** and o-

isopropylphenol to yield **16** and **17** respectively. The assigned structures are consistent with the  $^1\text{H}$  and  $^{13}\text{C}$  NMR data given in the Experimental Section.

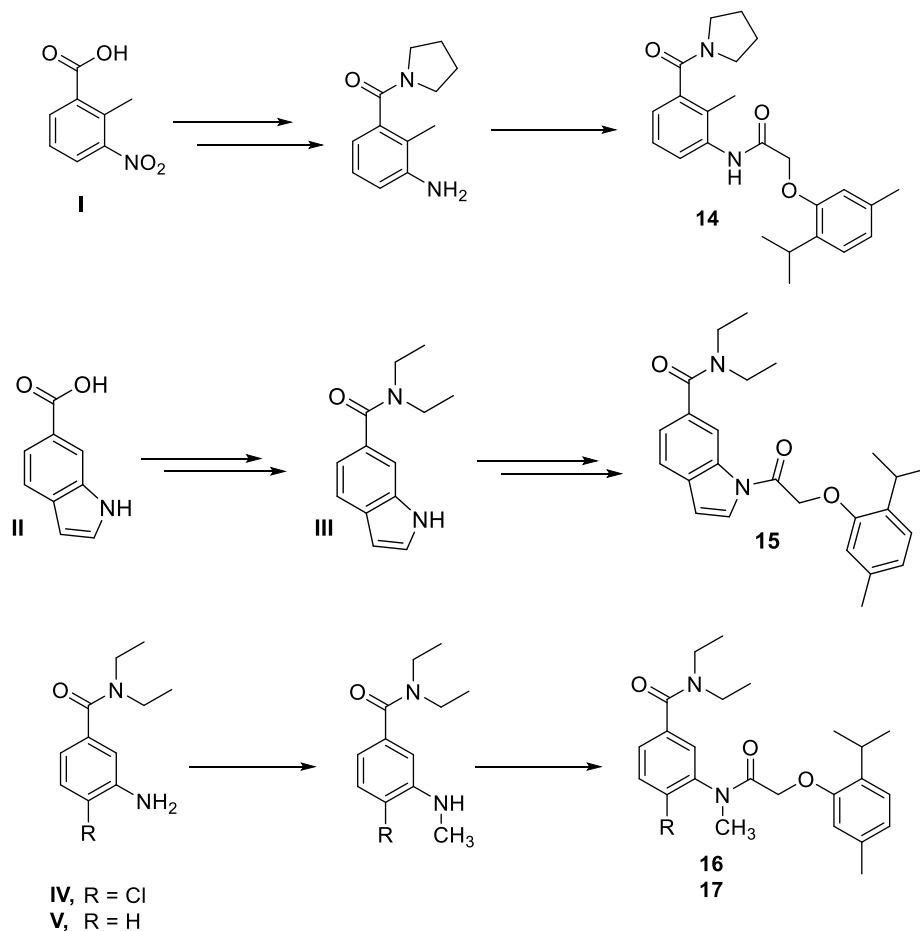


**Figure 2.2.4.2.2.** Preparation of analogs **14-17**.

The modifications introduced were expected to affect the shape of these molecules in the following ways. For compound **14**, the 2-methyl group should force 3-NHC(O)R substituent out of the plane of the B ring thereby changing the overall shape of the molecule relative to that shown in **Figure 2.2.4.2.1**. Meanwhile the indole ring in compound **15** should ensure the coplanarity of the B, C and D units. Finally, the *N*-methyl substituents in analogs **16** and **17** will eliminate the intramolecular hydrogen bonding observed in the X-Ray structure of **4**.

It is immediately obvious when looking at the results whether or not these changes are beneficial. Compound **14** is less potent based on a somewhat less favorable unit A. When compared to appropriate analogs with an equivalent unit A, **14** is only slightly less effective. This being said, the 2-methyl substituent appears to be a detrimental addition even from a proper point of comparison. Contrary to what was expected, analog **15** is relatively inactive. Similarly, the *N*-methylated derivatives **16-17** appear to be less potent than the corresponding NH analogs, with the differences between them not significant enough to draw important conclusions. This was unexpected if one assumes that the conformation resulting from the intramolecular hydrogen bond is an important feature of activity.

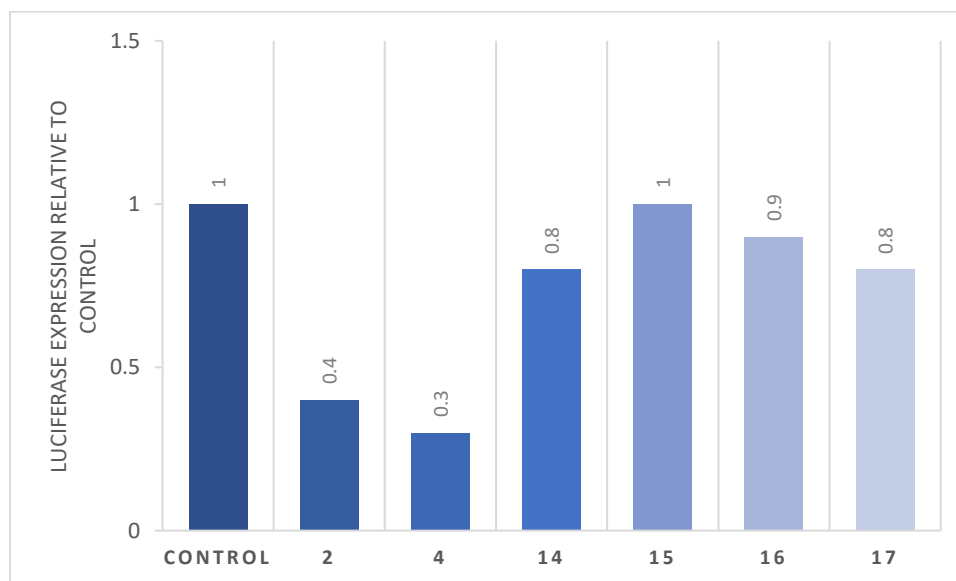


**Figure 2.2.4.2.3.** Luciferase expression assay results of analogs **14-17**.

A possible explanation for the results described above is that the presence of the NH between units B and C is absolutely required. This could be because of the intramolecular bond mentioned previously, or because it enables the formation of a hydrogen bond with the target. This would account for how analogs **15-17** that each modify the shape of the molecules differently all performed similarly poorly. It would also explain why compound **14** was the most effective of this series, despite having been

prepared from a less favorable unit A. When compared to similar analogs that lack the 2-methyl substituent, compound **14** is only slightly less potent. This indicates the possibility that the conformation in solution of these compounds is not a key element of their activity.

A few analogs were planned in addition to the compounds described above but could not be prepared for various reasons. An additional amount of indole analog **15** was used to attempt a reduction of the double bond on the five membered ring present in the compound. This hydrogenation was performed with H<sub>2</sub> and palladium on carbon. The equipment available on hand was unfortunately not sufficient to allow for high temperatures or H<sub>2</sub> pressure, and the reaction was unsuccessful.

The AB units **18** and **19** were prepared by alkylating the reduced AB units with allyl bromide and benzyl bromide. Every attempt to couple the two intermediates to thymol acetic acid (**3**) with either of the two amide bond formation methods described above resulted in the purification and identification of unchanged starting material. It is likely that the reactions failed to proceed due to increased steric constraints with the larger substituents, as similar problems were encountered to a smaller extent with compounds **15-17**. The coupled product could potentially have been obtained by performing the alkylation using an ABCD starting material rather than the AB units, and increasing the temperature or duration of the reflux. However, after the results from the analogs **15-17** were received and the previous conclusions made, this was not pursued further.

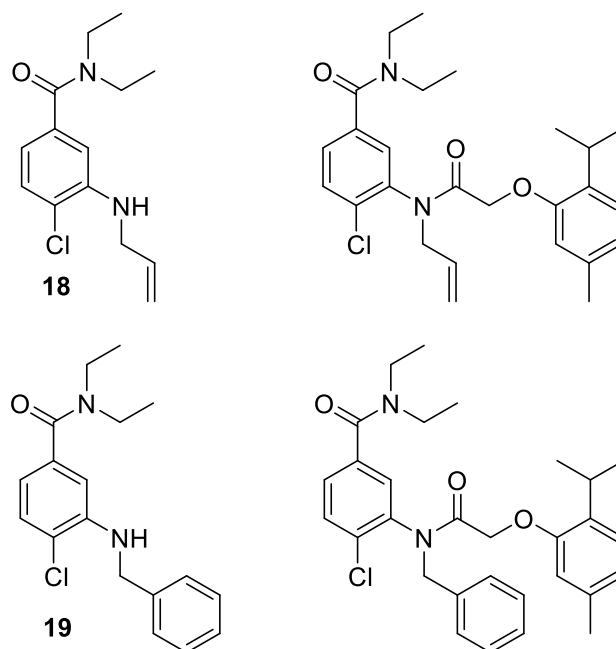


**Figure 2.2.4.3.** Chemical structure of compounds **18** and **19** as well as their respective final coupled products.

### 2.2.5 Analogs containing unit D modifications

Analogs investigating this portion of the structure were not a major focus of this work. Nonetheless, a pair of analogs (**22-23**) were prepared to test the importance of the 5-methyl substituent in ring D, which was always found in the most active compounds, but is absent in STL26 (**2**). A second pair (**20-21**) was prepared to investigate the effect of electronegative and slightly electron-withdrawing substituents in ring D, by introducing halogens at C4. Compound **24** is one of a number of compounds prepared by COOP student Kendra Lakevold, to investigate the hypothesis that larger aliphatic ortho substituents would be beneficial to the activity. Lastly, a very interesting structure (**25**) was synthesized accidentally while trying to prepare an AB unit from 3-aminobenzoic acid, where the oxalyl chloride itself was incorporated in the structure. As a considerable amount of pure compound was obtained, it was sent to be tested alongside other analogs. The compound was formed when, predictably, the chlorines of the oxalyl chloride were substituted by the two amine nucleophiles present in solution.

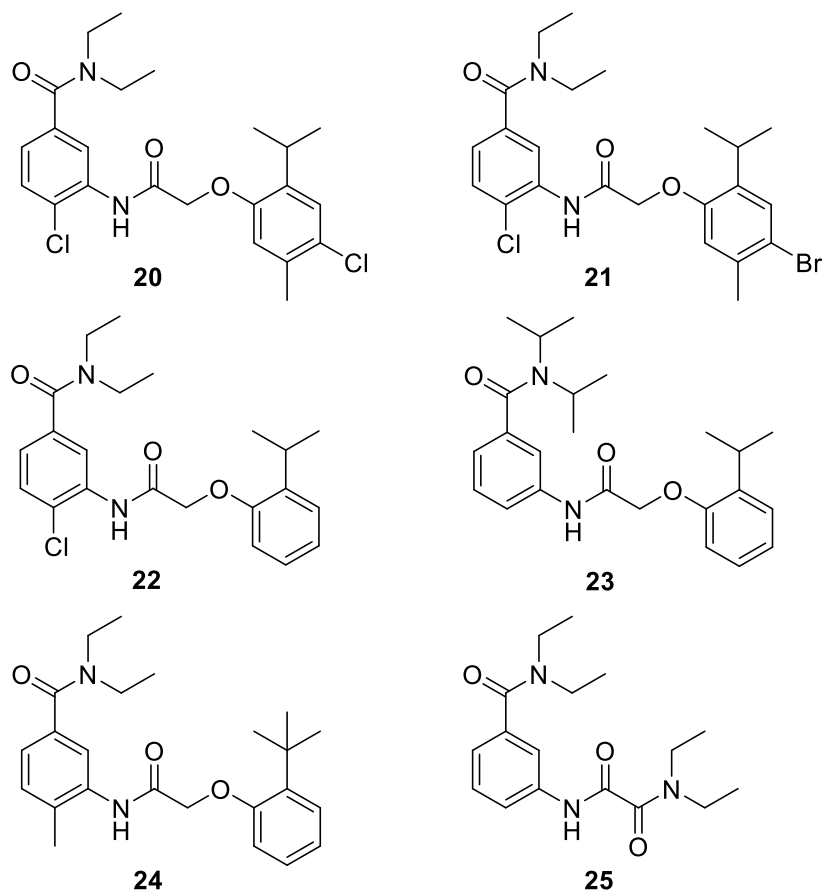


**Figure 2.2.5.1.** Chemical structure of analogs **20-25**, containing unit D modifications.

Unfortunately, the results for the analogs covered in this section were quite disappointing. The bioassays for compounds **20** and **21** were unsuccessful due to solubility issues, whereas the results for **24** and **25** were never received. The expectation for these compounds was that **20**, **21** and **24** were unlikely to cause significant changes to the activity, while any activity by **25** would have been considered an interesting new lead. The results for compounds **22** and **23** were received, but bring conflicting data to what was previously obtained. The two *o*-isopropyl analogs displayed very poor activity in this set of bioassays, which is unexpected considering their only change was the removal of the 5-methyl substituent. This is the same unit D as is present in STL26 (**2**), one of the most active compounds known. The analog **22** should not have showed such poor activity, considering its only difference with that of **2** is the presence of a 4-chloro substituent on ring B. The impact of this change was shown to be minor, as many active compounds were

prepared with this same B ring. Due to the conflicting nature of this data, conclusions cannot be drawn without further investigation. As these two lone data points are opposed to most previous data obtained and were tested in the same series, they should at least be retested to confirm there was no issue with their bioassays.

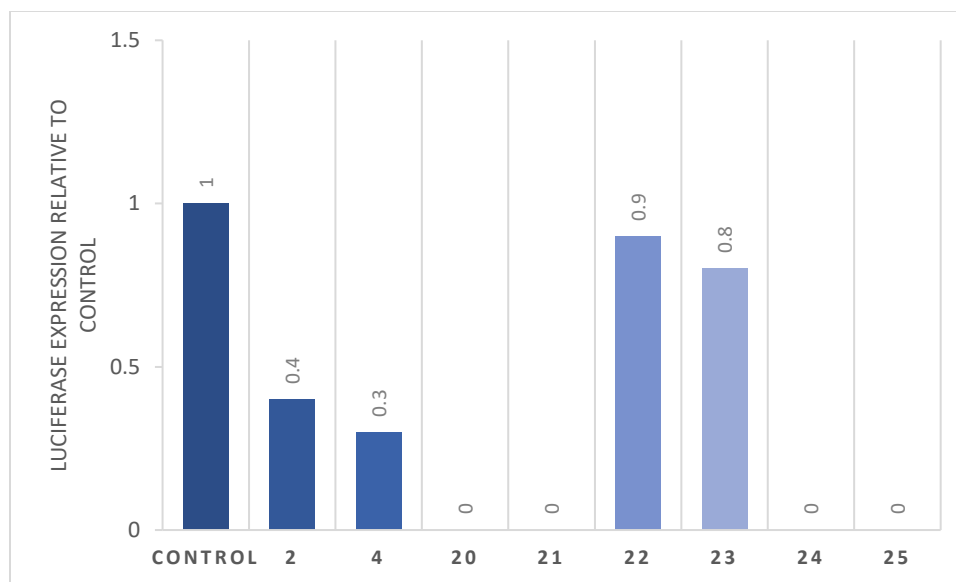


**Figure 2.2.5.2.** Luciferase expression assay results of analogs **20-25**.

The compounds containing modifications to unit D prepared as part of this work thus could not lead to any satisfying or helpful conclusions. A small number of analogs were prepared by undergraduate Ashleigh Lew containing units D based on 2-methyl and 2-chloro phenol that were not reported in this or previous works. However, none of these displayed any inhibitory activity whatsoever. Three additional analogs were prepared based on **21** in preparation for future work, and are described in the conclusion of this thesis. The SAR study of this region of the structure is ongoing, and will be a major focus from this point on.

## 2.2.6 Conclusion and future work

The solubility issues of these compounds were briefly mentioned in this thesis but deserved further emphasis considering the significant issues they caused in testing and with potential administration. The most straightforward way to improve the solubility of the compounds in water would be to introduce small acidic or basic groups, and converting them to salts. These additional groups could be added on units B or D where they, as discussed previously, should have little effect on the activity of the resulting analogs. Modifications to unit D would be preferred as they would be less likely to interfere with the synthesis, and could be done without additional protection and deprotection steps. This work was started in collaboration with the Organ group from the university of Ottawa. Our group supplied previously prepared compound **26**, to which they introduced three different amines by substitution to the chlorine in ring D. This was done using a method they developed, and allowed them to easily expand tests on the reliability of the reaction on molecules with different functional groups.<sup>25</sup> They graciously prepared compounds **27**, **28** and **29** on a small scale. The product yield was unfortunately not enough to send samples for testing of both the amines received and their corresponding hydrochloride salt. The latter were therefore not prepared. Compound **27** unfortunately only showed negligible activity; bioassay results from the other two compounds have not been received.

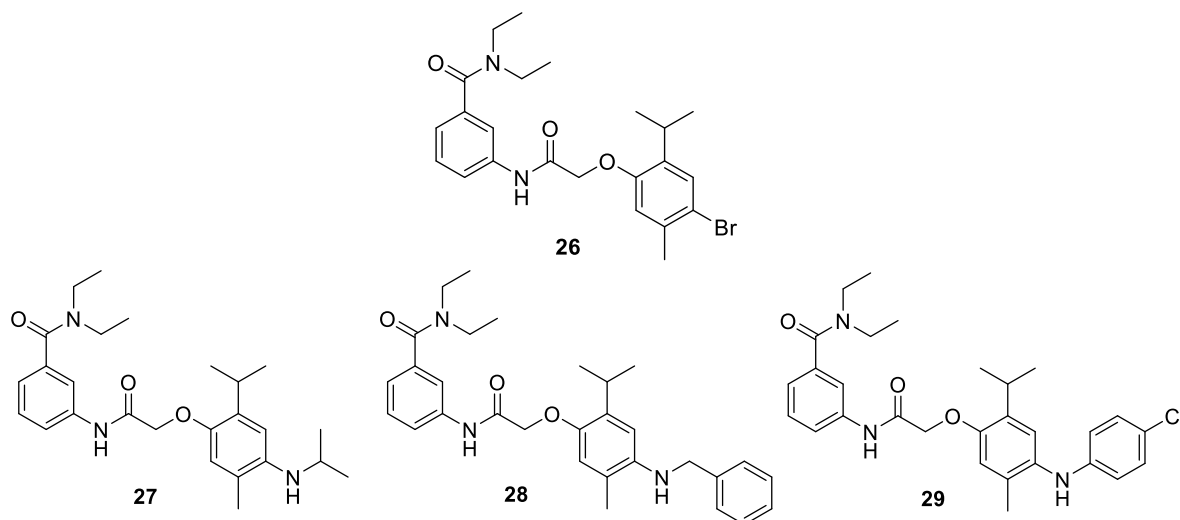


**Figure 2.2.6.1.** Structure of the three analogs prepared by the Organ group (**26-29**).

The next step will be the addition of a simple amine, and carboxylic acid to the same position. The amine analog can be prepared via the nitration of thymol, followed by a reduction after the formation of the other amide bonds. The acid analog would be prepared by hydroxymethylation of thymol with formaldehyde. The resulting alcohol would then be oxidized. Both compounds could then be easily converted to their respective salts, and should be readily soluble in water. The amine analog would be expected to be a better candidate as it should return to its deprotonated form when in the blood stream which could give it a better chance at reaching the spinal cord.

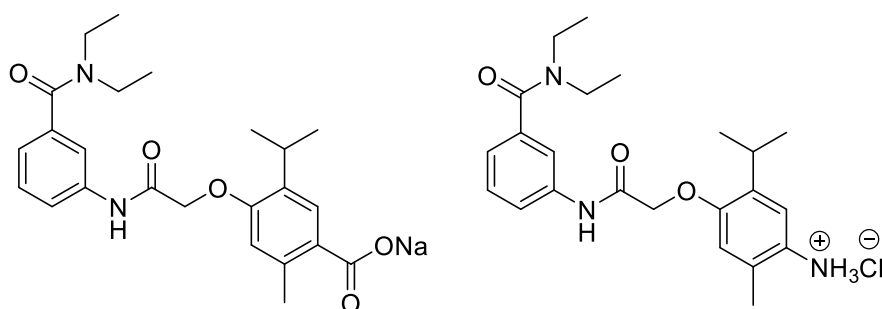


**Figure 2.2.6.2.** Structure of potential water-soluble analogs.

While attempts to improve activity by altering the primary conformation of the analogs were unsuccessful, different structures could be synthesized that could do so without forming a tertiary amide between units B and C as was done previously. While the 2-methyl analog had negative results despite retaining the intramolecular hydrogen bond, a compound retaining this bond while also locking the molecule in a planar conformation has not been prepared. Below are two example of compounds that could be prepared to investigate further in this direction.

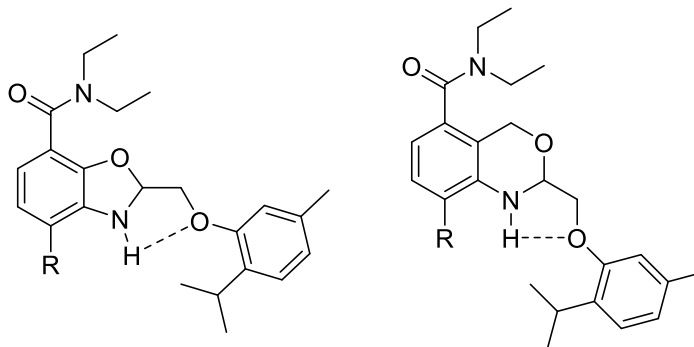


**Figure 2.2.6.3.** Structure of potential analogs containing a cyclic unit C.

Finally, while the activity of the current best analogs is not significantly superior to the lead structure ZO2 (**1**), the compound itself was already found to be somewhat effective at improving recovery post SCI even prior to the improvements discovered.<sup>15</sup> While optimization should continue for the analogs to become at least an order of magnitude more active, this seems unlikely to happen without deviating significantly from the structures currently in use. In this light, it would be a good idea to consider performing metabolic studies of these analogs. Having a general idea of the safety of these compounds, as well as their key metabolites would be useful before going further into this project.

## 2.3 Experimental Data

### 2.3.1 General information

The work presented in this chapter was done for and in collaboration with the Brown group. As such, only the compounds that they deemed important were fully characterized, and in those cases the characterization would be restricted to the minimum required to support future patent applications.

For the sake of space, while the compounds were characterized by at least  $^1\text{H}$  NMR at each step, only the completed AB, CD and final products will be reported in this section. A  $^{13}\text{C}$  NMR analysis was not always performed on the AB intermediates if they were used immediately.

#### TLC

Thin layer chromatography was used to analyze product formation during reactions, assess purity of final products, determine appropriate solvent mixtures for column chromatography where required and detect the desired fractions to combine after elution. The samples to analyze were deposited on aluminum-backed thin layers silica plates and eluted with an appropriate solvent mixture, typically composed of DCM, ethyl acetate and/or hexanes. As most of the compounds in this project contained aromatic rings or  $\pi$  systems, the eluted plates were visualized under UV light (254 nm) and stained with ceric ammonium molybdate and heat.

#### Column chromatography

When required, the finished products were purified via column chromatography if other purification methods were unsuccessful or not appropriate. SiliaFlash F60 (230-400 mesh) silica powder was used. The columns were packed with dry silica, before adding

the sample in a minimal amount of solvent and fully drying the column. The elution solvent system used was an ethyl acetate and hexane mixture. In all columns performed, the elution started with a small volume of pure hexanes, followed by a steady increase in ethyl acetate ratio. The gradients and solvent ratios used varied depending on the compounds being purified and were based on an initial TLC of the sample.

## **NMR**

The  $^1\text{H}$  and  $^{13}\text{C}$  NMR spectra were obtained on a Bruker Avance 400 MHz spectrometer, while NOE experiment spectra were obtained on a Bruker Avance II 600MHz spectrometer. The samples were prepared in  $\text{CDCl}_3$ , MeOD or  $\text{D}_2\text{O}$ . The solvent used for each sample is indicated with their respective spectra. The chemical shift values for all spectra are reported in parts per million (ppm) relative to tetramethylsilane (TMS) ( $\delta$  0.00 ppm). Coupling constants are reported in Hz where appropriate. Spectral information was processed using the TopSpin 4.06 software.

## 2.3.2 General procedures

### 2.3.2.1 Amide coupling via acyl chloride intermediate

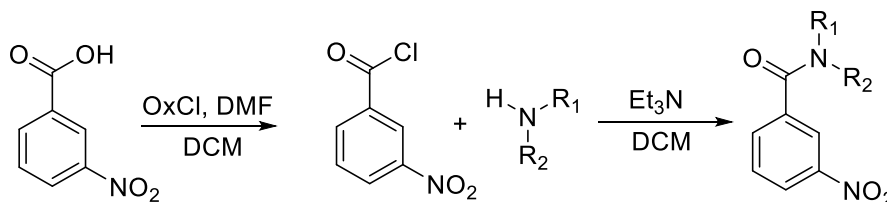


**Figure 2.3.2.1.1.** Preparation of amides from an acyl chloride intermediate.

The carboxylic acid substrate (1.00 eq.) was suspended in DCM in a round bottom flask. Oxalyl Chloride (3.00 eq.) was then added via syringe and the mixture was placed in an oil bath to heat gently for five minutes. A few drops of DMF were added to the solution to catalyze the reaction, which brought it to a boil. The solution was stirred at reflux in the oil bath for an hour after which the solvent was immediately removed on the rotary evaporator to obtain the acyl chloride intermediate. This intermediate was obtained either as an oil or a solid depending on the initial substrate.

During the reflux of the first solution, a second round bottom flask was prepared with the selected amine (1.00 eq.) and triethylamine (3.00 eq.) diluted in DCM. This solution was chilled in an ice bath in preparation for the next step.

The acyl chloride intermediate was dissolved or diluted in a small amount of DCM, then placed in the same as bath as the flask containing the amines. Once both solutions were cooled sufficiently, the acyl chloride solution was added dropwise over 5 minutes to the amines via a glass pipette. Over the course of this addition, the solution became progressively more yellow, with opaque white fumes appearing. The combined solution was left to sit at room temperature for half an hour, then quenched with water.

A separatory funnel was used to isolate the organic layer and wash it twice with  $\text{HCl}_{(\text{aq})}$  5%. The solution was dried over  $\text{MgSO}_4$ , filtered and evaporated in vacuo. The product was obtained as an oil, which solidified over time. The product was purified by recrystallisation in DCM and hexanes or by column chromatography depending on the purity of the crude product, and characterized by  $^1\text{H}$  and  $^{13}\text{C}$  NMR.

### 2.3.2.2 EDCI & DMAP amide coupling

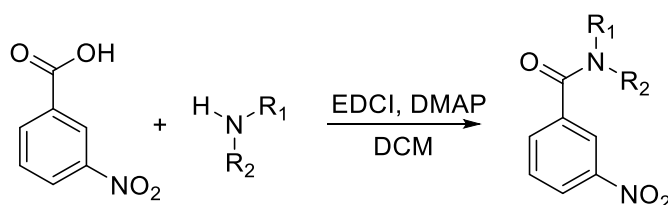


**Figure 2.3.2.2.1.** Amide bond formation using EDCI as coupling reagent.

The carboxylic acid substrate (1.00 eq.) was dissolved in dichloromethane. 1-Ethyl-3-(3-dimethylaminopropyl)carbodiimide hydrochloride (EDCI, 1.20 eq.) and dimethylaminopyridine (DMAP, 1.20 eq.) were added to the solution and fully dissolved. The amine reagent (1.00+ eq.) was added last. The reaction mixture was left to react at room conditions over night. Once done, the mixture was washed with a 5%  $\text{NaOH}_{(\text{aq})}$  solution to remove excess starting materials. The resulting organic phase was dried with magnesium sulfate, filtered, and evaporated to obtain the desired product. The crude product was then purified by recrystallisation in dichloromethane and hexanes or by column chromatography in silica gel, as appropriate, then characterized by  $^1\text{H}$  and  $^{13}\text{C}$  NMR.

### 2.3.2.3 Reduction of nitro groups to amines using Iron

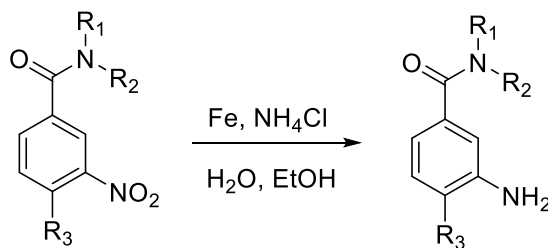


**Figure 2.3.2.3.1.** Fe reduction of nitro groups.

The nitro starting material (1.00 eq.) was dissolved in a 1:2 water and ethanol mixture (15 mL per g of starting material) in a round bottom flask. Iron Powder (6.00 eq.) was added, followed by saturated Ammonium Chloride in water (30 g/100 mL, 0.6 eq.). The mixture was placed in an oil bath at 100°C without a magnetic stirrer, and refluxed for an hour or until complete by TLC. The mixture was stirred regularly with a metal spatula to keep the iron in suspension.

After being removed from the oil bath and allowed to cool down, the solution was filtered by suction through a small amount of celite, to remove the Iron powder. NaOH<sub>(aq)</sub> 10% was added to the filtered solution, from which the amine product was extracted three times with 20 mL dichloromethane. The organic extract was dried with magnesium sulfate, then filtered by gravity to remove the deposits. The solvent was evaporated in vacuo to obtain the product as a yellow oil, which was placed in the freezer for a few minutes until it solidified. The product was obtained in good yields as yellow crystals, and characterized by <sup>1</sup>H and <sup>13</sup>C NMR.

#### 2.3.2.4 Nucleophilic substitution of chloroacetic chloride by phenols

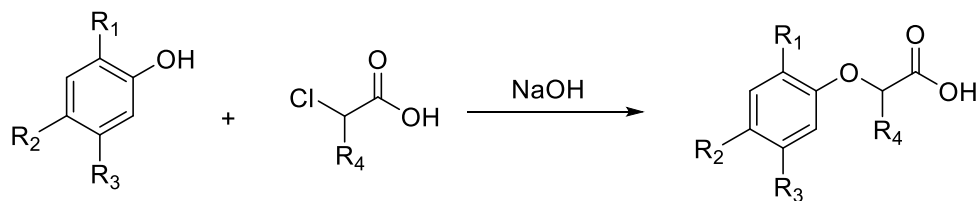


**Figure 2.3.2.4.1.** Formation of 2-phenoxyacetic acid derivatives.

The phenol starting material (1.00 eq.) was dissolved in an aqueous solution of NaOH (4.00 eq.). The chloroacetic acid was then added to the mixture, which was stirred at reflux in an oil bath until complete by TLC. The reactions usually took several days of heating to complete. The solution was washed thrice with dichloromethane, then acidified dropwise with concentrated HCl to precipitate the product. The product was obtained via suction filtration as a white solid and characterized by <sup>1</sup>H and <sup>13</sup>C NMR.

#### 2.3.2.5 Palladium-catalyzed substitution of aromatic bromine by amines

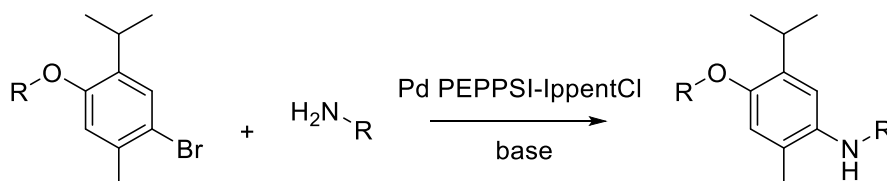


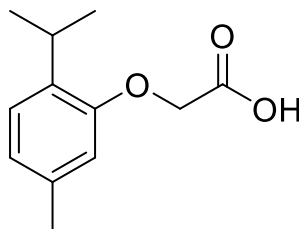
**Figure 2.3.2.5.1.** Substitution of aromatic bromines by amines.

This reaction was performed according to the following procedure by the Organ group on brominated compounds supplied by our lab. The brominated substrate (1.00 eq.), a base of choice such as tBuOK or NaBHT (1.10 eq.) and the palladium catalyst (3-5%) were placed in a round bottom flask and purged with argon. 1,4-dioxane was added as solvent, as well the desired amine (1.30 eq.). The mixture was heated at 80°C for 24 hours. The workup procedure was not shared with our group but most likely only consisted of acid-base extractions. Purification of the compounds by column chromatography on silica gel was performed afterwards by our group.

### 2.3.3 Experimental procedures and product characterization

Preparation of 2-(2-isopropyl-5-methylphenoxy)acetic acid, referred to as thymol acetic acid,

3



3

Procedure as described by Rowan Swan in a report of her experimental procedures. This document did not contain images of the obtained NMR spectra, only text data is available.

In a round bottom flask equipped with a magnetic stirrer, thymol (34.9 g, 232.8 mmol) was dissolved in a solution of NaOH (25.4 g, 635 mmol) in distilled water (75 mL). Chloroacetic acid (20 g, 211.7 mmol) was then added. The solution was stirred at reflux over several days, tracked by TLC. The solution was washed with dichloromethane and acidified to precipitate the product. No purification was required for this reaction, and the pure product was obtained as a beige powder (14.23 g, 32%).

**<sup>1</sup>H NMR (400 MHz; CDCl<sub>3</sub>):** δ 7.15 (d, J = 7.7 Hz, 1H), 6.83 (d, J = 7.7 Hz, 1H), 6.58 (s, 1H), 4.70 (s, 2H), 3.36 (m, J = 6.9 Hz, 1H), 2.33 (s, 3H), 1.24 (d, J = 6.9 Hz, 6H).

**<sup>13</sup>C NMR: (400 MHz; CDCl<sub>3</sub>):** δ 174.85, 155.01, 136.91, 135.01, 126.85, 123.12, 112.84, 65.63, 27.03, 23.25, 21.74.

### Preparation of 3-amino-4-chloro-*N,N*-diethylbenzamide.

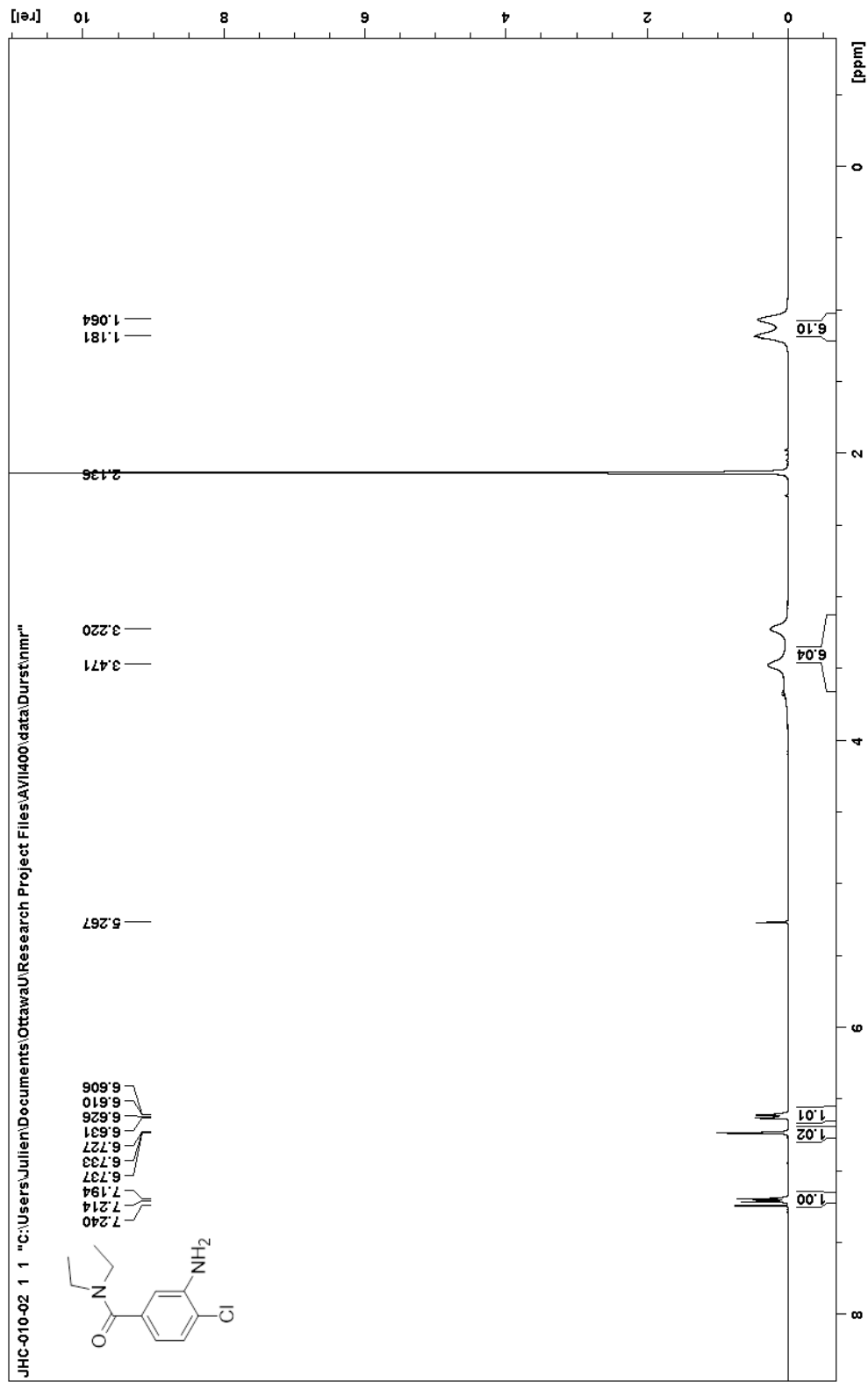


4-Chloro-3-nitrobenzoic acid (2.05 g, 10.2 mmol) was dissolved in DCM (60 mL) with oxalyl chloride (2.1 mL, 24.5 mmol). DMF (10 drops) was added before the solution was stirred for 40 minutes at 60°C. The solution was evaporated and new DCM was added. The solution was cooled, and added slowly to a solution of diethylamine (2.1 mL, 20.3 mmol) and triethylamine (7.5 mL, 53.8 mmol) in DCM in an ice bath. The combined solution was left to sit 30 minutes before adding water and separating the phases. The organic layer was washed once with 5% NaOH<sub>(aq)</sub>, once with 5% HCl<sub>(aq)</sub> and once with 2.5% NaOH<sub>(aq)</sub>, before being dried over MgSO<sub>4</sub>, filtered and evaporated in vacuo to yield the intermediate 3-nitro benzamide product (2.58 g, 99%).

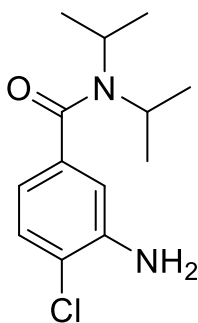
The intermediate (2.45 g, 9.54 mmol) was dissolved in a 2:1 mixture of ethanol and water. Iron powder (2.67 g, 47.8 mmol) and NH<sub>4</sub>Cl<sub>(aq)</sub> (30 g/100 mL, 0.85 mL, 4.7 mmol) were added to the mixture. The solution was refluxed without a stirrer at 100°C for 45 minutes, until complete by TLC. Afterwards, the iron was filtered out by suction filtration through a small layer of celite. The desired product was extracted in DCM and washed once with 5% HCl<sub>(aq)</sub>. The organic layer was dried over MgSO<sub>4</sub>, filtered by gravity and evaporated to yield the desired product as a solid (2.02 g, 93%). The total yield over both steps was 92%.

\*presence of acetone and dichloromethane can be seen in the <sup>1</sup>H spectrum.

<sup>1</sup>H NMR (400 MHz, CDCl<sub>3</sub>) δ, ppm: 7.20 (d, J = 8.0 Hz, 1H), 6.73 (d, J = 1.6 Hz, 1H), 6.62 (dd, J<sub>1</sub> = 8.0 Hz, J<sub>2</sub> = 2.0 Hz, 1H), 3.35 (m, 6H), 1.12 (br, 6H).



### Preparation of 3-amino-4-chloro-*N,N*-diisopropylbenzamide.

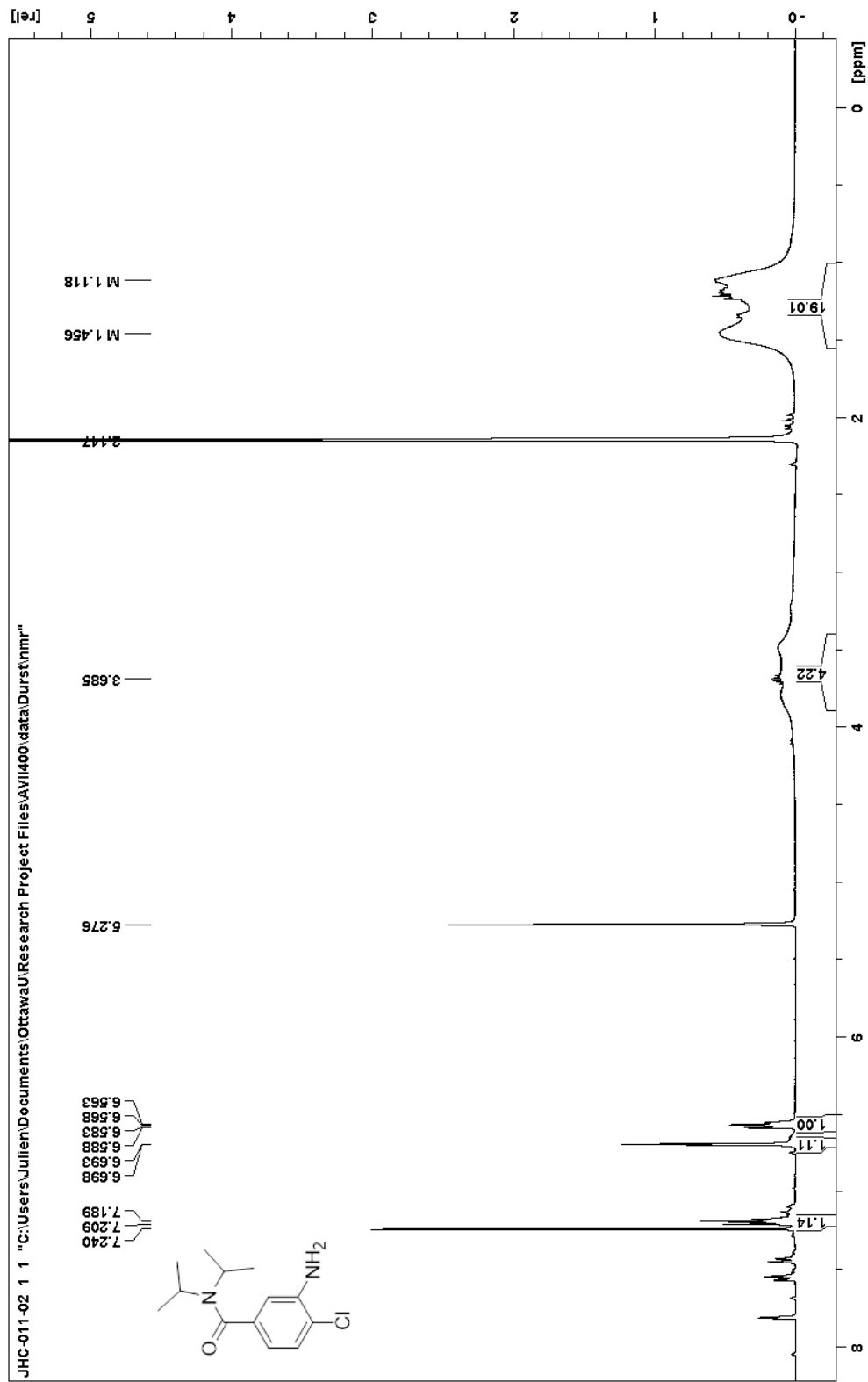


4-Chloro-3-nitrobenzoic acid (2.98 g, 14.8 mmol) was dissolved in DCM (60 mL) with oxalyl chloride (3.9 mL, 45.4 mmol). DMF (5 drops) was added before the solution was stirred for 40 minutes at 60°C. The solution was evaporated and new DCM was added. The solution was cooled, and added slowly to a solution of diisopropylamine (6.3 mL, 44.6 mmol) and triethylamine (12.5 mL, 89.7 mmol) in DCM in an ice bath. The combined solution was left to sit 30 minutes before adding water and separating the phases. The organic layer was washed once with 5% NaOH<sub>(aq)</sub>, once with 5% HCl<sub>(aq)</sub> and once with 2.5% NaOH<sub>(aq)</sub>, before being dried over MgSO<sub>4</sub>, filtered and evaporated in vacuo to yield the 3-nitro benzamide intermediate product (3.10 g, 74%).

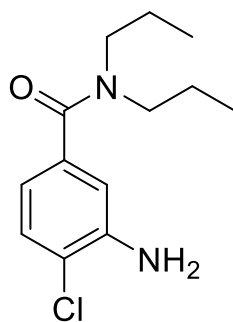
The intermediate (2.77 g, 9.7 mmol) was dissolved in a 2:1 mixture of ethanol and water. Iron powder (2.18 g, 39.0 mmol) and NH<sub>4</sub>Cl<sub>(aq)</sub> (30 g/100 mL, 0.70 mL, 3.9 mmol) were added to the mixture. The solution was refluxed without a stirrer at 100°C for 45 minutes, until complete by TLC. Afterwards, the iron was filtered out by suction filtration through a small layer of celite. The desired product was extracted in DCM and washed once with 5% HCl<sub>(aq)</sub>. The organic layer was dried over MgSO<sub>4</sub>, filtered by gravity and evaporated to yield a solid (1.99 g) composed of a 21:79 mixture of nitro starting material and the desired product (1.57 g, 42%), which were later separated. NMR data is unfortunately only available for the crude mixture containing some starting material. The total yield over both steps was 31%.

\*The spectrum shows presence of the nitro intermediate, DCM and acetone impurities.

**<sup>1</sup>H NMR (400 MHz, CDCl<sub>3</sub>) δ, ppm:** 7.19 (d, J = 8.0 Hz, 1H), 6.69 (d, J = 2.0 Hz, 1H), 6.57 (dd, J<sub>1</sub> = 8.0 Hz, J<sub>2</sub> = 2.0 Hz, 1H), 3.69 (br, 4H), 1.28 (br, 12H).



### Preparation of 3-amino-4-chloro-*N,N*-dipropylbenzamide.

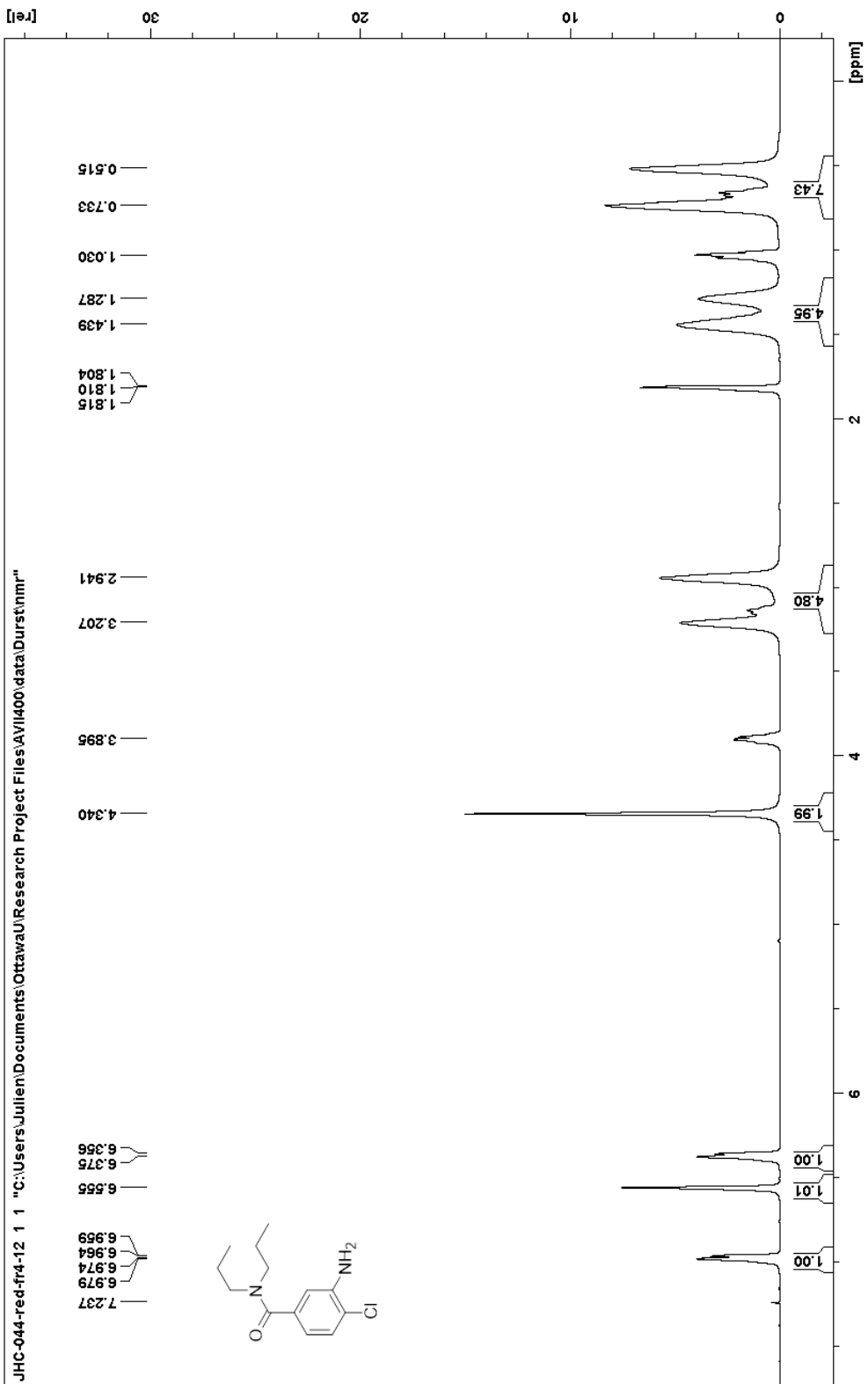


4-Chloro-3-nitrobenzoic acid (5.25 g, 26.04 mmol) was suspended in DCM (30 mL) in a round bottom flask. Oxalyl chloride (5.80 mL, 67.58 mmol) was subsequently added. DMF (5 drops) was added to the solution, which was then stirred at reflux for 1h 45 minutes in an oil bath at 60°C. Meanwhile, dipropylamine (1.35 mL, 9.84 mmol) and triethylamine (1.35 mL, 9.67 mmol) were diluted in DCM (5.0 mL) and chilled in an ice bath. The acyl chloride solution was evaporated, then redissolved in DCM. Half of this solution was added slowly to the solution of amines. The combined mixture was left to sit at room temperature for 30 minutes, after which water was added. The solution was washed once with 5% HCl<sub>(aq)</sub> and once with 5% NaOH<sub>(aq)</sub>, then dried over MgSO<sub>4</sub>, filtered and evaporated in vacuo to yield the 3-nitro benzamide intermediate product (1.44 g, 51%).

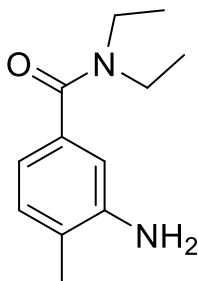
The intermediate (1.44 g, 5.05 mmol) was dissolved in a 2:1 mixture of ethanol and water (22 mL). Iron powder (1.40 g, 25.1 mmol) and NH<sub>4</sub>Cl<sub>(aq)</sub> (30 g/100 mL, 0.50 mL, 2.8 mmol) were added to the mixture. The solution was refluxed without a stirrer at 100°C for 60 minutes, until complete by TLC. Afterwards, the iron was filtered out by suction filtration through a small layer of celite. The desired product was extracted in DCM and washed once with 5% HCl<sub>(aq)</sub>. The organic layer was dried over MgSO<sub>4</sub>, filtered by gravity and evaporated to yield a yellow oil (0.72 g, 56%). The total yield over both steps was 29%

\*the concentration of the sample was too high, leading to broad peaks. This made it impossible to measure some coupling constants.

**<sup>1</sup>H NMR (400 MHz, CDCl<sub>3</sub>) δ, ppm:** 6.97 (dd, J<sub>1</sub> = 6.0 Hz, J<sub>2</sub> = 2.0 Hz, 1H), 6.56 (s, 1H), 6.36 (d, J = 7.6 Hz, 1H), 4.34 (s, 2H), 3.21 (t, 1H), 1.36 (d, 4H), 0.73 (t, 3H), 0.52 (t, 3H).



### Preparation of 3-amino-*N,N*-diethyl-4-methylbenzamide.

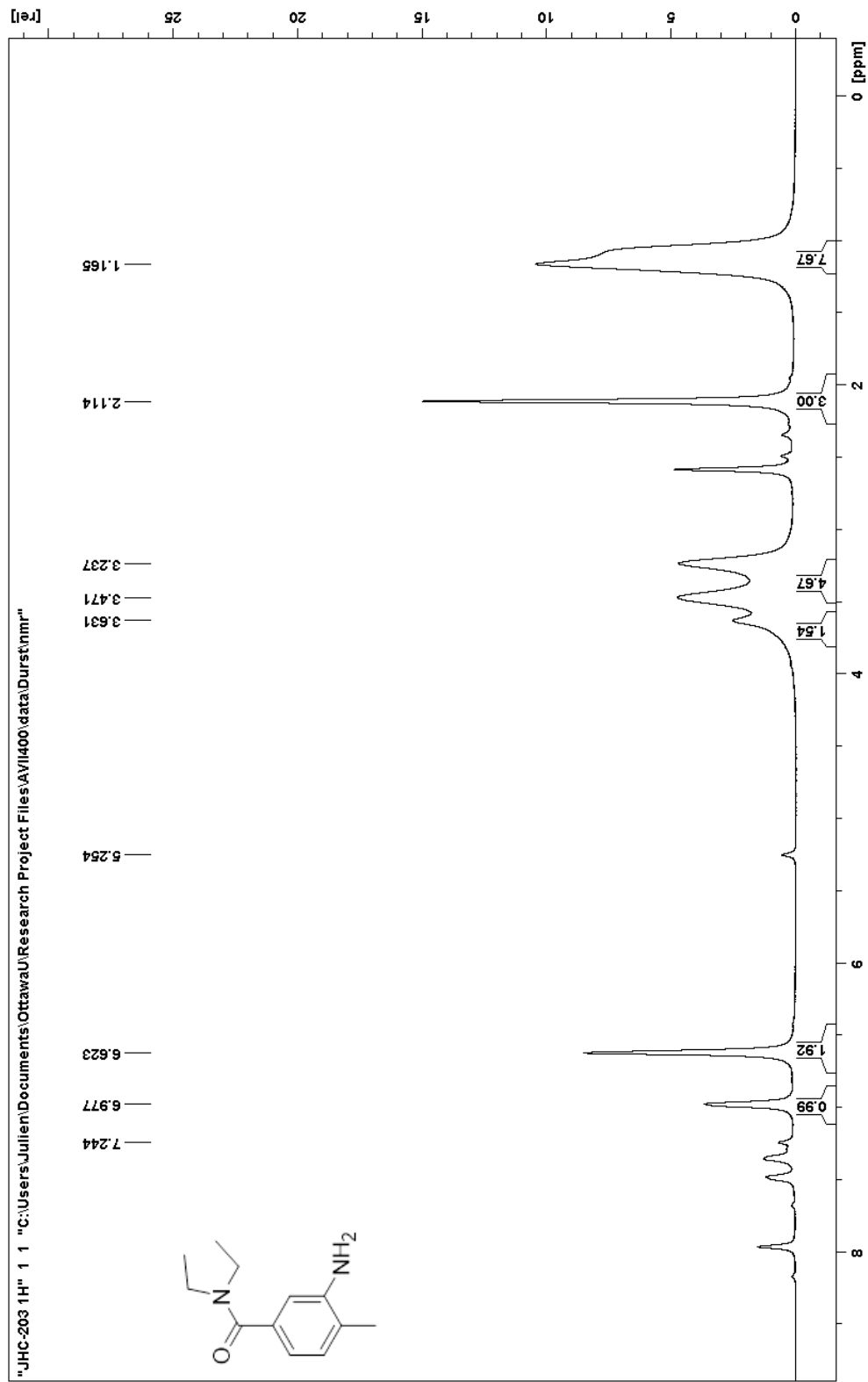


4-Methyl-3-nitrobenzoic acid (4.67 g, 25.8 mmol) was suspended in DCM with thionyl chloride (11.0 mL, 151 mmol) in a round bottom flask, and was heated gently in an oil bath around 50°C. The solution was left to reflux for 1 hour. Afterwards, the solvent was evaporated, and the contents of the flask were redissolved in a small amount of DCM. After cooling in an ice bath, the acyl chloride solution was added slowly to a cooled solution of diethylamine (8.5 mL, 82.2 mmol) in DCM. After 30 minutes at room temperature, water was added and the organic layer was isolated with a separatory funnel, then washed once with 5% HCl<sub>(aq)</sub> then 10% NaOH<sub>(aq)</sub>. The resulting organic layer was dried over MgSO<sub>4</sub>, filtered and evaporated. The intermediate product was obtained as a yellow oil (4.44 g, 73%) which was stored overnight in the freezer, but only solidified after scratching the walls of the flask with a spatula while blowing with air.

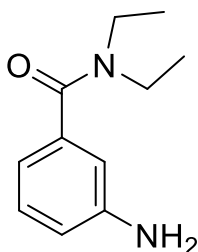
The intermediate (4.44 g, 18.8 mmol) was dissolved in a 2:1 mixture of ethanol and water (60 mL). Iron powder (6.67 g, 119 mmol) and NH<sub>4</sub>Cl<sub>(aq)</sub> (30 g/100 mL, 2.00 mL, 11.22 mmol) were added to the mixture. The solution was refluxed at 100°C until complete by TLC, while stirring by hand with a spatula every 5 minutes. Afterwards, the iron was filtered out by suction filtration through a small layer of celite. NaOH<sub>(aq)</sub> 10% was added to the solution, which was extracted thrice with DCM. The organic layer was dried over MgSO<sub>4</sub>, filtered by gravity and evaporated to yield the desired product as a yellow oil (3.41 g, 87%), which solidified after 5 minutes in the freezer. The total yield over both steps was 64%.

\*Traces of dichloromethane and starting material residue can be found in the NMR spectrum.

**<sup>1</sup>H NMR (400 MHz, CDCl<sub>3</sub>) δ, ppm:** 6.98 (s, 1H), 6.62 (s, 2H), 3.63 (br, 2H), 3.47 (br, 2H), 3.24 (br, 2H), 2.11 (s, 3H), 1.17 (s, 6H).



### Preparation of 3-amino-*N,N*-diethylbenzamide.

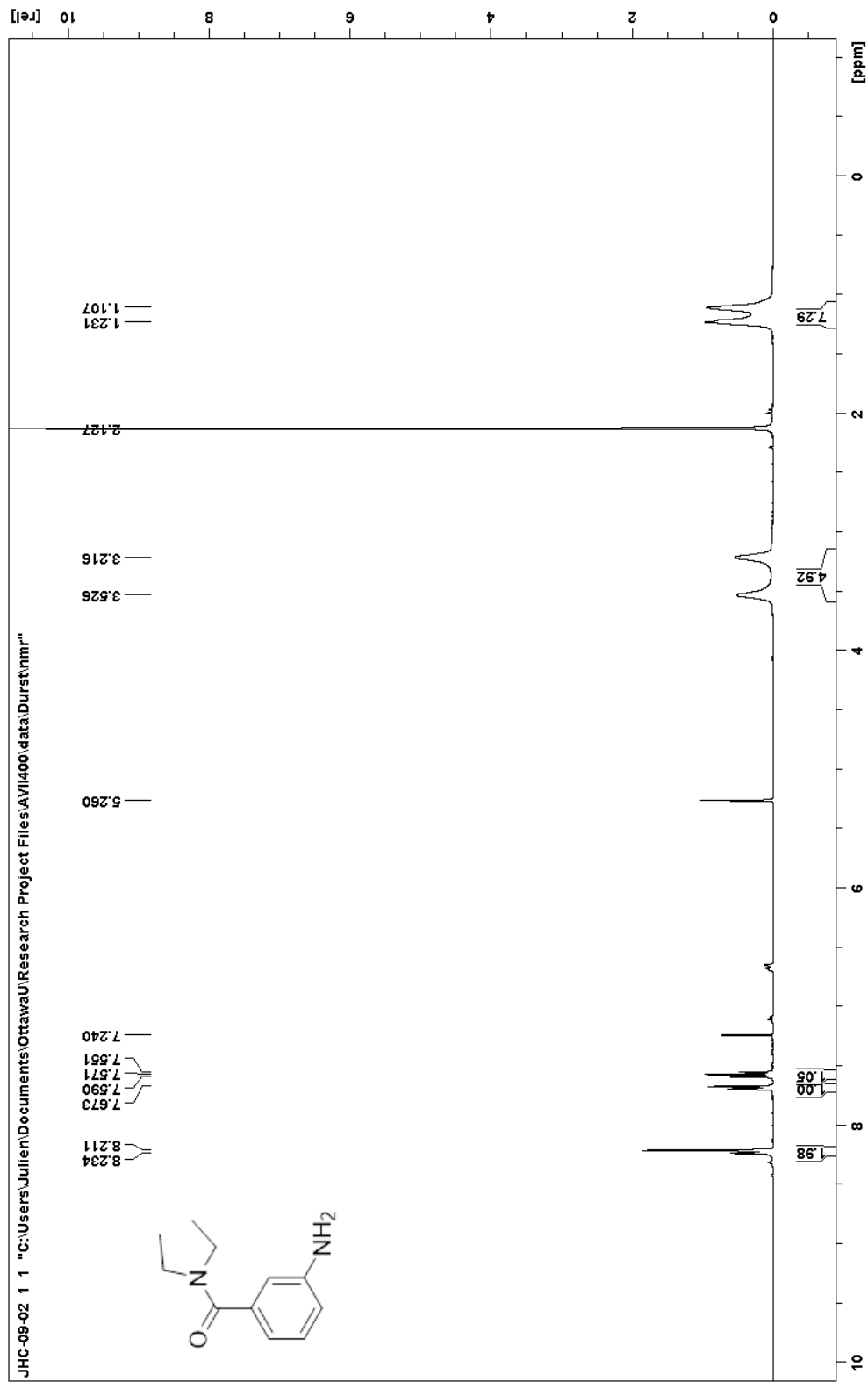


3-Nitrobenzoic acid (4.58 g, 27.4 mmol) was dissolved in DCM (100 mL) with oxalyl chloride (7.0 mL, 81.6 mmol). DMF (10 drops) was added before the solution was stirred for 40 minutes at 60°C. The solution was evaporated and new DCM was added. The solution was cooled, and added slowly to a solution of diethylamine (8.5 mL, 82.2 mmol) and triethylamine (23.0 mL, 165.0 mmol) in DCM in an ice bath. The combined solution was left to sit 30 minutes before adding water and separating the phases. The organic layer was washed once with 5% NaOH<sub>(aq)</sub>, once with 5% HCl<sub>(aq)</sub> and once with 2.5% NaOH<sub>(aq)</sub>, before being dried over MgSO<sub>4</sub>, filtered and evaporated in vacuo to yield the intermediate product (4.70 g, 77%).

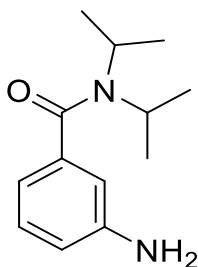
The intermediate (4.55 g, 20.5 mmol) was dissolved in a 2:1 mixture of ethanol and water. Iron powder (5.64 g, 101.0 mmol) and NH<sub>4</sub>Cl<sub>(aq)</sub> (30 g/100 mL, 2.2 mL, 12.1 mmol) were added to the mixture. The solution was refluxed without a stirrer at 100°C for 45 minutes, until complete by TLC. Afterwards, the iron was filtered out by suction filtration through a small layer of celite. The desired product was extracted in DCM and washed once with 5% HCl<sub>(aq)</sub>. The organic layer was dried over MgSO<sub>4</sub>, filtered by gravity and evaporated to yield the desired product as a solid (0.86 g, 22%). The total yield over both steps was 17%.

\*There were no chemical shift changes between the spectra of the nitro intermediate and the amine product. However the amine was successfully coupled into a finished ABCD compound. The spectrum shows presence of DCM and acetone.

**<sup>1</sup>H NMR (400 MHz, CDCl<sub>3</sub>) δ, ppm:** 8.22 (d, J = 9.2 Hz, 1H), 8.21 (s, 1H), 3.53 (br, 2H), 3.22 (br, 2H), 1.23 (br, 3H), 1.11 (br, 3H).



### Preparation of 3-amino-*N,N*-diisopropylbenzamide.



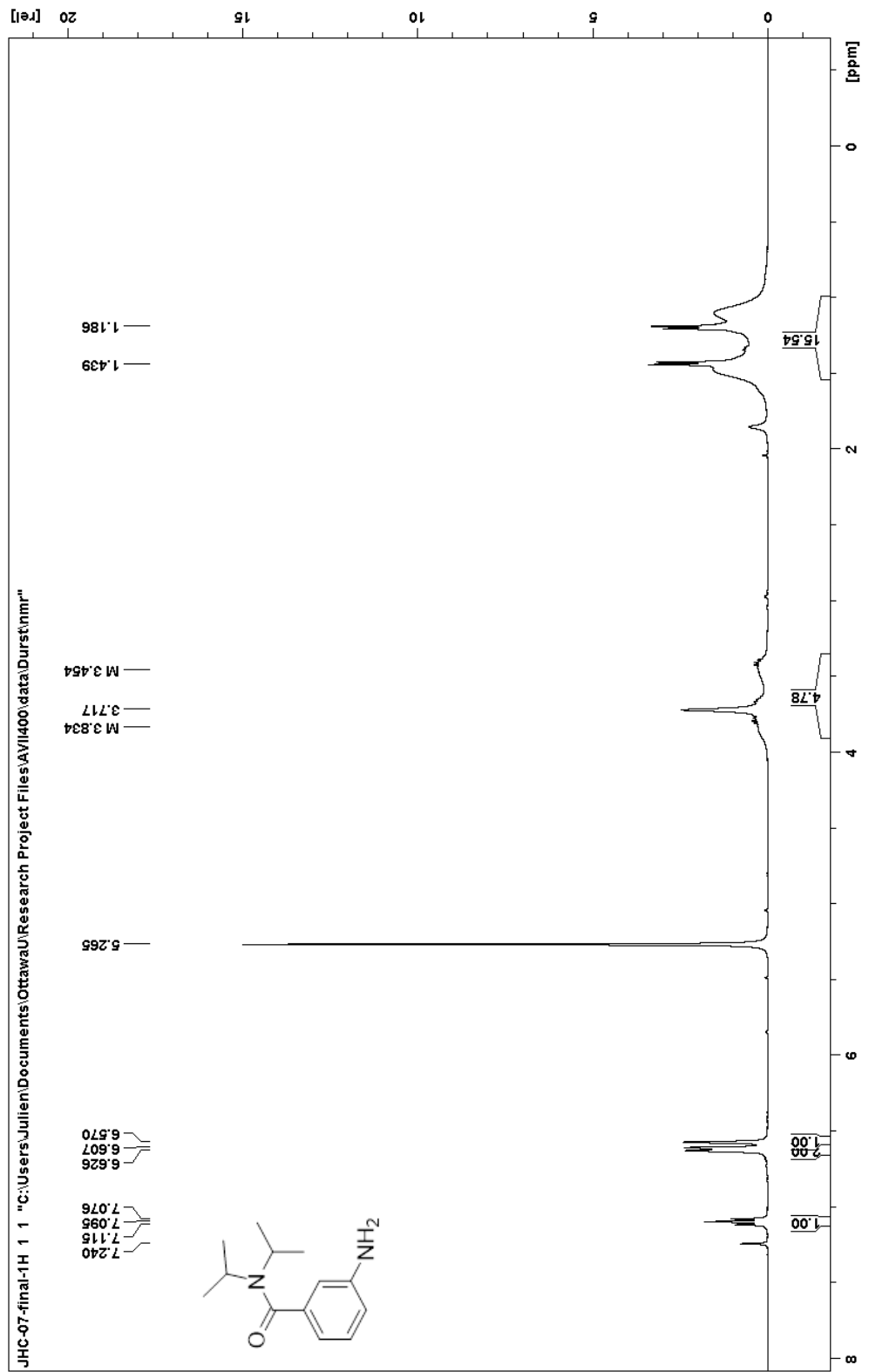
3-Nitrobenzoic acid (2.1 g, 12.56 mmol) was dissolved in DCM (50 mL) with oxalyl chloride (3.1 mL, 36.12 mmol). DMF (5 drops) was added before the solution was stirred for 30 minutes at 60°C. The solution was evaporated and new DCM was added. The solution was cooled, and added slowly to a solution of diisopropylamine (3.5 mL, 24.80 mmol) and triethylamine (10.0 mL, 71.75 mmol) in DCM in an ice bath. The combined solution was left to sit 30 minutes before adding water and separating the phases. The organic layer was washed once with 5% NaOH<sub>(aq)</sub> and twice with 5% HCl<sub>(aq)</sub>, before being dried over MgSO<sub>4</sub>, filtered and evaporated in vacuo to yield the intermediate product (2.67 g, 85%).

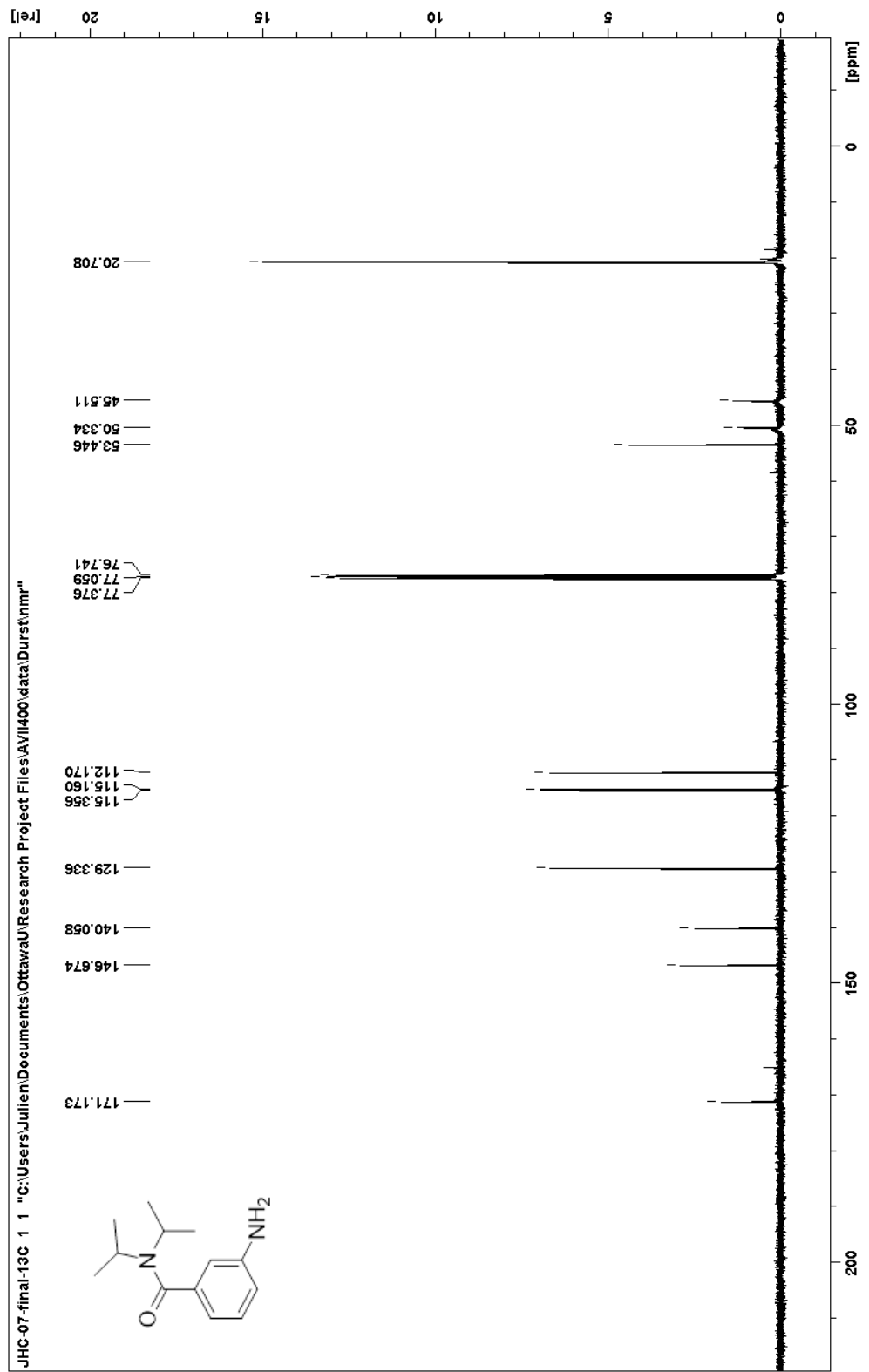
The intermediate was dissolved in a 2:1 mixture of ethanol and water (45.0 mL). Iron powder (3.49 g, 5.89 mmol) and NH<sub>4</sub>Cl<sub>(aq)</sub> (30 g/100 mL, 1.3 mL, 7.30 mmol) were added to the mixture. The solution was refluxed without a stirrer at 100°C for 45 minutes, until complete by TLC. Afterwards, the iron was filtered out by suction filtration through a small layer of celite. The desired product was extracted in DCM. The organic layer was dried over MgSO<sub>4</sub>, filtered by gravity and evaporated to yield the desired product as a solid (2.25 g, 96%). The total yield over both steps was 82%.

\*The spectrum show a large amount of DCM in the sample.

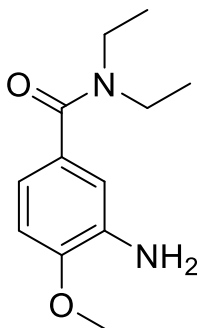
**<sup>1</sup>H NMR (400 MHz, CDCl<sub>3</sub>) δ, ppm:** 7.10 (t, J = 7.6 Hz, 1H), 6.61 (d, J = 7.6 Hz, 2H), 6.57 (s, 1H), 3.83 (br, 2H), 3.45 (br, 2H), 1.44 (br, 6H), 1.19 (br, 6H).

**<sup>13</sup>C NMR (400 MHz, CDCl<sub>3</sub>) δ, ppm:** 171.17, 146.67, 140.06, 129.34, 115.36, 115.16, 112.17, 50.33, 45.51, 20.71 (4C).



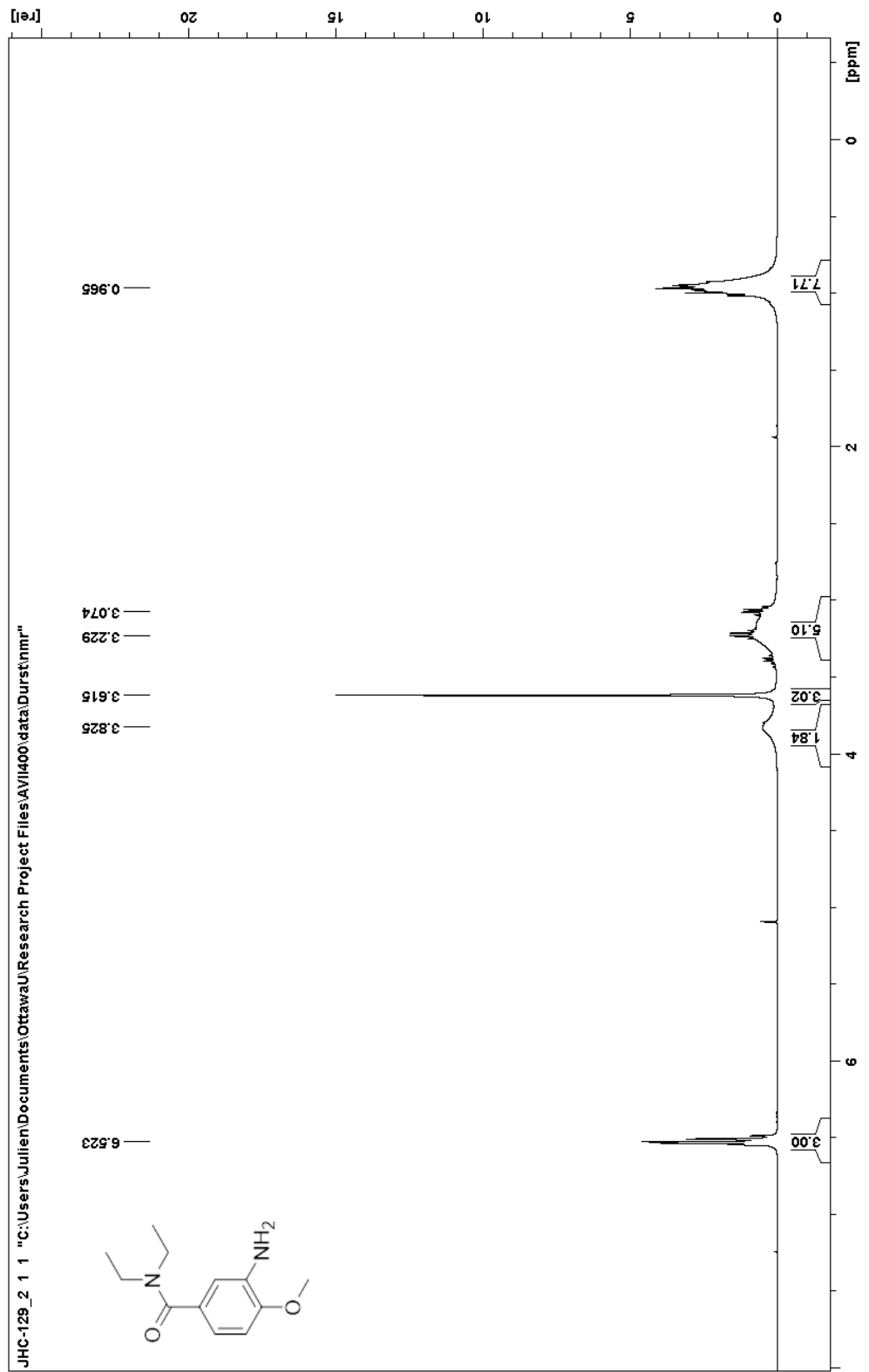


### Preparation of 3-amino-*N,N*-diethyl-4-methoxybenzamide.

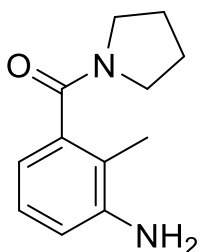


4-methoxy-3-nitrobenzoic acid (1.30 g, 6.59 mmol) was suspended in DCM (10 mL) in a round bottom flask. Oxalyl chloride (1.70 mL, 19.8 mmol) was subsequently added. DMF (2 drops) was added to the solution, which was then stirred at reflux for 1h in an oil bath at 70°C. Meanwhile, diethylamine (1.00 mL, 9.67 mmol) and triethylamine (3.00 mL, 21.5 mmol) were diluted in DCM and chilled in an ice bath. The acyl chloride solution was evaporated, then redissolved in DCM. This solution was added slowly to the solution of amines. The combined mixture was left to sit at room temperature for 30 minutes, after which water was added. The solution was washed once with 5% NaOH<sub>(aq)</sub>, then dried over MgSO<sub>4</sub>, filtered and evaporated in vacuo. The intermediate product obtained (1.52 g, 6.02 mmol, 91%) was then dissolved in a 2:1 mixture of ethanol and water, to which Iron powder (1.77 g, 31.5 mmol) was added. A saturated solution of ammonium chloride was added last (7.5 mL, 4.05 mmol). The mixture was stirred at reflux in an oil bath at 100°C for an hour. Afterwards, the solution was left to cool to room temperature, then filtered through celite. The solution was extracted with DCM, and the organic layer was dried over MgSO<sub>4</sub>, filtered and evaporated. The product was obtained as a slightly yellow solid (1.10 g, 82%). The total yield over both steps was 75%.

<sup>1</sup>H NMR (400 MHz, CDCl<sub>3</sub>) δ, ppm: 6.52 (m, 3H), 3.83 (br, 2H), 3.62 (s, 3H), 3.23 (br, 2H), 3.07 (br, 2H), 0.97 (br, 6H).



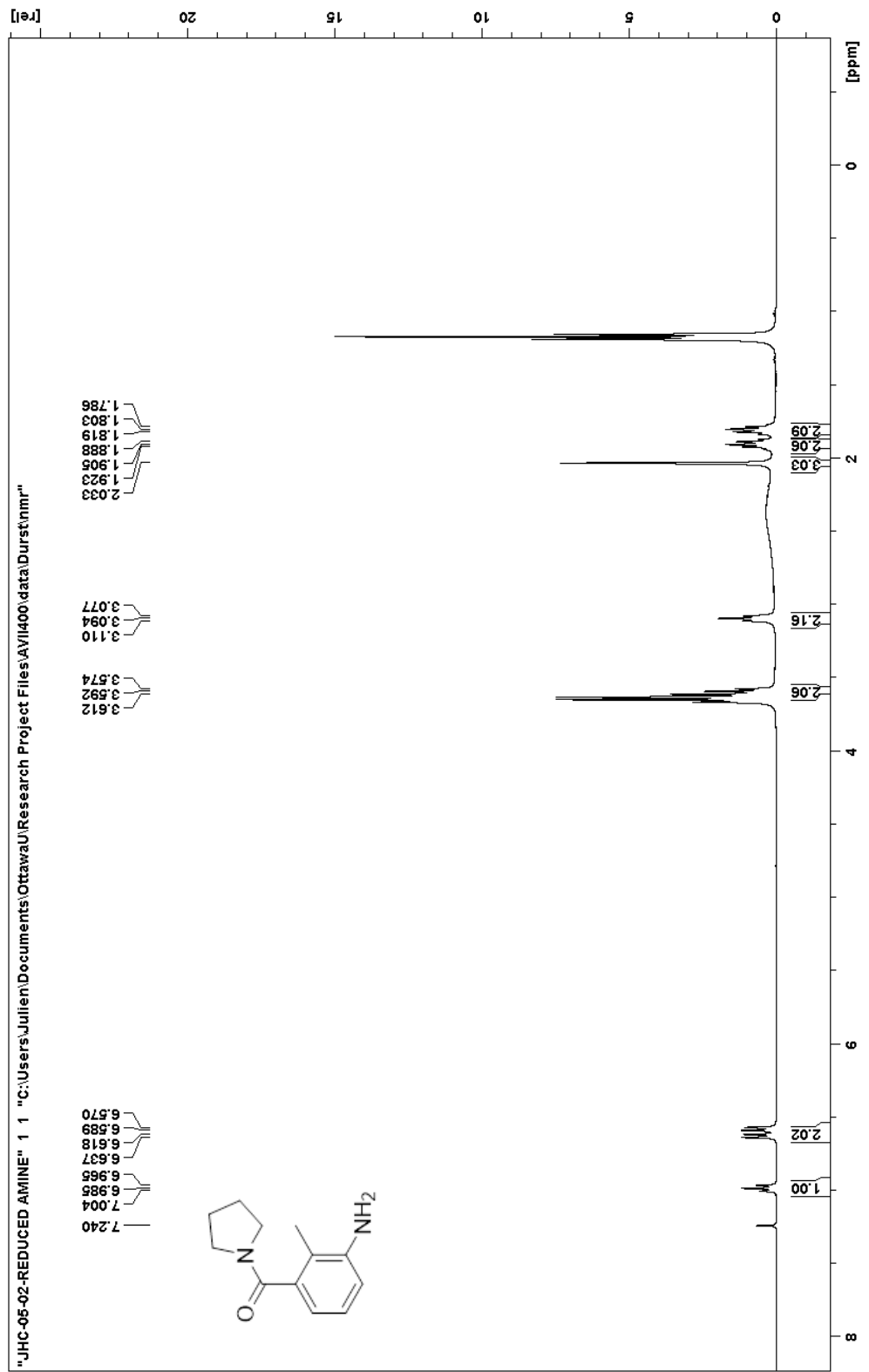
**Preparation of (3-amino-2-Methylphenyl)(pyrrolidin-1-yl)methanone.**



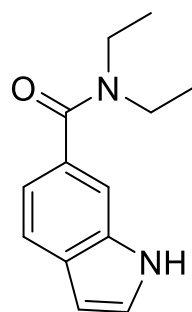
(2-Methyl-3-nitrophenyl)(pyrrolidin-1-yl)methanone (4.38 g, 18.70 mmol) was dissolved in a 2:1 mixture of ethanol and water (90 mL). Iron powder (6.00 g, 107.45 mmol) and  $\text{NH}_4\text{Cl}_{(\text{aq})}$  (30 g/100 mL, 2.1 mL, 11.79 mmol) were added to the mixture. The solution was refluxed without a stirrer at  $90^\circ\text{C}$  for 1h 30 minutes, until complete by TLC. Afterwards, the iron was filtered out by suction filtration through a small layer of celite. The desired product was extracted in DCM. The organic layer was dried over  $\text{MgSO}_4$ , filtered by gravity and evaporated to yield the desired product as a solid (2.91 g, 76%).

\*Ethanol was still present in the sample as of when the spectrum was taken.

**$^1\text{H}$  NMR (400 MHz,  $\text{CDCl}_3$ )  $\delta$ , ppm:** 6.99 (t,  $J = 7.6$  Hz, 1H), 6.63 (d,  $J = 7.6$  Hz, 1H), 6.58 (d,  $J = 7.6$  Hz, 1H), 3.59 (t,  $J = 7.2$  Hz, 2H), 3.09 (t,  $J = 6.8$  Hz, 2H), 2.03 (s, 3H), 1.91 (m,  $J = 7.2$  Hz, 2H), 1.80 (m,  $J = 6.8$  Hz).

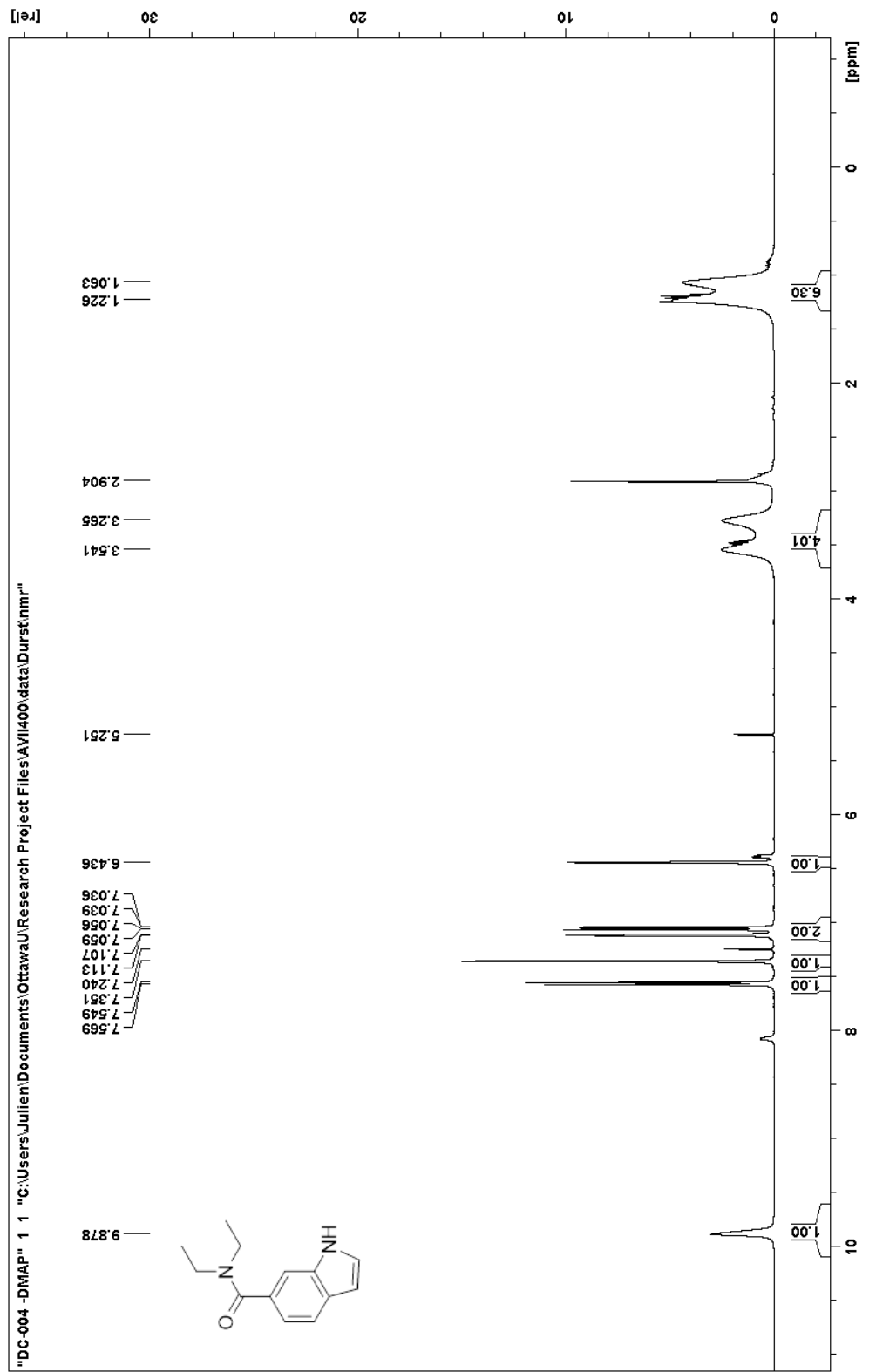


**Preparation of *N,N*-diethyl indole-6-carboxamide.**

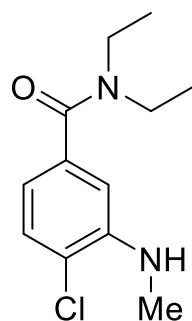


Procedure performed by undergraduate Danielle Causer. In a round bottom flask with DCM, indole-6-carboxylic acid (0.52 g, 3.23 mmol) was dissolved in DCM (15.0 mL). EDCI (0.97 g, 5.06 mmol) and DMAP (0.62 g, 5.07 mmol) were then added, followed by diethylamine (0.5 mL, 4.83 mmol). The solution was stirred at reflux for an hour in a heated oil bath. Afterwards, the solution was washed with 10% NaOH<sub>(aq)</sub>. The resulting organic layer was dried over MgSO<sub>4</sub>, filtered and evaporated. The crude product was purified by silica gel column chromatography with a gradient of hexanes and ethyl acetate. The purified product was obtained as colorless crystals (0.28 g, 40%)

**<sup>1</sup>H NMR (400 MHz, CDCl<sub>3</sub>) δ, ppm:** 9.88 (br, 1H), 7.56 (d, J = 8.0 Hz, 1H), 7.35 (s, 1H), 7.11 (t, J = 2,4 Hz, 1H), 7.05 (dd, J<sub>1</sub> = 8.0 Hz, J<sub>2</sub> = 1.2 Hz, 1H), 6.44 (s, 1H), 3.54 (br, 2H), 3.27 (br, 2H), 1.23 (br, 3H), 1.06 (br, 3H).



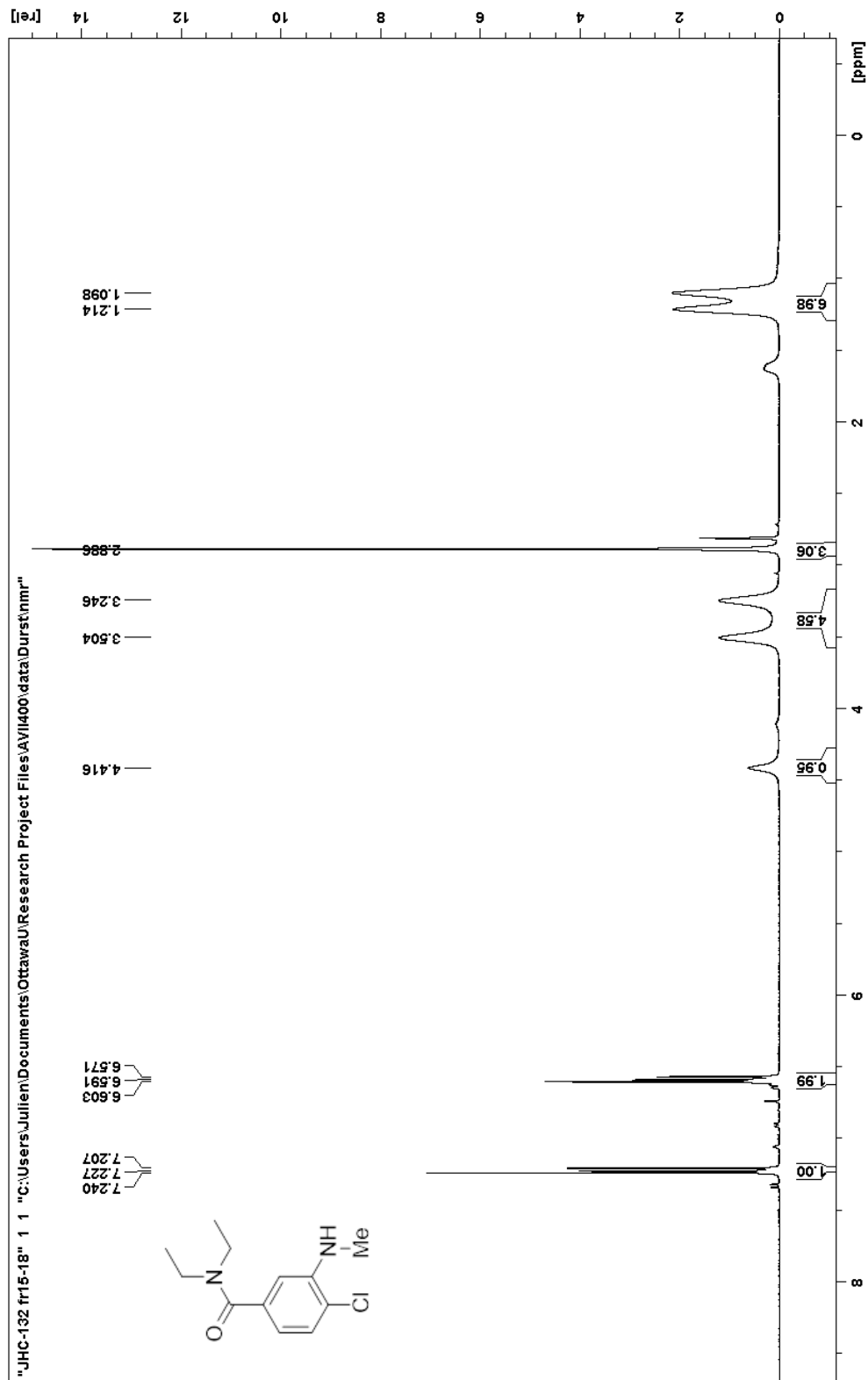
**Preparation of 3-(*N*-methylamino)-4-chloro-*N,N*-diethylbenzamide.**

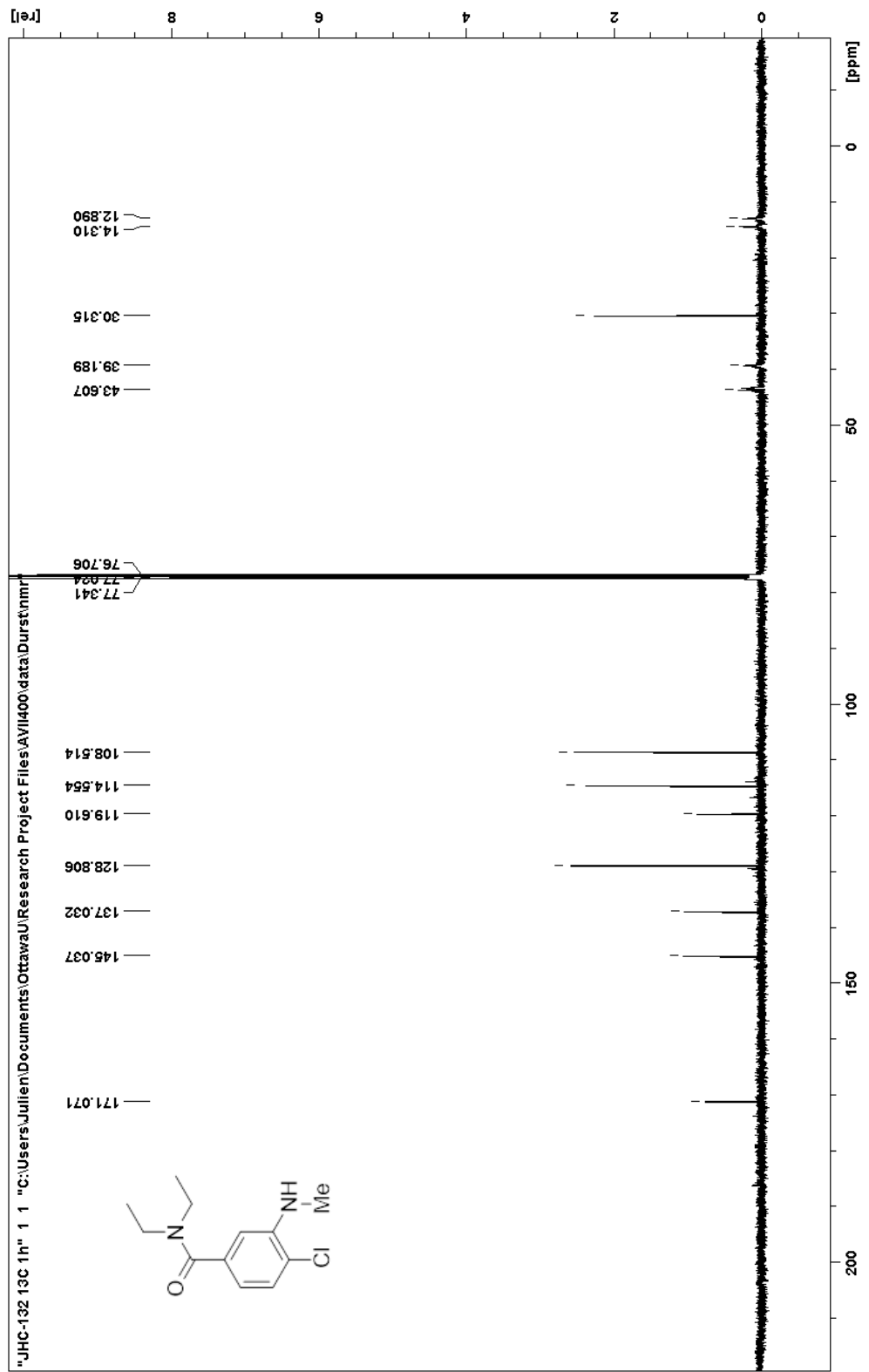


3-amino-4-chloro-*N,N*-diethylbenzamide (1.30 g, 5.73 mmol) was dissolved in toluene in a round bottom flask. Potassium carbonate powder (1.37 g, 9.91 mmol) was added, then dimethyl sulfate (0.55 mL, 5.81 mmol). The solution was stirred at reflux for a day, before adding additional dimethyl sulfate (0.35 mL, 3.70 mmol), and being refluxed for an additional day. After being cooled down to room temperature, the solution was immediately separated via silica gel column chromatography. The product was obtained as a yellow oil that crystallized overnight (0.51 g, 37%).

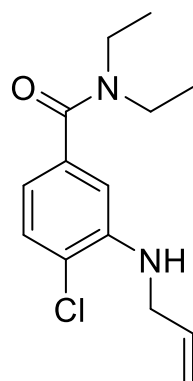
**<sup>1</sup>H NMR (400 MHz, CDCl<sub>3</sub>) δ, ppm:** 7.22 (d, J = 8.0 Hz, 1H), 6.60 (s, 1H), 6.58 (d, J = 8.0 Hz, 1H), 4.42 (br, 1H), 3.50 (br, 2H), 3.25 (br, 2H), 2.89 (s, 3H), 1.21 (br, 3H), 1.10 (br, 3H).

**<sup>13</sup>C NMR (400 MHz, CDCl<sub>3</sub>) δ, ppm:** 171.07, 145.04, 137.03, 128.81, 119.61, 114.55, 108.51, 43.61, 39.19, 30.32, 14.21, 12.89.





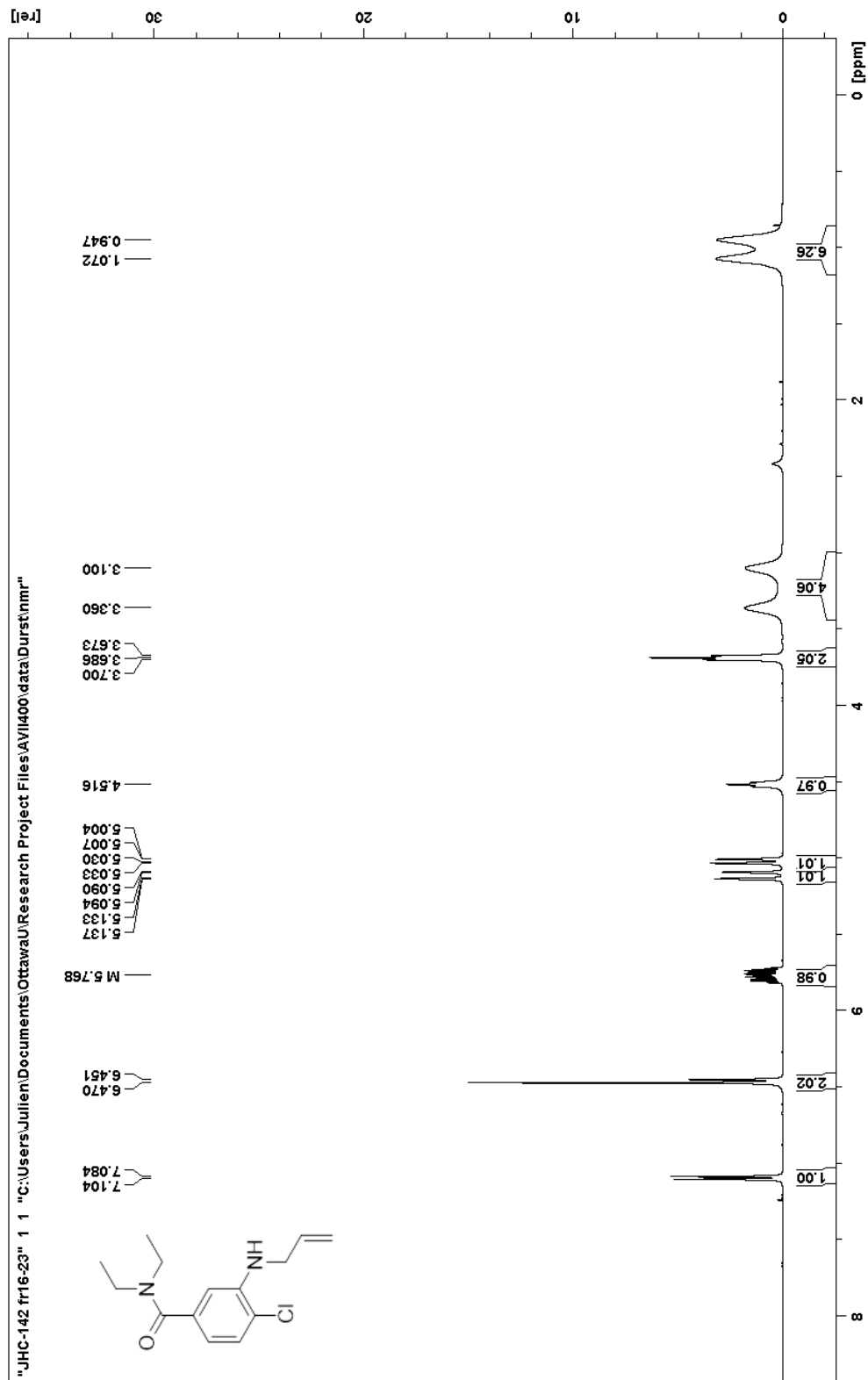
Preparation of 3-(*N*-2-propenylamino)-4-chloro-*N,N*-diethylbenzamide, **18**.



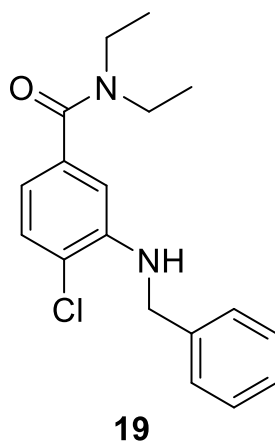
**18**

3-amino-4-chloro-*N,N*-diethylbenzamide (1.95 g, 8.60 mmol) was dissolved in toluene in a round bottom flask. Sodium carbonate powder (2.20 g, 20.7 mmol) was added, then allyl bromide (1.8 mL, 20.8 mmol). The solution was stirred at reflux for three days. After being cooled down to room temperature, the solution was immediately separated via silica gel column chromatography. The product was obtained as a yellow oil (0.29 g, 13%).

**<sup>1</sup>H NMR (400 MHz, CDCl<sub>3</sub>) δ, ppm:** 7.09 (d, *J* = 8.0 Hz, 1H), 6.47 (s, 1H), 6.46 (d, *J* = 8.0 Hz, 1H), 5.77 (m, 1H), 5.11 (dd, *J*<sub>1</sub> = 17.2 Hz, *J*<sub>2</sub> = 1.6 Hz, 1H), 5.02 (dd, *J*<sub>1</sub> = 10.4 Hz, *J*<sub>2</sub> = 1.2 Hz, 1H), 4.52 (s, 1H), 3.69 (t, *J* = 5.6 Hz, 2H), 3.36 (br, 2H), 3.10 (br, 2H), 1.07 (br, 3H), 0.95 (br, 3H).



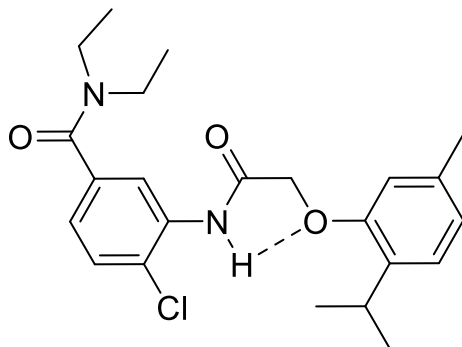
**Preparation of 3-(*N*-benzylamino)-4-chloro-*N,N*-diethylbenzamide, 19.**



3-amino-4-chloro-*N,N*-diethylbenzamide (0.65 g, 2.87 mmol) was dissolved in toluene (10 mL) in a round bottom flask. Potassium carbonate powder (0.38 g, 2.74 mmol) was added, then benzyl bromide (0.33 mL, 2.78 mmol). The solution was stirred at reflux until complete by TLC. After being cooled down to room temperature, the solution was immediately separated via silica gel column chromatography. A yellow oil was obtained, which was then recrystallized in hexanes and DCM. The product was obtained as a white solid (0.22 g, 24%).

A <sup>1</sup>H NMR was taken at the time to confirm the identity of the product, but was misplaced since

**Preparation of 3-(2-(2-isopropyl-5-methylphenoxy)acetamido)-4-chloro-*N,N*-diethyl benzamide, 4.**



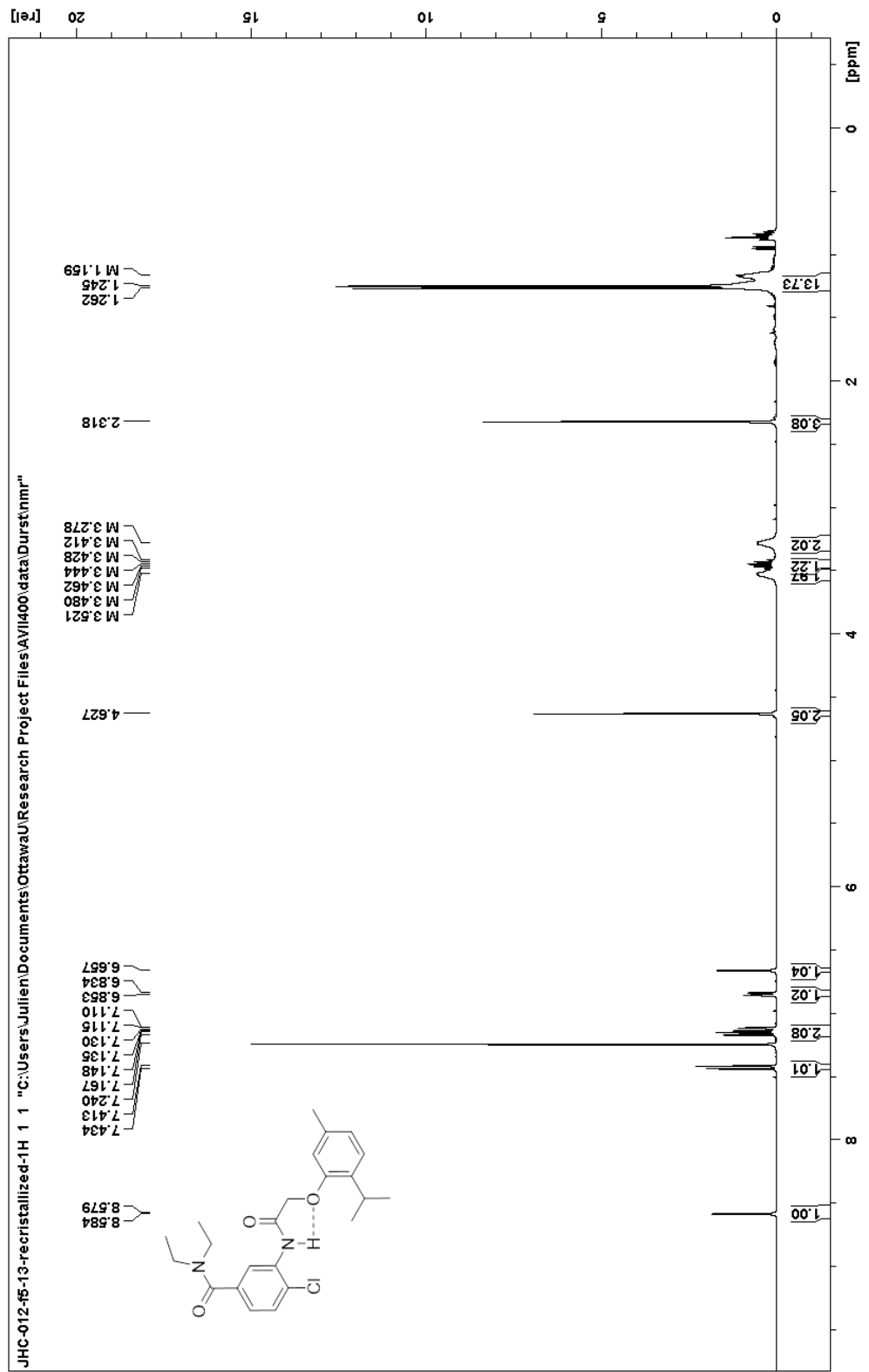
**4**

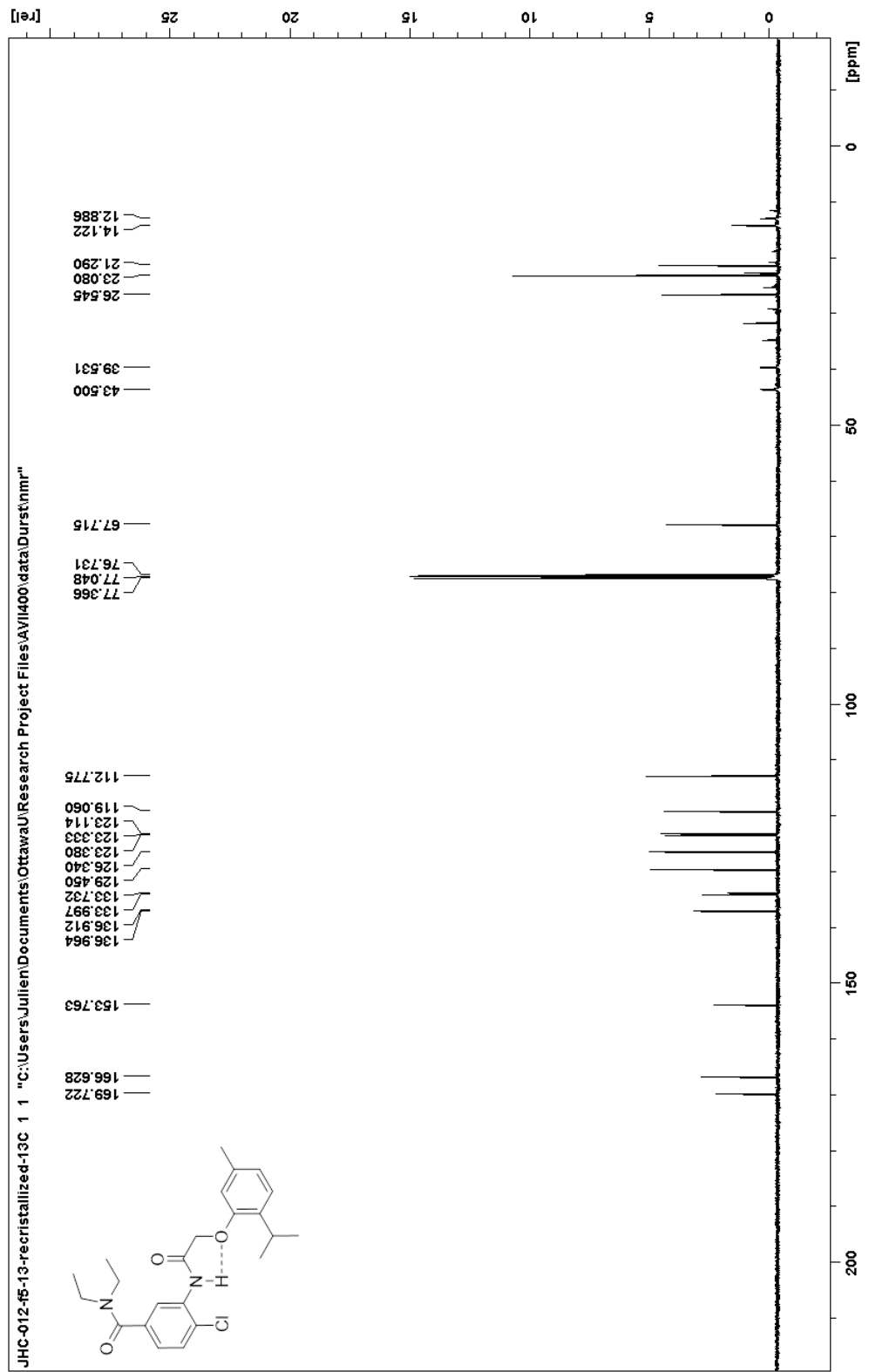
Thymol acetic acid (0.13 g, 0.62 mmol) was suspended in DCM (40 mL) in a round bottom flask. Oxalyl chloride (0.11 mL, 1.28 mmol) was subsequently added. The mixture was degassed with nitrogen, before beginning to heat the solution. DMF (5 drops) was added dropwise, bringing the solution to a boil. The solution was stirred at reflux for 1 hour, at 70°C. Afterwards, the solvent was evaporated in vacuo, and the solid was redissolved in DCM.

The acyl chloride solution was added slowly to a solution of 3-amino-4-chloro-*N,N*-diethyl benzamide (0.16 g, 0.71 mmol) and triethylamine (0.20 mL, 1.43 mmol) in DCM previously chilled in an ice bath. After resting for 30 minutes, the solution was washed twice with 5% HCl<sub>(aq)</sub> and twice with 5% NaOH<sub>(aq)</sub>. The organic layer was dried over MgSO<sub>4</sub>, filtered and evaporated to obtain the crude product. The product was isolated via column chromatography, then further purified via recrystallisation in a mixture of DCM and hexanes. The mass of finished product obtained was unfortunately lost.

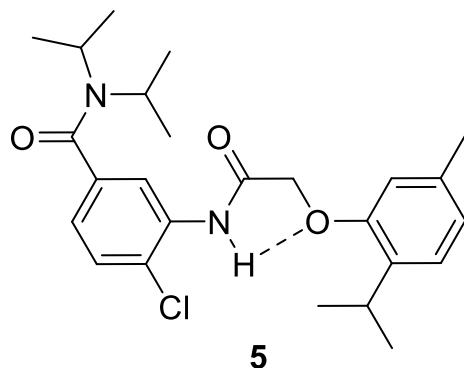
**<sup>1</sup>H NMR (400 MHz, CDCl<sub>3</sub>) δ, ppm:** 8.58 (d, *J* = 2.0 Hz, 1H), 7.42 (d, *J* = 8.4 Hz, 1H), 7.16 (d, *J* = 7.6 Hz, 1H), 7.12 (dd, *J*<sub>1</sub> = 8.0 Hz, *J*<sub>2</sub> = 2.0 Hz, 1H), 6.84 (d, *J* = 7.6 Hz, 1H), 6.66 (s, 1H), 4.63 (s, 2H), 3.52 (br, 2H), 3.44 (m, *J* = 7.2 Hz, 1H), 3.28 (br, 2H), 2.32 (s, 3H), 1.25 (d, *J* = 6.8 Hz, 6H), 1.20 (br, 6H).

**<sup>13</sup>C NMR (400 MHz, CDCl<sub>3</sub>) δ, ppm:** 169.72, 166.63, 153.76, 136.96, 136.91, 134.00, 133.73, 129.45, 126.34, 123.38, 123.33, 123.11, 119.06, 112.78, 67.72, 43.50, 39.53, 26.55, 23.08 (2C), 21.29, 14.12, 12.89.





**Preparation of 3-(2-(2-isopropyl-5-methylphenoxy)acetamido)-4-chloro-*N,N*-diisopropyl benzamide, 5.**



Thymol acetic acid (0.29 g, 1.4 mmol) was suspended in DCM (30 mL) in a round bottom flask. Oxalyl chloride (0.24 mL, 2.8 mmol) was subsequently added. The mixture was degassed with nitrogen, before beginning to heat the solution. DMF (5 drops) was added dropwise, bringing the solution to a boil. The solution was stirred at reflux for 1h 15 minutes, at 70°C. Afterwards, the solvent was evaporated in vacuo, and the solid was redissolved in 25 mL DCM. Only half (12.5 mL) of this new solution was used to prepare the final product, while the other half was kept for later use.

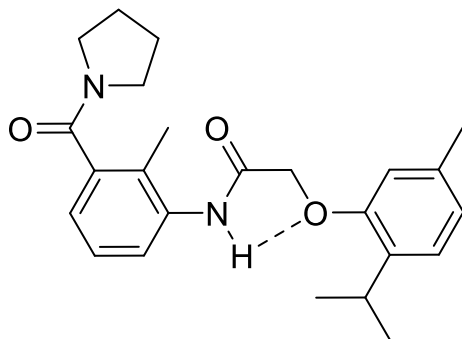
The acyl chloride solution was added slowly to a solution of 3-amino-4-chloro-*N,N*-diisopropyl benzamide (0.16 g, 0.63 mmol) and triethylamine (0.25 mL, 1.8 mmol) in DCM previously chilled in an ice bath. After resting for 30 minutes, the solution was washed twice with 5% HCl<sub>(aq)</sub> and twice with 5% NaOH<sub>(aq)</sub>. The organic layer was dried over MgSO<sub>4</sub>, filtered and evaporated to obtain the crude product. The product was isolated via column chromatography, then further purified via recrystallisation in a mixture of DCM and hexanes. The purified product was obtained as a fine beige powder (20.4 mg, 7%, mp: 176.4 - 176.5°C)

\*A small amount of residual ethyl acetate is visible in the <sup>1</sup>H spectrum.

**<sup>1</sup>H NMR (400 MHz, CDCl<sub>3</sub>) δ, ppm:** 7.41 (d, J = 8.0 Hz, 1H), 7.16 (d, J = 8.0 Hz, 1H), 7.07 (dd, J<sub>1</sub> = 8.0 Hz, J<sub>2</sub> = 1.6 Hz, 1H), 6.84 (d, J = 8.4 Hz, 1H), 6.66 (s, 1H), 4.62 (s, 2H), 3.87 (br, 2H), 3.50 (br, 2H), 2.32 (s, 3H), 1.51 (br, 6H), 1.25 (d, J = 6.8 Hz, 6H), 1.20 (br, 6H).



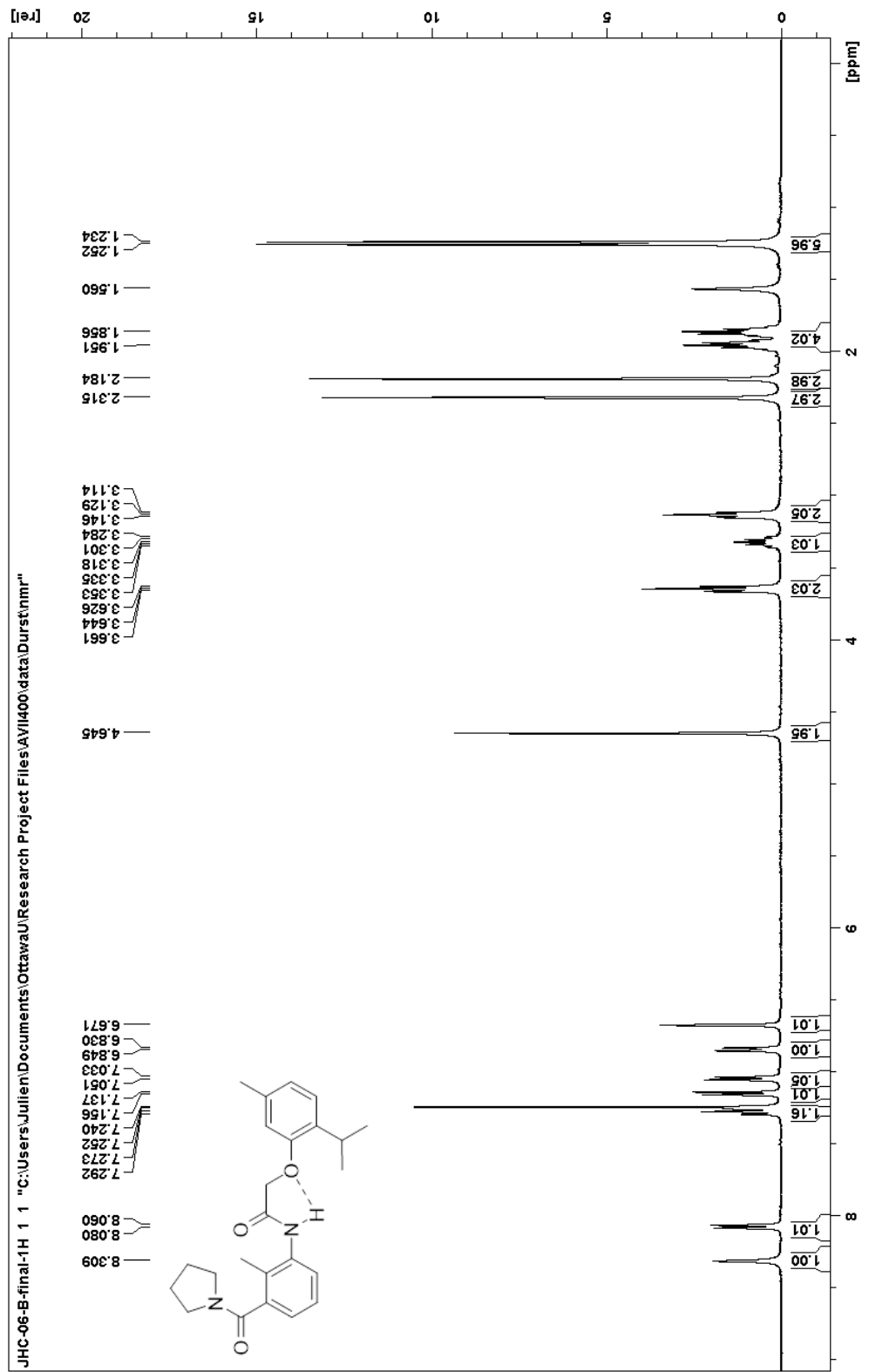
**Preparation of (3-(2-(2-isopropyl-5-methylphenoxy)acetamido)-2-methylphenyl)(pyrrolidin-1-yl)methanone, 14.**



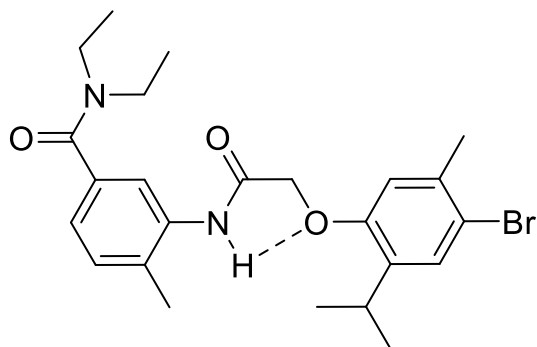
**14**

(3-amino-2-methylphenyl)(pyrrolidin-1-yl)methanone (0.10 g, 0.49 mmol) was dissolved in DCM with triethylamine (0.4 mL, 2.89 mmol) then chilled in an ice bath. Thymol acetic acid chloride was prepared by refluxing thymol acetic acid (0.256 g, 1.23 mmol), oxalyl chloride (0.3 mL, 3.50 mmol) and 5 drops of DMF, in DCM. The solution was heated at 60°C for 30 minutes. The solvent was evaporated and the intermediate was redissolved in a small amount of DCM, and cooled in the same ice bath. The acyl chloride solution was added dropwise to the amines. After resting for 30 minutes, the solution was washed twice with 5% HCl<sub>(aq)</sub>, then once with 5% NaOH<sub>(aq)</sub>. The organic layer was dried over MgSO<sub>4</sub>, filtered and evaporated to obtain the crude product. The product was purified via column chromatography to yield the solid product (18.2 mg, 9%).

**<sup>1</sup>H NMR (400 MHz, CDCl<sub>3</sub>) δ, ppm:** 8.31 (s, 1H), 8.07 (d, J = 8.0 Hz, 1H), 7.27 (t, J = 8.0 Hz, 1H), 7.15 (d, J = 7.6 Hz, 1H), 7.04 (d, J = 7.2 Hz, 1H), 6.84 (d, J = 7.6 Hz, 1H), 6.67 (s, 1H), 4.65 (s, 2H), 3.64 (t, J = 6.8 Hz, 2H), 3.32 (m, J = 6.8 Hz, 1H), 3.13 (t, J = 6.8 Hz, 2H), 2.32 (s, 3H), 2.18 (s, 3H), 1.90 (m, 4H), 1.24 (d, J = 7.2 Hz, 6H).



**Preparation of 3-(2-(4-bromo-2-isopropyl-5-methylphenoxy)acetamido)-*N,N*-diethyl-4-methylbenzamide.**

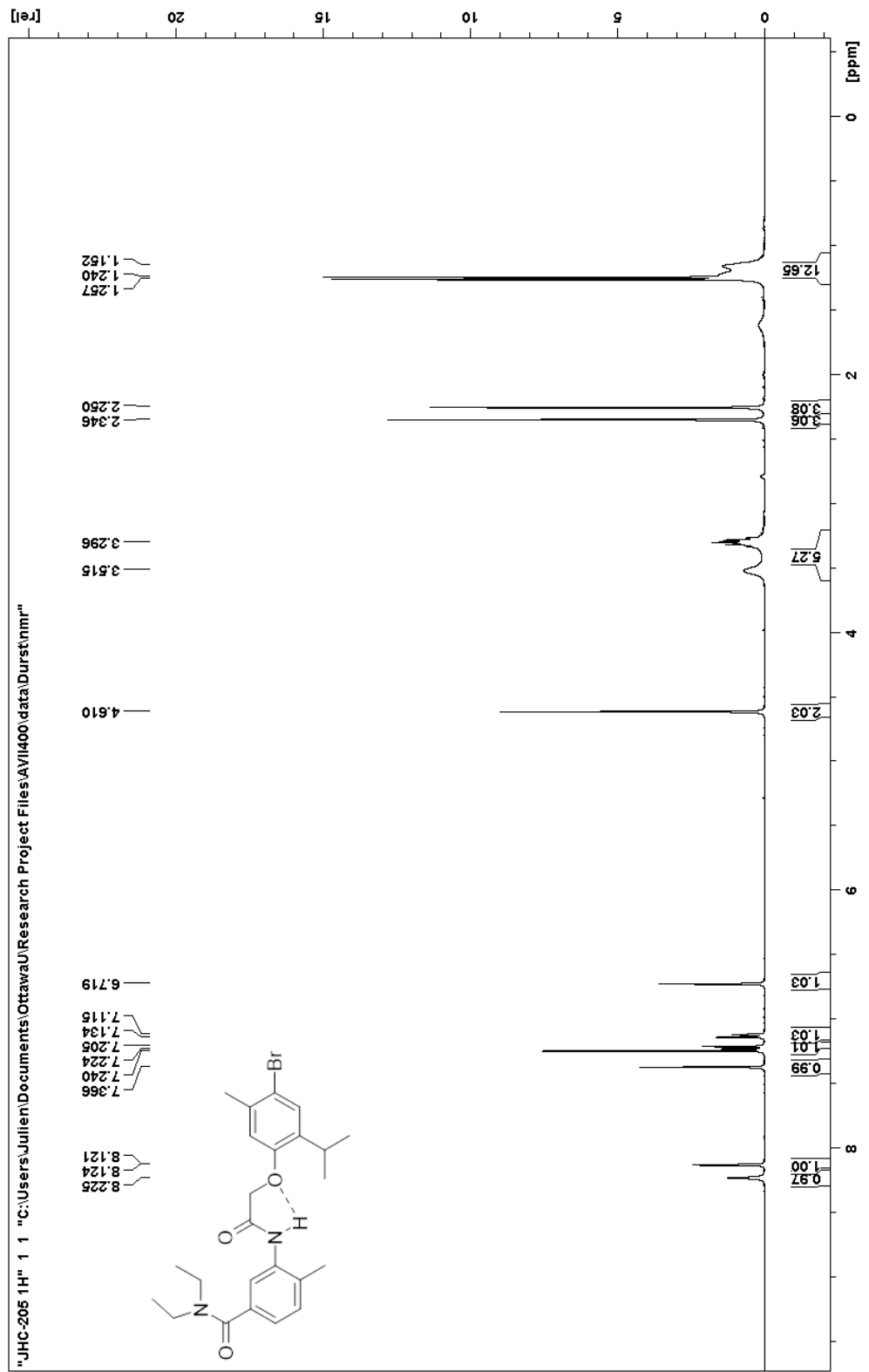


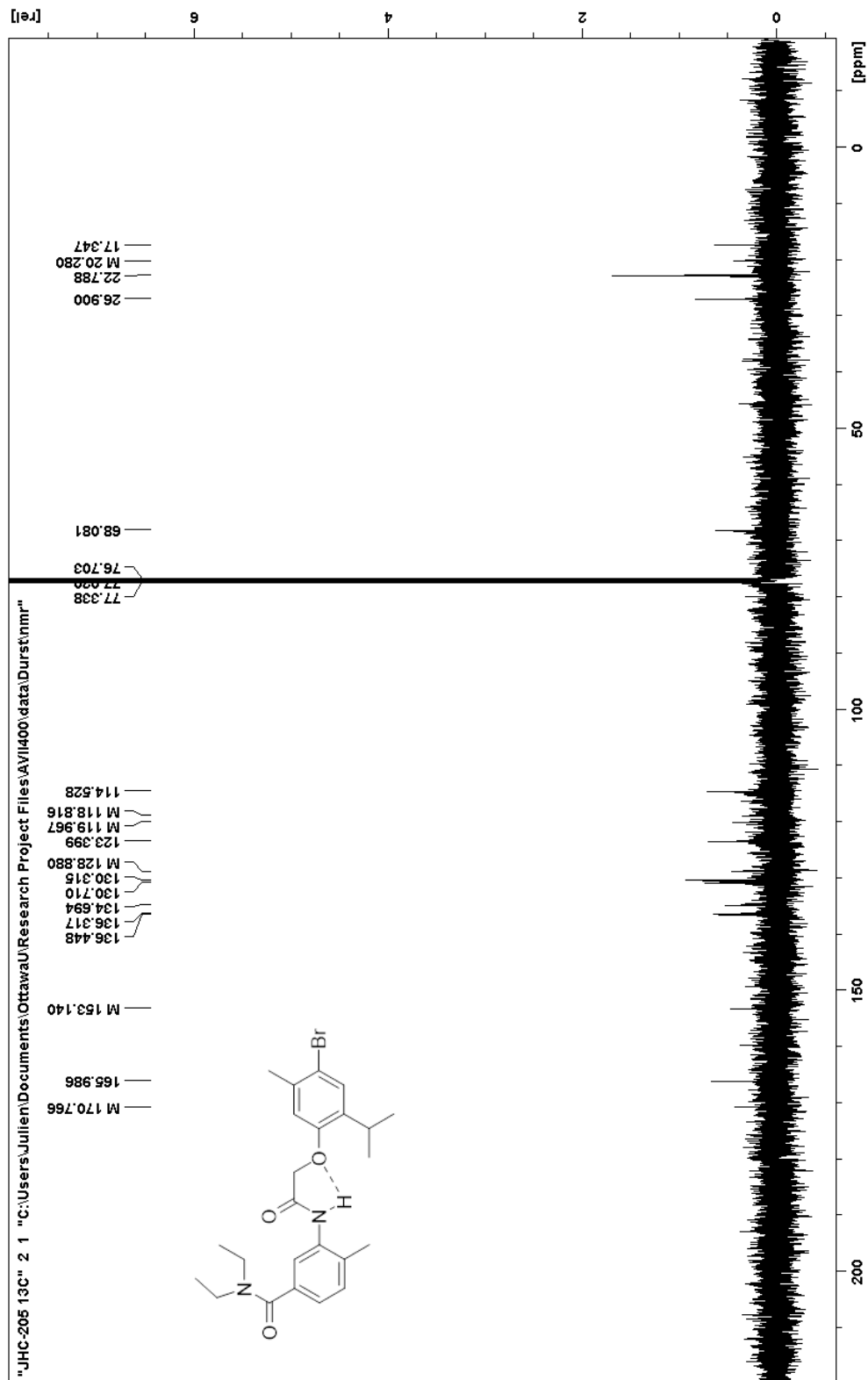
3-Amino-*N,N*-diethyl-4-methylbenzamide (1.01 g, 4.90 mmol) was dissolved in DCM with 2-(4-bromo-2-isopropyl-5-methylphenoxy)acetic acid (0.50 g, 1.74 mmol). DMAP (0.90 g, 7.37 mmol) and EDCI (0.90 g, 4.69 mmol) were subsequently added. The solution was left to sit overnight at room conditions with a rubber stopper. The next morning, the solution was washed once with 10% NaOH<sub>(aq)</sub> and once with 5% HCl<sub>(aq)</sub>, before drying over MgSO<sub>4</sub>, filtering by gravity and evaporating the solvent in vacuo. The crude product was obtained as a wet solid of poor quality (0.8 g). The crude product was dissolved in a mixture of warm DCM and hexanes, then placed in the freezer to solidify. Clear large crystals formed and were filtered by suction (0.13 g, 16%).

**<sup>1</sup>H NMR (400 MHz, CDCl<sub>3</sub>) δ, ppm:** 8.23 (s, 1H), 8.12 (d, *J* = 1.2 Hz, 1H), 7.37 (s, 1H), 7.21 (d, *J* = 7.6 Hz, 1H), 7.12 (dd, *J*<sub>1</sub> = 7.6 Hz, *J*<sub>2</sub> = 1.6 Hz, 1H), 6.72 (s, 1H), 4.61 (s, 2H), 3.41 (br, 4H), 3.29 (m, 1H), 2.35 (s, 3H), 2.25 (s, 3H), 1.25 (d, *J* = 6.8 Hz, 6H), 1.19 (br, 6H).

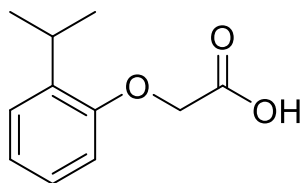
**<sup>13</sup>C NMR (400 MHz, CDCl<sub>3</sub>) δ, ppm:** 170.77, 165.99, 153.14, 136.45, 136.32, 134.69, 130.71, 130.32, 128.88, 123.40, 119.97, 118.82, 114.53, 68.08, 26.90, 22.79 (2C), 20.28, 17.35.

\*The low solubility of the product made the naturally faint diethylamine signals, and some of the quaternary carbons, very difficult to identify with certainty.





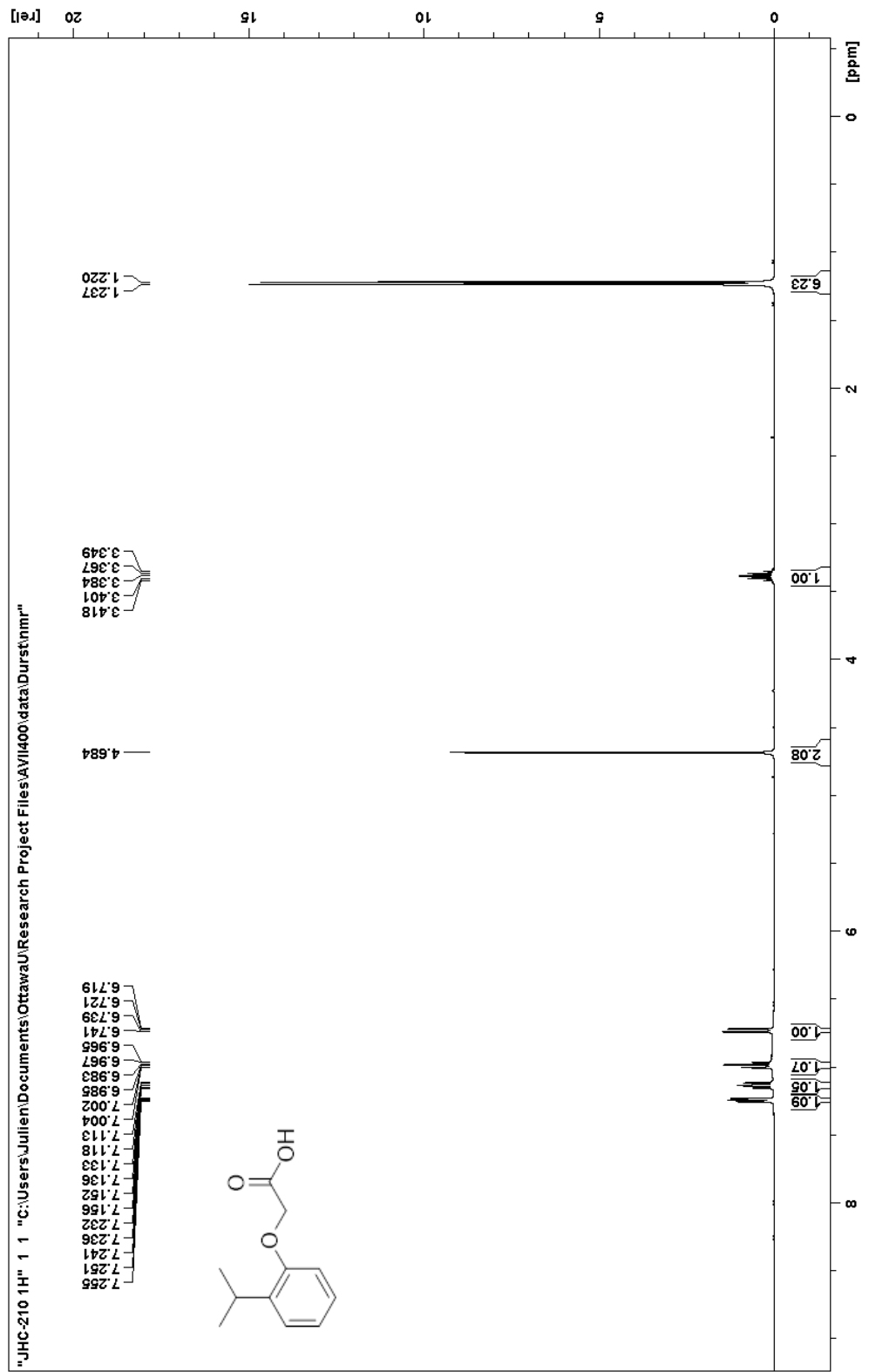
### Preparation of 2-(2-isopropylphenoxy)acetic acid.

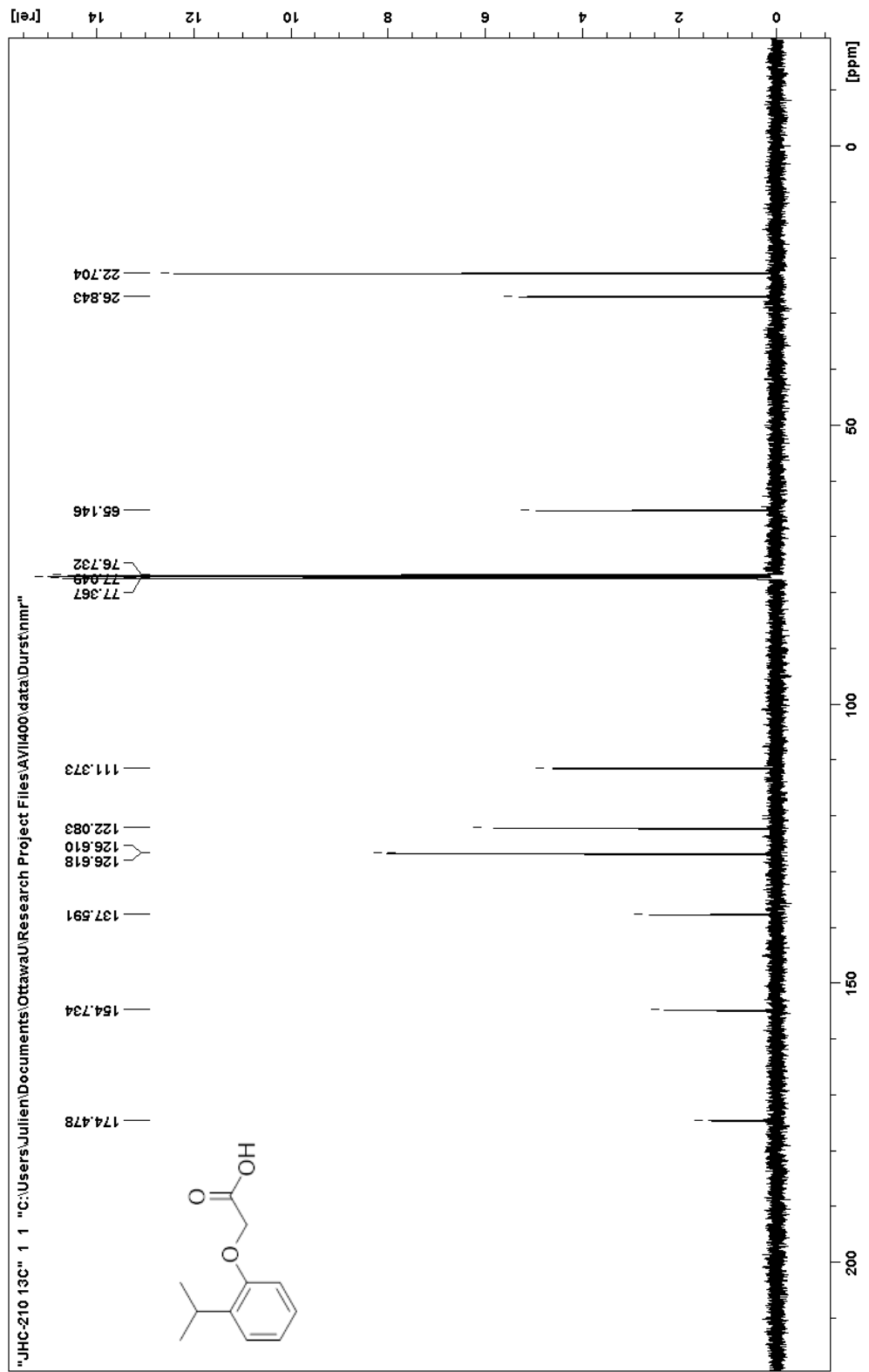


o-Isopropylphenol (13.61 g, 100 mmol) and chloroacetic acid (10.33 g, 110 mmol) were dissolved in a solution of NaOH (8.80 g, 220 mmol) in distilled water. The solution was stirred at reflux for several days at 100°C in an oil bath. A 10% sodium carbonate solution was added before washing with DCM. The aqueous phase obtained was acidified with concentrated HCl added dropwise to precipitate the desired product, which was then isolated via suction filtration. Yielded the product (18.23 g, 94%) as a white fluffy solid.

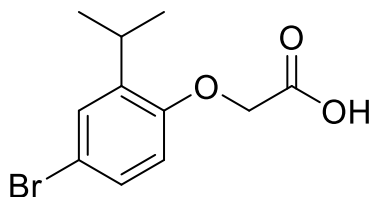
**<sup>1</sup>H NMR (400 MHz, CDCl<sub>3</sub>) δ, ppm:** 7.24 (dd,  $J_1 = 7.6$  Hz,  $J_2 = 1.6$  Hz, 1H), 7.13 (dt,  $J_1 = 8.0$  Hz,  $J_2 = 1.6$  Hz, 1H), 6.98 (dt,  $J_1 = 7.6$  Hz,  $J_2 = 0.8$  Hz, 1H), 6.73 (dd,  $J_1 = 8.0$  Hz,  $J_2 = 0.8$  Hz, 1H), 4.68 (s, 2H), 3.38 (m,  $J = 6.8$  Hz, 1H), 1.23 (d,  $J = 6.8$  Hz, 6H).

**<sup>13</sup>C NMR (400 MHz, CDCl<sub>3</sub>) δ, ppm:** 174.48, 154.73, 137.59, 126.62, 126.61, 122.08, 111.37, 65.15, 26.84, 22.70.



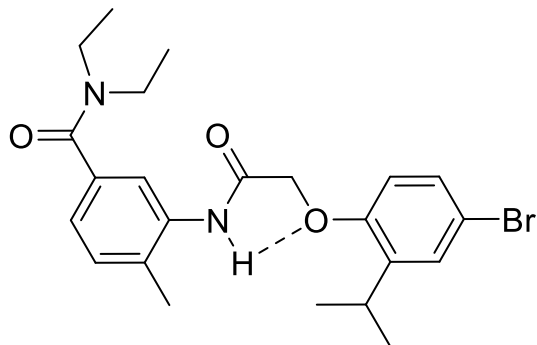


**Preparation of 2-(4-bromo-2-isopropylphenoxy)acetic acid.**



2-(2-isopropylphenoxy)acetic acid (10.42 g, 53.66 mmol), *N*-bromosuccinimide (9.55 g, 53.66 mmol) and *p*-toluenesulfonic acid (2.05 g, 10.78 mmol) were dissolved in DCM. The solution was stirred at room conditions for two days. Afterwards, the solution was washed with water, then dried over  $\text{MgSO}_4$ , filtered and evaporated in vacuo. Crude product was obtained as an orange paste (5.9 g). This paste was purified via recrystallization in a DCM/hexane mixture, and further washed with water. A white dry solid was recovered via suction filtration (0.75 g, 5%). A large amount of product was left behind during the purification process to obtain pure product.

Preparation of 3-(2-(4-bromo-2-isopropylphenoxy)acetamido)-*N,N*-diethyl-4-methylbenzamide.



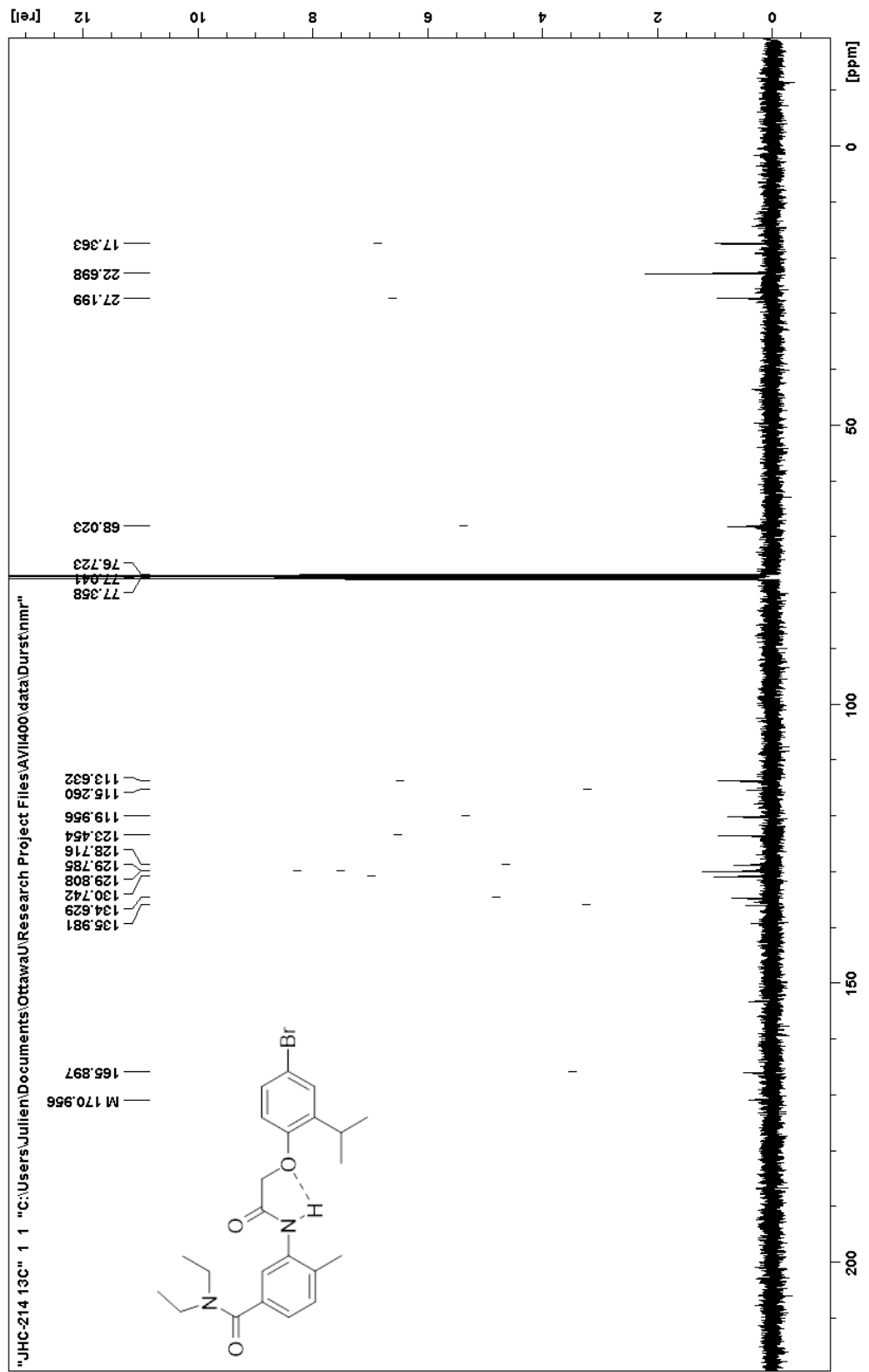
2-(4-bromo-2-isopropylphenoxy)acetic acid (0.75 g, 2.75 mmol), 3-amino-4-methyl-*N,N*-diethylbenzamide (0.57 g, 2.76 mmol), DMAP (0.34 g, 2.78 mmol) and EDCI (0.52 g, 3.35 mmol) were mixed together in a round bottom flask with DCM. The solution was stirred at room conditions overnight with a stopper. The next morning, the solution was washed once with 10% NaOH<sub>(aq)</sub> and once with 5% HCl<sub>(aq)</sub>, before drying over MgSO<sub>4</sub>, filtering by gravity and evaporating the solvent in vacuo. The product was obtained as a white powder (0.21 g, 17 %, mp: 116.5 - 118.0°C).

<sup>1</sup>H NMR (400 MHz, CDCl<sub>3</sub>) δ, ppm: 8.22 (br, 1H), 8.11 (d, J = 1.2 Hz, 1H), 7.36 (d, J = 2.4 Hz, 1H), 7.29 (dd, J<sub>1</sub> = 8.8 Hz, J<sub>2</sub> = 2.4 Hz, 1H), 7.21 (d, J = 7.6 Hz, 1H), 7.12 (dd, J<sub>1</sub> = 7.6 Hz, J<sub>2</sub> = 1.6 Hz, 1H), 6.73 (d, J = 8.8 Hz, 1H), 4.62 (s, 2H), 3.51 (br, 2H), 3.34 (m, 1H), 3.30 (br, 2H), 2.25 (s, 3H), 1.26 (d, J = 6.8 Hz, 6H), 1.20 (br, 6H).

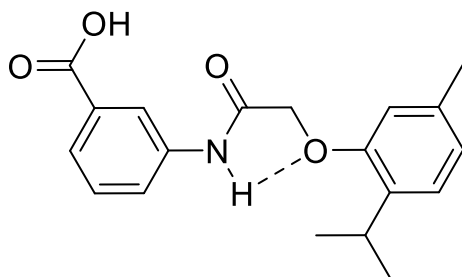
<sup>13</sup>C NMR (400 MHz, CDCl<sub>3</sub>) δ, ppm: 170.96, 165.90, 135.98, 134.63, 130.74, 129.81, 129.79, 128.72, 123.45, 119.96, 115.26, 113.63, 68.02, 27.20, 22.70 (2C), 17.36.

\*The solubility of the compound was too low for the diethylamine peaks to be visible by 13C NMR.





**Preparation of *N*-(3-carboxyphenyl)-2-(2-isopropyl-5-methyl)phenoxyacetamide.**

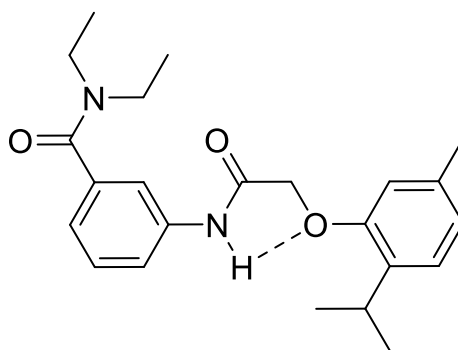


Thymol acetic acid (3.07 g, 14.70 mmol) was suspended in DCM (30 mL) in a round bottom flask. Oxalyl chloride (3.8 mL, 44.3 mmol) was added next. After heating gently in an oil bath, 5 drops of DMF were added, bringing the mixture to a boil. The solution was stirred at reflux for an hour. As solid material was still visible by this point, an additional quantity of oxalyl chloride was added (3.6 mL, 41.9 mmol). Reflux was continued for an additional hour.

A second solution of methyl 3-aminobenzoate (1.70 g, 11.2 mmol) in DCM was prepared, to which triethylamine (6.0 mL, 43.0 mmol) was added. This solution was cooled in an ice bath. The acyl chloride solution was cooled, then added slowly to the amines via glass pipette. Afterwards, water was added to the solution, which was washed twice with 5% HCl<sub>(aq)</sub>, dried with MgSO<sub>4</sub>, filtered and evaporated. A crude product was obtained as a brown oil (2.74 g), which solidified after roughly half an hour at room conditions. This product was purified by column chromatography and recrystallisation in a mixture of hexanes and DCM. The intermediate product was obtained by suction filtration as a white solid (1.07 g, 28%).

This intermediate (0.67 g, 1.96 mmol) was deprotected by dissolving it methanol (30 mL) with Potassium hydroxide (0.51 g, 9.09 mmol). The solution was stirred at reflux in an oil bath at 70°C for 9 hours. The solvent was mostly evaporated to facilitate the extraction of leftover starting material. 10% NaOH<sub>(aq)</sub> was added and the solution was washed once with DCM. The product was obtained by acidifying the aqueous layer with concentrated HCl, then suction filtration. The product was obtained as a white solid (0.43 g, 67%). The overall yield for both steps was 19%.

**Preparation of 3-(2-(2-isopropyl-5-methylphenoxy)acetamido)-*N,N*-diethyl benzamide, 13.**

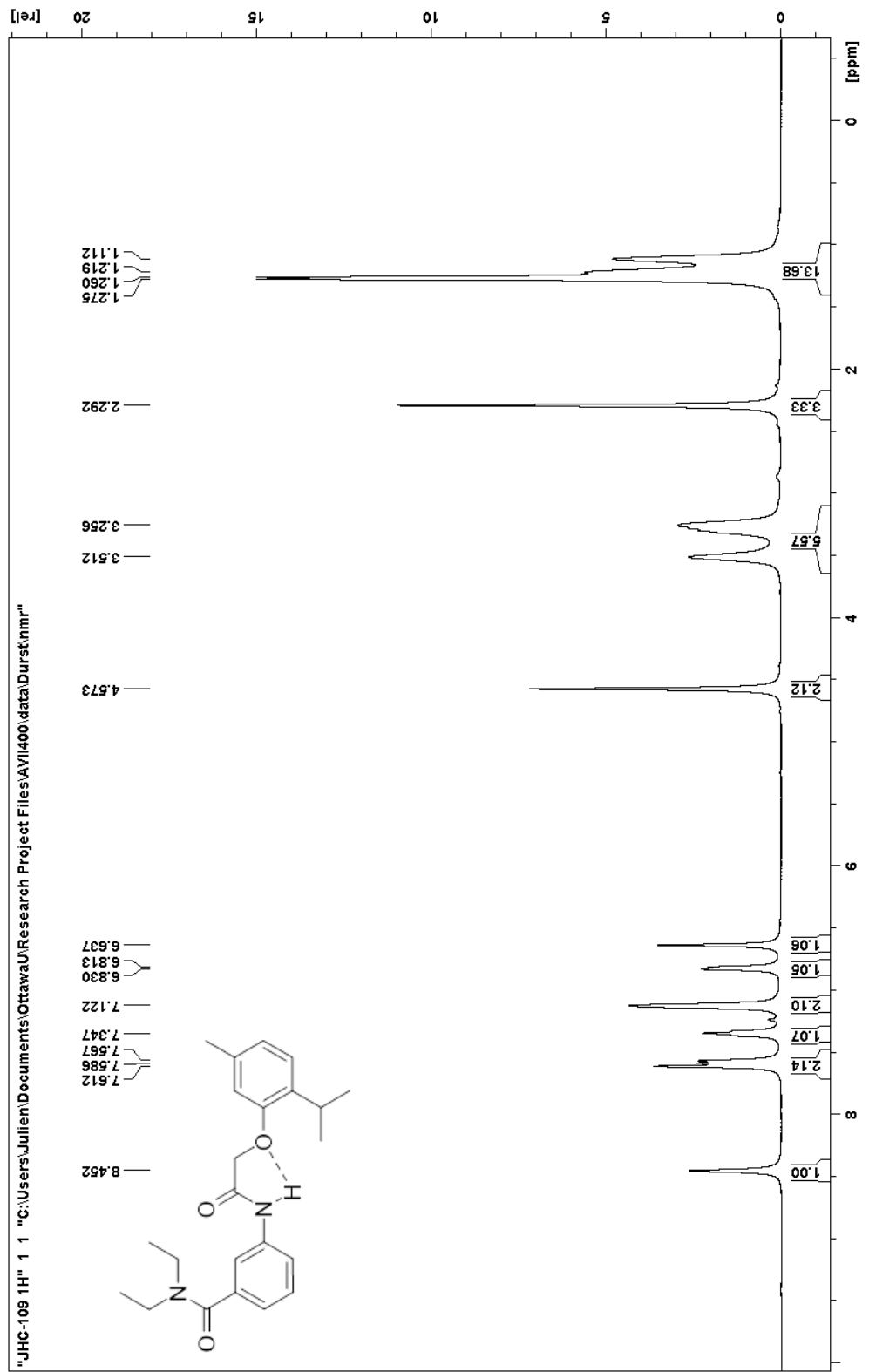


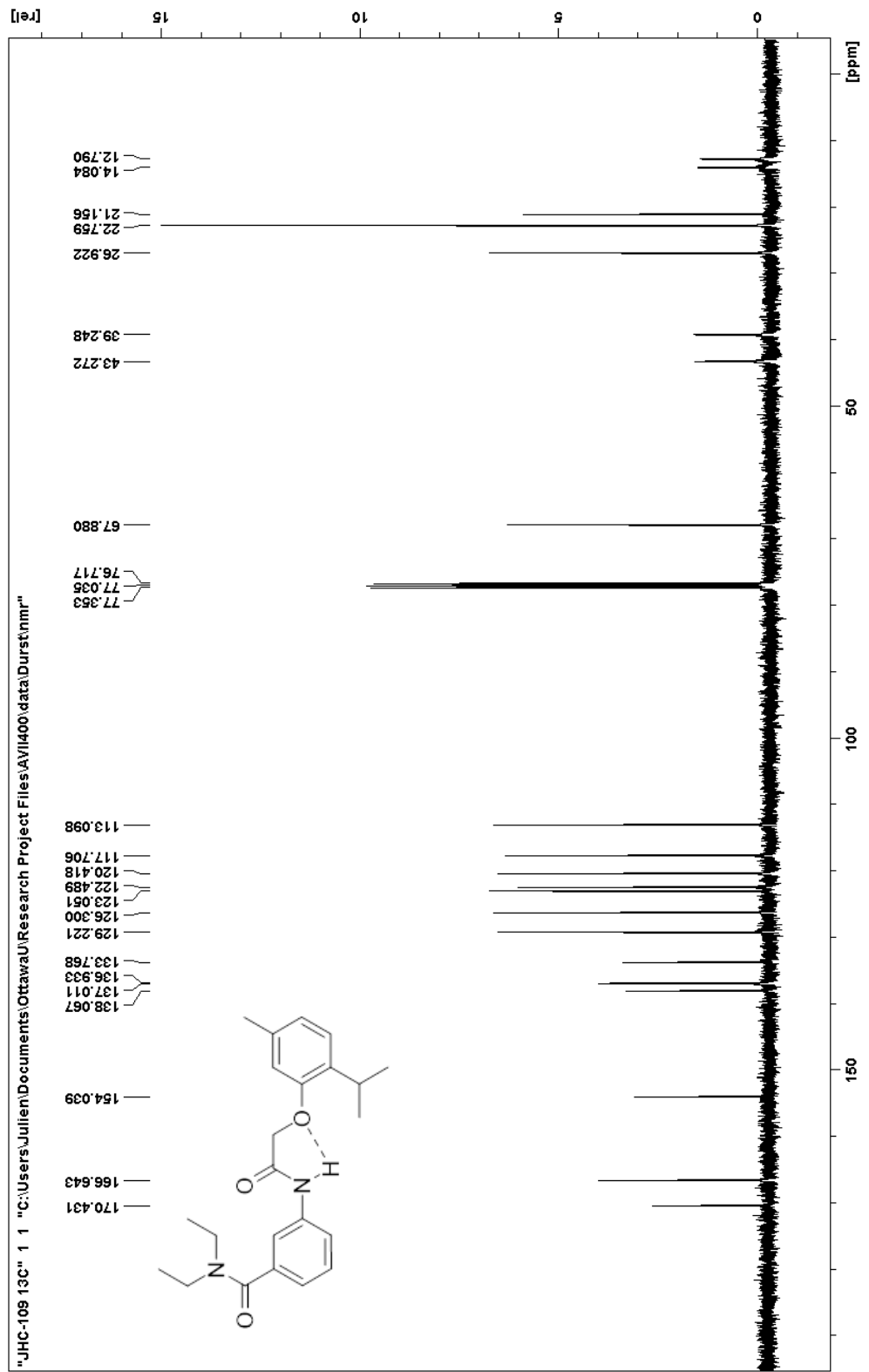
*N*-(3-carboxyphenyl)-2-(2-isopropyl-5-methyl)phenoxyacetamide (0.43 g, 1.31 mmol) was dissolved in DCM (15 mL) with oxalyl chloride (0.35 mL, 4.08 mmol). 3 drops of DMF were added, and the solution was placed in an oil bath at 70°C to reflux for an hour. As the reaction had not visually progressed, an additional amount (0.50 mL, 5.83 mmol) of oxalyl chloride was added. The solution was allowed an additional hour at reflux. Afterwards, the solvent was evaporated in vacuo, and a small amount of DCM was added to dissolve the solid.

Meanwhile, a solution of diethylamine (2.0 mL, 19.3 mmol) in DCM was prepared, and cooled in an ice bath. The acyl chloride solution was cooled, then added slowly to the amines via a glass pipette. After letting the mixture sit 30 minutes at room temperature, water was added. The solution was extracted with DCM. The organic layer was then washed once with 10% NaOH-<sub>(aq)</sub>, then dried over MgSO<sub>4</sub>, filtered and evaporated. A yellow oil was obtained, which was recrystallized in a mixture of DCM and hexanes. The product was obtained by suction filtration as white shiny flakes (0.16 g, 42%, mp: 108.9 - 110.4°C).

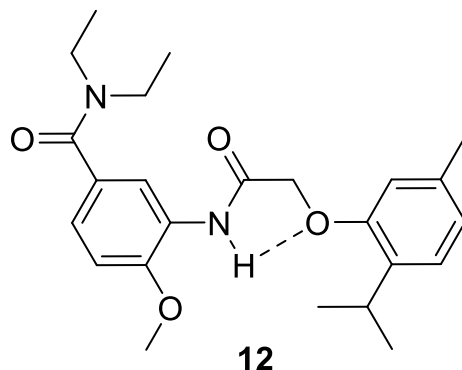
**<sup>1</sup>H NMR (400 MHz, CDCl<sub>3</sub>) δ, ppm:** 8.45 (br, 1H), 7.61 (s, 1H), 7.58 (d, *J* = 7.6 Hz, 1H), 7.35 (s, 1H), 7.12 (s, 2H), 6.82 (d, *J* = 6.8 Hz, 1H), 6.64 (s, 1H), 4.57 (s, 2H), 3.51 (br, 2H), 3.26 (br, 3H), 2.29 (s, 3H), 1.27 (d, *J* = 6.0 Hz, 6H), 1.22 (br, 3H), 1.11 (br, 3H).

**<sup>13</sup>C NMR (400 MHz, CDCl<sub>3</sub>) δ, ppm:** 170.43, 166.64, 154.04, 138.07, 137.01, 136.93, 133.77, 129.22, 126.30, 123.05, 122.49, 120.42, 117.71, 113.10, 67.88, 43.27, 39.25, 26.92, 22.76 (2C), 21.16, 14.08, 12.79.





**Preparation of 3-(2-(2-isopropyl-5-methylphenoxy)acetamido)-4-methoxy-*N,N*-diethylbenzamide, 12.**

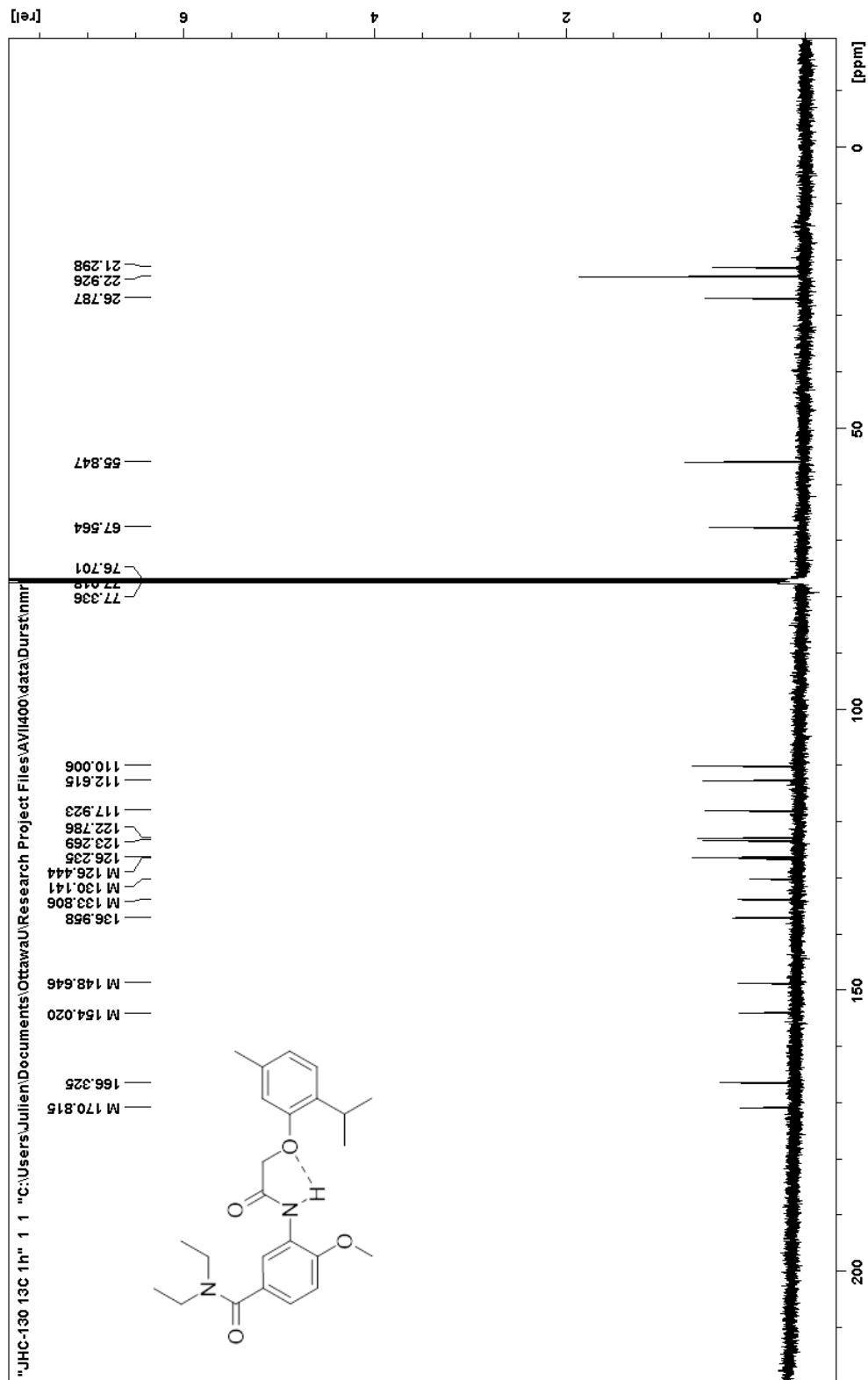


3-amino-4-methoxy-*N,N*-diethylbenzamide (0.15 g, 0.67 mmol) was dissolved in DCM with triethylamine (0.3 mL, 2.15 mmol) and cooled in an ice bath. A prepared solution of thymol acetic acid in DCM (1 mmol/mL, 0.8 mL, 0.8 mmol) was then added slowly via syringe. The mixture was left to sit at room conditions for 30 minutes, before adding water. The solution was then extracted with DCM. The organic layer was washed once with 5% HCl (aq), then dried over MgSO<sub>4</sub>, filtered and evaporated. The crude solid obtained was recrystallised multiple times in a mixture of DCM and hexanes. The product was obtained via suction filtration as a white solid (0.02 g, 7%).

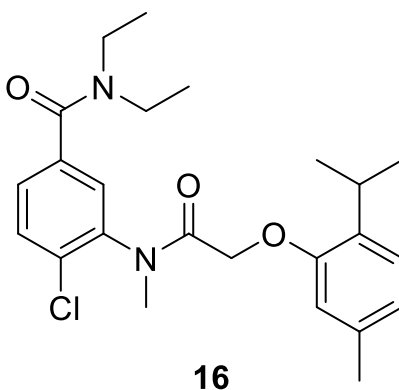
**<sup>1</sup>H NMR (400 MHz, CDCl<sub>3</sub>) δ, ppm:** 9.14 (br, 1H), 8.55 (d, *J* = 2.4 Hz, 1H), 7.18 (dd, *J*<sub>1</sub> = 8.4 Hz, *J*<sub>2</sub> = 2.0 Hz, 1H), 7.15 (d, *J* = 7.6 Hz, 1H), 6.91 (d, *J* = 8.4 Hz, 1H), 6.83 (d, *J* = 7.6 Hz, 1H), 6.65 (s, 1H), 4.59 (s, 2H), 3.89 (s, 3H), 3.42 (br, 5H), 2.32 (s, 3H), 1.29 (d, *J* = 6.8 Hz, 6H), 1.20 (br, 6H).

**<sup>13</sup>C NMR (400 MHz, CDCl<sub>3</sub>) δ, ppm:** 170.82, 166.33, 154.02, 148.65, 136.96, 133.81, 130.14, 126.44, 126.24, 123.27, 122.79, 117.92, 112.62, 110.00, 67.56, 55.85, 26.79, 22.93 (2C), 21.30.





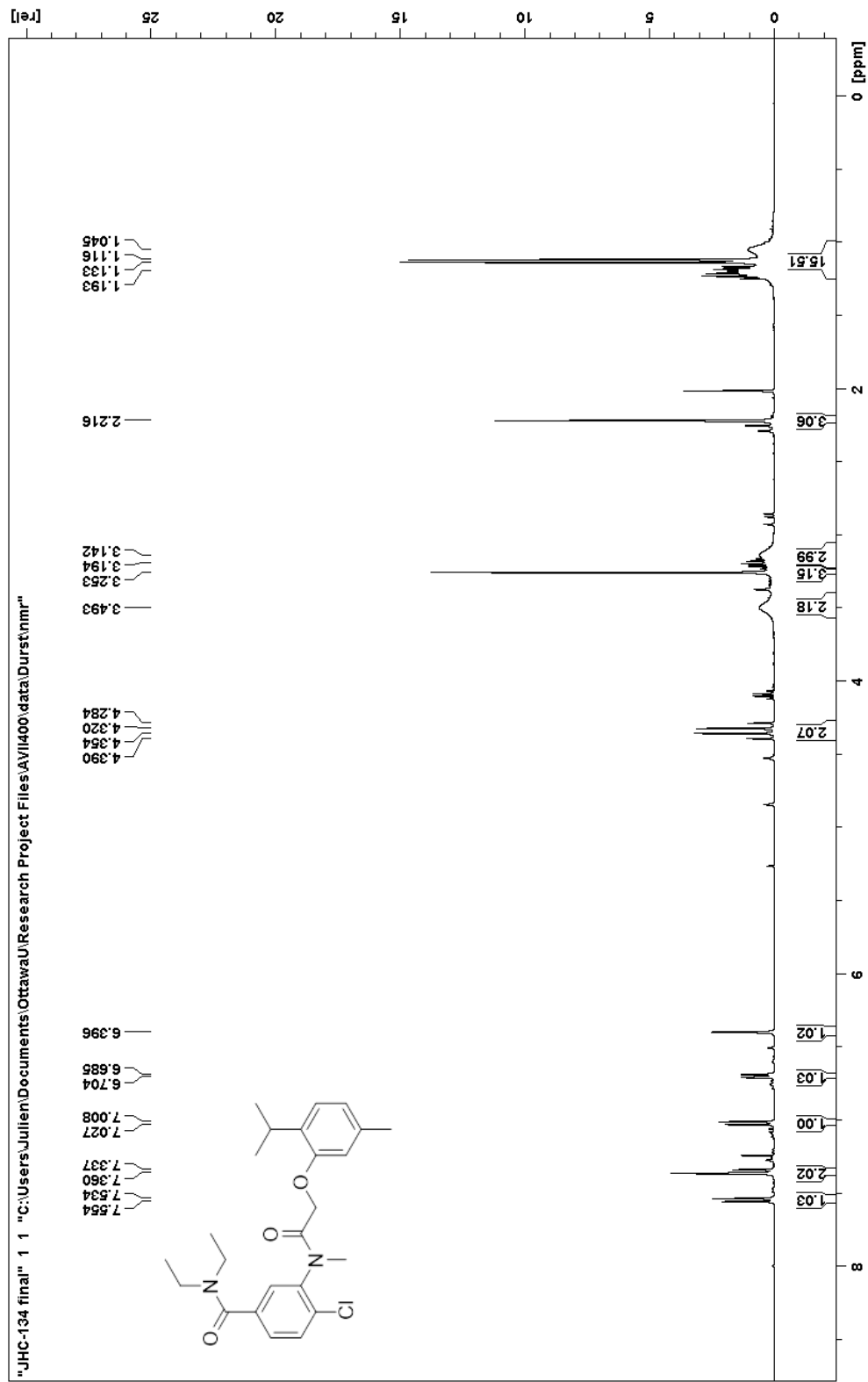
### Preparation of compound 16.

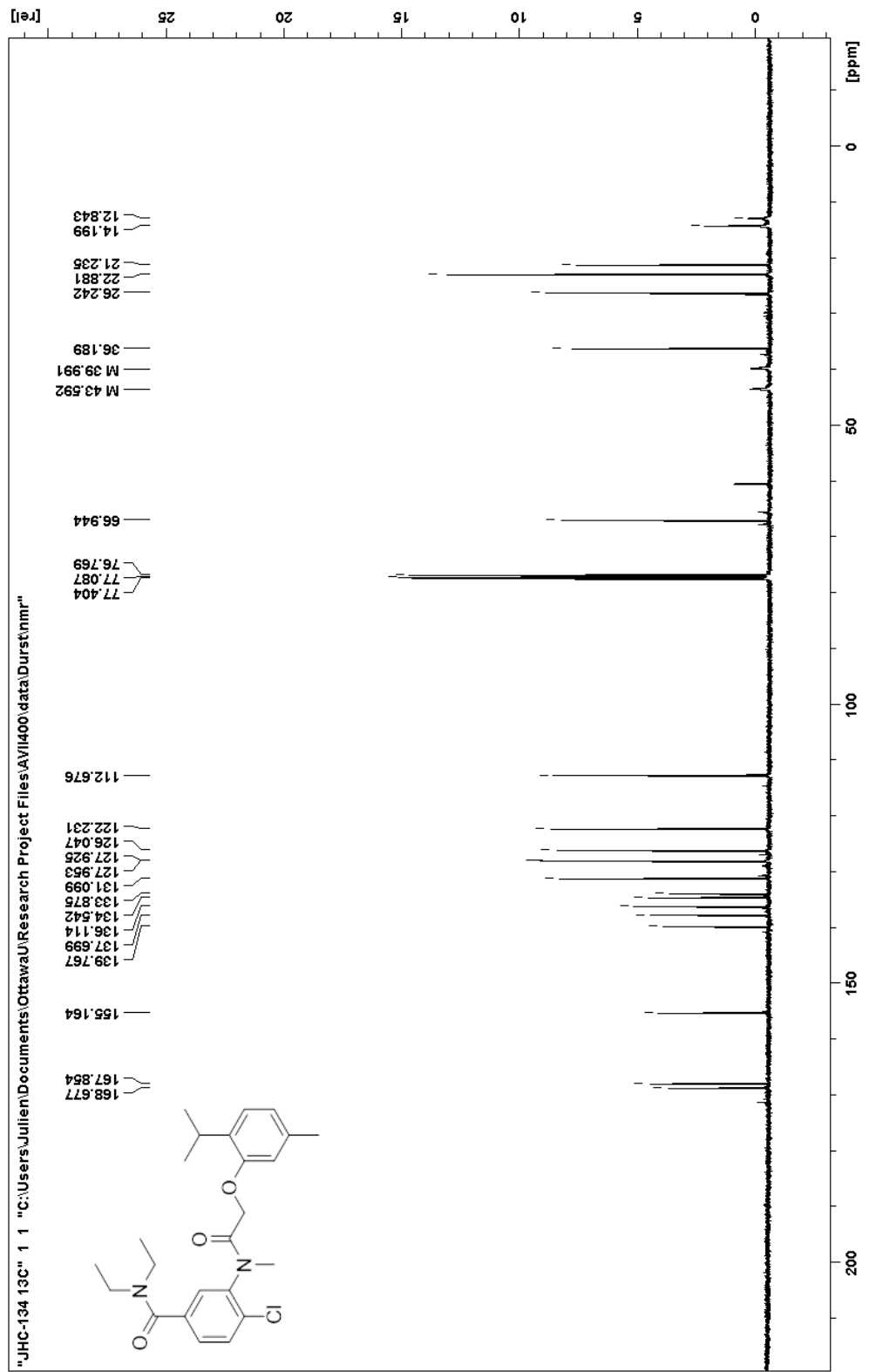


3-(*N*-methylamino)-4-chloro-*N,N*-diethylbenzamide (0.26 g, 1.08 mmol) and thymol acetic acyl chloride (0.37 g, 1.63 mmol) were dissolved in DCM in separate flasks. Triethylamine (0.20 mL, 1.43 mmol) was added to the solution containing the amine substrate. Both flasks were chilled in an ice bath, then the acyl chloride was slowly added to the solution of amines. The combined mixture sat at room conditions for 30 minutes, after which it was quenched with water. The solution was washed once with 10% NaOH<sub>(aq)</sub>, once with 5% HCl<sub>(aq)</sub>, dried over MgSO<sub>4</sub>, filtered and evaporated. The crude product was isolated and purified by two separate column chromatographies. The product was sent for testing before the weight and yield were measured.

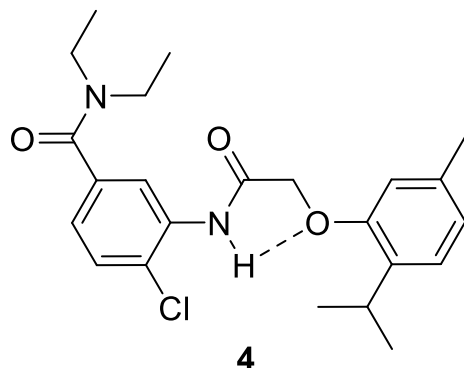
<sup>1</sup>H NMR (400 MHz, CDCl<sub>3</sub>) δ, ppm: 7.54 (d, J = 8.0 Hz, 1H), 7.36 (s, 1H), 7.35 (d, J = 9.2 Hz, 1H), 7.01 (d, J = 7.6 Hz, 1H), 6.69 (d, J = 7.6 Hz, 1H), 6.40 (s, 1H), 4.34 (q, J = 14.4 Hz, 2H), 3.49 (br, 2H), 3.25 (s, 3H), 3.19 (m, 1H), 3.14 (br, 2H), 2.22 (s, 3H), 1.19 (br, 3H), 1.12 (d, J = 6.8 Hz, 6H), 1.05 (br, 3H).

<sup>13</sup>C NMR (400 MHz, CDCl<sub>3</sub>) δ, ppm: 168.68, 167.85, 155.16, 139.77, 137.70, 136.11, 134.54, 133.88, 131.10, 127.95, 127.93, 126.05, 122.23, 112.68, 66.94, 43.59, 39.99, 36.19, 26.24, 22.88 (2C), 21.24, 14.20, 12.84.





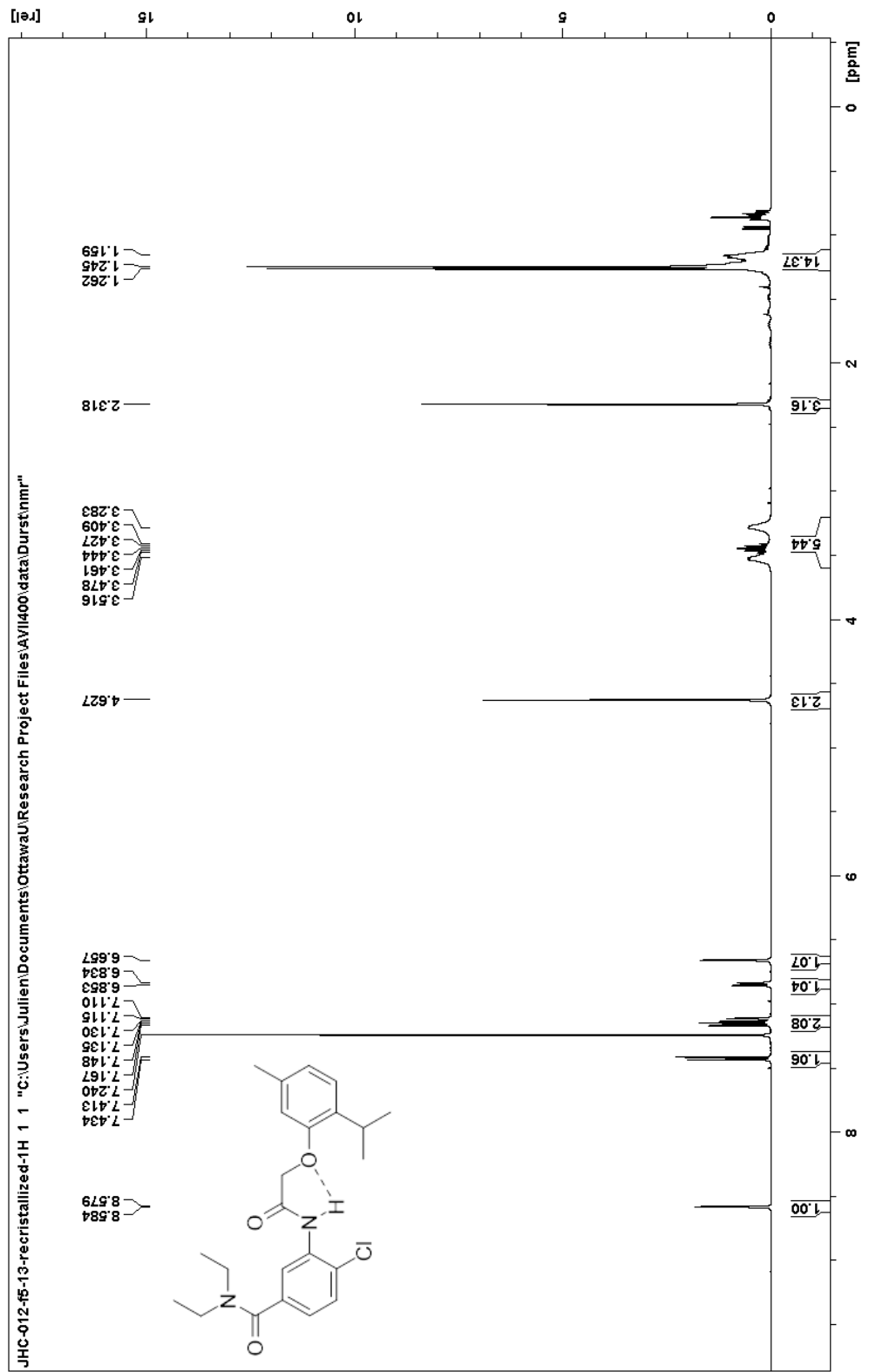
**Preparation of 3-(2-(2-isopropyl-5-methylphenoxy)-*N*-methylacetamido)-4-chloro-*N,N*-diethylbenzamide, 4.**

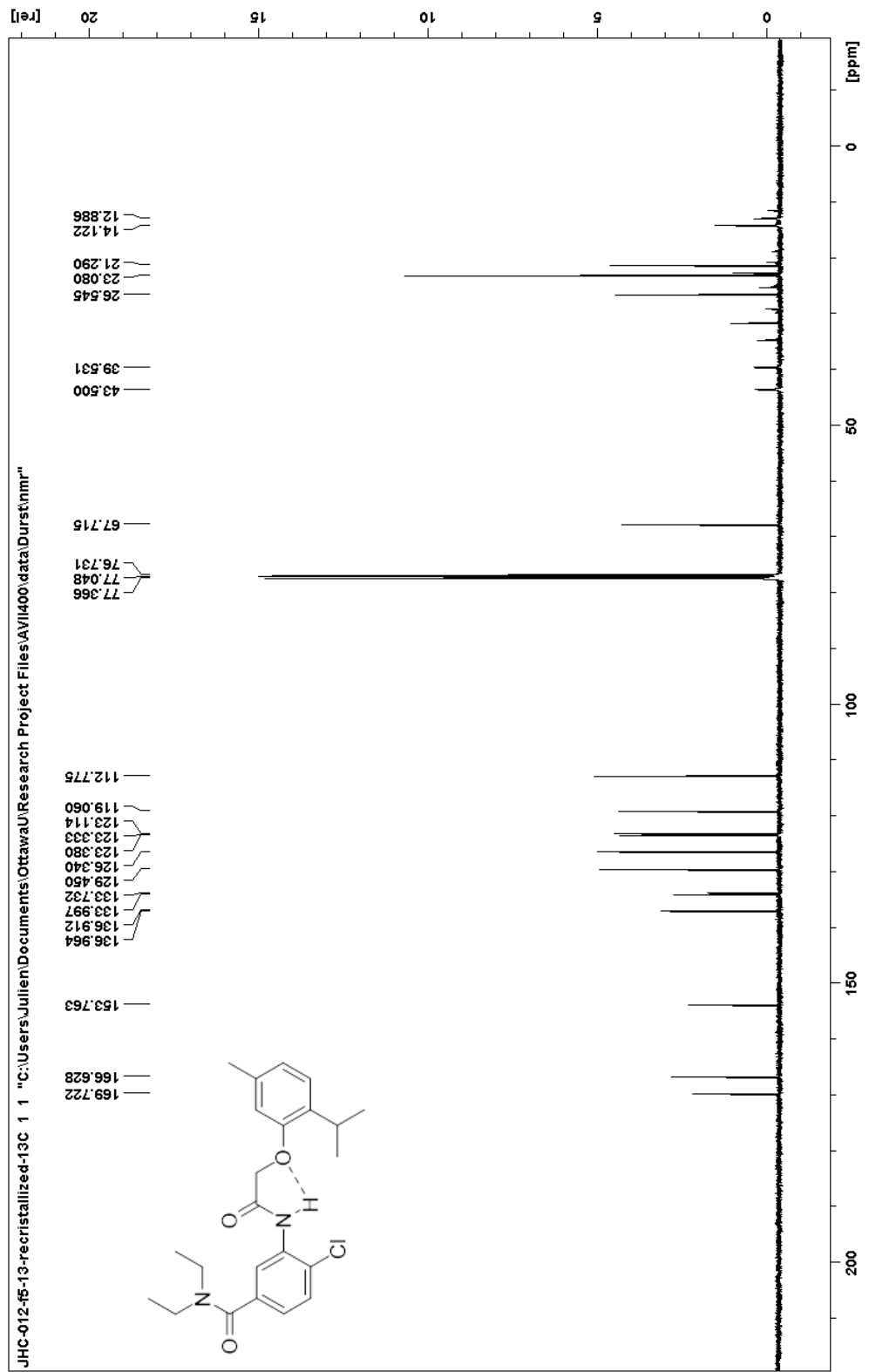


In a round bottom flask with DCM, 3-amino-4-chloro-*N,N*-diethylbenzamide (0.74 g, 3.26 mmol) and thymol acetic acyl chloride (0.37 g, 1.63 mmol) were dissolved in DCM in separate flasks. Triethylamine (0.20 mL, 1.43 mmol) was added to the solution containing the amine substrate. Both flasks were chilled in an ice bath, then the acyl chloride was slowly added to the solution of amines. The combined mixture sat at room conditions for 30 minutes, after which it was quenched with water. The solution was washed once with 10% NaOH<sub>(aq)</sub>, once with 5% HCl<sub>(aq)</sub>, dried over MgSO<sub>4</sub>, filtered and evaporated. The crude product was isolated and purified by two separate column chromatographies. The mass of product was unfortunately not recorded prior to sending the compound for analysis.

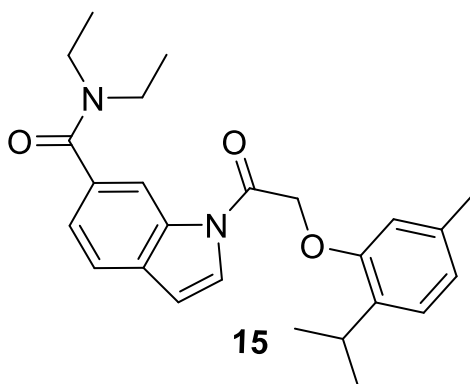
**<sup>1</sup>H NMR (400 MHz, CDCl<sub>3</sub>) δ, ppm:** 8.58 (d, *J* = 2.0 Hz, 1H), 7.42 (d, *J* = 8.4 Hz, 1H), 7.16 (d, *J* = 7.6 Hz, 1H), 7.12 (dd, *J*<sub>1</sub> = 8.0 Hz, *J*<sub>2</sub> = 2.0 Hz, 1H), 6.84 (d, *J* = 7.6 Hz, 1H), 6.66 (s, 1H), 4.63 (s, 2H), 3.52 (br, 2H), 3.44 (m, *J* = 6.8 Hz, 1H), 3.28 (br, 2H), 2.32 (s, 3H), 1.25 (d, *J* = 6.8 Hz, 6H), 1.20 (br, 6H).

**<sup>13</sup>C NMR (400 MHz, CDCl<sub>3</sub>) δ, ppm:** 169.72, 166.63, 153.76, 136.96, 136.91, 134.00, 133.73, 129.45, 126.34, 123.38, 123.33, 123.11, 119.06, 112.78, 67.72, 43.50, 39.53, 26.55, 23.08 (2C), 21.29, 14.12, 12.89.





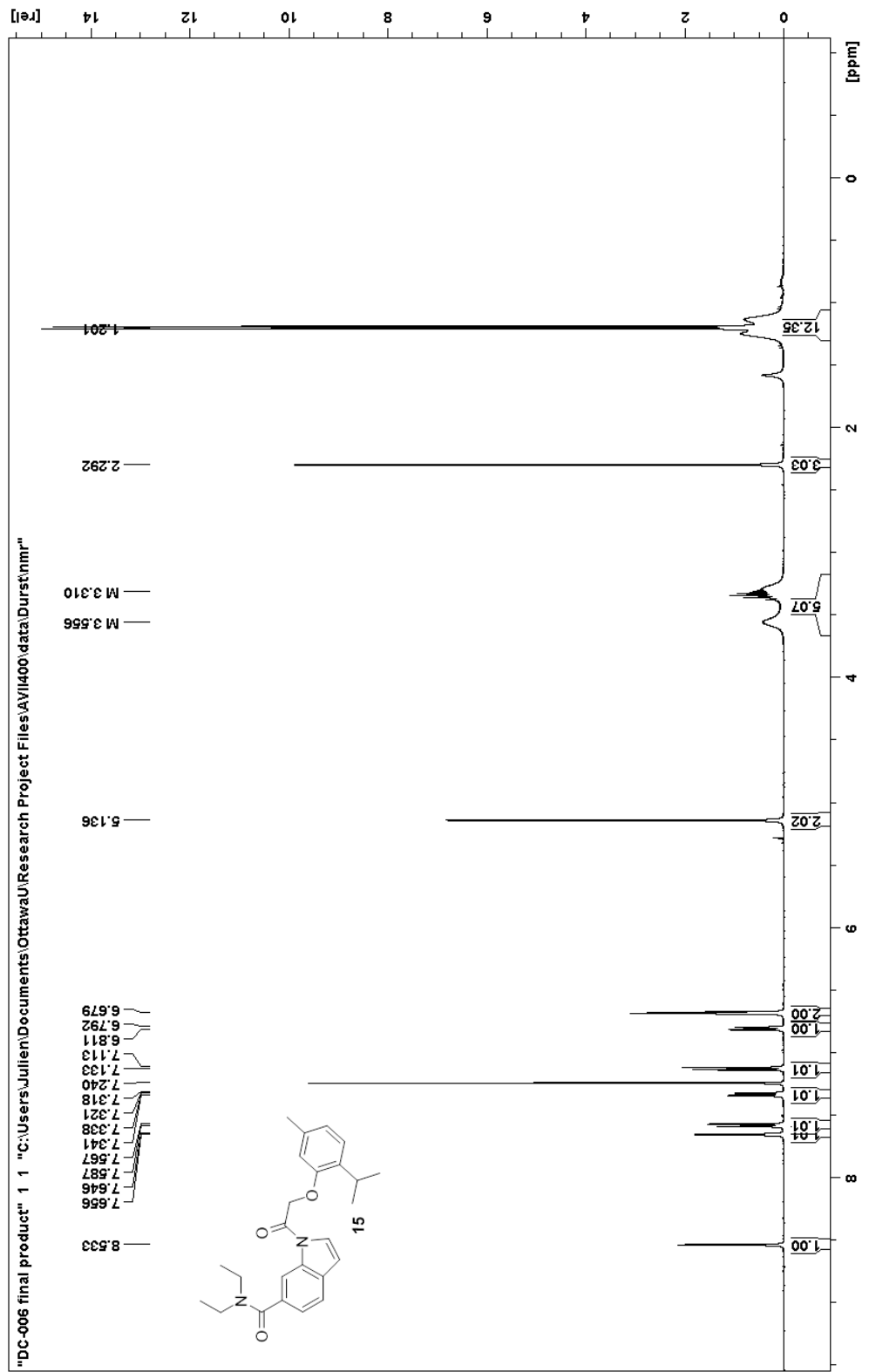
### Preparation of compound 15.

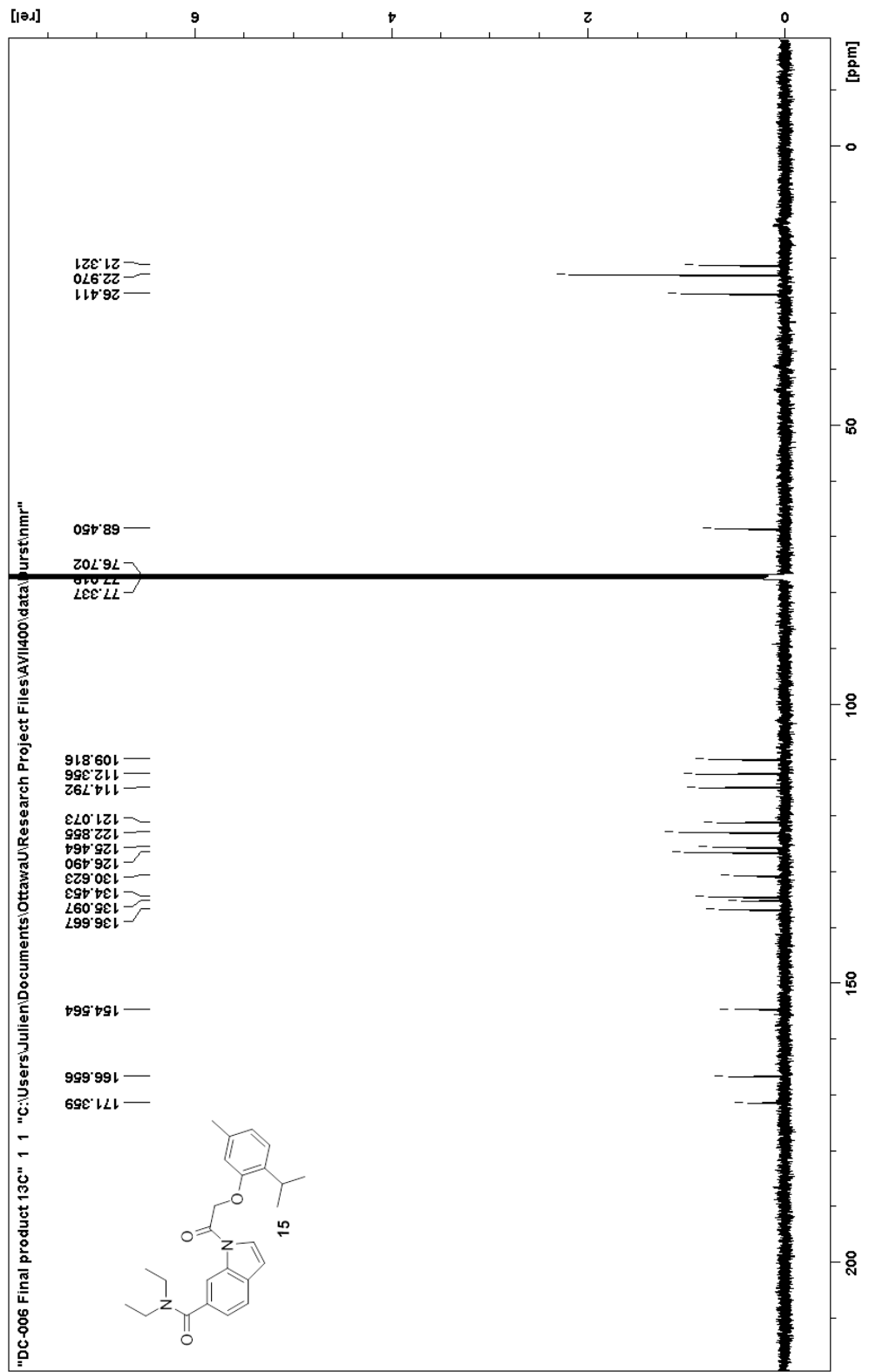


Protocol performed by undergraduate Danielle Causer. The previously prepared *N,N*-diethyl indole-6-carboxamide (1.01 g, 4.67 mmol) was added with thymol acetic acid (0.97 g, 4.66 mmol) to a round bottom flask. DMAP (0.71 g, 5.81 mmol) and EDCI (1.07 g, 5.58 mmol) were added next, before dissolving the combined solids in DCM (15.0 mL). The solution was stirred over two days at 40°C with a stopper. The solution was washed twice with 10% NaOH<sub>(aq)</sub> and twice with 5% HCl<sub>(aq)</sub>. The organic layer was dried over MgSO<sub>4</sub>, filtered and evaporated, yielding the crude product as a brown oil with some solid pieces. The crude product was purified via silica gel column chromatography using a gradient of hexanes and ethyl acetate. NMR analysis was used to identify the fractions containing the product, which was then recrystallized in a mixture of hexanes and DCM. The purified product was obtained by suction filtration as a white powder (103 mg, 5%).

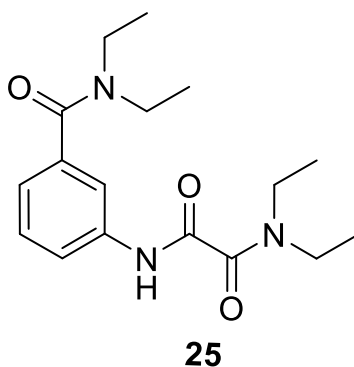
**<sup>1</sup>H NMR (400 MHz, CDCl<sub>3</sub>) δ, ppm:** 8.53 (s, 1H), 6.65 (d, J = 4.0 Hz, 1H), 7.58 (d, J = 8.0 Hz, 1H), 7.33 (d, J = 8.0 Hz, 1H), 7.12 (d, J = 8.0 Hz, 1H), 6.80 (d, J = 7.6 Hz, 1H), 6.68 (s, 1H), 6.67 (d, J = 4.8 Hz, 1H), 5.14 (s, 2H), 3.44 (m, 5H), 2.29 (s, 3H), 1.20 (m, 12H).

**<sup>13</sup>C NMR (400 MHz, CDCl<sub>3</sub>) δ, ppm:** 171.34, 166.66, 154.57, 136.67, 135.10, 134.45, 130.62, 126.49, 125.46, 122.86, 121.07, 114.79, 112.36, 109.82, 68.45, 26.41, 22.97, 21.32.





### Preparation of compound 25.

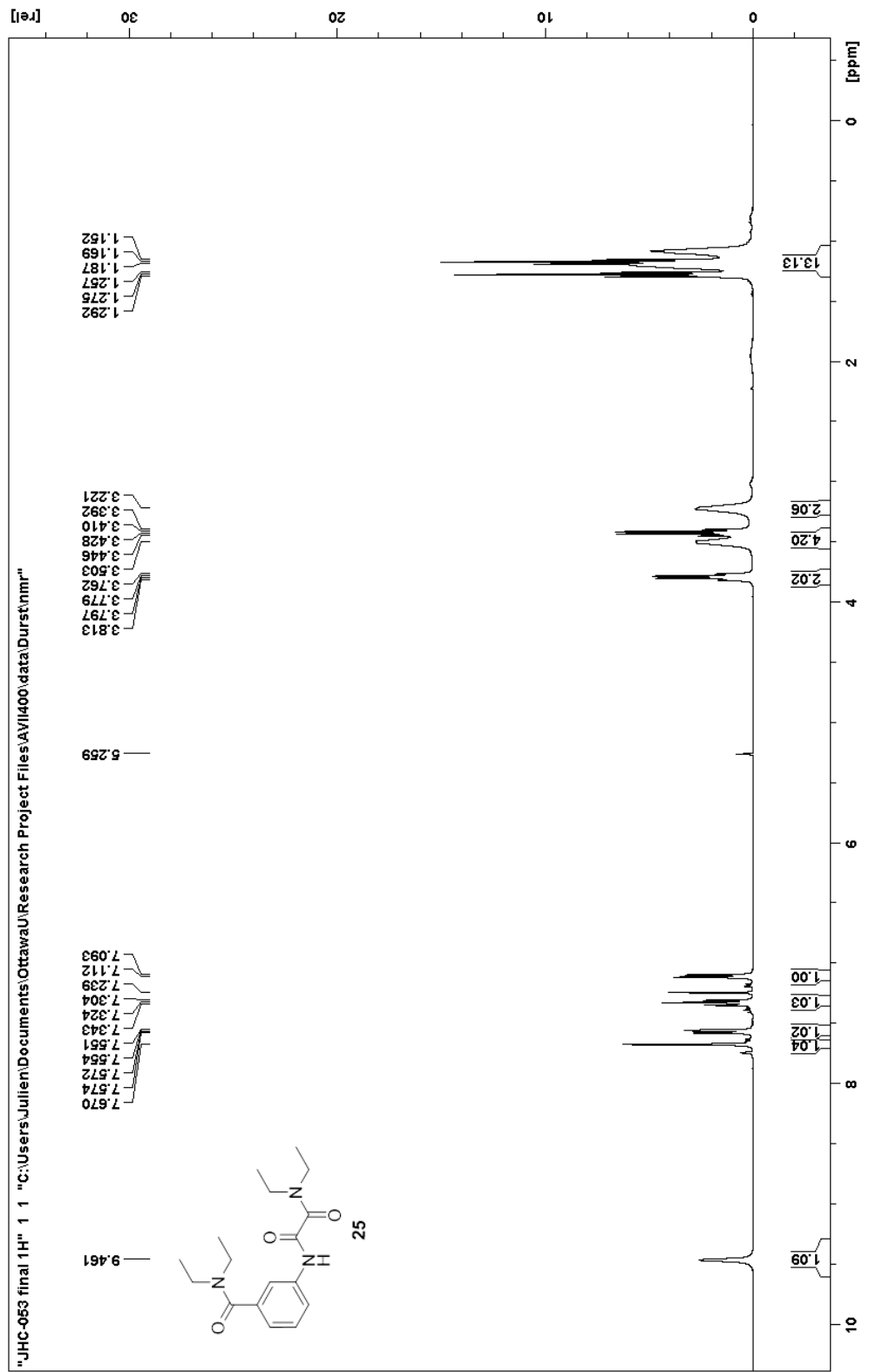


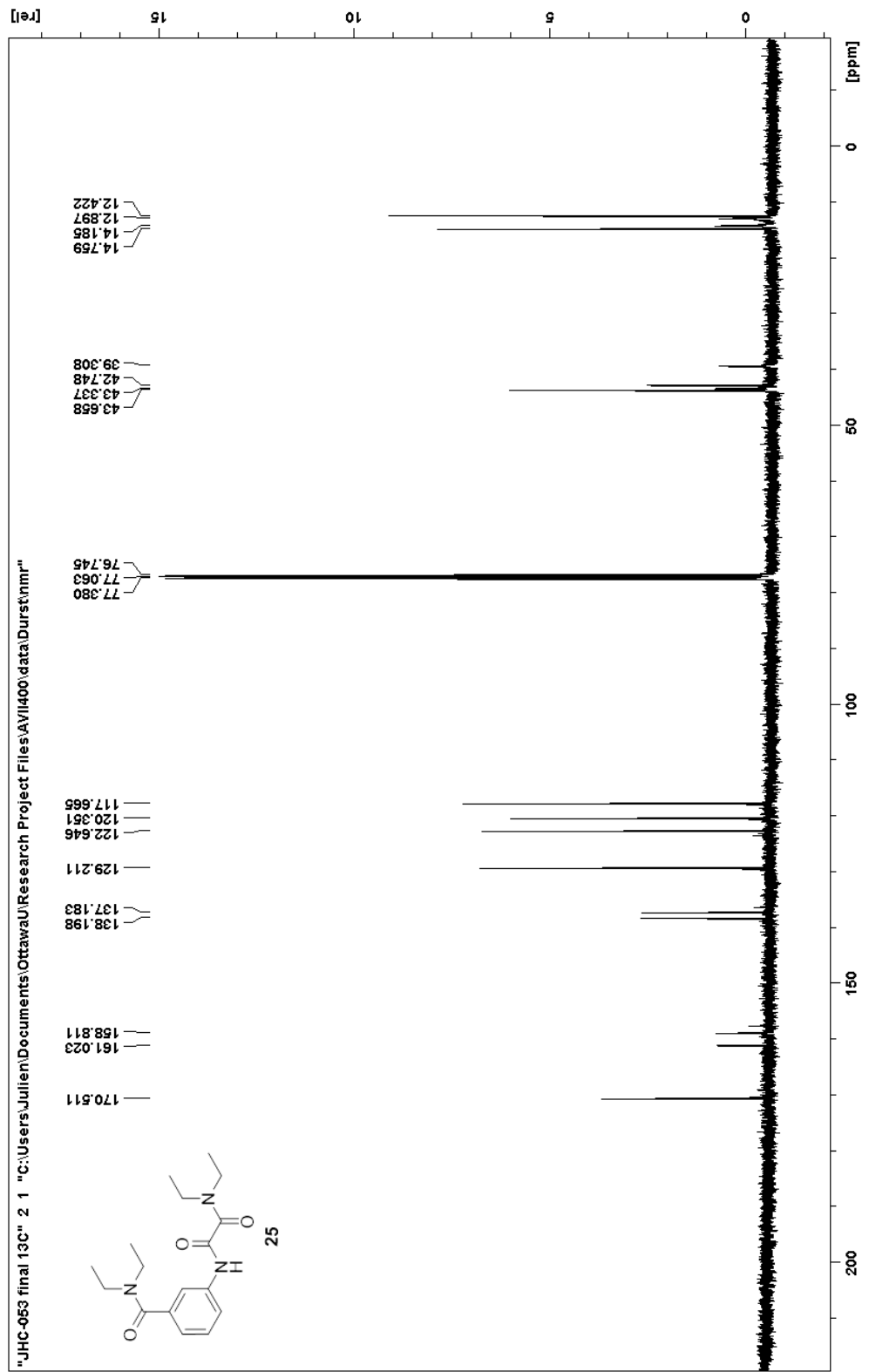
3-aminobenzoic acid (3.15 g, 23.0 mmol) and oxalyl chloride (4.5 mL, 52 mmol) were dissolved in DCM (30 mL) in a round bottom flask with a stirrer. The flask was warmed in an oil bath at 70°C, before adding 5 drops of DMF, beginning the reflux. The solution was refluxed for 1 hour and 30 minutes, after which the solvent was evaporated in vacuo. The solids were dissolved again in DCM, then cooled in an ice bath.

The solution of acyl chloride was added dropwise to a cooled solution of excess diethylamine and triethylamine in DCM. The solution was left to rest at room temperature for 30 minutes, then the solvent was evaporated. Water was added to quench the reaction, which was then washed once with 5% HCl<sub>(aq)</sub>. The organic layer was dried with MgSO<sub>4</sub>, filtered and evaporated. A small quantity (0.75 g) of the obtained solid was kept for a different experiment. The remaining product was purified by recrystallisation in a mixture of DCM and hexanes. The purified product was obtained by suction filtration as a white powder (3.56 g, 49%).

**<sup>1</sup>H NMR (400 MHz, CDCl<sub>3</sub>) δ, ppm:** 9.46 (s, 1H), 7.67 (s, 1H), 7.56 (d, J = 8.0 Hz, 1H), 7.32 (t, J = 8.0 Hz, 1H), 7.10 (d, J = 7.6 Hz, 1H), 3.79 (q, J = 6.8 Hz, 2H), 3.50 (br, 2H), 3.42 (q, J = 7.2 Hz, 2H), 3.22 (br, 2H), 1.28 (t, J = 6.8 Hz, 3H), 1.19 (br, 3H), 1.17 (t, J = 7.2 Hz, 3H), 1.10 (br, 3H).

**<sup>13</sup>C NMR (400 MHz, CDCl<sub>3</sub>) δ, ppm:** 170.51, 161.02, 158.851, 138.20, 137.18, 129.21, 122.65, 120.35, 117.67, 43.66, 43.34, 42.75, 39.31, 14.76, 14.19, 12.90, 12.42.





## 2.4 References

- (1) World Health Organization. Spinal cord injury Facts Sheet <https://www.who.int/news-room/fact-sheets/detail/spinal-cord-injury> (accessed Jul 16, 2020).
- (2) Spinal Cord Injury Facts & Statistics <https://www.sci-info-pages.com/spinal-cord-injury-facts-and-statistics/> (accessed Jul 14, 2020).
- (3) Spinal cord injury - Symptoms and causes <https://www.mayoclinic.org/diseases-conditions/spinal-cord-injury/symptoms-causes/syc-20377890> (accessed Jul 17, 2020).
- (4) *Neurological Disorders: Public Health Challenges*; World Health Organization, Ed.; World Health Organization: Geneva, 2006.
- (5) Lin, C.-W.; Huang, Y.-P.; Pan, S.-L. Spinal Cord Injury Is Related to an Increased Risk of Multiple Sclerosis: A Population-Based, Propensity Score-Matched, Longitudinal Follow-up Study. *J. Neurotrauma* **2015**, *32* (9), 655–659. <https://doi.org/10.1089/neu.2014.3723>.
- (6) Shepherd Center. Spinal Cord Injury Information: Levels, Causes, Recovery <https://www.shepherd.org/patient-programs/spinal-cord-injury/about#FAQ1> (accessed Jul 16, 2020).
- (7) New, P. W.; Cripps, R. A.; Bonne Lee, B. Global Maps of Non-Traumatic Spinal Cord Injury Epidemiology: Towards a Living Data Repository. *Spinal Cord* **2014**, *52* (2), 97–109. <https://doi.org/10.1038/sc.2012.165>.
- (8) American Association of Neurological Surgeons. Spinal Cord Injury – Types of Injury, Diagnosis and Treatment <https://www.aans.org/> (accessed Jul 20, 2020).
- (9) National Spinal Cord Injury Statistical Center. NSCISC 2019 Spinal Cord Injury Facts and Figures at a Glance. 2019.
- (10) Gater, D. R. Obesity After Spinal Cord Injury. *Phys. Med. Rehabil. Clin. N. Am.* **2007**, *18* (2), 333–351. <https://doi.org/10.1016/j.pmr.2007.03.004>.
- (11) Brown, R.; DiMarco, A. F.; Hoit, J. D.; Garshick, E. Respiratory Dysfunction and Management in Spinal Cord Injury. *Respir. Care* **2006**, *51* (8), 853–870.
- (12) Jackson, A. B.; Groomes, T. E. Incidence of Respiratory Complications Following Spinal Cord Injury. *Arch. Phys. Med. Rehabil.* **1994**, *75* (3), 270–275. [https://doi.org/10.1016/0003-9993\(94\)90027-2](https://doi.org/10.1016/0003-9993(94)90027-2).
- (13) Krueger, H.; Noonan, V. K.; Trenaman, L. M.; Joshi, P.; Rivers, C. S. The Economic Burden of Traumatic Spinal Cord Injury in Canada. *Chronic Dis. Inj. Can.* **2013**, *33* (3), 11.
- (14) Thuret, S.; Moon, L. D. F.; Gage, F. H. Therapeutic Interventions after Spinal Cord Injury. *Nat. Rev. Neurosci.* **2006**, *7* (8), 628–643. <https://doi.org/10.1038/nrn1955>.
- (15) Brown, A. CIHR Grant Application: Developing SOX9 Inhibitors for Spinal Cord Injury. 2017.
- (16) Fawcett, J. W.; Asher, R. A. The Glial Scar and Central Nervous System Repair. *Brain Res. Bull.* **1999**, *49* (6), 377–391. [https://doi.org/10.1016/s0361-9230\(99\)00072-6](https://doi.org/10.1016/s0361-9230(99)00072-6).
- (17) Galtrey, C. M.; Fawcett, J. W. The Role of Chondroitin Sulfate Proteoglycans in Regeneration and Plasticity in the Central Nervous System. *Brain Res. Rev.* **2007**, *54* (1), 1–18. <https://doi.org/10.1016/j.brainresrev.2006.09.006>.

- (18) MCKILLOP, W. M.; DRAGAN, M.; SCHEDL, A.; BROWN, A. Conditional Sox9 Ablation Reduces Chondroitin Sulfate Proteoglycan Levels and Improves Motor Function Following Spinal Cord Injury. *Glia* **2013**, *61* (2), 164–177. <https://doi.org/10.1002/glia.22424>.
- (19) Xu, X.; Bass, B.; McKillop, W. M.; Mailloux, J.; Liu, T.; Geremia, N. M.; Hryciw, T.; Brown, A. Sox9 Knockout Mice Have Improved Recovery Following Stroke. *Exp. Neurol.* **2018**, *303*, 59–71. <https://doi.org/10.1016/j.expneurol.2018.02.001>.
- (20) Arthur Brown. Private Communication: SAR Data of the ZO2 Analogs.
- (21) Fluet-Chouinard, Adrien. Synthesis of Analogs of a Potential Drug for Treatment of Epilepsy. Thesis, Université d'Ottawa / University of Ottawa, 2019.
- (22) Raina, V. Part B. Synthesis of Analogs of ZO2; Compounds with Potential to Help Regenerate Partially Severed Spinal Cords. **2018**, 263.
- (23) Kurzer, F.; Douraghi-Zadeh, K. Advances in the Chemistry of Carbodiimides. *Chem. Rev.* **1967**, *67* (2), 107–152. <https://doi.org/10.1021/cr60246a001>.
- (24) Watté, J.; Van Gompel, W.; Lommens, P.; De Buysser, K.; Van Driessche, I. Titania Nanocrystal Surface Functionalization through Silane Chemistry for Low Temperature Deposition on Polymers. *ACS Appl. Mater. Interfaces* **2016**, *8* (43), 29759–29769. <https://doi.org/10.1021/acsami.6b08931>.
- (25) Lombardi, C.; Day, J.; Chandrasoma, N.; Mitchell, D.; Rodriguez, M. J.; Farmer, J. L.; Organ, M. G. Selective Cross-Coupling of (Hetero)Aryl Halides with Ammonia To Produce Primary Arylamines Using Pd-NHC Complexes. *Organometallics* **2017**, *36* (2), 251–254. <https://doi.org/10.1021/acs.organomet.6b00830>.